To the Graduate Council:

I am submitting herewith a dissertation written by Feng Yu entitled "Experimental Design and Mathematical Modeling of Trichloroethylene Cometabolism in a Packed Bed Biofilm Reactor by *Pseudomonas putida* F1". I have examined the final copy of this dissertation for form and content and recommend that it be accepted in partial fulfillment of the requirements for the degree of Doctor of Philosophy, with a major in Chemical Engineering.

Paul R. Bienkowski, Major Professor

We have read this dissertation
and recommend its acceptance:

Accepted for the Council:

Associate Vice Chancellor and
Dean of the Graduate School

# Experimental Design and Mathematical Modeling of Trichloroethylene Cometabolism in a Packed Bed Biofilm Reactor by *Pseudomonas putida* F1

A Dissertation

Presented for the

Doctor of Philosophy Degree

The University of Tennessee, Knoxville

Feng Yu

August 1998

Copyright ©1998 by Feng Yu

All rights reserved

## Dedication

This dissertation is dedicated to Jiajun Jin, Xun Yu, Yun Yu, Xunxi Chen,

Weibo Chen, and my Parents Meixian Chen and Yigen Yu.

## Acknowledgments

I would like to thank Dr. Paul Bienkowski, my major advisor, who always willing to help me and trust. He makes me think and work independently to face any difficult problems. Highly appreciation goes to Dr. Gary Sayler, who takes care of me as his own student, gave me the great chance to work in the Center for Environmental Biotechnology where I could gain a lot of useful knowledge of microbiology, and financially support me in my final year towards Ph. D. Special thanks to Dr. Allen Baker who taught me the finite element method, always give me insight advise and make me complete the model computation successfully. Warmly thanks for Dr. Paul Frymier, serving as my committee, the time and effort. I also would like to thank Dr. Donlad Bogue, I will always remember him.

I would like to thank Dr. John Sanseverino for his help and advice when I was in difficulties. Many thanks to Dr. Chris Cox for his generosity, and Dr. Xiaobing Feng, a professor from Mathematical Department, giving useful advise. I want to thank Dr. Curtis Lajoie, Dr. Chris Kelly, and Dr. Raymond Stapleton.

I would say that I am lucky to have a friend like Hae-jin (Hae-jin Woo). Thanks Hae-jin for her kindness, her love, always sharing difficulties for me, and giving me inspirations, more like a sister. Many thanks goes to Mike Taylor whom I learned a lot computer knowledge from, for his assistance in the numerical calculation. I also appreciate Zhou Shi, for spending time discussing technique issues with me.

Deepest gratitude goes to my mentor Professor Jiajun Jin, my parents Meixian Chen, and Yigen Yu, my sister Yun Yu, brother Xun Yu, and Xunxi Chen. They are always be there for me. Thanks for the love, the encouragement, and emotional support that let me go through all hard time and get to this point.

Finally, I would thank other friends and lab coworkers include Catherine Cheng, Yee-kyung Ku, Meng Meng Wang, Justin Shingleton, CJ O'Lenick, Qinping Deng, Min Liang, and Kathy Chang. Special thanks to my friend Thada Somphone.

## Abstract

Trichloroethylene (TCE) as a suspected human carcinogen is one of the most common pollutants found in contaminated groundwater. Biofilm reactors have been extensively used in the bioremediation of hazardous organic compounds such as TCE. The biological background of TCE biodegradation is cometabolism. Limitations in the successful removal of TCE include competitive inhibition of primary substrate, TCE product toxicity, and oxygen limitation. In this study, an effective packed-bed bioreactor system was developed for the treatment of aqueous phase TCE by the toluene dioxygenases system of *Pseudomonas putida* F1. The reactor was a glass chromatography column 60 cm long and 2.5 cm in diameter. Glass beads (4 mm in diameter) were used to pack the column and support growth of the biofilm. The reactor was operated as a trickling filter with a recycled effluent to maintain low toluene concentrations throughout the column. The aqueous influent contained a minimal salts medium, toluene and TCE in various concentration range. Oxygen supply was directly connected to the column. The gas stream was also recirculated back into the column to prevent the loss of TCE in the vapor phase. Operational conditions that were tested included influent toluene concentration, influent TCE concentration, influent flow rate, and recycle rate. TCE removal efficiencies ranged from 94.5% to 60% with TCE influent concentrations of 0.31 to 1.06 ppm, and influent toluene concentrations of 30 to

53 ppm, respectively.

Modeling of biofilm kinetics is the first step for bioreactor design and process optimization. Although numerous biofilm models have been developed in various situations, very few models are reported for TCE cometabolism, probably due to its biological complexity and computational difficulties. In this study, a relatively comprehensive steady-state biofilm model was proposed for TCE coox-idation by *Pseudomonas putida* F1 using toluene as a primary substrate. This model coupled diffusion process with substrates competitive inhibition reaction in the biofilm. The Model assumed that TCE degradation was carried out by active biomass only, which was balanced by cell growth and TCE transformation product toxicity effect. Finally, the effective biofilm thickness was calculated. Finite element method was used for the implementation of numerical solutions of non-linear ordinary differential equations. TCE and toluene fluxes under different toluene and TCE bulk concentrations were investigated. The influence of mass transfer, TCE product toxicity on TCE degradation were analyzed. Combining TCE cometabolic biofilm model with dispersion, convection, mass transfer between biofilm phase and liquid phase, and physical equilibrium between gas phase and liquid phase, a bioreactor model was developed for the system of interest. At low TCE influent concentration, model calculation results match experimental data fairly well. Comparing with the experiments, model prediction errors were

below 30%. The inverse of TCE removal efficiency was found to be a function of the inverse of transformation capacity in a form of second order polynomial. This enabled the model to predict TCE removal efficiency at high TCE concentration when transformation product toxicity was significant. Similar results were obtained from model simulation by varying influent flow rates, influent TCE concentrations, influent toluene concentrations, and recycle rates as from the experiments, quantitatively or qualitatively. This bioreactor model can be used to design a bioreactor and to optimize operation for TCE cometabolism.

## Table of Symbols

$A$: Group constant

$A_r$: Cross section area of the column ($cm^2$)

$A_s$: Specific area of particle ($cm^{-1}$)

$b_d$: Cell decay constant (1/day)

$b_s$: Decay by shear loss (1/day)

$b'$: Overall decay constant (1/day)

$C_i$: Concentration in liquid phase (mg/L)

$C_{i0}$: Concentration at time zero (mg/L)

$C_{bi}$: Concentration in the bulk liquid (mg/L)

$C_{bi}{}^{in}$: Liquid concentrations in the inlet of the reactor (mg/L)

$C_{bi}{}^{ef}$: Effluent concentration (mg/L)

$C_{bi}{}^{if}$: Influent concentration (mg/L)

$C_{gi}$: Gas phase concentration (mg/L)

$C_{pi}$: Concentration in the biofilm (mg/L)

$C_{pi}|_{x=0}$: Concentrations at the interface of liquid film and biofilm (mg/L)

$C_{si}$: Concentrations at the surface of biofilm (mg/L)

$C_i^*$: Gas-Liquid interfacial concentration (mg/L)

$d_0$: Sauter mean diameter (cm)

$D_i$: Diffusion coefficient in the liquid phase ($cm^2$/day)

$D_{fi}$: Diffusivity of in the biofilm ($cm^2$/day)

$d_p$: Particle diameter (cm)

$E_i$: Dispersion coefficient ($cm^2$/day)

$f_a$: Active biomass fraction in the biofilm

$F$: A defined function

$F_f$: Liquid flow rate (ml/min)

$H_i$: Henry's law constant

$J_i$: Flux to the biofilm (mg/$cm^2$/day)

$J_i^i$: Toluene or TCE flux at sublayer $i$ (mg/$cm^2$/day)

$J_i^{i+1}$: Toluene or TCE flux at sublayer $i+1$ (mg/$cm^2$/day)

$k_i$: Reaction rate constant (mg substrate/mg cell/day)

$K_i$: Substrate saturation parameter (mg/L)

$K_{Gi}$: Gas phase mass transfer coefficient (cm/day)

$k_{Li}$: Liquid phase mass transfer coefficient (cm/day)

$l_e$: Element length (cm)

$L_i$: Liquid film thickness (cm)

$L_f$: Effective biofilm thickness (cm)

$L_r$: Length of the reactor (cm)

$M_b$: Molecular weight of solvent

$R$: Recycle ratio

$t$: Time (minute)

$t_i$: Standard biofilm depth (cm)

$t_a$: Geometric average of $t_1$ and $t_2$

$T$: Absolute temperature (K)

$T_c$: TCE transformation capacity (mg TCE/mg cell)

$u$: Superficial velocity (cm/min)

$v$: Gas velocity (cm/min)

$V_a$: Molar volume of solute as liquid at its boiling point

$V^g$: Vapor phase volume (ml)

$V^l$: Liquid phase volume (ml)

$x$: Coordinate in the biofilm (cm)

$X$: Biomass concentration (mg/L)

$X_f$: Biofilm density (mg/cm$^3$)

$X_0$: Initial biomass concentration (mg/L)

$Y$: Toluene yield coefficient (mg cell/mg toluene)

$z$: Reactor coordinate (cm)

**Dimensionless Group**

$Pe_i$: Peclet number

$R_{em}$: Reynolds number

$S_c$: Schmidt number

$Sh_i$: Sherwood number

### Greek letters

$\alpha_i$: Liquid-Biofilm mass transfer number

$\alpha$: Fitting parameter

$\beta$: Fitting parameter

$\beta_i$: Liquid-Gas mass transfer number

$\delta l$: Subunit biofilm thickness (cm)

$\epsilon$: Porosity of the bed

$\eta$: Dimensionless biofilm coordinate

$\eta_{ei}$: Effectiveness factor

$\gamma_i$: Gas phase mass transfer number

$\mu_g$: specific growth rate ($hr^{-1}$)

$\mu$: Absolute viscosity of solution (cp)

$\phi_i$: Linear base function

$\psi_b$: Association parameter

$\rho$: Solution density ($g/cm^3$)

$\sigma$: Shear stress

$\theta_G$: Gas hold-up

$\theta_L$: Liquid hold-up

$\theta_s$: Standard biofilm time for toluene (min)

$\zeta$: Dimensionless reactor coordinate

$i = 1$: for toluene, and $i = 2$: for TCE

# Contents


**1 Introduction** **1**

1.1 General Description . . . . . 1

1.2 Research Objectives . . . . . 3

**2 Background and Literature Review** **4**

2.1 Trichloroethylene . . . . . 4

2.2 TCE Treatment Techniques . . . . . 5

2.3 Cometabolism of TCE by *Pseudomonas putida* F1 . . . . . 7

2.4 Bioreactor Design . . . . . 10

2.5 Mathematical Modeling . . . . . 12

2.5.1 Reaction Kinetics . . . . . 12

2.5.2 Biofilm Model and Bioreactor Model . . . . . 13

2.6 Finite Element Method . . . . . 14

**3 Material and Methods** **17**

3.1 Cell Preparation for Growth Curve Study . . . . . 17

3.2 Batch Test for Toluene and/or TCE Degradation . . . . . 18

3.3 Analytical Method . . . . . 19

3.3.1 Cell Mass Determination . . . . . 19

3.3.2 Toluene and TCE Measurement . . . . . 20

3.3.3 Gas Phase Oxygen Measurement . . . . . 20

3.4 Minimal Salts Medium . . . . . 21

**4 Batch Experimental Results** **24**

4.1 Growth Characteristic of *Pseudomonas putida* F1 . . . . . 25

4.2 Toluene Degradation . . . . . 25

4.3 Cometabolism of TCE and Toluene . . . . . 26

4.4 TCE Degradation by Resting Cell . . . . . 29

4.5 Experimental Verification of TCE Toxicity . . . . . 31

**5 Toluene and TCE Degradation Kinetics** **35**

5.1 Determination of Yield Coefficient $Y$ . . . . . 36

5.2 Determination of $K_1$ and $k_1$ for Toluene . . . . . 37

5.3 Determination of $K_2$ and $k_2$ for TCE . . . . . 40

5.4 Determination of Transformation Capacity $T_c$ . . . . . 41

5.5 Parameters' Correction . . . . . 45

5.6 Comparing of Model Calculation with Experimental Data . . . . . 49

**6 Bioreactor System Development** **60**

6.1 Bioreactor System . . . . . 61

6.2 Abiotic Experiment . . . . . 64

6.3 Growth of Biofilm . . . . . 66

6.4 Measuring of Liquid Hold-up and Gas Recycle Rate . . . . . 67

6.4.1 Liquid Hold-up . . . . . 67

6.4.2 Gas Recycle Rate . . . . . 68

**7 Column Analysis** **70**

7.1 Toluene Degradation in the Column . . . . . 70

7.2 Oxygen Distribution in the Column . . . . . 73

7.3 Biomass Activity Test and Biomass Distribution . . . . . 74

**8 TCE Cometabolism in a Packed Bed Biofilm Reactor** **77**

8.1 Dynamic TCE Breakthrough Curve . . . . . 77

8.2 Toluene Concentration Affects TCE Degradation . . . . . 79
8.3 TCE Concentration Affects Its Degradation . . . . . 83
8.4 Recycle Rate Affects TCE Degradation . . . . . 86
8.5 Flow Rate Affects TCE Degradation . . . . . 88
8.6 Oxygen Affects TCE and Toluene Degradation . . . . . 90
8.7 Summary of the Column Experiments . . . . . 91

**9 Biofilm Model** **95**

9.1 Model Development . . . . . 97
9.2 Non-Dimensionalization of Model Equations . . . . . 103
9.3 Effectiveness Factor . . . . . 105
9.4 Solving Procedure . . . . . 106
9.5 Numerical Implementation by Finite Element Method . . . . . 106
9.6 Computational Results . . . . . 110

**10 Bioreactor Model** **126**

10.1 Model Development . . . . . 128
10.2 Dimensionless Form of Model Equation . . . . . 130
10.3 Solving Procedure . . . . . 132

10.4 Finite Element Method . . . . . 132

10.5 Sample Model Calculation Results . . . . . 135

10.6 Model Sensitivity Analysis . . . . . 141

10.6.1 Toluene Yield Coefficient . . . . . 142

10.6.2 TCE Transformation Capacity $T_c$ . . . . . 142

10.6.3 Specific Area of Mass Transfer and Reactor Length . . . . 144

10.6.4 TCE Saturation Parameter $K_2$ . . . . . 145

10.6.5 Recycle Ratio . . . . . 146

10.7 Comparison of Model with Experimental Results . . . . . 148

10.7.1 Influent Flow Rate Affects TCE Degradation . . . . . 149

10.7.2 TCE Loading Rate Affects TCE Degradation . . . . . 150

10.7.3 Toluene Affects TCE Degradation . . . . . 154

**11 Conclusions** **160**

**Bibliography** **166**

**Appendices** **182**

**A Calibration Curve of O.D vs Biomass** **183**

**B Procedure for Making Solution B** **185**

**C Calculation of Oxygen Demanding in the Column** **187**

**D Code for Kinetic Calculation** **189**

**E Finite Element Method Related Issues** **193**

E.1 Notations Used in the Finite Element Methods . . . . . 193

E.1.1 Notations in the Biofilm Model . . . . . 193

E.1.2 Notations in the Bioreactor Model . . . . . 194

E.2 Sample Operation of Jacobian Form in the Biofilm Model . . . . . 195

E.3 Finite Element Library Matrices . . . . . 196

**F Code for Solving Biofilm Model** **198**

F.1 Template for Solving Biofilm Concentrations . . . . . 198

F.2 Main Program for Biofilm Equations . . . . . 200

F.3 Residuals and Jacbians for Concentrations in the Biofilm . . . . . 205

F.4 Code for Element Assembling . . . . . 207

**G Code for Solving Bioreactor Model** **209**

G.1 Template for Bulk Fluid Equations . . . . . 209

G.2 Main Program for Bioreactor Model . . . . . 212

G.3 Residuals and Jacobians for Bulk Fluid Equations . . . . . 216

G.4 Subroutine for Solving the Biofilm Equations . . . . . 218

G.5 Matrices Dimension Set-up . . . . . 221

G.6 Parameter Evaluation . . . . . 221

# List of Figures

2.1 (A) Oxidation of toluene to *cis*-toluene dihydrodiol by toluene dioxygenase. (B) Diagrammatic representation of recombinant clone pDTG601[85]. . . . . 9

2.2 Diagnostic products and proposed intermediate in TCE dioxygenation by toluene dioxygenase[35] . . . . . 9

3.1 Diagram of Cell Cultivation in a Flask . . . . . 18

4.1 Growth Curve of *Pseudomonas putida* F1 . . . . . 26

4.2 Toluene Degradation: using initial 10, 30, 50 ppm concentrations . 27

4.3 TCE Cometabolism: 40 ppm Toluene and 1 ppm TCE. Top Figure: Toluene Concentration Changes with Time; Bottom Figure: TCE Concentration Changes with Time . . . . . 28

4.4 TCE Cometabolism: 10 ppm Toluene and 1 ppm TCE. Top Figure: Toluene Concentration Changes with Time; Bottom Figure: TCE Concentration Changes with Time . . . . . 30

4.5 TCE Degradation by Resting Cell . . . . . 31

4.6 TCE Degradation with and without Adding Succinate . . . . . 32

4.7 TCE Degradation under the Influence of Toluene. Top Figure: TCE Concentration Changes with Time; Bottom Figure: Toluene Concentration Changes with Time . . . . . 33

5.1 Determination of Yield Coefficient of Toluene . . . . . 37

5.2 Determination of $k_1$ at Different Initial Toluene Concentrations (Symbols are the experimental data: '$\diamond$'=test1, '$\circ$'=test2, '$*$'=test3) 38

5.3 $K_1$ Evaluation at 20 ppm Initial Toluene Concentration . . . . . 39

5.4 Determination of $K_2$ and $k_2$ of TCE . . . . . 41

5.5 5 ppm TCE Degradation . . . . . 42

5.6 0.5 ppm TCE Degradation by Repeating Injection . . . . . 43

5.7 1 ppm TCE Degradation by Repeating Injection . . . . . 44

5.8 2 ppm TCE Degradation by Repeating Injection . . . . . 44

5.9 Relationship of TCE and Toluene Concentration . . . . . 47

5.10 Comparison of Model Estimation with Experimental Data . . . . 50

5.11 Model Calculations of Toluene Reaction Rates . . . . . 50

5.12 Comparison of Model Estimation with Experimental Data for TCE Degradation by Resting Cells . . . . . 51

5.13 TCE Reaction Rate and Active Biomass Change with Time (1 ppm TCE) . . . . . 52

5.14 TCE Reaction Rate and Active Biomass Change with Time (4.7 ppm TCE) . . . . . 53

5.15 Comparison of Model Estimation with Experimental Data (40 ppm toluene and 1 ppm TCE). Top Figure: Toluene Concentration Changes with Time; Bottom Figure: TCE Concentration Changes with Time. . . . . 55

5.16 Calculation Results of Toluene and TCE Reaction Rates Changing with Time (40 ppm toluene and 1 ppm TCE) . . . . . 56

5.17 Comparison of Model Estimation with Experimental Data (8 ppm toluene and 1 ppm TCE). Top Figure: Toluene Concentration Changes with Time; Bottom Figure: TCE Concentration Changes with Time. . . . . 57

5.18 Toluene and TCE Reaction Rate Changes with Time (8 ppm toluene and 1 ppm TCE) . . . . . 58

6.1 Reactor System Schematic . . . . . 63

6.2 Abiotic Toluene and TCE Breakthrough Curve . . . . . 65

6.3 Liquid Hold-up Changes with Total Flow Rate . . . . . 68

6.4 Gas Recycle Rate Changes with Influent Flow Rate . . . . . 69

7.1 Gas and Liquid Phase Toluene Concentration Distribution in the Column at Different Toluene Loading Rate . . . . . 72

7.2 Oxygen Distribution in the Column at Different Toluene Loading 74

7.3 Toluene Degradation by Active Growing Cell and Immobilized Cell 76

7.4 Cell Mass Distribution along the Column . . . . . 76

8.1 Effluent TCE Concentration Changes with Time . . . . . 78

8.2 TCE Degradation by Step Changing Toluene Concentration (The corresponding toluene concentrations entered the column after dilution by the recycle were: (1)=0.58 ppm; (2)=3.37 ppm; (3)=6.33 ppm.) . . . . . 80

8.3 Effluent TCE Concentration Changes with Time after Stop Toluene Feeding . . . . . 81

8.4 Toluene Concentration Affects TCE Removal Efficiency . . . . . 82

8.5 Influent TCE Concentration Affects TCE Degradation . . . . . 84

8.6 Gas Phase TCE Concentration and Oxygen Distribution in the Column . . . . . 85

8.7 Recycle Rate Affects TCE Degradation . . . . . 87

8.8 Influent Flow Rate Affects TCE Degradation . . . . . 89

8.9 TCE Removal Efficiency Changes with Influent Flow Rate . . . . 89

8.10 Gas Phase TCE Distribution in the Column . . . . . 90

8.11 Oxygen Affects Toluene and TCE Degradation . . . . . 92

8.12 Summary of TCE Degradation in the Packed Bed Reactor . . . . 93

9.1 Biofilm discretization and toluene TCE concentration profiles . . . 99

9.2 Solving Procedure for the Biofilm System . . . . . 107

9.3 Toluene and TCE Concentrations in the Biofilm . . . . . 113

9.4 Active Biomass Distributions in the Biofilm . . . . . 113

9.5 Toluene Flux in the Biofilm . . . . . 114

9.6 TCE Flux in the Biofilm . . . . . 114

9.7 Toluene and TCE Concentrations in the Biofilm . . . . . 116

9.8 Active Biomass in the Biofilm . . . . . 116

9.9 Toluene Flux in the Biofilm . . . . . 117

9.10 TCE Flux in the Biofilm . . . . . 117

9.11 Toluene/TCE Flux Ratio in the Biofilm . . . . . 118

9.12 Toluene and TCE Concentrations in the Biofilm . . . . . 118

9.13 Toluene and TCE Concentrations in the Biofilm . . . . . 120

9.14 Active Biomass in the Biofilm . . . . . 120

9.15 Toluene Flux in the Biofilm . . . . . 121

9.16 TCE Flux in the Biofilm . . . . . 121

9.17 Toluene/TCE Flux in the Biofilm . . . . . 122

9.18 Toluene and TCE Concentrations in the Biofilm . . . . . 122

9.19 Toluene Flux in the Biofilm . . . . . 124

9.20 TCE Flux in the Biofilm . . . . . 124

9.21 Toluene/TCE Flux in the Biofilm . . . . . 125

9.22 Active Biomass in the Biofilm . . . . . 125

10.1 Illustrations of Numerical Model for the Biofilm and Bioreactor . 127

10.2 Solving Procedure for Concentrations in the Bioreactor . . . . . 133

10.3 Toluene Concentrations in the Bioreactor . . . . . 137

10.4 TCE Concentrations in the Bioreactor . . . . . 137

10.5 Biofilm Thickness Distribution in the Reactor . . . . . 139

10.6 Toluene Concentrations in the Biofilm . . . . . 139

10.7 TCE Concentrations in the Biofilm . . . . . 140

10.8 Toluene and TCE Flux in the Reactor . . . . . 140

10.9 Toluene and TCE Effectiveness Factor . . . . . 141

10.10Toluene Yield Coefficient Affects TCE Degradation . . . . . 143

10.11TCE Product Toxicity Affects Its Degradation . . . . . 144

10.12Specific Area Affects TCE Degradation . . . . . 145

10.13Reactor Length Affects TCE Degradation . . . . . 146

10.14TCE Saturation Parameter Affects TCE Degradation . . . . . 147

10.15Recycle Rate Affects TCE Degradation . . . . . 148

10.16Influent Flow Affects TCE Degradation . . . . . 149

10.17Comparison of Model Predictions with Experimental Results at Different Flow Rate. (Numbers refer to influent flow rates in the unit of in ml/min) . . . . . 150

10.18Correlation of Removal Efficiency vs $T_c$ . . . . . 152

10.19Extrapolation of TCE Removal Efficiency at Low $T_c$ Value . . . . 153

10.20TCE Removal Efficiency at Different TCE Concentrations . . . . 153

10.21Comparison of Model Prediction with Experimental Data . . . . 154

10.22Correlation of TCE Removal Efficiency to $T_c$ . . . . . 156

10.23TCE Removal Efficiency at Different Influent Toluene Concentration 156

10.24Correlation of TCE Removal Efficiency vs $T_c$ at High Toluene Concentrations . . . . . 157

10.25Toluene Concentration Entering the Reactor at Its Corresponding Influent Toluene Concentration under Recycle Ratio 9.82 . . . . . 158

10.26Comparison of Model Prediction with Experimental Data . . . . 159

A.1 Calibration Curve of O.D vs Dried Mass . . . . . 184

# List of Tables


2.1 Physical Characteristics of Trichloroethylene[12] . . . . . 5

3.1 Composition of Minimal Salts Media . . . . . 22

3.2 Composition of Metals 44 Solution . . . . . 23

5.1 Estimated $K_1$ at Different Initial Toluene Concentration . . . . . 40

5.2 Estimated $T_c^{app}$ at Different Initial TCE Concentration by Repeating Injection . . . . . 45

5.3 Kinetic Parameters of Toluene and TCE Degradation . . . . . 47

5.4 Values of Kinetic Parameters Reported in Literature (M.C. refers to mixture culture) . . . . . 48

9.1 Parameters Used in the Biofilm Model Calculation . . . . . 111

# Chapter 1

# Introduction

## 1.1 General Description

Trichloroethylene is widely used as a solvent and degreasing agent[40]. Spillage and improper disposal caused it become one of the most common chlorinated compounds in the contaminated groundwater[81]. It is a suspected human carcinogen[18]. Its presence in drinking water supplies is a potential hazard. Treatment of TCE and other chlorinated compounds include physical process and biological process. Biological treatment has great advantages over many conventional physical-chemical techniques. Physical techniques, for example adsorption and stripping[37], only transfer contaminants from one phase to another. Extra cost will be required for contaminants destruction in the subsequent treatment step. In a biologi-

cal process, the polluted groundwater is pumped into a bioreactor where contaminants are degraded through the metabolism of microorganisms. No report has been found that microorganisms can use TCE as a growth substrate under aerobic conditions. TCE degradation is under the mechanism of cometabolism that TCE is oxidized by non-specific oxygenases in the presence of an inducing growth substrate and oxygen. These enzymes are called inducible enzymes, such as methane monoxygenase[74], propane monooxygenase[79], and toluene dioxygenases[80]. They are produced only when the corresponding growth substrate exists in the environment. Limitations in the successful biotransformation of TCE include product toxicity[1][63][65], competitive inhibition between TCE and primary substrate[43], and dissolved oxygen limitation[13]. The objective of this research is to develop a packed bed bioreactor system to degrade TCE in liquid phase, test different operating conditions. The primary goal is to develop a mathematical model for process optimization and future design. The application of this bioreactor system could be extended to the treatment of groundwater contaminated with other chlorinated aliphatic compounds. The information gained can be applied to the design and improvement of packed bed biofilm reactor systems for the above-ground treatment of TCE and other problematic enviromental contaminants.

## 1.2 Research Objectives

This research involved a development and an investigation of the feasibility of a biofilm reactor system for the treatment of groundwater contaminated with TCE. On the basis of cometabolic theory, *Pseudomonas putida* F1 was used as the biocatalyst to degrade TCE with toluene as a primary substrate. The specific objectives include:

1. To develop a packed bed biofilm reactor system that can be effectively used for aqueous phase TCE removal.

2. To understand the effects of cometabolism on the biodegradation of TCE and toluene in batch and fixed-film cultures.

3. To evaluate the kinetic parameters of TCE and toluene degradation by batch reaction.

4. To study TCE removal in the bioreactor under various operating conditions.

5. To develop a mathematical model, based on the information obtained above, to simulate TCE and toluene biodegradation in the biofilm and in the packed bed reactor and to solve the system of equations by finite element method.

# Chapter 2

# Background and Literature Review

## 2.1 Trichloroethylene

Trichloroethylene is a nonflammable volatile organic compound. It is used mainly as a solvent for metal degreasing, solvent extraction, dissolving and cleaning in industries and household products like typewrite correction fluid, paint removers, and spot removers. Its physical properties are summarized in Table 2.1[12]. Careless disposal, spillage, and leakage make TCE among the most common pollutants in the contaminated groundwater in United States[17]. Great concern has been established because of its toxicity and possible carcinogenic

Table 2.1: Physical Characteristics of Trichloroethylene[12]

| | |
|---|---|
| Chemical formula | $CHCl:CCl_2$ |
| Molecular weight | 131 |
| Density at 20°C | 1.4642 |
| Solubility at 25°C | 1100 mg/L |
| Odor | chloroform-like |
| Color | colorless |
| Boiling point | 87°C |
| Volatility | $P_{vapor}$=77 mm Hg at 25°C |
| Henry's Law | 0.5 (C air/C water) |
| Flammability | nonflammable |

properties[76]. Chemical stability and poor biodegradability leads to its persist over years[23][78]. Proposed drinking water standard for TCE is 5 $\mu$g/L[75]. However, contamination levels in mg/L range can be found near polluted sources[31][42].

## 2.2 TCE Treatment Techniques

TCE remediation technologies have been developed for years. Air stripping and granulated-active carbon(GAC) adsorption have been proved as the most effec-

tive methods for removing volatile organic compounds (VOCs) from contaminated groundwater[37]. 99% removal of TCE can be achieved by air stripping[23]. TCE concentration was reduced to below 5 $\mu$g/L by adsorption[37]. However, they are both mass transfer operations. Contaminants are only transferred from one media to another without complete destruction. In addition, regeneration of the used carbon often make the adsorption process more expensive. Biological treatment is an alternative way which overcomes disadvantages in the conventional process. Contaminants are usually converted to $CO_2$, $H_2O$ and other non-toxic products. TCE can be transformed under both anaerobic and aerobic environments. Studies demonstrated that the main mechanism of anaerobic TCE degradation is reductive dehalogenation[45]. Anaerobically, vinyl chloride can be formed as one of the main products, and this organic compound is identified as mutagen and carcinogen[39]. The other disadvantage of anaerobic treatment is that the reaction rate is very slow[8][9]. Biotransformation of TCE under aerobic conditions does not result in the formation of toxic compounds[82]. However, TCE can not be used as a growth substrate in the aerobic process. It can only be transformed under the mechanism of cometabolism in which non-specific oxygenases of microorganisms catalyze the oxidation of TCE in the presence of primary substrate. These microorganisms include methanotrophs[74], toluene oxidizers[62][80], propane oxidizers[79], phenol utilizers[28][29], and ammonia oxidizers[77]. Many studies have been given on

in-situ bioremediation for restoring aquifers contaminated by liquid fuels and halogenated organics using indigenous microorganisms in the environment. Growth substrate, oxygen, and other nutrients need to be added to stimulate the growth of microbial populations[34]. Some times in-situ bioremediations are difficult to control. They mostly depend on the subsurface and the hydrogeology conditions of site. When in-situ biodegradation is not possible, pump-and-treat system becomes another promising choice. During this process, contaminated groundwater is pumped into a bioreactor, with the action of microorganisms, the contaminants are destroyed[38][44]. Also great efforts have been made for simulating degradation and performing fundamental researches in bioreactor system in recent years.

## 2.3 Cometabolism of TCE by *Pseudomonas putida* F1

Cometabolism is the transformation of a nongrowth substrate at the expense of a growth substrate or other transformable compound[16] for microorganisms. A growth substrate is defined as an electron donor that provides reducing power and energy, or carbon for cell growth and maintenance. In a cometabolic reaction, the cometabolic enzyme is induced by the growth substrate, which simultaneously catalyzes the transformation of the nongrowth substrate. *Pseudomonas putida* F1

was used as biocatalyst carrier in this study. Wackett and Gibson[80] demonstrated that initial TCE removal rate by *Pseudomonas putida* F1 was significant greater than by methanotroph *Methylosinus trichosporium* OB3b. In addition, maximum TCE degradation activity of methanotrophs is due to the expression of methane monooxygenase (MMO) in a soluble form under conditions of copper starvation[20][49][70]. It can be predicted that removal efficiency would be limited when copper in a concentration greater than 0.25 $\mu M$ exists in the groundwater system[72]. The biological background of *Pseudomonas putida* F1 has been well documented. The ability of this microorganism to mineralize TCE is through cooxidation when toluene serves as a growth substrate[80]. The enzyme responsible for TCE metabolism is toluene dioxygenase[47]. It is a three-component enzyme system induced in the presence of toluene[85]. The component proteins are flavoprotein, ferredoxin, and iron sulfur protein. They transfer electrons from NADH to the terminal component that catalyzes the formation of *cis*-toluene dihydrodiol from toluene (Figure 2.1). It has been confirmed that *tod*$C_1C_2$BA genes encode for the production of toluene dioxygenase for TCE degradation. Toluene dioxygenase has a broad substrate specificity. Its oxidation mechanism of TCE is dioxygen insertion[35](Figure 2.2). The major products of TCE oxidation are formic acid and glyoxylic acid. TCE remediation by *Pseudomonas putida* F1 also suffers from intermediates toxicity[80]. TCE oxidization results in cytotox-

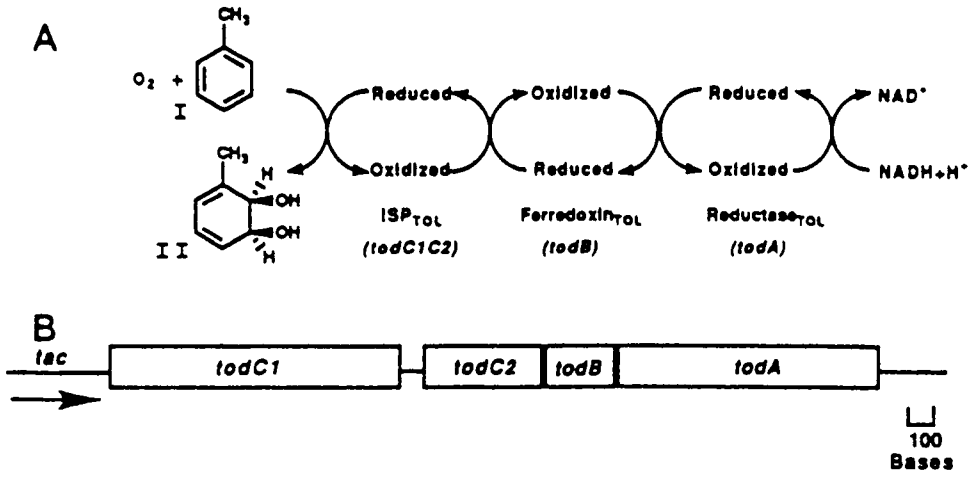



Figure 2.1: (A) Oxidation of toluene to *cis*-toluene dihydrodiol by toluene dioxygenase. (B) Diagrammatic representation of recombinant clone pDTG601[85].

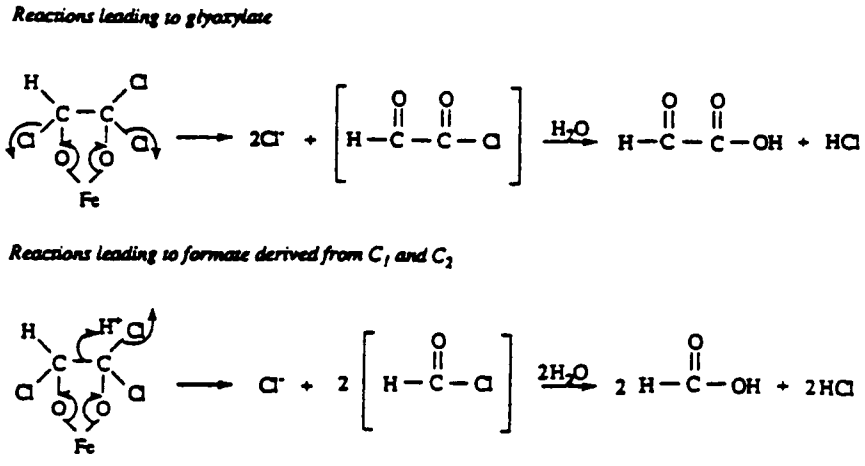



Figure 2.2: Diagnostic products and proposed intermediate in TCE dioxygenation by toluene dioxygenase[35]

icity and loss of toluene dioxygenase activity[35]. Heald and Jenkins[26] showed that TCE oxidation toxicity is mediated by toluene dioxygenase. TCE product toxicity decreases the transformation capacity of bioreactor system and becomes a major problem in the bioremediation process.

## 2.4 Bioreactor Design

Due to the complexity of TCE cometabolism, bioreactor system design seems to be quite different from conventional reactors. Usually growth phase and transformation phase are separated to avoid growth substrate competitive inhibition. Alvarez-Cohen and McCarty[1] first proposed a two-stage dispersed-growth system for the treatment of TCE. After being well grown on methane in a CSTR, cells were transferred to a plug flow reactor for TCE transformation. Two-stage biological treatment system have been used successfully when competitive inhibition between primary substrate and secondary substrate is involved[24][43]. Tschantz[73] extended their work by using multi-stage bioreactor for TCE degradation by *Methylosinus trichosporium* OB3b. Most recent work for dual chlorinated compounds degradation was reported by Chang and Alvarez-Cohen[13].

Biofilm reactors have been received great attention in TCE and other VOCs biodegradation in recent years, mainly because of their high cell concentration, resistant to shock loading of inhibitory compounds, especially well performance in

the degradation of recalcitrant organic compounds[20][36][48][64]. In TCE degradation, cell growth and TCE transformation phase are separated by using sequencing biofilm reactor[21][60], in which TCE is degraded in the absence of growth substrate, and enzyme activity which lost due to TCE product toxicity was recovered in the growth mode alternatively. However, TCE removal efficiency decreased with time[21], usually TCE degradation ability can not be completely regenerated. Similar results were obtained by Shimomura[63] for TCE degradation in a fluidized-bed reactor. This is not a stable operation. Oxygen is necessary in the oxidation of TCE. It acts as a co-substrate as well as a terminal electron acceptor for cellar respiration[33]. Insufficient oxygen may decrease the rate of TCE degradation. Chang and Alvarez-Cohen[13] used a sealed chamber with pressurized pure oxygen to increase dissolved oxygen level in the influent. Directly introducing air into the reactor will cause stripping problem[70]. Strand[69] developed a sparged biofilm reactor where gas was recycled and pumped upward into the reactor. Supplying sufficient oxygen is a big issue in the in-situ groundwater treatment[29][30].

## 2.5 Mathematical Modeling

### 2.5.1 Reaction Kinetics

TCE removal kinetics in the absence of growth substrate can be described by Michaelis-Menten kinetics for single substrate. Alvarez-Cohen and McCarty[1] proposed the concept of transformation capacity to modify the active cell loss by product toxicity, which yields the following rate equation:

$$r_c = \frac{k[X_0 - \frac{1}{T_c}(C_0 - C)]C}{K_c + C} \tag{2.1}$$

where $C_0$ and $C$ are TCE concentrations (mg/L) at initial time $t_0$ and at time $t$ (day); $X_0$ (mg/L) is the initial active biomass concentration; k (mg TCE/mg cell/day) is TCE reaction rate constant, $K_c$ (mg/L) is the TCE substrate saturation parameter, and $T_c$ is the transformation capacity (mg TCE/mg cell). This model has been applied successfully in later studies[13][65]. Competitive inhibition Michaelis-Menten kinetics was employed in the steady-state continuous system with simultaneous conversion of toluene and TCE by Landa et al[32]. Model calculation results fit the experimental data very well. Chang and Alvarez-Cohen[14] developed a kinetic model for the cometabolic biodegradation of chlorinated compounds, in which NADP limitation was also considered besides competitive inhibition and product toxicity. This is the most comprehensive model so far for TCE degradation. Cometabolic kinetics under different conditions was evaluated

by Criddle[15].

### 2.5.2 Biofilm Model and Bioreactor Model

Steady-state biofilm model was first developed by Rittmann and McCarty[55]. Biofilm with no net growth or decay over time is defined as a steady-state biofilm. The model predicts substrate flux and biofilm thickness under given condition in steady state. Biofilm kinetics determines three substrate utilization conditions: deep, shallow, and fully penetrated biofilm[71]. For deep biofilm, the rate of degradation is fast that substrate concentration at the attachment surface is merely zero. In contrast, for fully penetrated biofilm, the reaction rate is too slow to establish a concentration gradient within the biofilm. Biofilm with reaction rate between deep biofilm and fully penetrated one is the shallow biofilm. This becomes the fundamental biofilm model for other model development, such as multi-species biofilm model[57], dual limitation biofilm model[58], and steady-state biofilm model with biofilm growth[66]. Models of chlorinated compound degradation in the biofilm are also based on the cometabolic theory. Those secondary substrates can not support a stable biofilm. A primary substrate must be provided as a carbon and energy source for the biofilm activity[10][11]. A few theoretical model have been developed to predict cometabolic degradation of TCE in the biofilm. Model developed by Anderson and McCarty[2] was the only one to

in-cooperate TCE transformation product toxicity into the biofilm kinetics with methane as the primary growth substrate. Difficulties in the successful biofilm modeling of TCE cometabolism may because of the complex biological process in the oxidation of TCE. The characteristics of TCE cometabolic biofilm process and unsteady bioreactor operation make the bioreactor modeling difficult. Very few bioreactor models have been developed when one considers all facts of competitive inhibition, product toxicity in the biofilm, and convection, dispersion, mass transfer in a packed bed biofilm reactor for TCE remediation.

## 2.6 Finite Element Method

The finite element method is a procedure for constructing approximate solution to initial-boundary value partial differential equation (PDE) system in engineering and mathematical physics[5][6][7]. Its solution is implemented through a discrete approximate equation called weak statement, which combines the calculus and vector field theory, and the concepts of extremization, orthogonality and completeness for computing. A general approximate solution for a given partial differential equation $L(q) = 0$ with specified boundary conditions can be written as:

$$q(x) \approx q^N(x) = \sum_{i=1}^{N} a_i \phi_i(x) \tag{2.2}$$

for a steady-state problem, and as

$$q(x,t) \approx q^N(x,t) = \sum_{i=1}^{N} a_i(t)\phi_i(x) \tag{2.3}$$

for an unsteady-state problem, where $1 \leq i \leq N$, $N$ is the number of terms for approximation, $\phi_i(x)$ are set of trial functions that span the physical domain, they can be linear, quadratic, or cubic piecewise polynomials. The unknown expansion coefficient set $a_i$ or $a_i(t)$ is the nodal solution. The measure of the error caused by numerical approximate solution is then given by:

$$L(e^N) = L(q) - L(q^N) \tag{2.4}$$

Weak statement enables the approximation error vanishing over the entire domain:

$$WS^N = \int_\Omega \omega_i(x) L(q^N) d\tau = 0 \tag{2.5}$$

where $\Omega$ is the physical domain, and $\omega_i(x)$ is a set of weight functions. In Galerkin weak statement, the weight functions $\omega_i(x)$ are equated to the trial functions $\phi_i(x)$ term by term:

$$GWS^N = \int_\Omega \phi_i(x) L(q^N) d\tau = 0 \tag{2.6}$$

Galerkin weak statement is optimal as it requires the error in $q^N$ to be orthogonal to every number of the trial space defined to support $q^N$. Specific boundary conditions are automatically incorporated into the weak statement. Solution domain is discretized into finite elements. In one element domain, the solution can be

interpolated in terms of the basis function as:

$$Q_e(x,t) = \{N_k\}^T \{Q(t)\}_e \tag{2.7}$$

where $N_k$ is the finite element basis of the associated trial function $\phi_i$, $k = 1, 2, 3$ for linear, quadratic, and cubic function, respectively, and $\{Q(t)\}_e$ is the nodal solution. Non-overlapping assembling of each finite element domain leads to the mathematical statement of finite element approximate solution:

$$Q^h(x,t) = U_e \{N_k\}^T \{Q(t)\}_e \tag{2.8}$$

In steady state, solution is only a function of space, no time is concerned. Applying Galerkin weak statement to each element and assembling them yields the global matrix statement:

$$[Matrix]\{Q\} - \{b(data)\} = \{0\} \tag{2.9}$$

where [Matrix] and $\{b(data)\}$ are global matrices in which $\{b(data)\}$ is the user-supplied data in a form of column matrix. For an unsteady-state case, the solution is also a function of time:

$$[JACOBIAN](\{Q^{n+1}\} - \{Q^n\}) + \Delta t\{RESIDUAL\}^n = \{0\} \tag{2.10}$$

This equation can be solved by Newton algorithm and linear algebra operations. Error estimation is accomplished in the form of norm suitable for the selected trial and test spaces, which is bounded by some measure by the given information(data).

# Chapter 3

# Material and Methods

## 3.1 Cell Preparation for Growth Curve Study

50 ml MSB media (Section 3.4) in a 250 ml flask was inoculated with a loop of *Pseudomonas putida* F1 frozen cells stored in a -80°C freezer. Toluene was used as a carbon source and supplied in a vapor phase through a suspended glass ball fixed in the rubber stopper (Figure 3.1). About 60 to 100 $\mu$l pure toluene was added inside. By shaking, toluene vaporized through a hole in the ball and dissolved in the media. After one day shaking at a rate of 108 rpm, a light yellow-green color was developed in the solution in the bottom of the flask. This first culture was transferred into another fresh growth media and grew in the same condition until O.D (600 nm) reached to 0.95 A.U. Cells were centrifuged at 10K

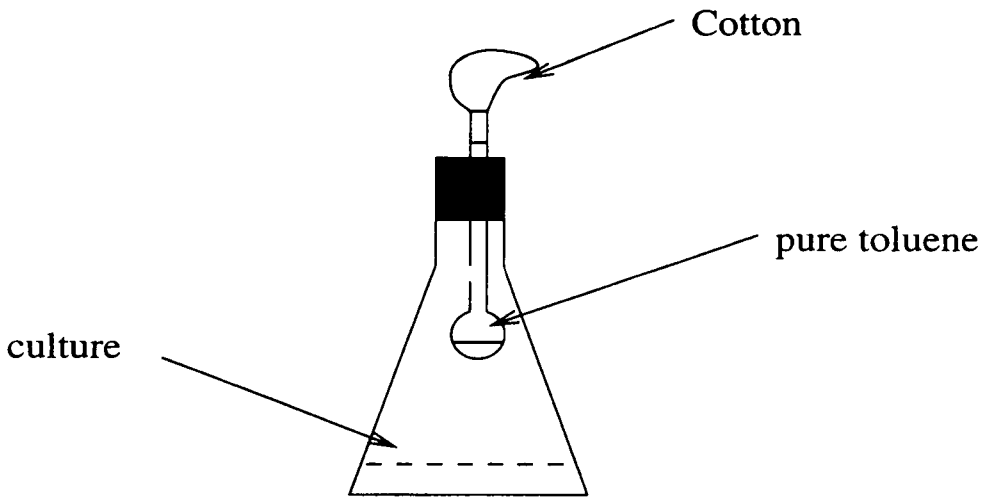



Figure 3.1: Diagram of Cell Cultivation in a Flask

rpm for ten minutes and resuspended in fresh media adjusting O.D to about 1.0 A.U. This second culture was then ready for growth curve study. At time zero, the concentrated cells were inoculated to 50 ml media. Repeated tests were conducted with starting O.D 0.0491 A.U. and 0.0585 A.U., respectively. 1 ml samples were taken at every one hour interval.

## 3.2 Batch Test for Toluene and/or TCE Degradation

Batch experiments were performed in a series of 25 ml Mininert vials with Teflon sealed cap. Second culture was used. The preparing procedure for active

cells was the same as for the growth study, except O.D was at about 1.0 for the whole experiments. Specific amounts of prepared cell solution were added into vials. Vials with cell solution were kept in an ice container. Fifteen minutes were necessary to warm it up before use. Toluene and/or TCE saturated water were introduced into the vials through a open-close valve on the cap by a gas tight syringe right before starting the experiment. The volumes of toluene and/or TCE saturated water to be transferred depended on toluene and/or TCE concentration for the testing. The finial liquid volume was fixed at 5 ml at different initial toluene and TCE concentrations to keep the vapor phase volume/liquid phase volume to 4:1. Vials were shaken at a rate of 180 rpm. Head space samples were taken at different intervals to monitor toluene and TCE degradation rate.

## 3.3 Analytical Method

### 3.3.1 Cell Mass Determination

Cell concentration was estimated by optical density (O.D) at a wavelength of 600 nm on a Beckman DU -70 spectrophotometer (La Jolla, Ca.). Biomass concentration in the unit of mg per liter was then determined by reading in the calibration curve of O.D vs biomass concentration, which was made by standard method in Appendix A.

### 3.3.2 Toluene and TCE Measurement

Toluene and TCE concentrations were determined by taking a gas phase sample and measuring in a Shimadzu GC 9AM gas chromatograph (Shimadzu Analytical Instruments Co., Kyoto, Japan) equipped a 60 m long, 0.75 mm I.D. glass capillary column (Supelco). TCE was detected by an electron capture detector (ECD), and toluene was detected by a flame ionization detector (FID). Helium was the carrier gas, and nitrogen was the makeup gas. Samples passing through the column reached ECD first then FID. Operation conditions for GC were: flow rate of helium 7 ml/min, nitrogen 50 ml/min, hydrogen 35 ml/min, and air 425 ml/min; temperature for oven 150°C, injection 250°C, and detector 250°C. 25 $\mu$l gas phase sample was taken for GC analysis. In the column experiments, 0.4 ml influent and effluent liquid samples were transferred into a 2 ml Teflon sealed cap vial by a 0.5 ml gas tight syringe. Vials were shaken rigorously for about 3 minutes by hand before headspace sample. Calibration curves for toluene and TCE were made every day. Total concentration was determined by comparing measured GC area with the calibration curve.

### 3.3.3 Gas Phase Oxygen Measurement

Oxygen in the gas phase from the column was also measured by GC analysis. By comparing area of air peak from sample to standard curve air peak with 21%

oxygen, the oxygen amount in the particular position of the column could be estimated.

## 3.4 Minimal Salts Medium

Minimal salts medium used in the experiments was made up of solution B and C. It is a modified mineral salt buffer[67]. The compositions of B and C are listed in Tables 3.1 and 3.2. Method for making solution B was detailed in Appendix B. Solutions B and C were filter sterilized, and solution B was stored in a refrigerator at 4 - 10°C. In preparing of 1.0 liter MSB, 20 ml solution B and 5 ml solution C were added into 1 liter phosphate buffer solution composed of 2.15 g/L $KH_2PO_4$ and 5.30 g/L $K_2HPO_4$ with pH 7.2, which was autoclaved in advanced. In batch degradation studies, toluene saturated water and/or TCE saturated water was transferred into vials by gas tight syringe to bring toluene and TCE to a designed concentration. In column system, the synthetic wastewater was made up continuously, in which MSB was 50% diluted by deionized water. Water saturated toluene and TCE were mixed with MSB to the top of the reactor. Concentrations were controlled by an HPLC pump for toluene feeding and a syringe pump for TCE feeding.

Table 3.1: Composition of Minimal Salts Media

| Chemical formula | Concentration (g/L) |
|---|---|
| Solution B | |
| Nitrilo triacetic acid | 10 |
| $MgSO_4.7H_2O$ | 14.45 |
| $CaCl_2.2H_2O$ | 3.33 |
| $(NH_4)_6Mo_7O_{24}.4H_2O$ | 0.00925 |
| $FeSO_4.7H_2O$ | 0.099 |
| Metals 44 (Table 3.2) | 50 ml |
| Solution C | |
| $(NH_4)_2SO_4$ | 60 g/300 ml $dH_2O$ |

Table 3.2: Composition of Metals 44 Solution

| Chemical formula | Concentration (mg/100 ml) |
|---|---|
| EDTA | 250 |
| $ZnSO_4.7H_2O$ | 109.5 |
| $MnSO_4.H_2O$ | 154 |
| $FeSO_4.7H_2O$ | 500 |
| $CuSO_4.5H_2O$ | 39.20 |
| $Co(NO_3)_2.6H_2O$ | 24.80 |
| $Na_2B_4O_7.10H_2O$ | 17.70 |

# Chapter 4

# Batch Experimental Results

A number of studies have been done by batch scale experiments for TCE degradation[14][26][52], either using methanotrophic, or phenol, or toluene oxidizing bacteria. These studies provide the fundamental knowledge of competitive inhibition, TCE transformation product toxicity, or reducing power limitation in the TCE cometabolism[14], not only qualitatively, but also quantitatively in kinetics. Different bacteria have different biochemical characteristics. To understand more about *Pseudomonas putida* F1, Some basic experiments for toluene and TCE degradation in batch scale were conducted.

## 4.1 Growth Characteristic of *Pseudomonas putida* F1

The growth of *Pseudomonas putida* F1 was measured by the increase of O.D in the flask. O.D vs time is plotted in Figure 4.1. O.D. can be converted into cell density by the calibration curve prepared before (Appendix A). Like other batch culture, lag phase occurred after inoculation. Cells experienced adjusting themselves to the new environment. In three hours, cells started to grow very fast. This was the exponential phase which continued to 8 hours in this experiment. O.D was in the range of 0.6. During this period, the growth rate can be described by following equation:

$$\frac{dX}{dt} = \mu_g X \tag{4.1}$$

where $X$ is the cell concentration (mg/L), and $\mu_g$ is the maximum specific growth rate ($hr^{-1}$). The determined value is 0.43 $hr^{-1}$. Time for doubling the population is 1.6 hr.

## 4.2 Toluene Degradation

Five initial toluene concentrations were investigated: 10 ppm, 20 ppm, 30 ppm, 40 ppm, and 50 ppm. Triple tests were addressed. The results of total toluene

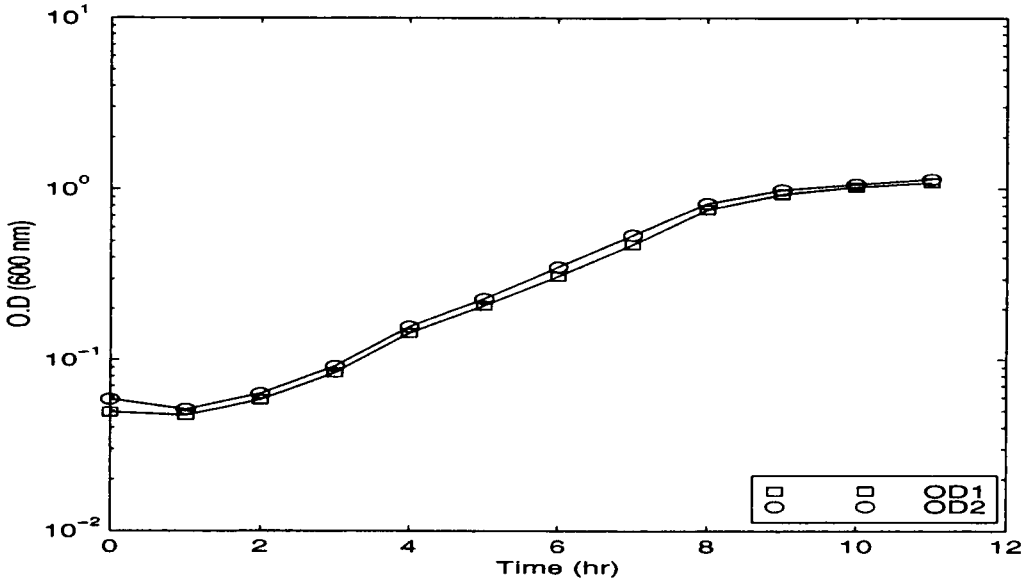



Figure 4.1: Growth Curve of *Pseudomonas putida* F1

concentration changing with time using 10 ppm, 30 ppm, and 50 ppm initial concentrations are shown in Figure 4.2. As a primary substrate, toluene was degraded rapidly. For approximately same biomass concentration, the toluene degradation rate kept the same in high concentration ranges.

## 4.3 Cometabolism of TCE and Toluene

TCE degradation character of *Pseudomonas putida* F1 in the presence of toluene was tested. Enzymes were fully induced for growing cells in a MSB media using toluene as the carbon source. Two sets of TCE degradation experiments were con-

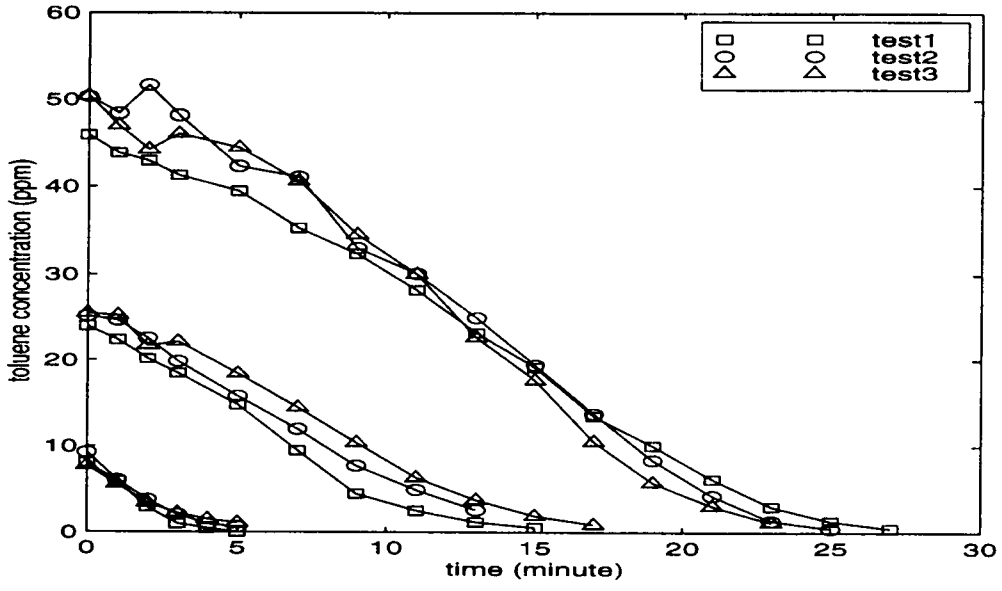



Figure 4.2: Toluene Degradation: using initial 10, 30, 50 ppm concentrations

ducted: high toluene concentration and low toluene concentration. Initial TCE concentration was fixed at 1 ppm. With an initial mixture of 40 ppm toluene and 1 ppm TCE, toluene was removed in 20 minutes (Figure 4.3). As they share a same enzyme system, there exists a competitive inhibition, with both toluene and TCE competing for the common active site of the enzyme. Due to much higher concentration of toluene than TCE and larger toluene degradation rate, TCE concentration remained almost unchanged until most of the toluene has been removed. The rate of TCE oxidation increased at toluene concentration below 10 ppm, and then TCE was degraded continuously. However, the degradation rate was not constant; it decreased with time. This phenomena has been

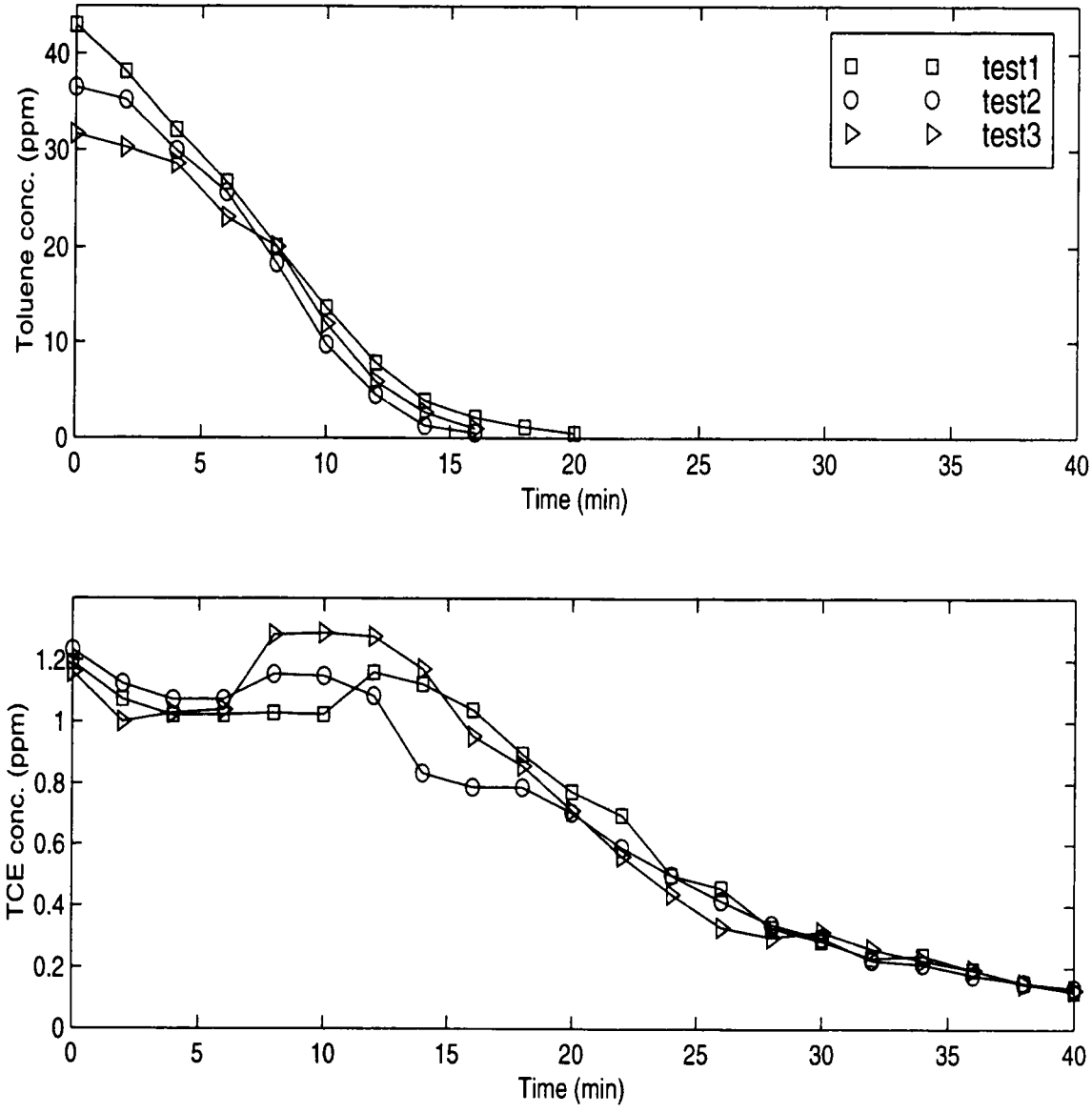



Figure 4.3: TCE Cometabolism: 40 ppm Toluene and 1 ppm TCE. Top Figure: Toluene Concentration Changes with Time; Bottom Figure: TCE Concentration Changes with Time

explained as TCE associated intermediate products toxicity[1]. At this time, no more enzyme was generated as of no toluene in the environment, and the toxicity of TCE transformation products inactivated the enzyme system responsible for TCE degradation. Another experiment was also performed with initial mixture of 10 ppm toluene and 1 ppm TCE (Figure 4.4). Slow TCE degradation lag phase was not observed under this condition, because toluene concentration was not high enough to show the significant competitive inhibition. But decreasing in TCE removal rate after toluene has been consumed still happened.

## 4.4 TCE Degradation by Resting Cell

Based on the theory of cometabolism, TCE transformation is catalyzed by the same enzyme system for toluene oxidation. If there is no toluene in the environment, TCE degradation will not be competitively inhibited by toluene. And initial TCE reaction rate will reach to maximum. Cells harvested from growth in a toluene media are called resting cell[1]. They have transformation ability of TCE in the absence of toluene. Results of TCE degradation with initial TCE concentrations at 0.5 ppm, 1 ppm, and 2 ppm are shown in Figure 4.5. In contrast with Figure 4.3, no lag phase occurred. This indicates that competitive inhibition was avoided. This has been found applications in engineering design, in which growth period and degradation period were separated[13][43][73] to enhance

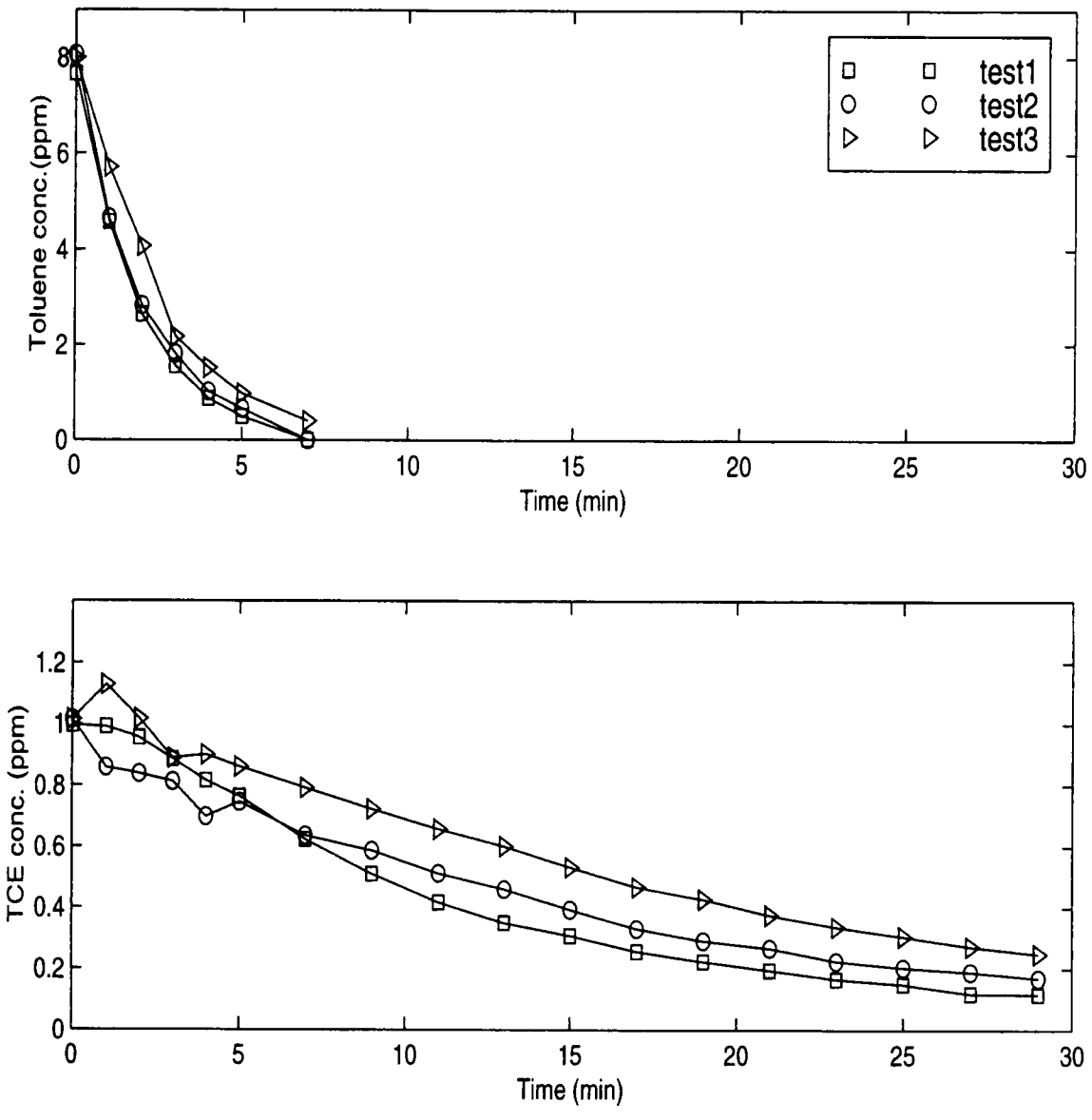



Figure 4.4: TCE Cometabolism: 10 ppm Toluene and 1 ppm TCE. Top Figure: Toluene Concentration Changes with Time; Bottom Figure: TCE Concentration Changes with Time

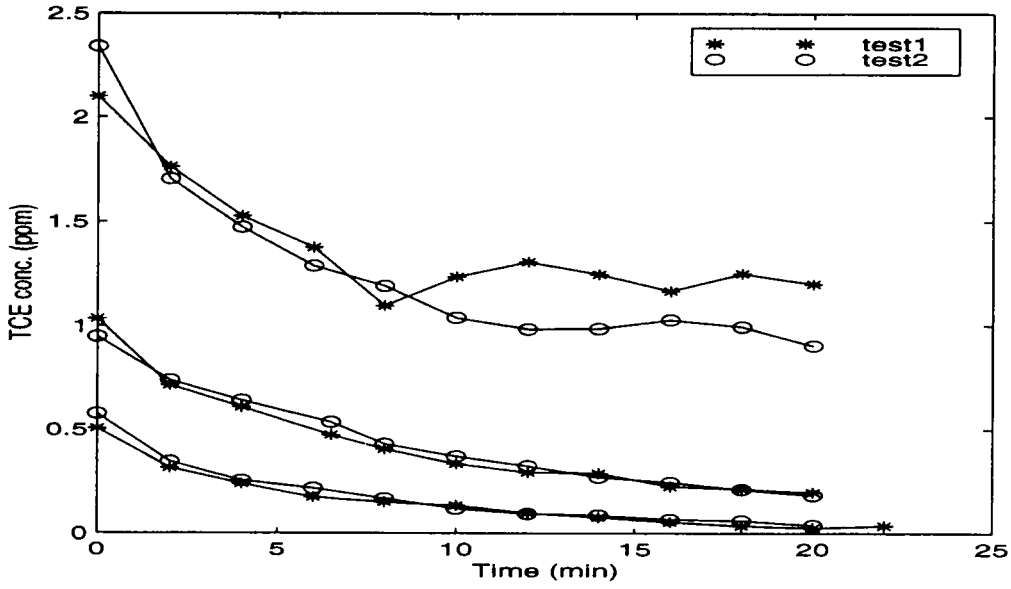



Figure 4.5: TCE Degradation by Resting Cell

TCE removal efficiency. Most of TCE was degraded within ten minutes, and the reaction rate decreased with time. TCE can not be removed completely due to lack of active enzyme system. There is a transformation limit for resting cells. As for the biofilm reactor system, an enzyme recover phase is necessary to regenerate new active enzyme[21][60].

## 4.5 Experimental Verification of TCE Toxicity

The finite TCE transformation limit is also called transformation capacity $T_c$. It is defined as amount of TCE has been transformed per amount of resting cell.

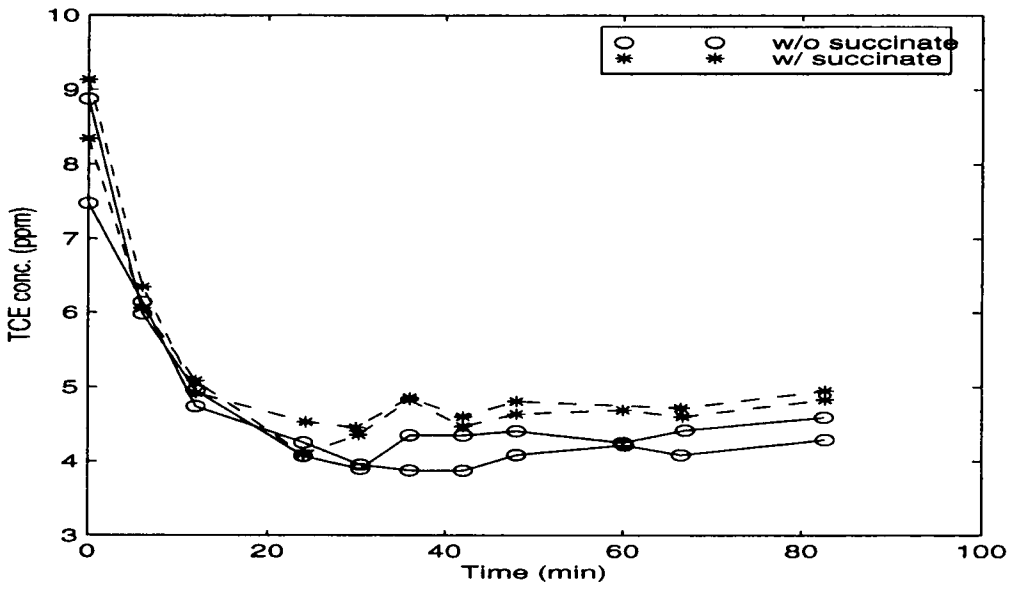



Figure 4.6: TCE Degradation with and without Adding Succinate

In order to prove that a transformation limit is caused by toxic effect of TCE degradation but not by insufficient of energy source or NADH, an experiment was conducted by comparing TCE degradation with and without adding sodium succinate which is a carbon and energy source for the growth of cell. The initial sodium succinate concentration was 50 mg/L, and initial TCE concentration was about 10 mg/L. The results plotted in Figure 4.6 show that TCE degradation was not improved by addition of sodium succinate. The source of finite TCE transformation is TCE related toxicity. If cells have already been toxified, they are still alive. However, they are incapable of TCE degradation. Figure 4.7 illustrates TCE degradation as a result of toxicity. Initial TCE concentration was

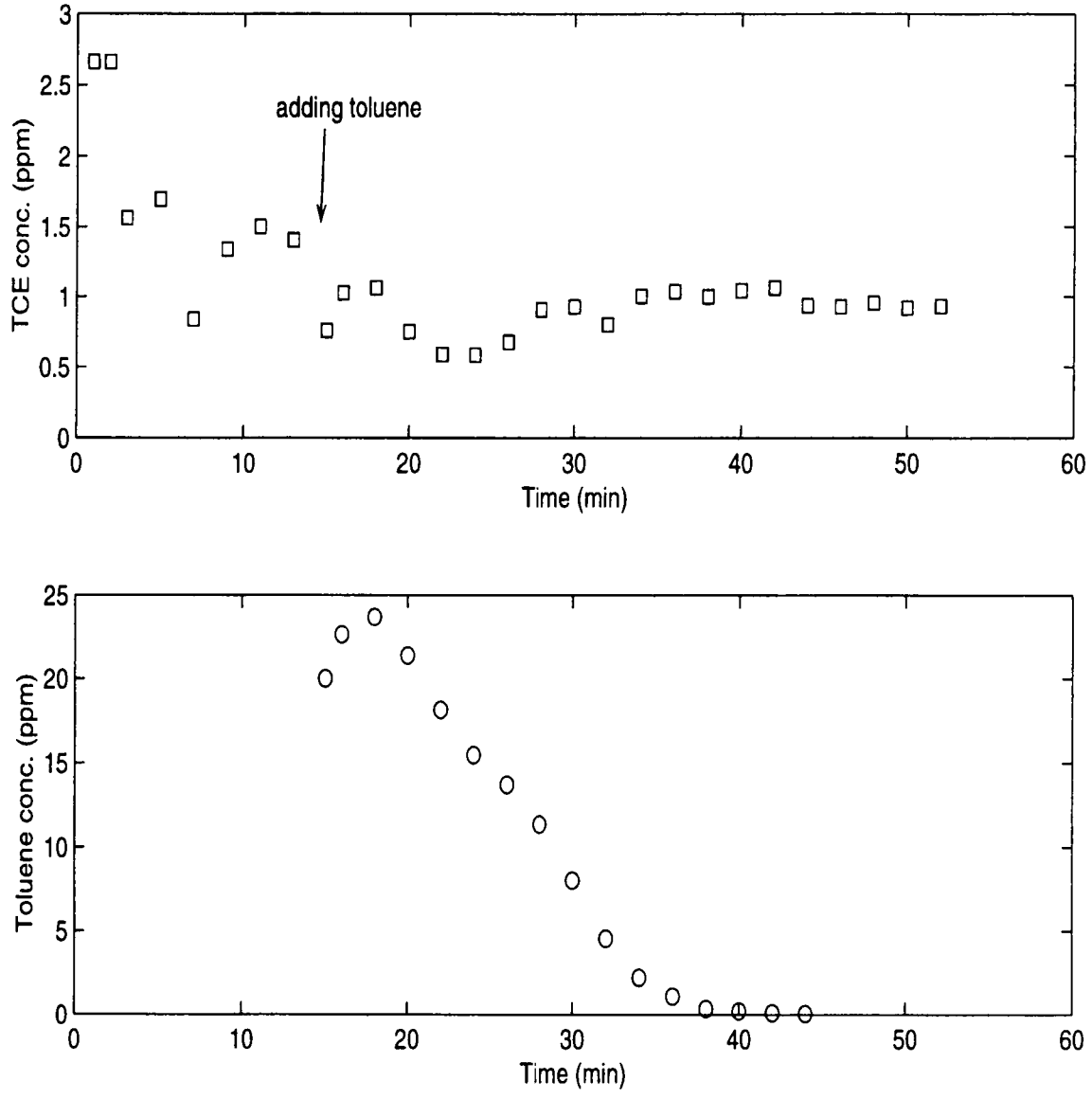



Figure 4.7: TCE Degradation under the Influence of Toluene. Top Figure: TCE Concentration Changes with Time; Bottom Figure: Toluene Concentration Changes with Time

2.66 ppm in the vial. TCE concentration dropped quickly in the first 10 minutes. Toxicity decreased reaction rate. In attempt to recover TCE oxidation activity, toluene was introduced in 15 minutes, which brought toluene concentration to about 20 ppm at this point. Toluene could still be removed, but no significant TCE degradation happened. This shows the fact that small amount of toluene in a short period can not make cell regain TCE degradation activity. Shimomura et al (1997)[63] also reported this result from their TCE degradation in a fluidized-bed bioreactor.

# Chapter 5

# Toluene and TCE Degradation Kinetics

General competitive enzyme reaction model[4] was employed for the cometabolism of TCE and toluene. The rate of toluene or TCE degradation is then given by the following expression:

$$-\frac{dC_i}{dt} = \frac{k_i X C_i}{C_i + K_i(1 + \frac{C_j}{K_j})} \tag{5.1}$$

where $i, j = 1, 2$, if $i = 1$, then $j = 2$, and $i = 2$, $j = 1$; $X$ is the cell concentration; $C_i$, and $C_j$ are concentrations of toluene or TCE, respectively; $K_i$, $K_j$ are substrate saturation constants; $k_i$, $k_j$ are rate constants of toluene or TCE. In batch condition, toluene and TCE participate in both gas phase and liquid phase. In this case, all concentrations in the right hand side of Equation 5.1 stand for

concentrations in the liquid phase. With rigorous shaking, no mass transfer resistance is assumed. Correction in the left hand side of Equation 5.1 should be made by multiplying a factor of $1 + H_i V^g / V^l$ to account for substances partitioned in the vapor phase. $H_i$ is Henry's law constant. $V^g$ and $V^l$ are the gas phase volume and liquid phase volume. Biomass growth is corrected by growth on toluene and toxicity of TCE:

$$\frac{dX}{dt} = Y(-\frac{dC_1}{dt}) - \frac{1}{T_c}(-\frac{dC_2}{dt}) - b_d X \tag{5.2}$$

where $Y$ is the yield coefficient (mg cell/mg toluene), $T_c$ is the transformation capacity of TCE (mg TCE/mg cell), and $b_d$ is the cell decay rate (1/day), $C_1$ is toluene concentration (mg/L), $C_2$ is TCE concentration (mg/L) in the solution. This model also predicts TCE degradation in the absence of toluene. In this situation, the net rate of cell growth is negative. TCE degradation stops when cells are completely inactivated.

## 5.1 Determination of Yield Coefficient $Y$

Yield coefficient of toluene was measured by batch experiment. The definition is given by:

$$Y = \frac{\Delta X}{\Delta C_1} \tag{5.3}$$

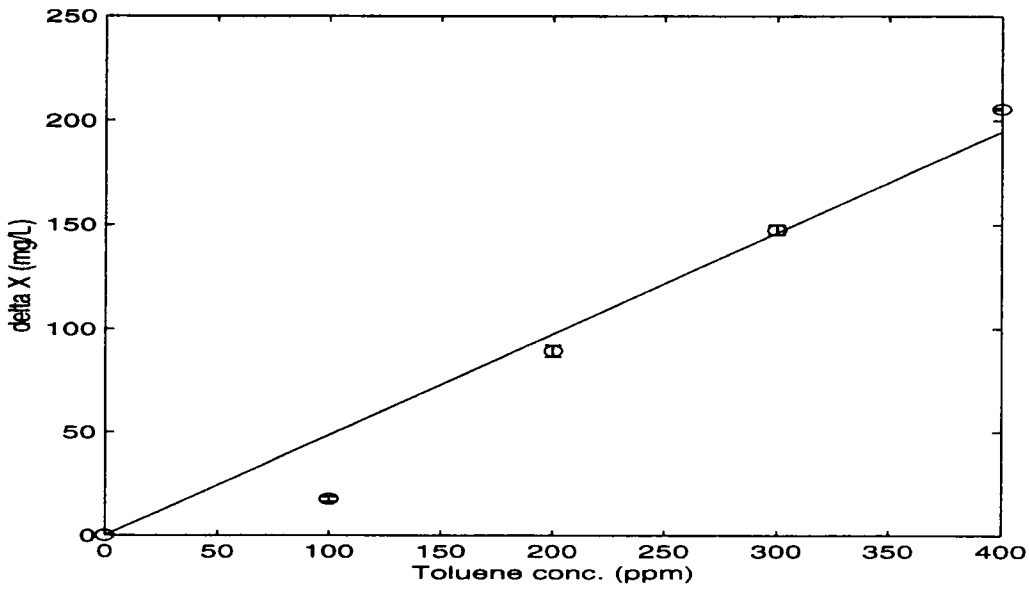



Figure 5.1: Determination of Yield Coefficient of Toluene

By setting a series of different initial toluene concentrations in the vials, shaking until all toluene was consumed, and measuring the final increase of biomass, a straight line can be obtained in Figure 5.1, where the slope is toluene yield coefficient. The value is 0.4872 mg dried cell/mg toluene.

## 5.2 Determination of $K_1$ and $k_1$ for Toluene

Equation 5.1 is simplified to Michaelis-Menten kinetics for a single compound toluene degradation. Constant toluene degradation rate when toluene concentration was large (Figure 5.2) indicates that in this range where $C_1 >> K_1$, the

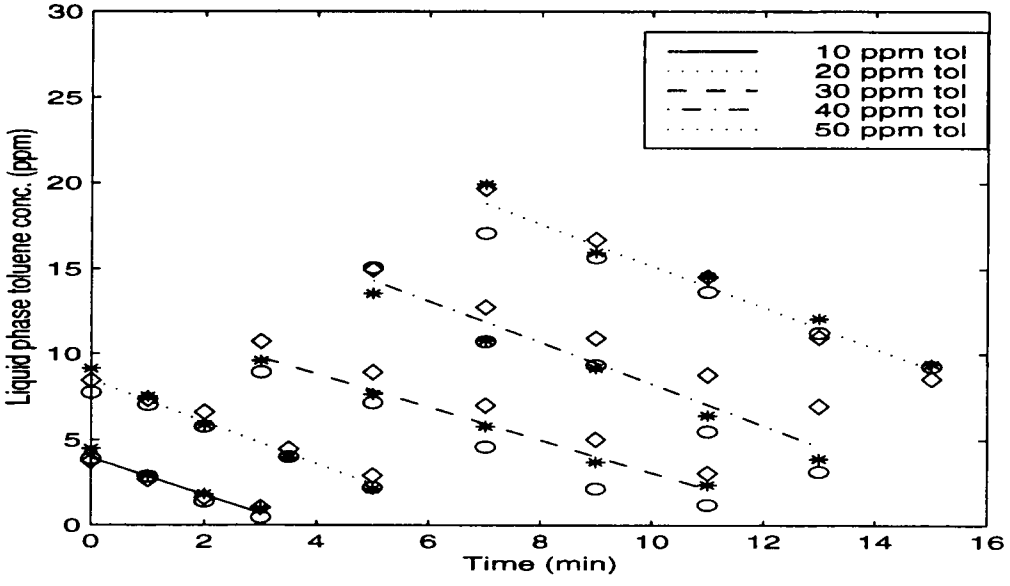



Figure 5.2: Determination of $k_1$ at Different Initial Toluene Concentrations (Symbols are the experimental data: '$\diamond$'=test1, '$o$'=test2, '$*$'=test3.)

kinetics follows zero order reaction. In a short time comparing with the doubling time of *Pseudomonas putida* F1, biomass was assumed to be constant. Thus the plot of toluene concentration vs time in that range is a straight line (Figure 5.2). The slope divided by cell mass and gas phase partition correction factor is the rate constant of toluene. The estimated value is: $k_1 = 8.4385 \pm 0.8640$ (mg toluene/mg cell/day). When toluene concentration is small, the integrated Michaelis-Menten equation form is used:

$$\frac{k_1 X}{(1 + H_1 V^g / V^l)}(t - t_0) - (C_{10} - C_1) = K_1 ln \frac{C_{10}}{C_1} \tag{5.4}$$

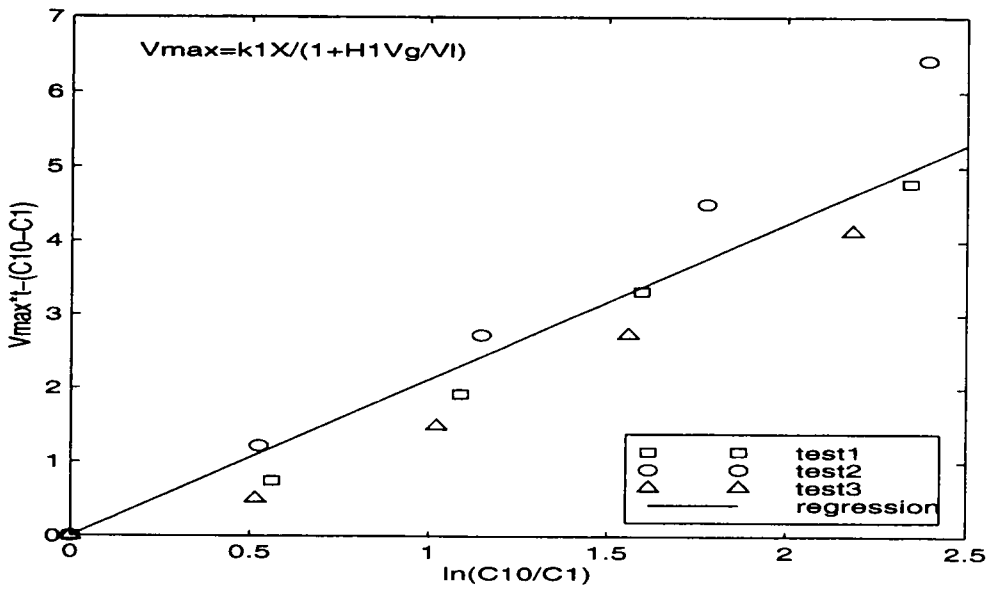



Figure 5.3: $K_1$ Evaluation at 20 ppm Initial Toluene Concentration

where $t$ refers to time and $C_1$ refers to liquid phase toluene concentration. Subscript zero is the time for concentration starting to integrate. By plotting left hand side over right hand side of Equation 5.4, the substrate saturation constant of toluene is evaluated. A sample plotting is shown in Figure 5.3. The data were selected from toluene degradation at 20 ppm initial concentration. $K_1$ estimated from other concentrations are listed in Table 5.1. The average value is: $K_1 = 1.1060 \pm 0.6465$ (mg/L). Comparing to $k_1$, $K_1$ value is more scattered.

Table 5.1: Estimated $K_1$ at Different Initial Toluene Concentration

| Toluene Concentration (ppm) | 10 | 20 | 30 | 40 | 50 |
|---|---|---|---|---|---|
| $K_1$ (mg/L) | 0.6588 | 2.1194 | 0.6733 | 1.3917 | 0.6867 |

## 5.3 Determination of $K_2$ and $k_2$ for TCE

In the absence of toluene, TCE degradation also follows single compound enzyme kinetics. Different from toluene degradation, active cell mass will change with time because of the toxic effect of TCE degradation product. This brings more non-linearity in Equation 5.1 in the estimation of kinetic parameters of TCE degradation. Therefore, initial rate method was used to avoid toxicity affection. All cells were assumed to be active in the beginning. By setting initial TCE concentrations at 0.2 ppm, 0.5 ppm, 1 ppm, 1.5 ppm, and 2 ppm, respectively, and measuring the TCE concentration changing with time, a plot of the inverse of initial reaction rate vs the inverse of initial TCE concentration should result in a straight line (Figure 5.4):

$$\frac{1}{-cons\frac{dC_2}{dt}} = \frac{K_2}{k_2 X}\frac{1}{C_2} + \frac{1}{k_2 X} \tag{5.5}$$

where *cons* is the correction factor for TCE partitioning between gas phase and liquid phase. With the known initial cell mass, rate constant was determined from the intercept, and saturation parameter was calculated from the slope. The

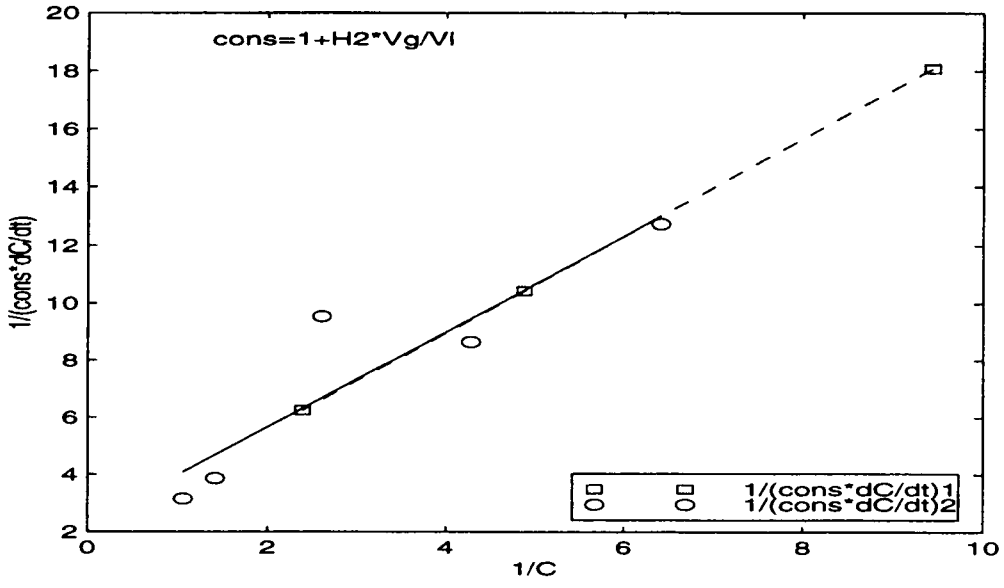



Figure 5.4: Determination of $K_2$ and $k_2$ of TCE

values are: $k_2 = 1.5783 \pm 0.0457$ (mg TCE/mg cell/day), and $K_2 = 0.7330 \pm 0.0254$ (mg/L). Two different symbols in Figure 5.4 refer to two experimental data sets.

## 5.4 Determination of Transformation Capacity $T_c$

The inactivation of TCE degradation enzyme is not only caused by toxicity of TCE transformation product, but also by self-decay. That means enzyme which is induced by toluene will lose activity by time. Hence, resting cells at different physical conditions have different transformation capacity. This was proved by

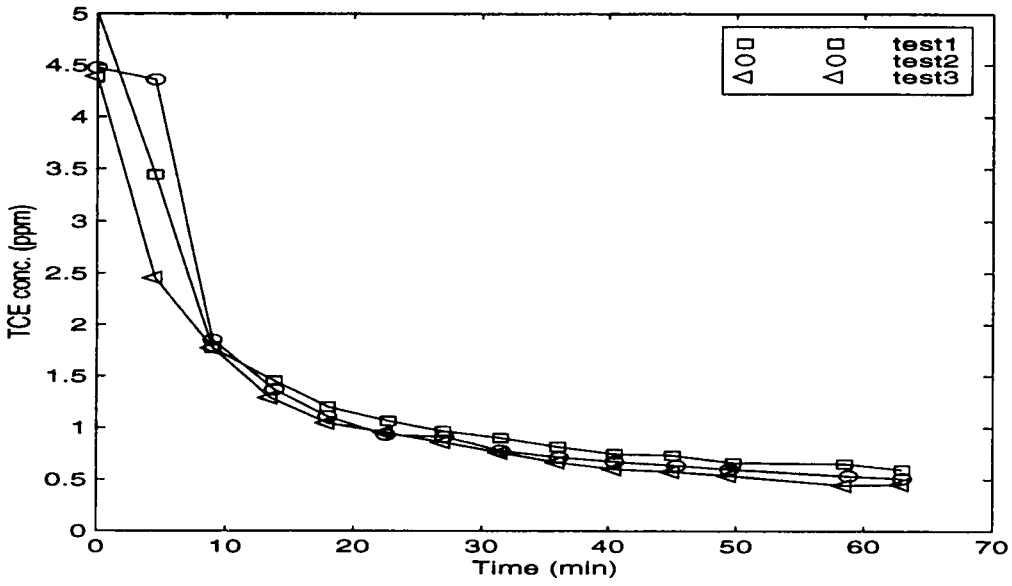



Figure 5.5: 5 ppm TCE Degradation

the following repeated injection of TCE to resting cells experiments. Initial TCE concentration were set at 0.5 ppm, 1.0 ppm, 1.5 ppm, 2 ppm, and 5 ppm. TCE concentrations in different vials were monitored at different time. Once TCE was undetectable, second time TCE injection was performed to reach to the original concentration. 5 ppm initial TCE couldn't be degraded completely (Figure 5.5), while 0.5 ppm initial TCE concentration vial was injected three times (Figure 5.6). Figure 5.6 shows that TCE degradation rate was significantly decreased after third injection. Enzyme was inactivated. This could be contributed from both toxicity and natural decay. Although TCE degradation lasted longer than 5 ppm initial TCE concentration whose degradation almost stopped at about 40 minutes,

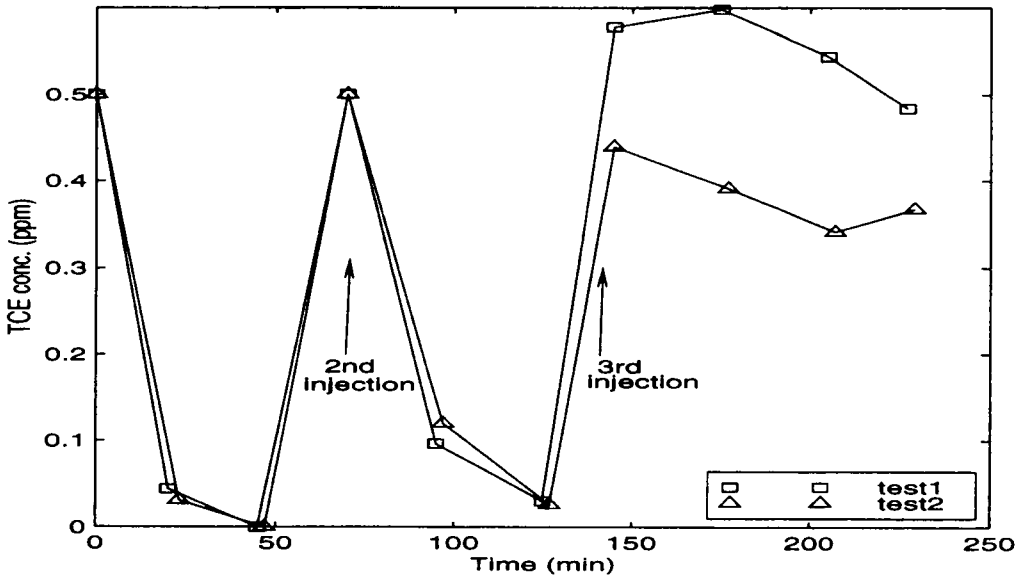



Figure 5.6: 0.5 ppm TCE Degradation by Repeating Injection

total amount of TCE had been transformed was much smaller than 5 ppm initial TCE concentration. This indicates that natural decay also plays a very important role in enzyme inactivation. Two injections were done for 1 ppm (Figure 5.7), 1.5 ppm, and 2 ppm (Figure 5.8) initial TCE concentration. In a short period of time, the lost of transformation activity mainly comes from toxicity. Transformation capacity was estimated from the repeating TCE injection experiments with initial TCE concentrations at 0.5 ppm, 1.0 ppm, 1.5 ppm, and 2.0 ppm:

$$T_c = \frac{\Delta C_2}{\Delta X} \tag{5.6}$$

The apparent values of $T_c$ in the repeating injection experiment for each different initial TCE concentrations are in Table 5.2. The average value was: $T_c = 0.0047$

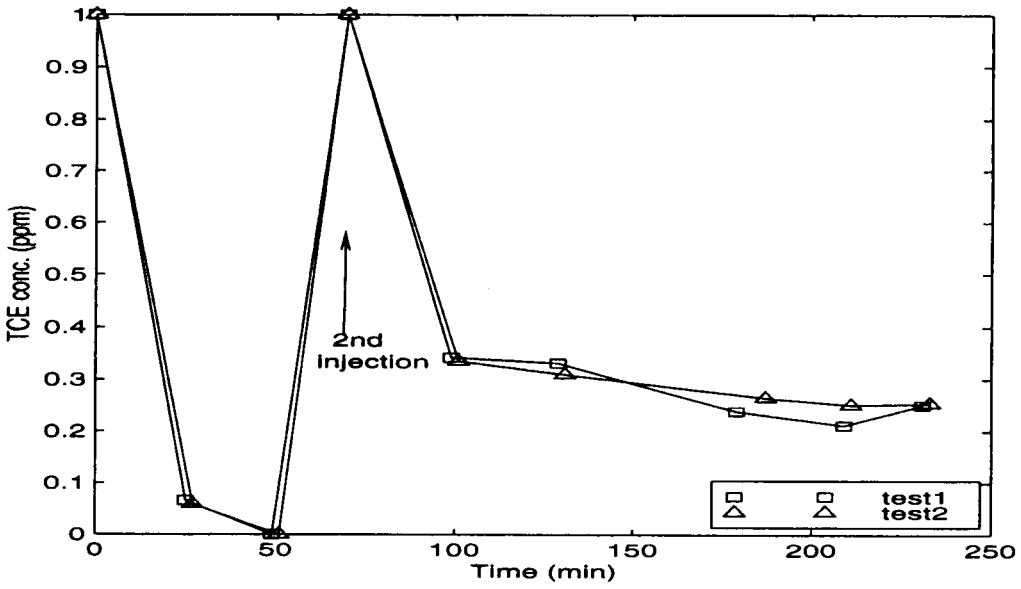



Figure 5.7: 1 ppm TCE Degradation by Repeating Injection

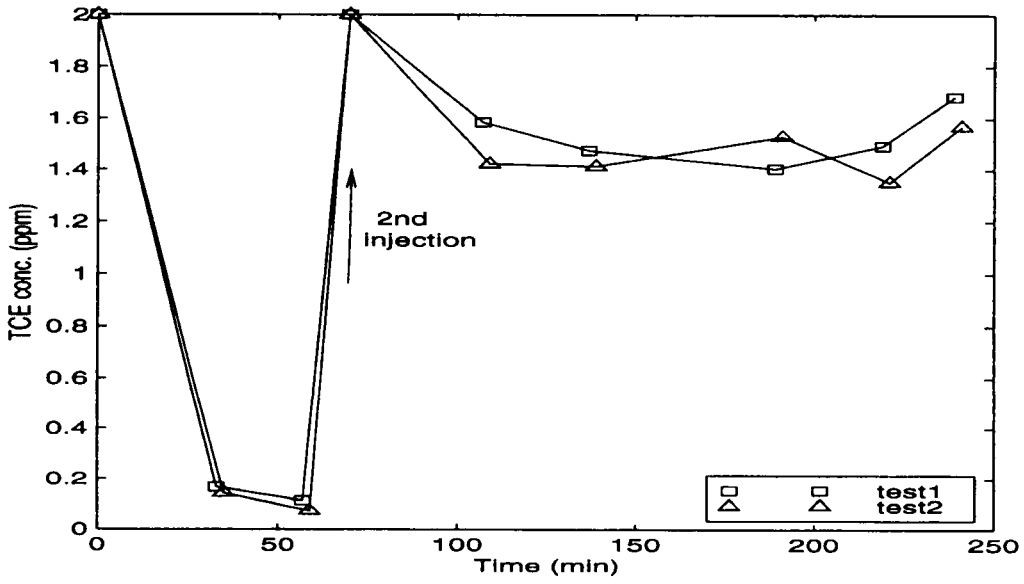



Figure 5.8: 2 ppm TCE Degradation by Repeating Injection

Table 5.2: Estimated $T_c^{app}$ at Different Initial TCE Concentration by Repeating Injection

| TCE Concentration (ppm) | 0.5 | 1.0 | 1.5 | 2.0 |
|---|---|---|---|---|
| Total TCE(mg) Transformed | 0.0071 | 0.00875 | 0.01065 | 0.01185 |
| Apparent $T_c$ (mg TCE/mg cell) | 0.00355 | 0.00438 | 0.00533 | 0.00593 |

(mg TCE/mg cell). The maximum value obtained in this study is 0.02 mg TCE/mg cell (Chapter 4, Section 4.5).

## 5.5 Parameters' Correction

Comparing with other people's work (H. Chang and L. Cohen, 1995)[14], two major differences are toluene reaction rate constant and TCE half-saturation parameter. The rate constant of toluene for *Pseudomonas putida* F1 is much greater than other toluene oxidizer[14], and TCE half-saturation parameter is smaller. Kinetic model calculations by using these fitting parameters showed that some disagreement of TCE degradation existed between experimental data (Figure 4.3) and calculation results. Because of the uncertainty in the estimation of $K_2$ and $k_2$ by using initial rate method, it seems that $K_2$ was underestimated and should be corrected. Divided Equation 5.1 yields the following form, where toluene is

set to 1 and TCE is set to 2:

$$\frac{dC_2}{dC_1} = \frac{k_2}{K_2}\frac{K_1}{k_1}\frac{1 + H_1\frac{Vg}{Vl}}{1 + H_2\frac{Vg}{Vl}}\frac{C_2}{C_1} \tag{5.7}$$

and integrating the above equation gives:

$$lnC_2 = AlnC_1 + ln\frac{C_{20}}{{C_{10}}^A} \tag{5.8}$$

where $A$ is a group coefficient defined in the right hand side of Equation 5.7, $C_{20}$ and $C_{10}$ are the initial TCE and toluene concentrations starting to integrate. This is the concentration constrain between TCE and toluene. If the model is good enough to describe cometabolism of TCE and toluene, then the plot of TCE concentration with toluene concentration in the log-log scale should end up with a straight line. Data from Figure 4.4 before toluene was consumed was reorganized in Figure 5.9. It is a linear relationship in the log-log plot. The slope is the coefficient $A$. The $A$ value from that experiment is 0.1157. Substituting $K_1$, $k_1$, and $k_2$ into the expression of $A$ equating to 0.1157, $K_2$ was re-estimated with a value of 1.524 mg/L. All parameters obtained here and some comparison values reported in literature are summarized in Table 5.3 and Table 5.4, respectively.

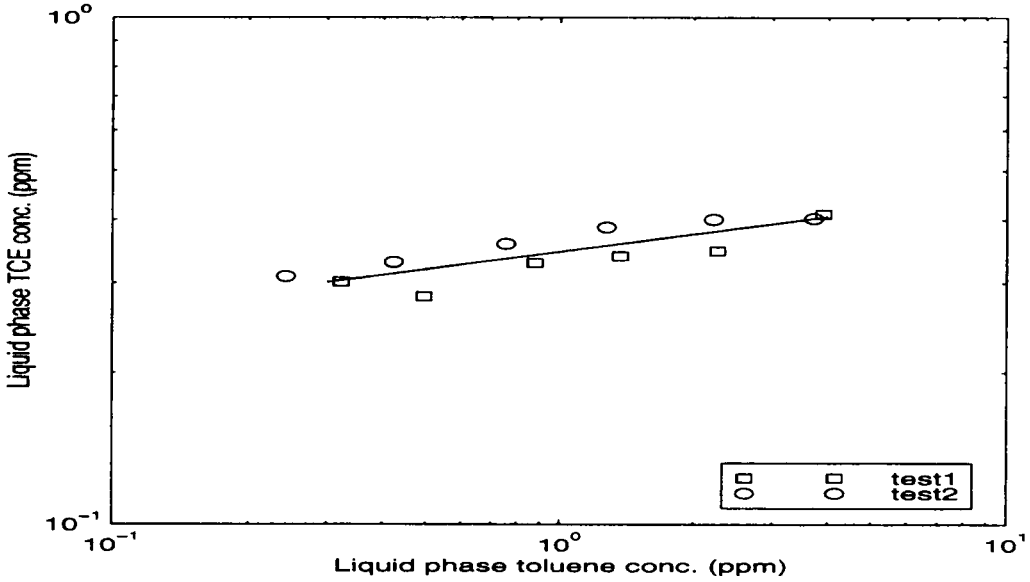



Figure 5.9: Relationship of TCE and Toluene Concentration

Table 5.3: Kinetic Parameters of Toluene and TCE Degradation

| Parameter | Estimated Value | Unit |
|---|---|---|
| $K_1$ | 1.1060±0.6465 | mg/L |
| $k_1$ | 8.4385±0.8640 | mg/mg/day |
| $K_2$ | 1.5240±0.0441 | mg/L |
| $k_2$ | 1.5783±0.0457 | mg/mg/day |
| $Y$ | 0.4872 | mg/mg |
| $T_c$ | 0.0047 | mg/mg |

Table 5.4: Values of Kinetic Parameters Reported in Literature (M.C. refers to mixture culture)

| Strain | $K_1$ (mg/L) | $k_1$ (mg/mg/L) | $K_2$ (mg/L) | $k_2$ (mg/mg/day) | Ref. |
|---|---|---|---|---|---|
| *P.* G4 (chemostat) | 2.3 | 9.27 | 0.79 | 0.95 | [32] |
| M.C. (batch) | 1.02 | 0.44 | 8.64 | 0.17 | [14] |
| M.C. (biofilm) | 0.027 | 1.53 | 0.097 | 0.377 | [3] |
| *P.* F1 (batch) | | | | 0.68 | [80] |
| *P.* F1 (biofilm) | 13.8 | 16.4 | | 0.0362 | [54] |
| *P.* F1 (batch) | 1.11 | 8.44 | 1.52 | 1.58 | this work |

## 5.6 Comparing of Model Calculation with Experimental Data

In batch system when cell decay term is much smaller than TCE toxic term, then $b$ term can be neglected, and Equation 5.2 is converted into following expression:

$$X = X_0 + Y(C_{10} - C_1) - \frac{1}{T_c}(C_{20} - C_2) \tag{5.9}$$

Combining with Equation 5.1, this system can be solved simultaneously. Finite difference method was used for integration. The code was written in Matlab syntax (Appendix D). Final model calculations are compared with the experimental data from both TCE and toluene cometabolism and TCE degradation by resting cell.

Figure 5.10 is toluene degradation curve with average initial concentrations of 17.4 ppm and 37 ppm. Scattered symbols are experimental data, and lines are model calculations. They match quite well. Toluene degradation rate kept constant until its total concentration in the vial below 10 ppm. The relationship of toluene reaction rate calculated from kinetic model and toluene concentration is plotted in Figure 5.11. It is a typical Monod type curve.

TCE transformation by resting cells with initial concentrations of 1 ppm, 4.7 ppm, and 10 ppm are shown in Figure 5.12. Good agreement was achieved for 1 ppm TCE degradation in the period of testing. TCE reaction rate in the experiments was found by taking the first derivative of TCE concentration with respect

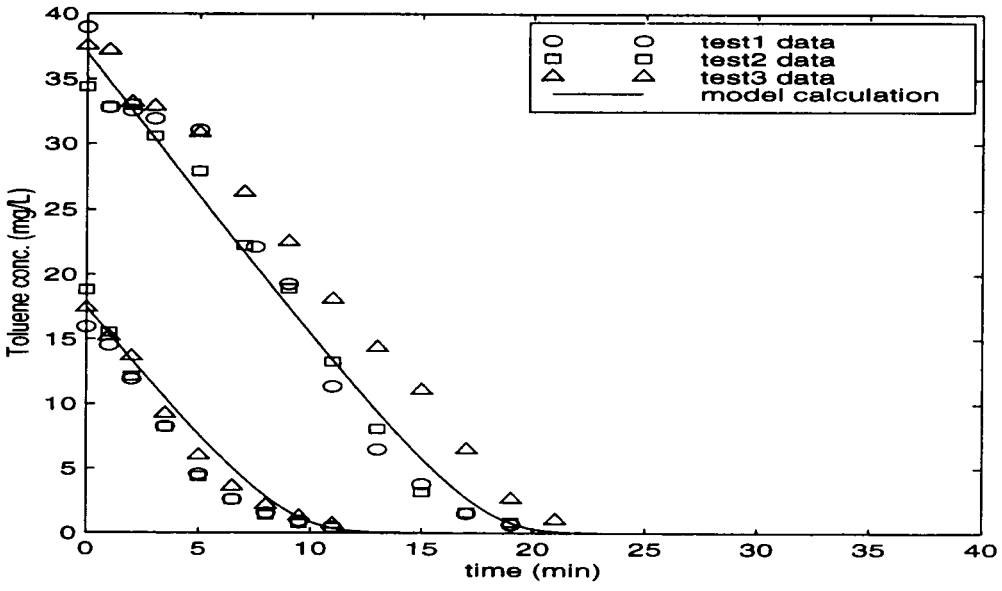



Figure 5.10: Comparison of Model Estimation with Experimental Data

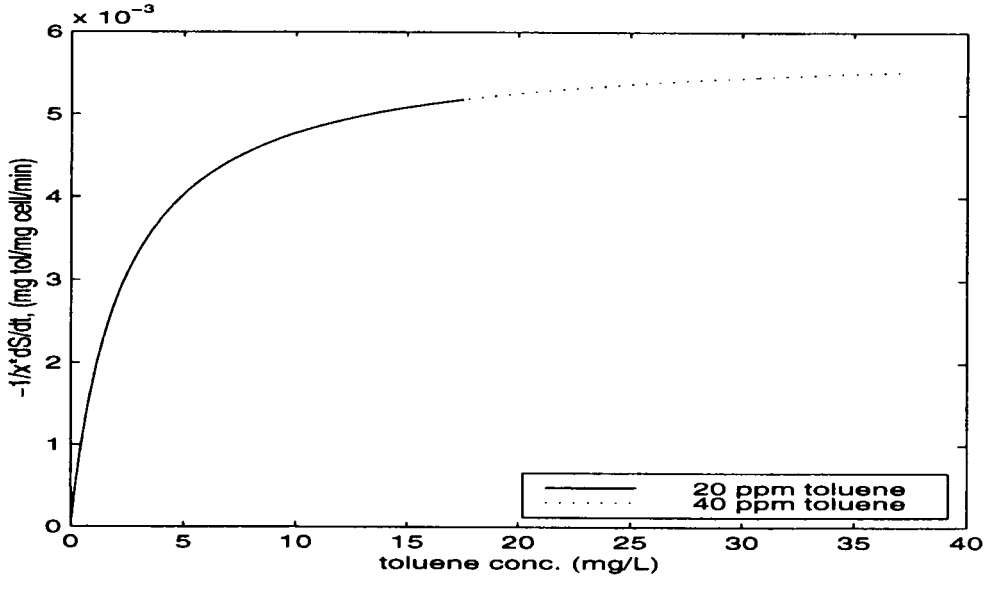



Figure 5.11: Model Calculations of Toluene Reaction Rates

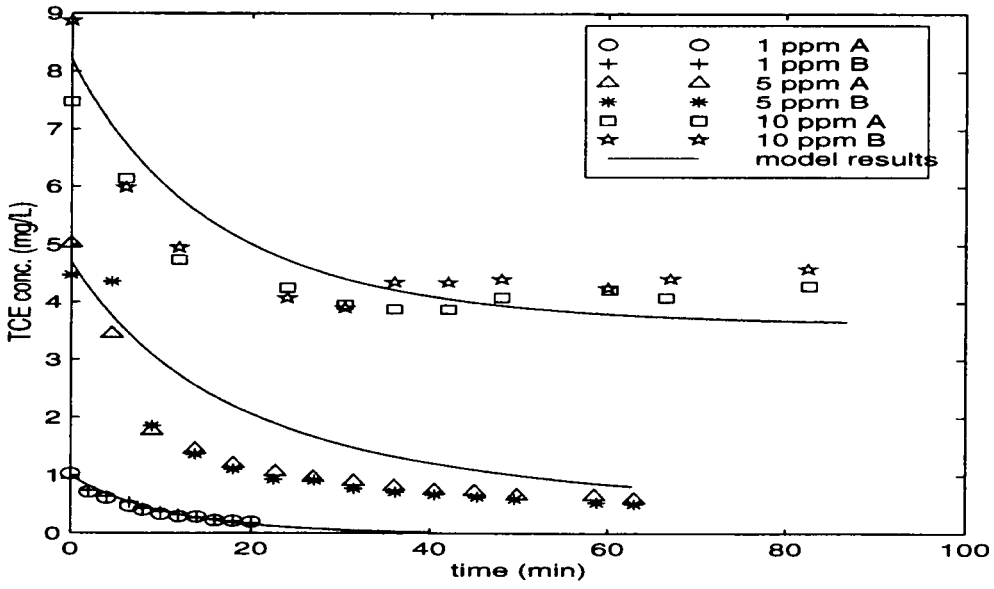



Figure 5.12: Comparison of Model Estimation with Experimental Data for TCE Degradation by Resting Cells

to time. This calculation was performed by using the data display and analysis software package, KaleidaGraph (Synergy Software). Unlike the toluene degradation rate which did not change as a function of time when toluene concentration was large (see Figure 5.2), the rate of TCE oxidation monotonically decreased with time (Figure 5.13 and Figure 5.14). Two reasons cause this effect: one is the decreasing of TCE concentration, the other is the toxicity of TCE transformation product to the cells. Although O.D was almost constant in the time of interest, the amount of active cell decreased. Active cell mass was calculated by the model. The higher was TCE concentration,the faster active cell mass dropped. In about

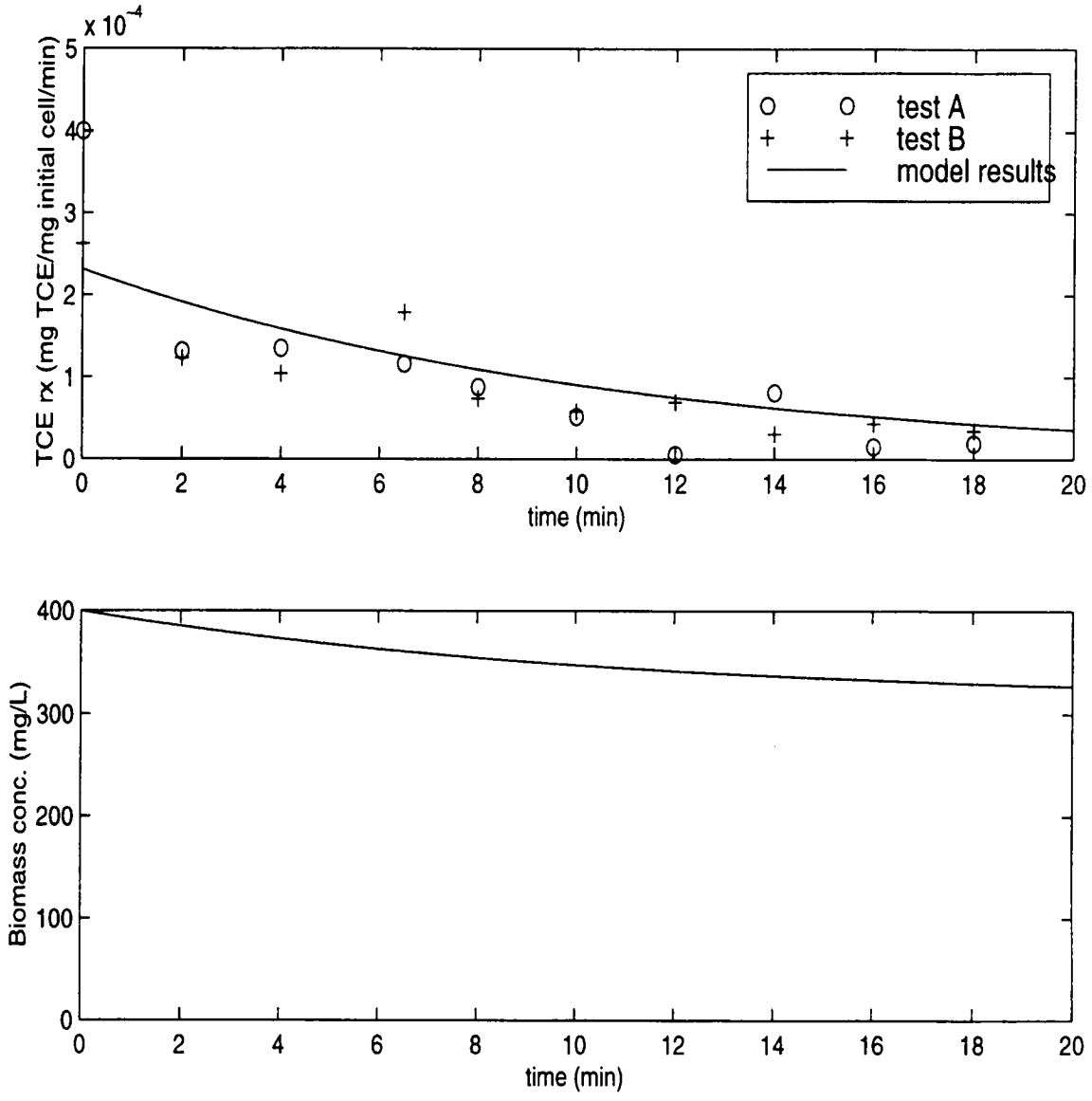



Figure 5.13: TCE Reaction Rate and Active Biomass Change with Time (1 ppm TCE)

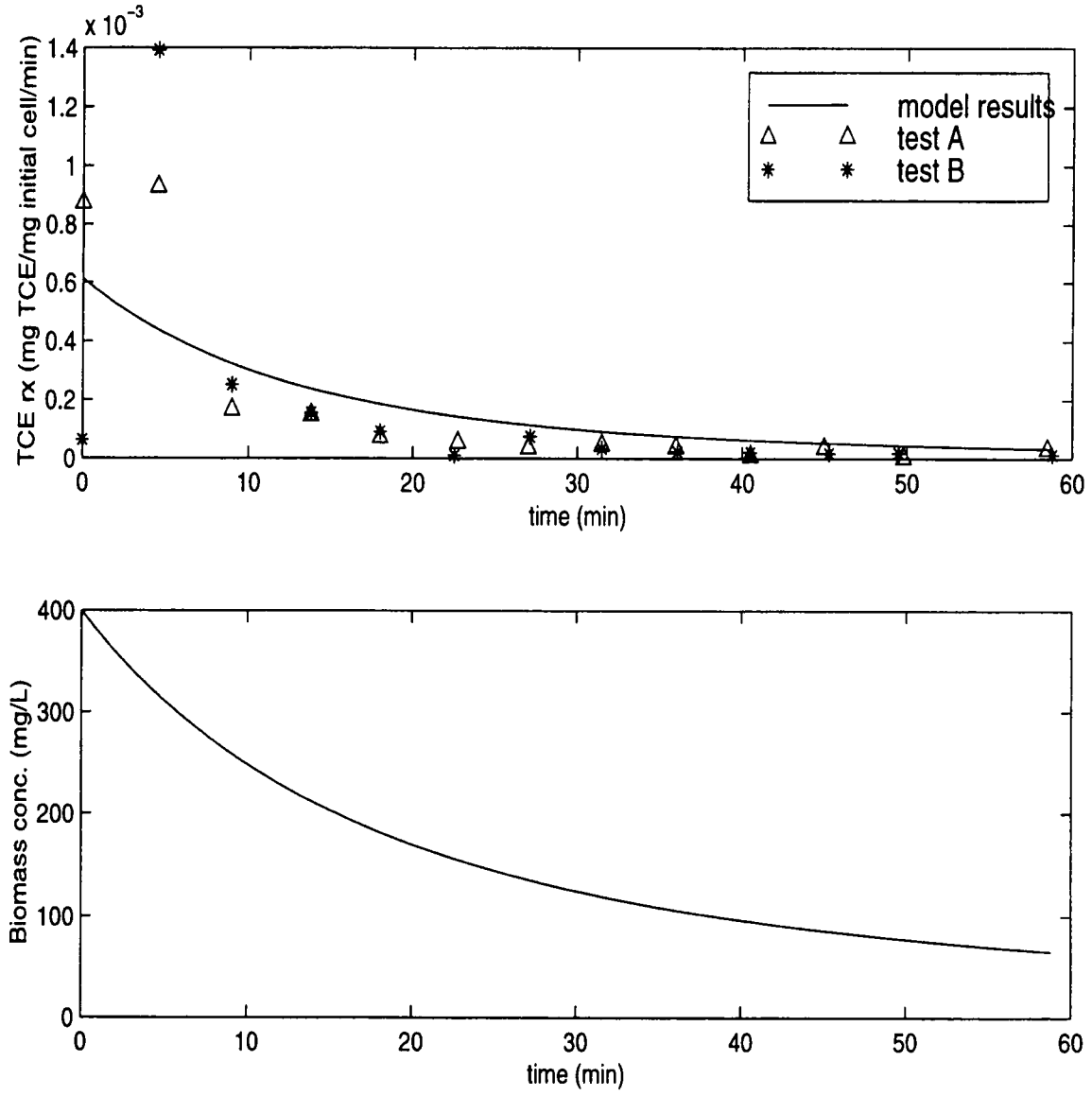



Figure 5.14: TCE Reaction Rate and Active Biomass Change with Time (4.7 ppm TCE)

20 minutes, about 17.5% cell was inactivated for 1 ppm TCE, while 59% cell was inactivated for 5 ppm TCE.

Three ranges can be classified in the cometabolism system (Figure 5.15): inhibition range when toluene concentration is high and TCE degradation is inhibited; fast degradation range where toluene concentration was under 10 ppm with volume ratio of gas phase to liquid phase 4 and most of TCE is removed ; decay range in which enzyme decays due to TCE transformation product toxicity and enzyme natural decay, TCE degradation rate decreases. TCE degradation rate has a maximum value at a certain time (Figure 5.16). Toluene degradation rate was much faster than TCE degradation rate. Concentration profile and reaction rate for average initial 8 ppm toluene and 1 ppm TCE were also shown in Figure 5.17 and Figure 5.18. From the fact that although cells were unable to further degrade TCE because of TCE toxic effect, they still had the ability to use toluene if TCE concentration was not high enough to kill the cells, cell mass for toluene and TCE degradation in Equation 5.1 should be different. The following expression could be used for quantifying toluene degradation biomass:

$$X = X_0 + Y(C_{10} - C_1) \tag{5.10}$$

While biomass from Equation 5.9 is the active cell participating in TCE degradation. Under this batch conditions of TCE and toluene cometabolism, calculation results from both kinetics before and after modification were very close, because

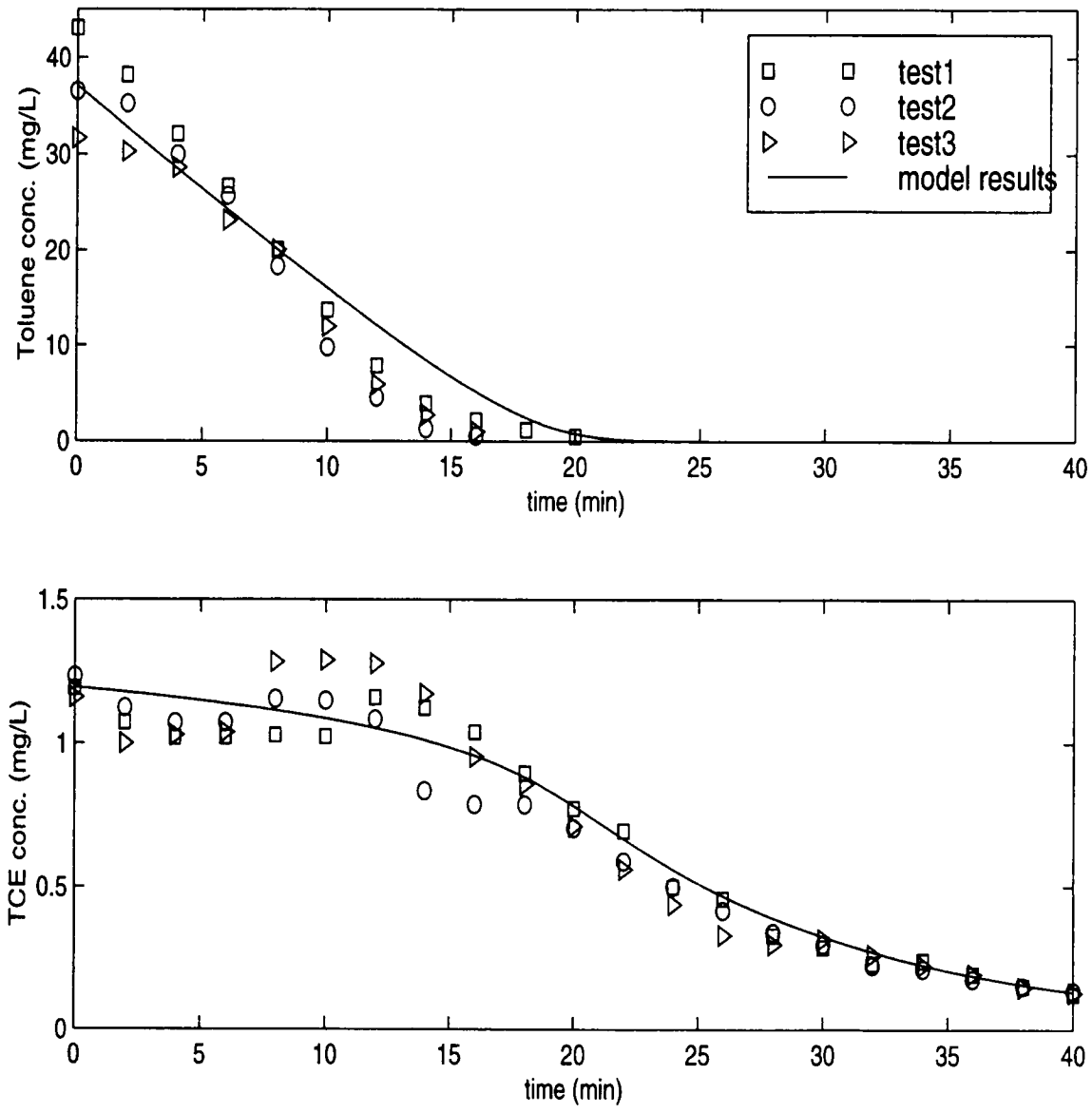



Figure 5.15: Comparison of Model Estimation with Experimental Data (40 ppm toluene and 1 ppm TCE). Top Figure: Toluene Concentration Changes with Time; Bottom Figure: TCE Concentration Changes with Time.

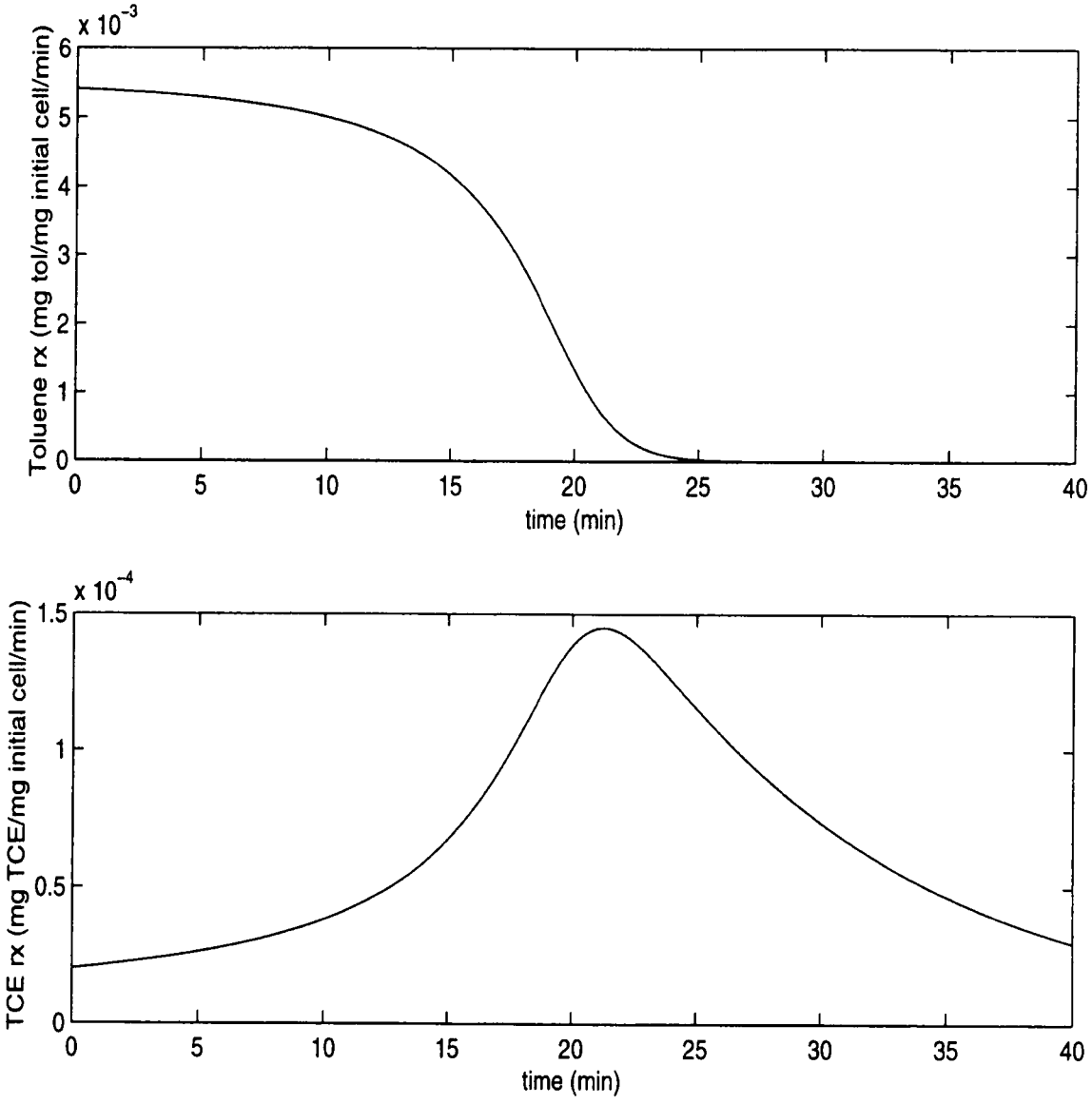



Figure 5.16: Calculation Results of Toluene and TCE Reaction Rates Changing with Time (40 ppm toluene and 1 ppm TCE)

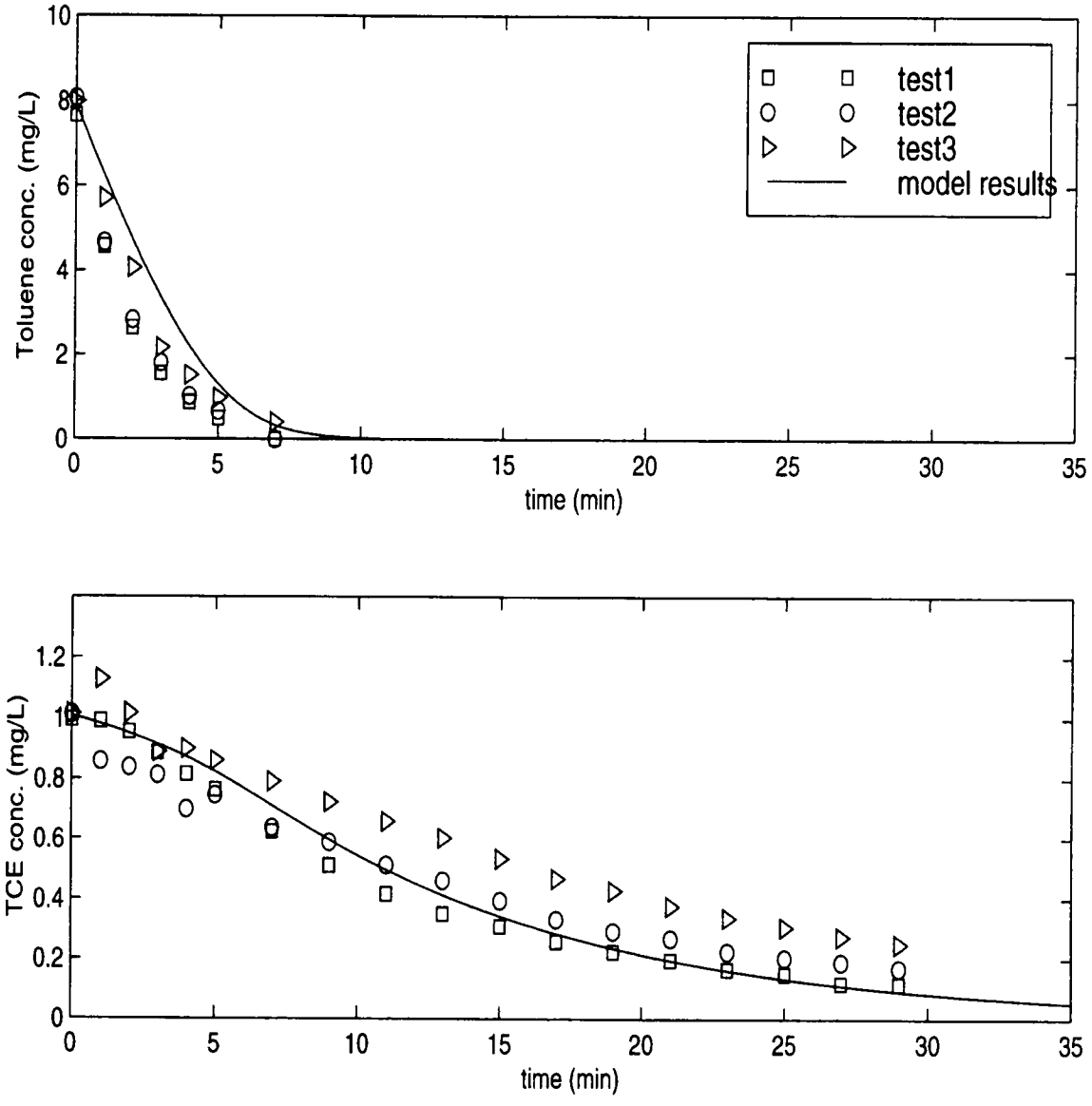



Figure 5.17: Comparison of Model Estimation with Experimental Data (8 ppm toluene and 1 ppm TCE). Top Figure: Toluene Concentration Changes with Time; Bottom Figure: TCE Concentration Changes with Time.

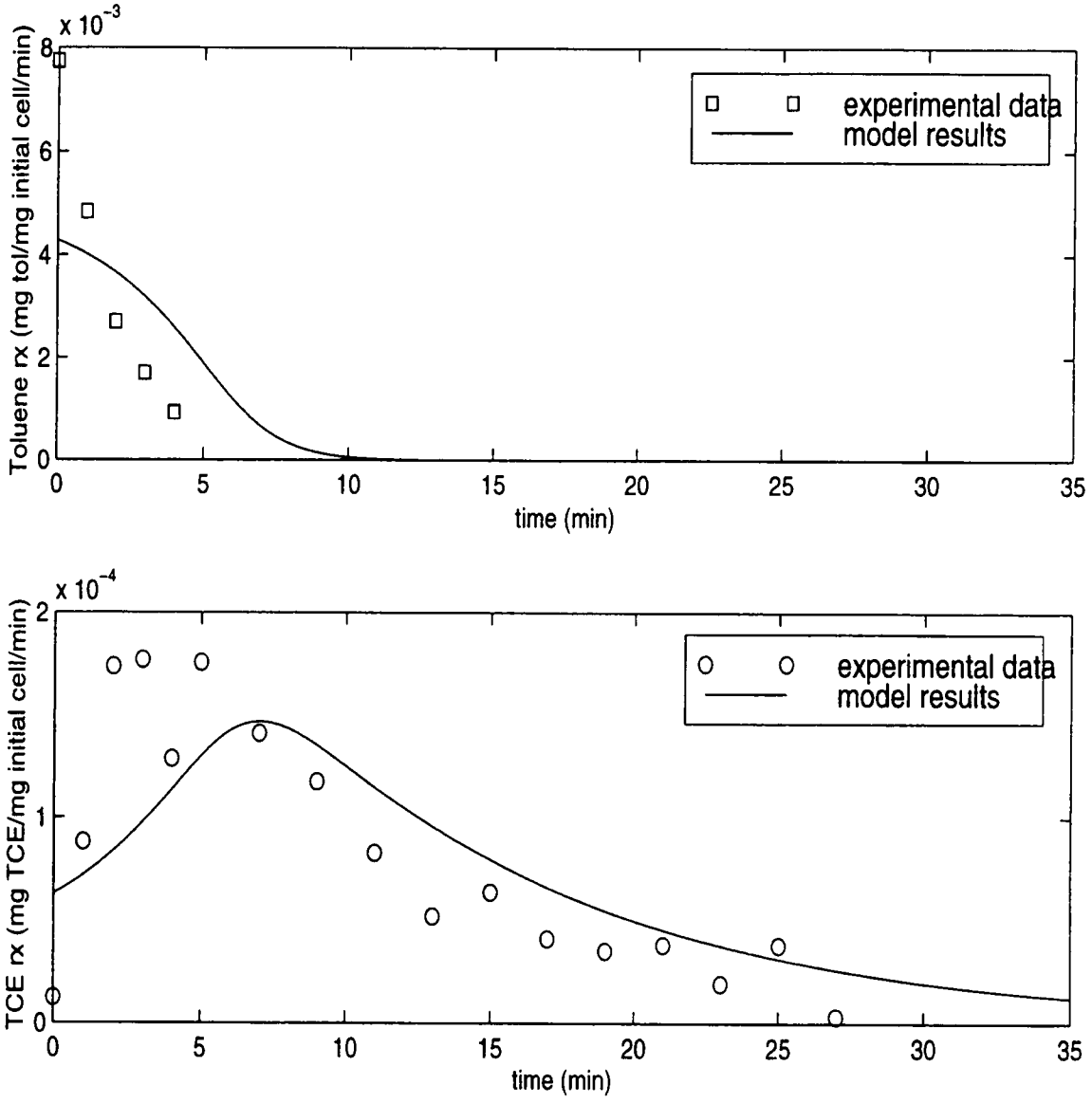



Figure 5.18: Toluene and TCE Reaction Rate Changes with Time (8 ppm toluene and 1 ppm TCE)

the initial cell concentration was high, and TCE concentration was not high enough to cause a large mount loss of active cells in the presence of toluene.

# Chapter 6

# Bioreactor System Development

Numerous bioreactor systems have been studied for continuous biotransformation of chlorinated organic compounds. There are mainly two kinds of reactor systems: one is a suspended cell system with the growth phase and degradation phase spatially separated. They include two-stage[1][13] bioreactors or multi-stage[73] bioreactors. Because of the elimination of competitive inhibition by primary substrate, TCE was degraded successfully. The other is a biofilm reactor in which cells are immobilized either on the surface of packing material[21] or in gel beads[63]. They are operated in sequence to avoid competitive inhibition, in the process where growth and degradation are separated by time. Thus two periods are required alternatively: one for the growth of biomass and inducement of enzyme, the other for the oxidation of chlorinated compounds in the absence

of growth substrate. High degradation rate and removal efficiency were achieved at the beginning due to high biomass concentration in the biofilm. However, product toxicity made the removal efficiency decrease gradually and sometimes caused reactor shutdown[63]. This is an unsteady operation. Oxygen as the final electron acceptor is very important in the entire biochemical reaction. Sufficient oxygen has to be supplied to satisfy oxidization reaction. Air directly pumped into the reactor caused a stripping problem[70], as many chlorinated compounds are volatile organics. A packed bed, developed by Strand et al[69], with biomass growth on glass beads was operated in a submerged mode, where recycled oxygen was directly pumped into the reactor. The report has found that the biomass didn't attached very well[53]. This kind of reactor operation may be subjected to loss of biomass as a result of high shear stress. To take advantage of the biofilm reactor as well as to minimize competitive inhibition, toxicity, and oxygen limitation, an effective biofilm reactor system was developed for TCE treatment by *Pseudomonas putida* F1.

## 6.1 Bioreactor System

A 2.5 cm in diameter, 60 cm long glass chromatography column with PTFE end fittings (Kontes, Inc.) was used for the column experiments. 4 mm diameter glass beads were packed in the column, which provided the physical support for the

growth of the biofilm. The operating system diagram is shown in Figure 6.1. All valves, tubings, and fittings are PTFE or stainless steel to prevent the loss of TCE. A ceramic piston pump (model Q, Fluid Metering, Inc.) pumped the minimum salt buffer in the feed reservoir to the reactor through a line where it mixed with TCE and toluene saturated water coming from two different high pressure pumps (Model 222C HPLC Pump, Scientific System, Inc., for toluene supply; ISCO Model 384 High Pressure Pump, Instrumentation Specialties Co., for TCE supply), forming the influent stream. Liquid flowed down in the reactor. Some of the effluent was pumped back to the reactor by another ceramic piston pump (model QD, Fluid Metering, Inc.) through blending with an influent aqueous line. The recycled effluent diluted the influent solution. Not only did the toluene concentration to the reactor fall well below inhibition level, but TCE was also diluted, which consequently lowered the toxic effect. Thus, the whole reactor ran under no competitive inhibition. The reactor was operated in a trickling manner, where oxygen was introduced into the column whenever needed in a very small amount. Oxygen was supplied by an oxygen tank. Gas flowed concurrently with the liquid stream from the top to the bottom of the reactor. Due to the direct contact of gas with liquid phase, oxygen could be transferred to the liquid phase continuously. Oxygen limitation for both toluene and TCE oxidation was avoided. As for the flow of the liquid, some gas went out together with the liquid, causing

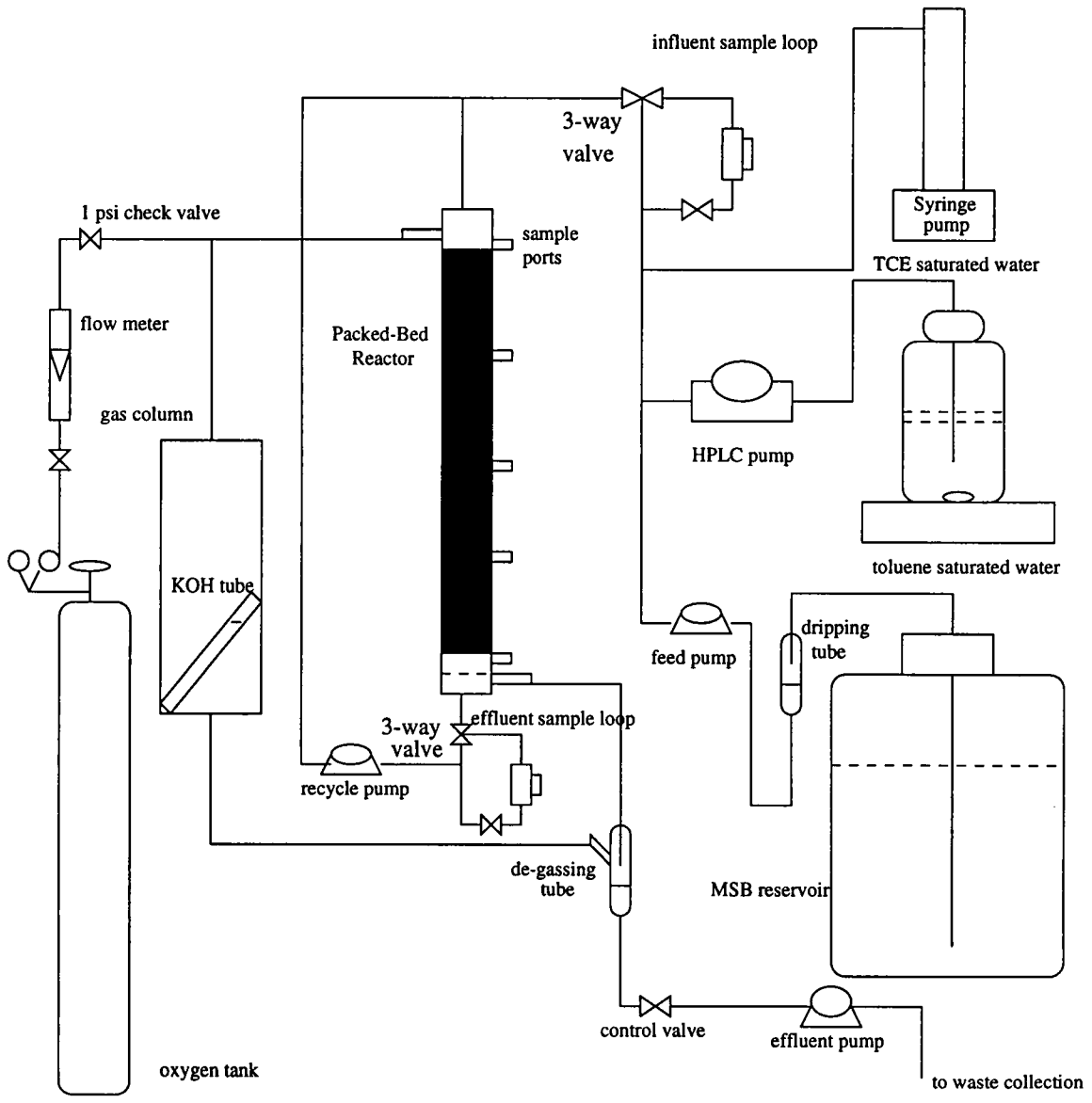



Figure 6.1: Reactor System Schematic

some degree of vacuum at the top part of the reactor. A de-gassing tube was used for the separation of gas-liquid mixture. Upon the separation of gas from liquid, gas was recycled back to the reactor automatically through a gas storage column (290 ml volume) (originally it was thought to store oxygen by daily replenishment). This operation approach also served a good attachment of biomass to the surface of packing material. An 8 ml 10 N KOH solution was placed in the gas storage column for catching $CO_2$ from bio-oxidation. This solution was replaced every three to five days. Influent and effluent aqueous samples were taken from sample ports for GC analysis. Gas phase samples could be taken from sample ports along the reactor. The liquid effluent was introduced into a waste collection carboy. A pump was used to keep the flow rate the same as that of the influent.

## 6.2 Abiotic Experiment

One of the bed properties can be examined by an abiotic toluene and TCE breakthrough experiment. A clean bed was used, and each item was sterilized by autoclaving or by a 70% ethanol solution. Total influent flow rate was set at 3 ml/min. The liquid recycle rate was about 27.5 ml/min. Influent toluene concentration was about 28 ppm, and influent TCE concentration was about 0.72 ppm. Effluent samples were taken continuously. TCE and toluene breakthrough curves are plotted in Figure 6.2. Both TCE and toluene came out from the

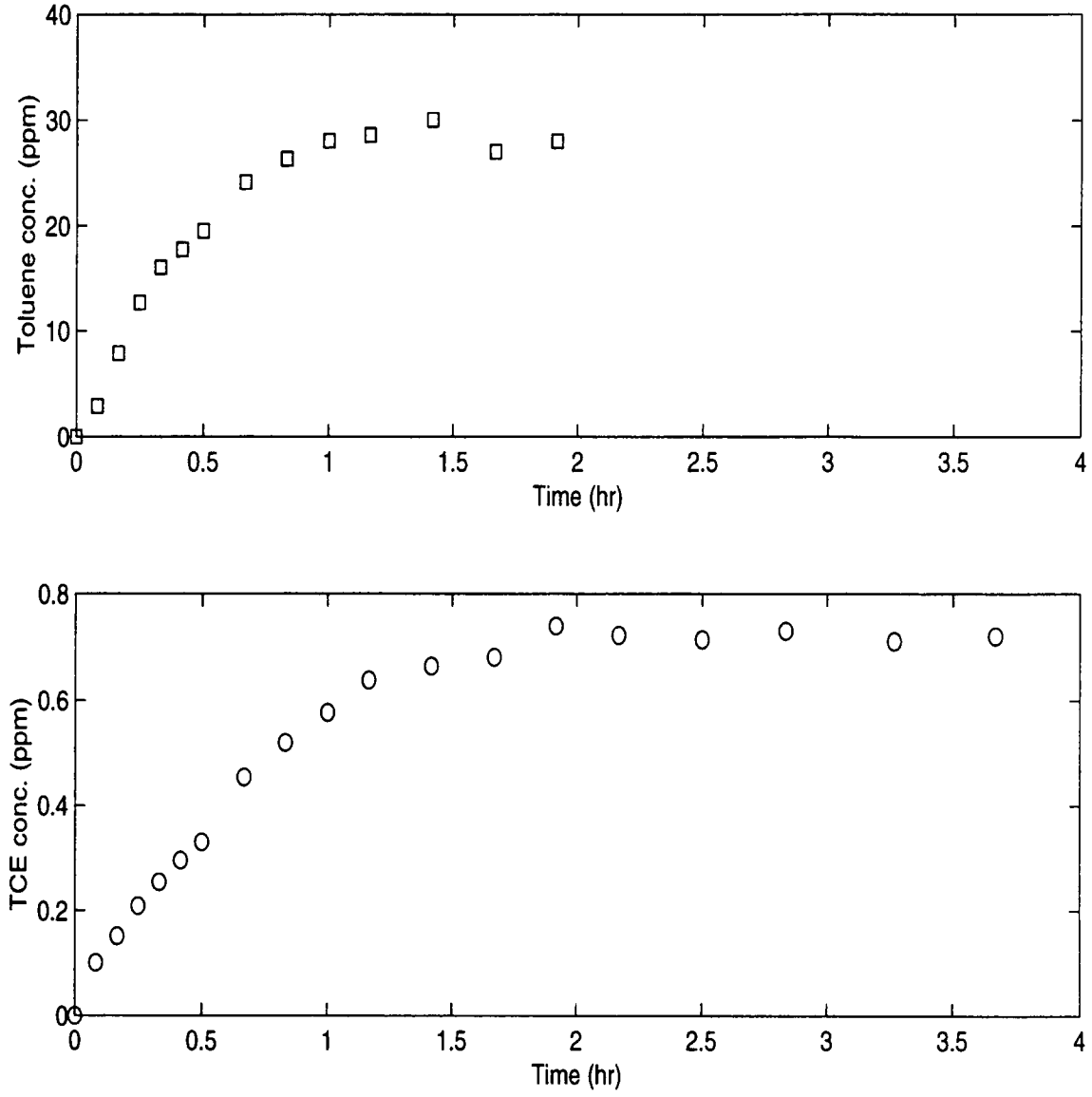



Figure 6.2: Abiotic Toluene and TCE Breakthrough Curve

column in 5 minutes. Because of the dilute effect of the reactor and gas storage column, effluents reached their influent values at 1 hour for toluene, and 1.66 hours for TCE.

## 6.3 Growth of Biofilm

The reactor was seeded with concentrated 20 ml of exponentially growing *Pseudomonas putida* F1 collected from a 250 ml flask after shaking incubation. The flow rate of feed from the media reservoir was set at 0.5 ml/min, while toluene saturated water was pumped at 0.2 ml/min, which made the influent toluene concentration of 147 ppm (loading rate at 0.1483 g/day) during the biofilm growth phase. TCE was not fed in this stage. Biomass was diluted at the beginning. Once it attached to the beads, it started to grow. In the first two days, recycle rate was kept at 14.5 ml/min. It was increased later to make less accumulation of cells on the top part of the reactor. Recycling enabled the cells to be relatively evenly distributed in the column, and also the high flow rate and dilution of the influent allowed toluene to reach the bottom part of the column. This made the growth of biofilm occur not only at the top part of the column, but also in the whole column, reducing the biomass gradient. Unlike in submerged operation, cells might be washed out after inoculation; the trickling bed offered a good condition for cell attachment. The growth of the cells could be observed

after 24 hours of inoculation, when a brown white color appeared. Effluent O.D. was monitored. No toluene was detected in the effluent. Because of the growth of bacteria, O.D. increased. But after it got to a steady state with detachment equilibrium with attachment and growth, O.D. remained almost unchanged. Biofilm was well formed in two weeks.

## 6.4 Measuring of Liquid Hold-up and Gas Recycle Rate

Bioreactor parameters such as liquid hold-up and gas recycle rate can be correlated by liquid flow rate in the reactor given by following power law expression[53]:

$$Parameter = \alpha(\frac{F_f}{A_r})^{\beta} \tag{6.1}$$

Where $A_r$ is the cross section area of the column ($cm^2$), $F_f$ is the liquid flow rate (ml/min), and $\alpha$ and $\beta$ are fitting coefficients. These coefficients were determined through experimental measurements with biofilm grown in the reactor.

### 6.4.1 Liquid Hold-up

Liquid hold-up is a function of both influent flow rate and recycle rate. $F$ in Equation 6.1 here is the total liquid flow rate in the bioreactor. By changing the

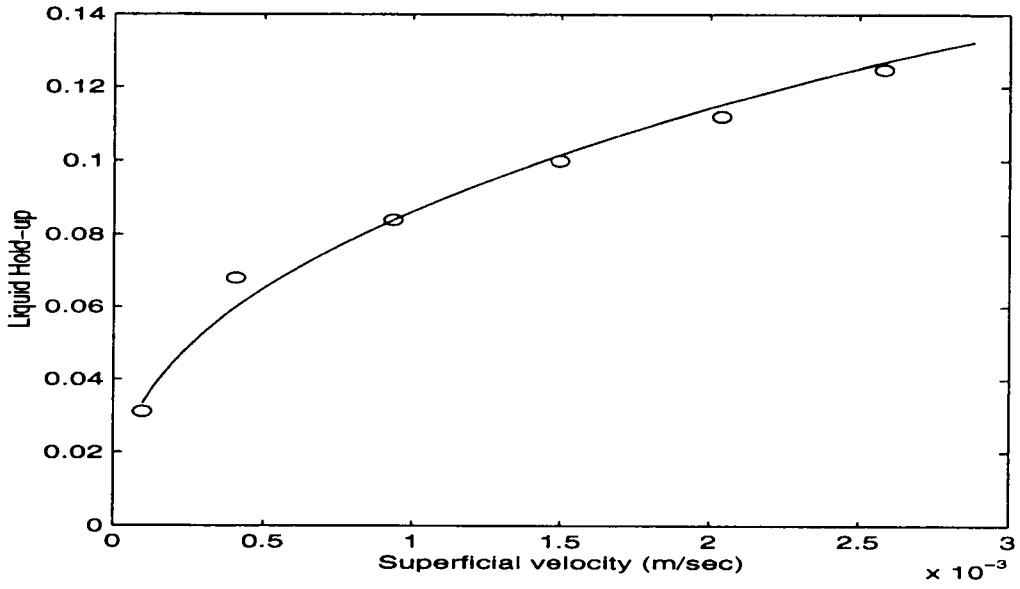



Figure 6.3: Liquid Hold-up Changes with Total Flow Rate

total liquid flow rate, and stopping feeding and recycling, fluid from the effluent was collected by a graduated cylinder to measure the liquid hold-up. Figure 6.3 shows the experimental data and fitting curve. The correlated form for liquid hold-up is:

$$\theta_L = 1.4287(\frac{F_f}{A_r} * 0.01/60)^{0.4065} \tag{6.2}$$

### 6.4.2 Gas Recycle Rate

The driving force of gas flow is the flow of liquid. Gas flow only depends on how much liquid comes out from the reactor. It is a function of total influent flow rate only. The liquid recycle doesn't affect its value. A gas bubble flow meter

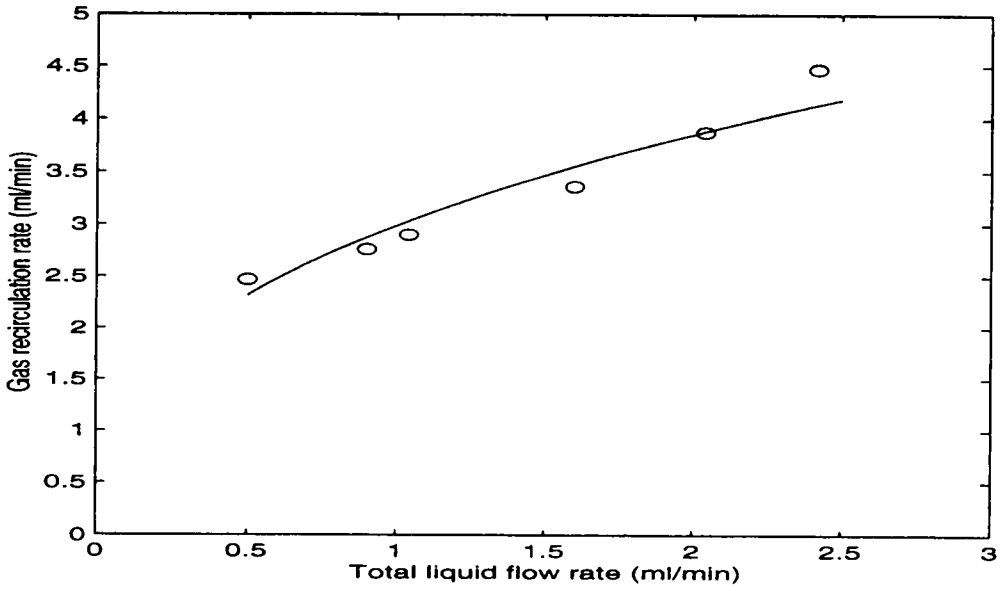



Figure 6.4: Gas Recycle Rate Changes with Influent Flow Rate

was connected between the de-gassing tube and the gas storage column. Once the experiment had started, the volume through which the gas bubble passed and the time were recorded. Gas recycle rates were then calculated at a certain range of influent liquid flow rate. The correlation is obtained:

$$r_g = 2.9879 F_f^{0.3674} \tag{6.3}$$

The experimental data and fitting curve are shown in Figure 6.4.

# Chapter 7

# Column Analysis

Some properties of the bioreactor were investigated. Toluene degradation activity, biomass growth, and oxygen distribution will be discussed in this chapter.

## 7.1 Toluene Degradation in the Column

Toluene as a primary substrate is very important in cell growth and enzyme production for the cometabolism of TCE. According to the kinetics studies, toluene is an easily degraded compound by *Pseudomonas putida* F1. Its concentration and distribution in the column have a tremendous influence on biofilm growth and TCE removal efficiency of the column. Gas samples from sample ports were taken to measure toluene concentration along the column. However, except for the first stage with no beads around in that space, no toluene was detected in the rest of

the stages. This doesn't mean that all toluene was used up in the first 1/4 part of the column. One explanation might be that the fluid was not evenly distributed in the radial direction; there existed short cuts in the column. In fact, it could be seen that liquid flowed un-uniformly. And because the reaction catalyzed by cells was so fast, toluene had already been transformed before it diffused to the sample port. If the influent toluene concentration was adjusted and measured instantly without overnight stabilization, a toluene concentration profile could be obtained. In this case, the growth of biomass could not catch up with the sudden change of toluene concentration. Figure 7.1 shows the change of the gas phase and liquid phase toluene concentrations along the column. Liquid phase concentrations were calculated by Henry's law assuming quick equilibrium achieved in each local position. Again, these concentration profiles might not ideal. The operation conditions were: MSB flow rate: 3 ml/min; recycle rate: 27.5 ml/min. Toluene was fed in three different flow rates: 0.4 ml/min, 0.7 ml/min, 1.0 ml/min, ending up with three different influent feed concentrations: 61 mg/L, 97 mg/L, and 129 mg/L. Actual toluene concentrations that went into the reactor after the dilution by recycling were: 6.7 mg/L, 11.6 mg/L, and 16.3 mg/L. The partition of toluene to the gas phase made liquid phase concentration even smaller. Figure 7.1 shows that toluene concentration was greatly reduced in the column. Due to a fast removal rate, measured values in the 2nd, 3rd, and 4th stage were still less

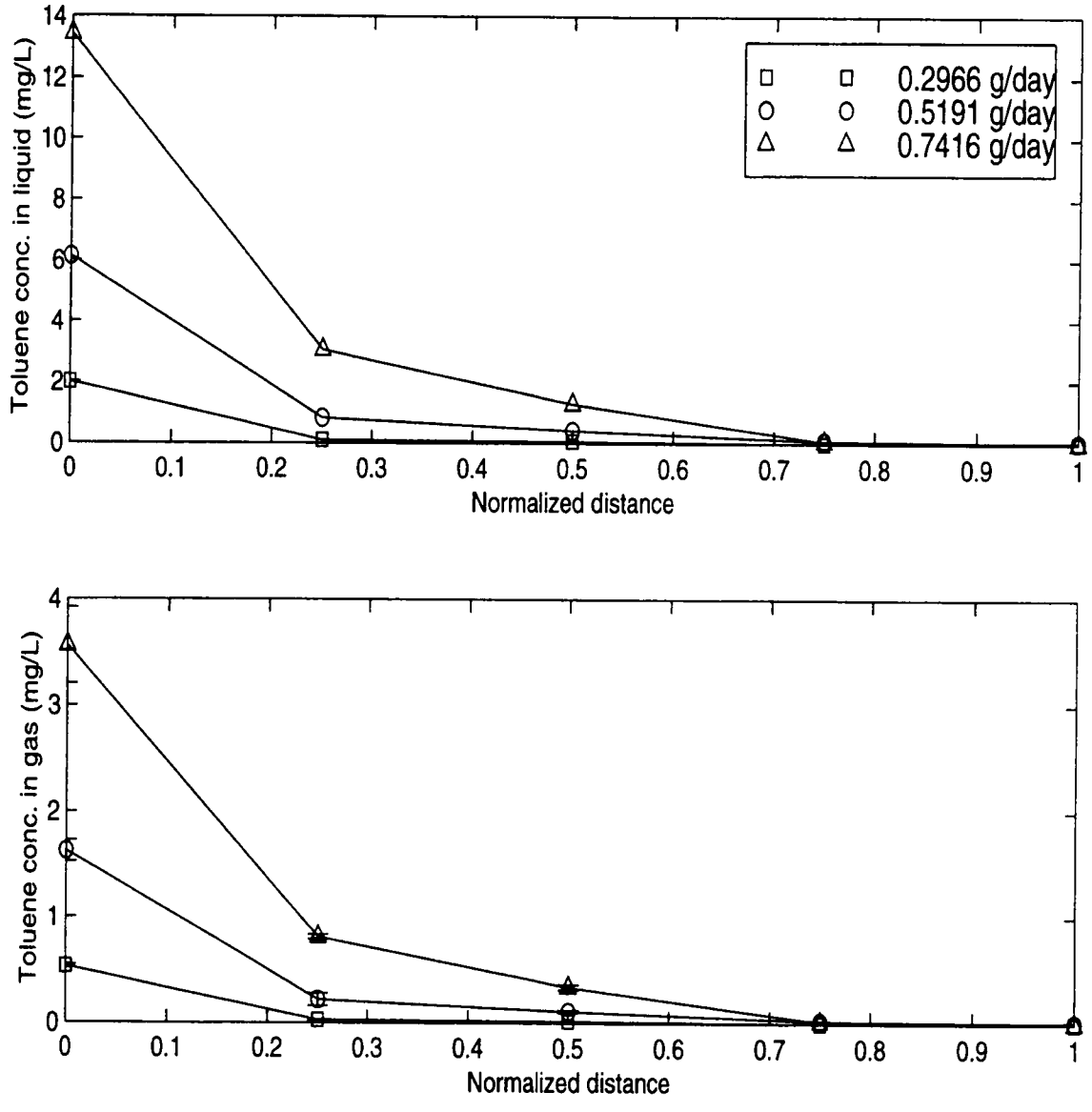



Figure 7.1: Gas and Liquid Phase Toluene Concentration Distribution in the Column at Different Toluene Loading Rate

than actual concentrations. In the last stage, the gas phase equilibrium with the effluent liquid, the sample value should be close to actual concentration.

## 7.2 Oxygen Distribution in the Column

Oxygen distribution was also checked in some sets of experiments. Regarding the above toluene degradation tests, corresponding gas phase oxygen concentration profiles are shown in Figure 7.2. Oxygen dropped from an average of 53% (volume percentage) from the top of the column to 28% (volume percentage) at the bottom of the column. Compared with 21% oxygen in the atmosphere, it was sufficient for the degradation. The flow of the liquid fluid led to the recirculation of gas phase; oxygen was continuously transferred from gas phase to the liquid thin film. The transfer of oxygen from liquid phase to biofilm phase was through the mechanism of molecular diffusion. A higher dissolved oxygen level must be achieved in the liquid phase due to pure oxygen feeding. This kind of reactor can be viewed as having no oxygen limitation for aqueous phase biodegradation, which is a common problem in groundwater treatment. Occasionally, when gas didn't recycle well, there was not enough oxygen to meet the oxygen demanded in the reactor, and effluent toluene concentration would increase immediately.

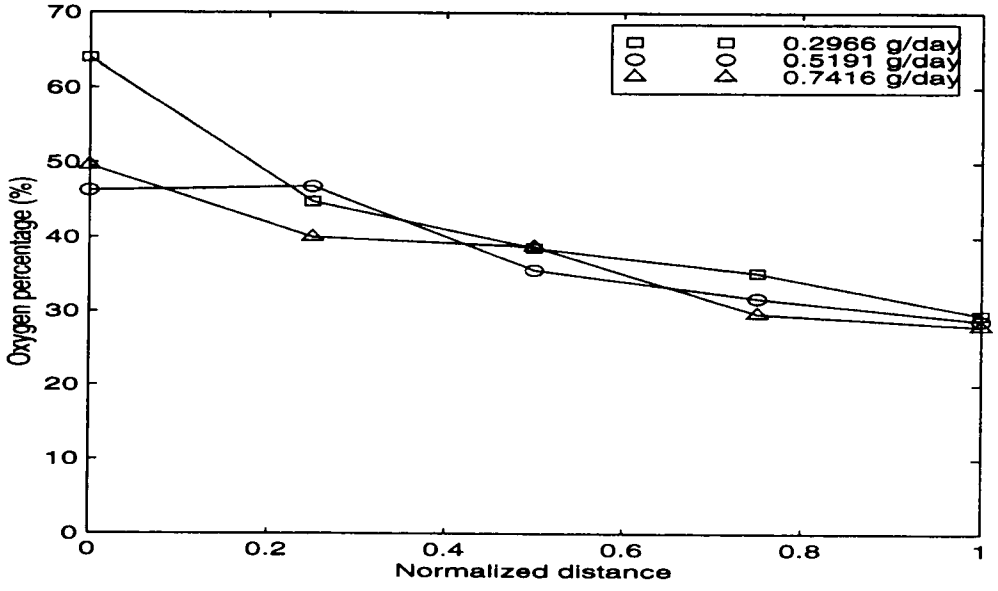



Figure 7.2: Oxygen Distribution in the Column at Different Toluene Loading

## 7.3 Biomass Activity Test and Biomass Distribution

Batch toluene degradation experiment was performed to test the reaction activity of the cells from the column. Three beads were taken out from stage No.1 and No.3. They were put into two 25 ml vials with MSB media inside. Vortex vials until biofilm was completely stripped from the surface of beads and broke into tiny pieces. 291 $\mu$l toluene saturated water was then injected into the vial. Final solution volume was 5 ml with initial toluene concentration at about 30 ppm. Vials were shaken at 180 rpm, and headspace was sampled continuously to

monitor toluene degradation. Results are plotted in Figure 7.3. The triangles were toluene degradation by exponential growing free cell. It took much more time for cells from the biofilm to degrade 30 ppm toluene than the active growing cell in the vials. Cell concentrations in each vial were: 400 mg/L for active free cell; 480 mg/L for cells from stage 1; and 240 mg/L for cells from stage 3. This illustrates the fact that within the biofilm not all cells are living cells; some are just dead body and exopolymeric substances (EPS). Three beads were also taken from each stage to analyze biomass distribution in the column. This experiment was done in 20 days after back wash of the column. Dried cell mass per bead vs. bed position was shown in Figure 7.4. Because of the toluene concentration gradient, cells grew more at the top part of the reactor, then decreased down the column.

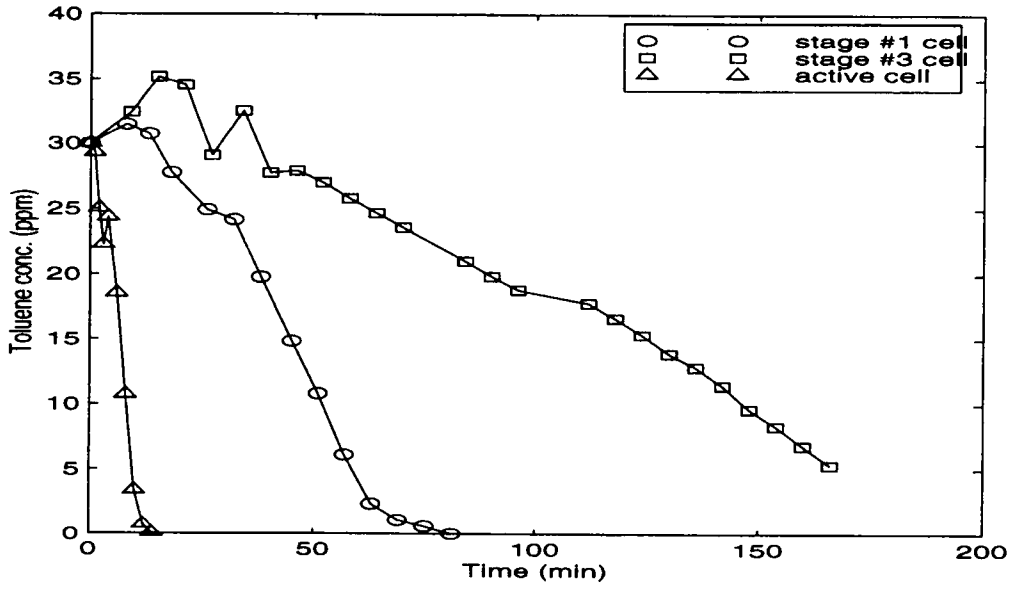



Figure 7.3: Toluene Degradation by Active Growing Cell and Immobilized Cell

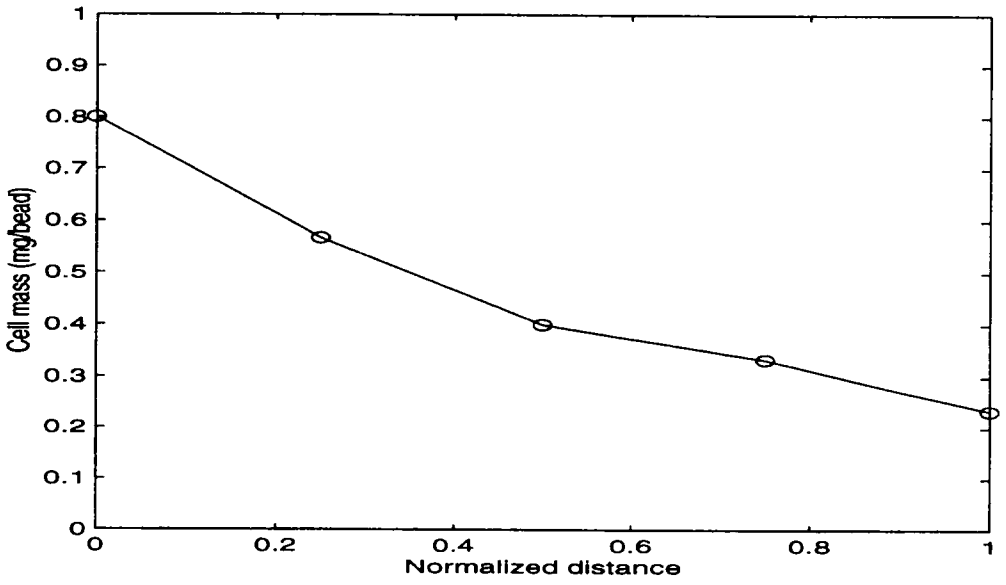



Figure 7.4: Cell Mass Distribution along the Column

# Chapter 8

# TCE Cometabolism in a Packed Bed Biofilm Reactor

After the growth of biofilm, different operational variables were tested to examine the performance of the bioreactor. They include: the influence of influent toluene concentration, influent TCE concentration, influent flow rate, and recycle rate to the TCE degradation.

## 8.1 Dynamic TCE Breakthrough Curve

Once biofilm had been fully developed, TCE was introduced into the column by a syringe pump. Influent toluene was maintained at about 28 mg/L. Total influent flow rate was 3.2 mg/L, and recycle rate was set at 27.5 ml/min. In-

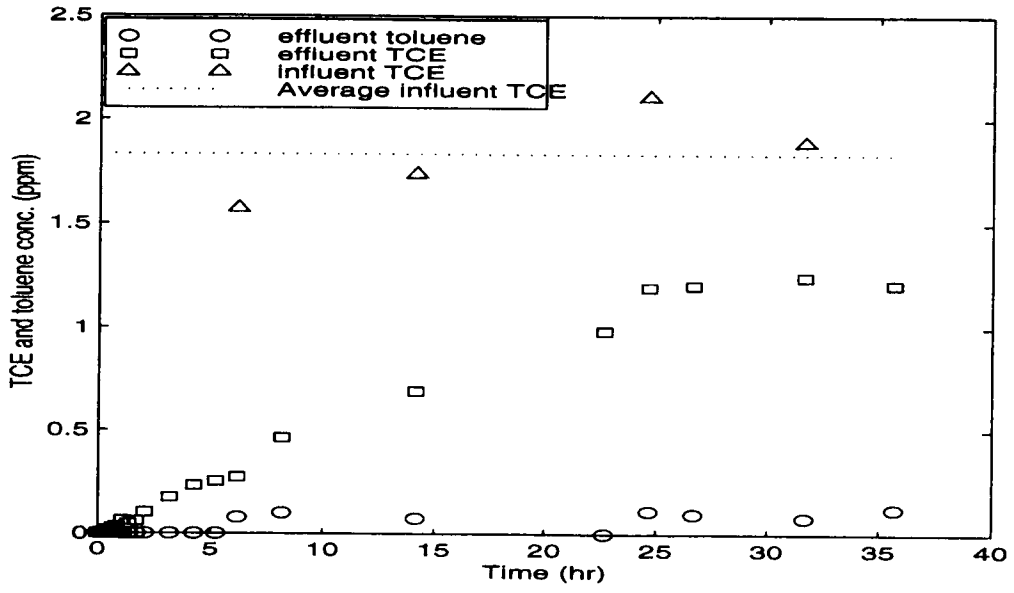



Figure 8.1: Effluent TCE Concentration Changes with Time

fluent and effluent were sampled; and their concentrations changing over time were plotted in Figure 8.1. Different from the abiotic experiment (Figure 6.2), a very small amount of toluene was detected; most of toluene was degraded by the biofilm. Besides dilution and adsorption effects, effluent TCE concentration increased very slowly. The level was much lower than abiotic experimental results in the first several hours. The difference was the amount that was consumed by the biodegradation. In this experiment, TCE came out of the reactor in 15 minutes, and toluene showed up in 6.17 hours. The average influent TCE concentration was 1.8 ppm.

## 8.2 Toluene Concentration Affects TCE Degradation

Toluene concentration was increased as a step function by adjusting the flow rate of the HPLC pump. Effluent TCE concentration was measured to see its response to the changing of toluene concentration in the column. Average influent TCE concentration was about 2.22 ppm, and the influent flow rate was about 3.2 ml/min. Three average influent toluene concentrations were tested: $\sim$ 5 ppm, $\sim$ 29 ppm, and $\sim$ 54.4 ppm. If influent toluene concentration was less than 10 ppm, only 13.7% TCE has been degraded. Increasing influent toluene leads to the decreasing of effluent TCE concentration. TCE removal efficiency increased to 31.4% of influent toluene at about 29 ppm. Under this condition, actual toluene concentration at the top of the reactor was 3.5 ppm after dilution by recycle stream. However, TCE removal was not significantly enhanced (about 34.4% removal) by further increasing of influent toluene concentration in this experiment (Figure 8.2). At this high toluene concentration, suddenly stopping toluene feeding resulted in the decreasing of effluent TCE concentration (Figure 8.3), which enabled the whole enzyme system for TCE degradation. But because of enzyme decay and product toxicity, effluent TCE concentration backed up promptly. In 6 hours, it reached to its influent value with zero degradation. Further examination

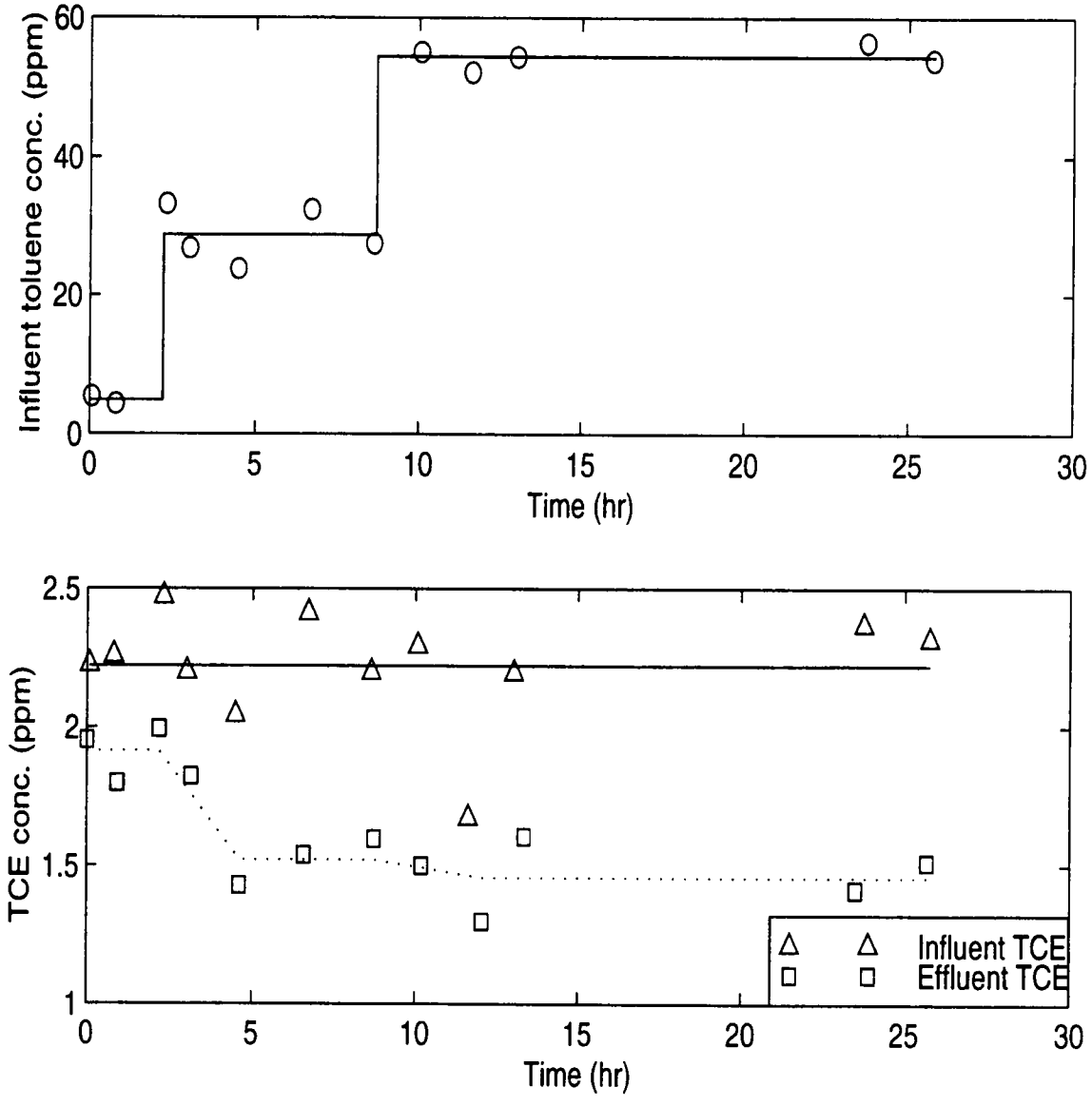



Figure 8.2: TCE Degradation by Step Changing Toluene Concentration (The corresponding toluene concentrations entered the column after dilution by the recycle were: (1)=0.58 ppm; (2)=3.37 ppm; (3)=6.33 ppm.)

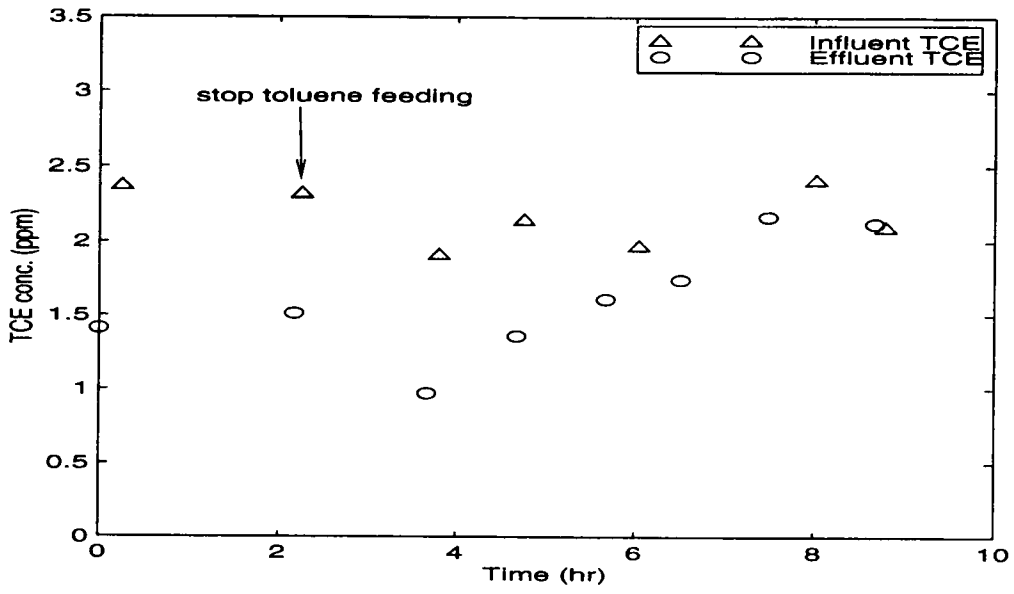



Figure 8.3: Effluent TCE Concentration Changes with Time after Stop Toluene Feeding

of how toluene concentrations affect TCE degradation was done by varying influent toluene concentrations on the daily bases (Figure 8.4). Two sets of influent TCE concentrations were explored with one 1.86 ppm and the other 1.06 ppm on the average. The influent flow rate was kept the same as 2.8 ml/min. In the first series, the decreasing of effluent TCE concentration was very obvious when influent toluene concentration was increased. Removal efficiency dropped to 32% when toluene concentration was 69.44 ppm. In the second round where influent TCE concentration was kept at about 1.06 ppm, it had the same trend. Low toluene concentrations resulted in small TCE degradation. At influent toluene

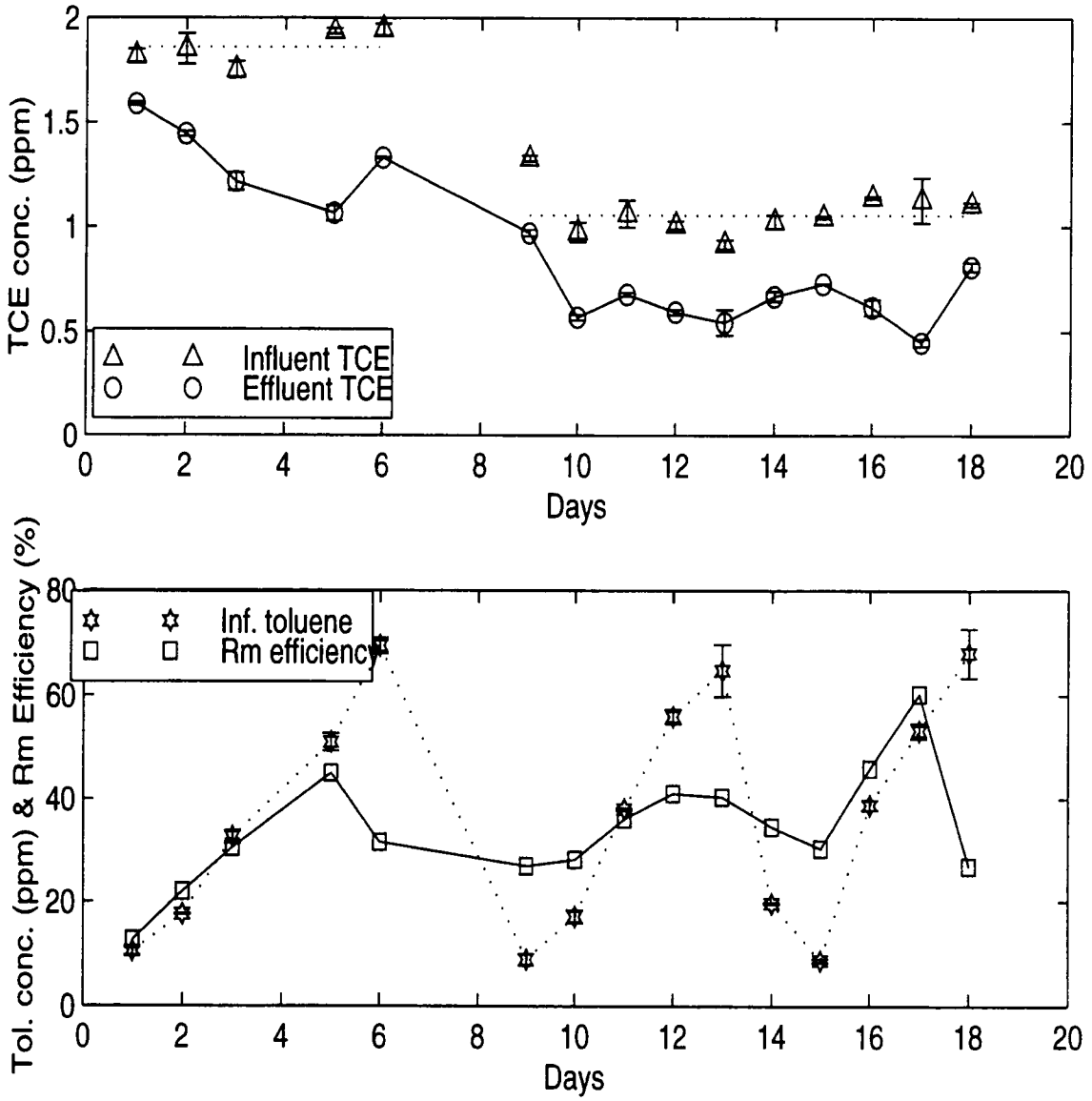



Figure 8.4: Toluene Concentration Affects TCE Removal Efficiency

concentration of 53 ppm, 60% TCE removal efficiency was achieved. Again, 68 ppm toluene caused efficiency to drop to 26.9%. This experiment shows that a certain level of toluene supply is necessary to maintain stable TCE degradation in the cometabolism.

## 8.3 TCE Concentration Affects Its Degradation

At a total influent rate of 3.02 to 3.3 ml/min and toluene loading of 0.1483 g/day, influent TCE concentration was increased daily. 94.5% TCE was removed at low influent TCE concentration (about 0.31 mg/L). Effluent TCE concentration increased with the increasing of influent TCE concentration (Figure 8.5). Removal efficiency went down to 13.7% at high influent concentration (about 7.2 ppm). In the low range of TCE concentration, it showed a linear relation of influent and effluent TCE concentration. Similar results were obtained by Strandberg et al (1989)[70]. Decreasing of removal efficiency at high influent TCE concentration implies product toxicity that destroyed the enzyme system. Measured gas phase TCE and oxygen concentration profile in the reactor for influent TCE concentration of 0.75 mg/L is plotted in Figure 8.6. The removal efficiency was 63%.

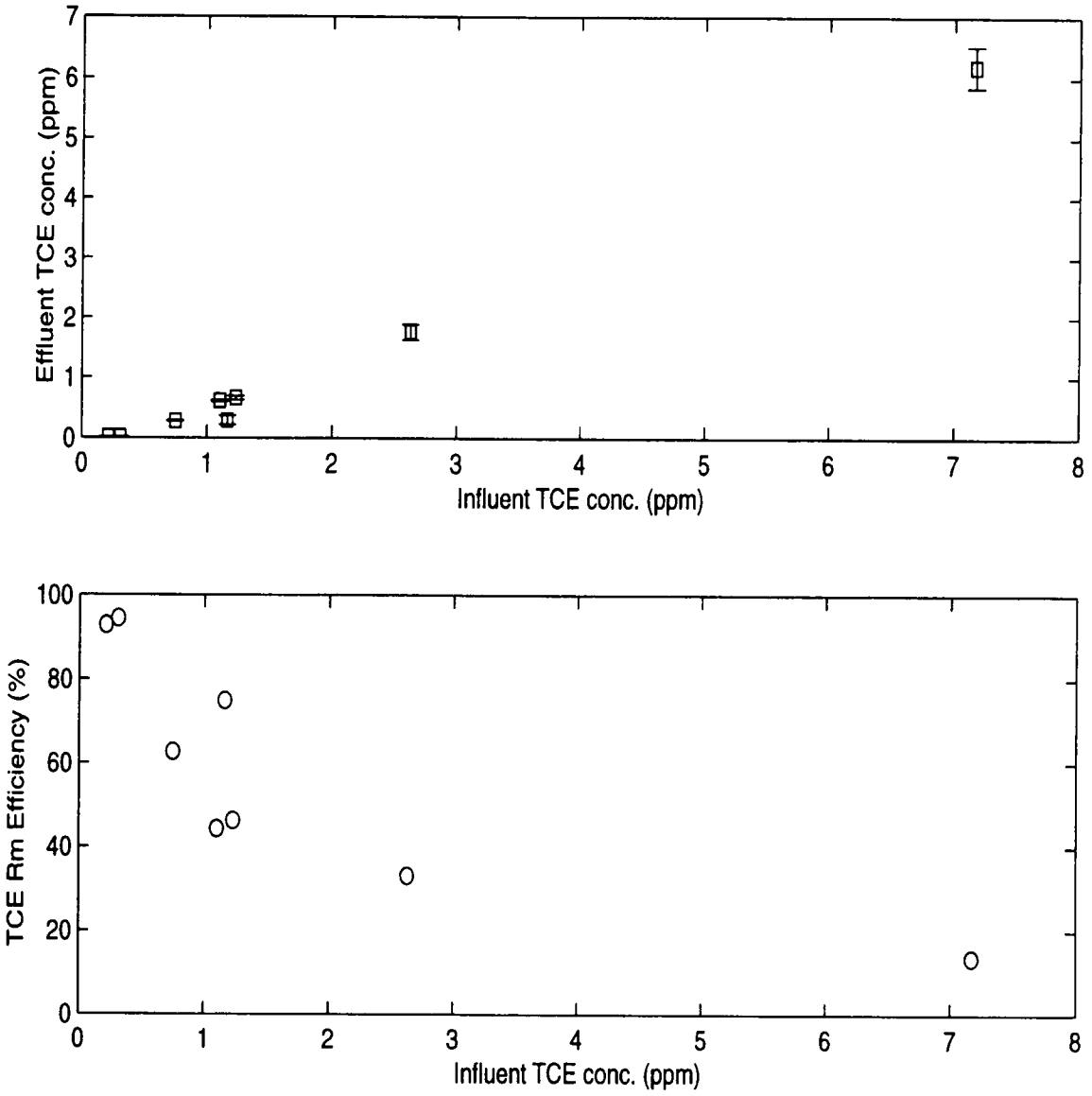



Figure 8.5: Influent TCE Concentration Affects TCE Degradation

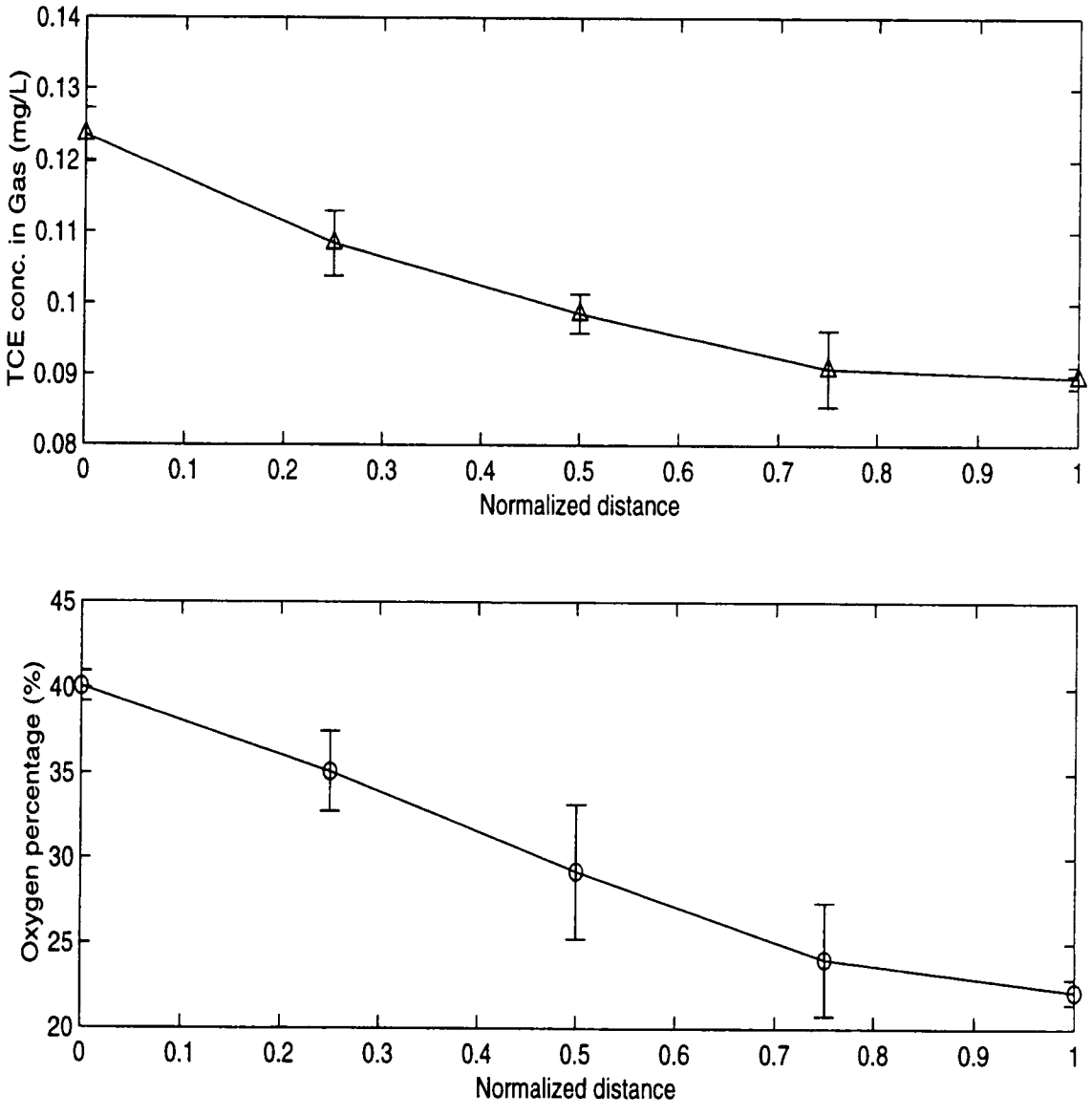



Figure 8.6: Gas Phase TCE Concentration and Oxygen Distribution in the Column

## 8.4 Recycle Rate Affects TCE Degradation

Liquid recycle affects toluene concentrations and toluene distribution in the column. If the influent toluene concentration is high, then most of the cells will grow in the upper part of the column. The accumulation of cells may cause column flooding. With more cells, more toluene will be consumed. No toluene will be supplied to the rest of the column, leaving that part very low in regards to loading of biomass. For the cometabolism of TCE, the degradation efficiency will be low, too, because toluene competitive inhibition dominates the upper part of the column, while in the bottom part, only a very small amount of active cells are present. All these make the column low in efficiency. Recycling part of the effluent back to the reactor results in dilution of the influent toluene concentration. Also, a high recycle rate enhances toluene transport from the top to the bottom of the column to keep up with toluene reaction rate. Thus, cells can be more uniformly distributed in the column. Figure 8.7 shows the effect of recycle rate on TCE degradation. Five recycle rates were tested: 12 ml/min, 27.5 ml/min, 44 ml/min, 60 ml/min, and 76 ml/min. A recycle rate greater than 27.5 ml/min didn't help much for TCE degradation in this experiment. Other operational conditions were: average influent toluene concentration: 29.82 mg/L; influent TCE concentration: 1.57 mg/L; total influent flow rate: 3.21 ml/min.

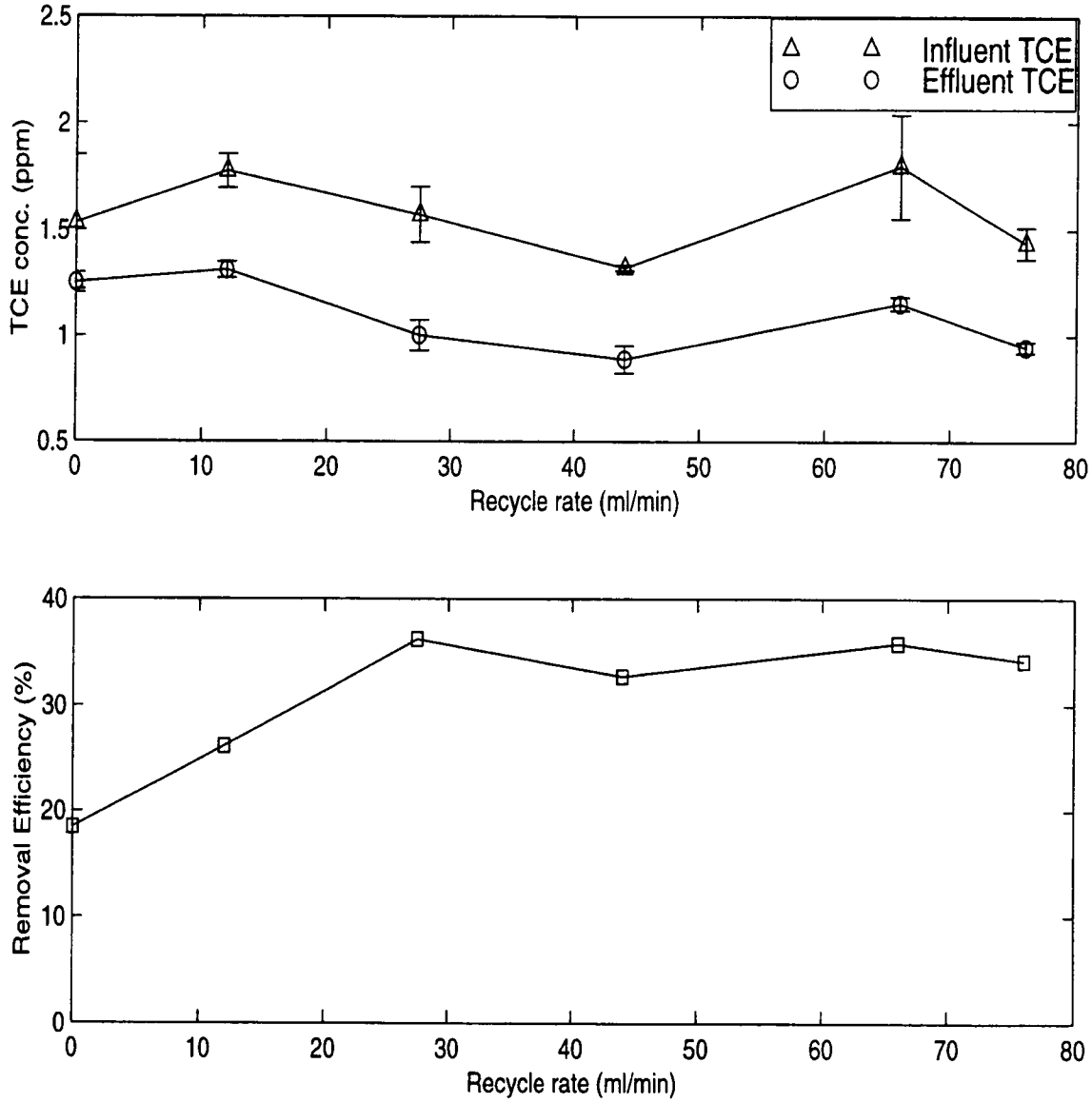



Figure 8.7: Recycle Rate Affects TCE Degradation

## 8.5 Flow Rate Affects TCE Degradation

Flow rate affects retention time in the column, thus affecting TCE degradation. Usually, the longer the retention time, the more TCE will be removed. Different from a conventional packed bed reactor where liquid is filled up in the whole column, liquid hold-up is much smaller, thus retention time was shorter. Sample estimation of retention time is given as follows. For total influent flow rate at 3.4 ml/min with 27.5 ml/min recycle rate, liquid hold-up calculated from Equation 6.2 is 0.04265. If the volume of the reactor is 280 ml, then total liquid in the reactor will be 11.9 ml. Residence time is gained by dividing liquid volume over influent flow rate. The value under this flow condition is 3.5 minutes. Three different flow rates were tested at the same toluene loading: 1.82 ml/min, 3.49 ml/min, and 4.67 ml/min. For each fixed flow rate, TCE concentration was adjusted day by day. Results are shown in Figures 8.8 and 8.9. The corresponding retention times are: 6.40 min, 3.43 min, and 2.61 min. Although increasing flow rate will increase liquid hold-up, compared to the increasing of flow rate, it contributed much less to make retention time change. Therefore, the lower flow rate got high TCE removal efficiency. The same results were obtained by Parvatiyar[50] in gas phase TCE transformation. For the total flow rate of 1.9 ml/min with influent TCE concentrations of 0.53 mg/L and 2.02 mg/L, the gas phase TCE concentration profile in the column is plotted in Figure 8.10. Removal efficiencies were 76%

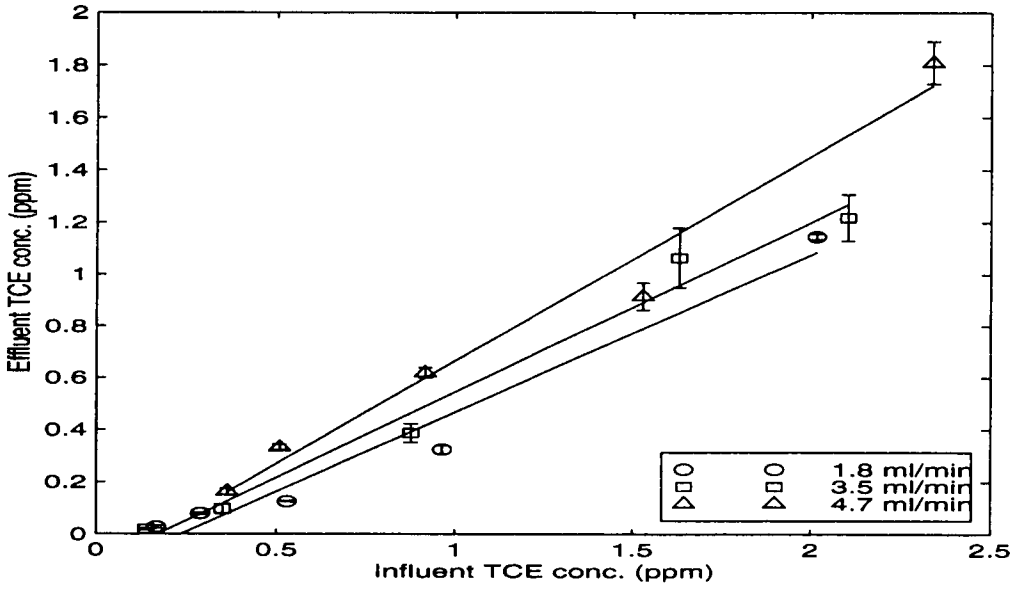



Figure 8.8: Influent Flow Rate Affects TCE Degradation

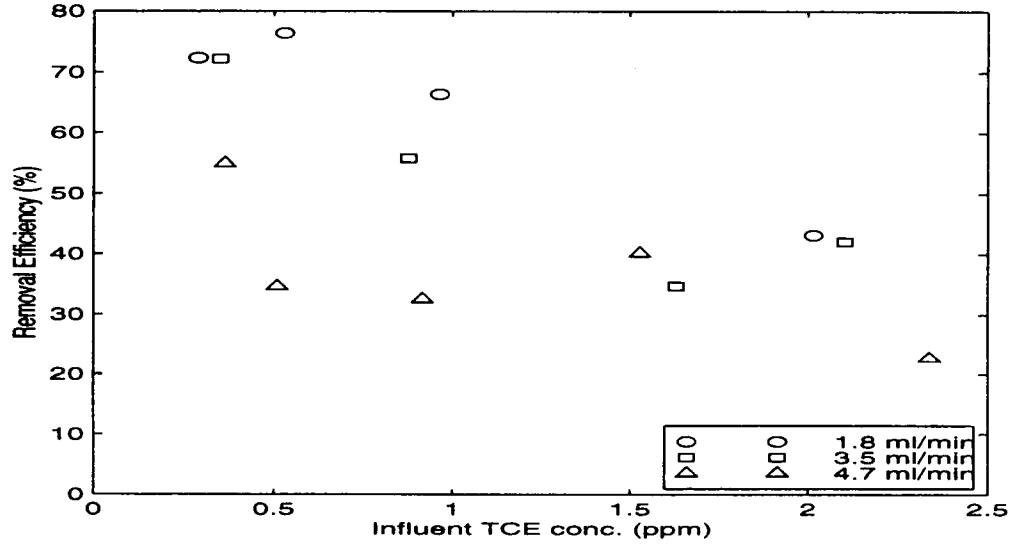



Figure 8.9: TCE Removal Efficiency Changes with Influent Flow Rate

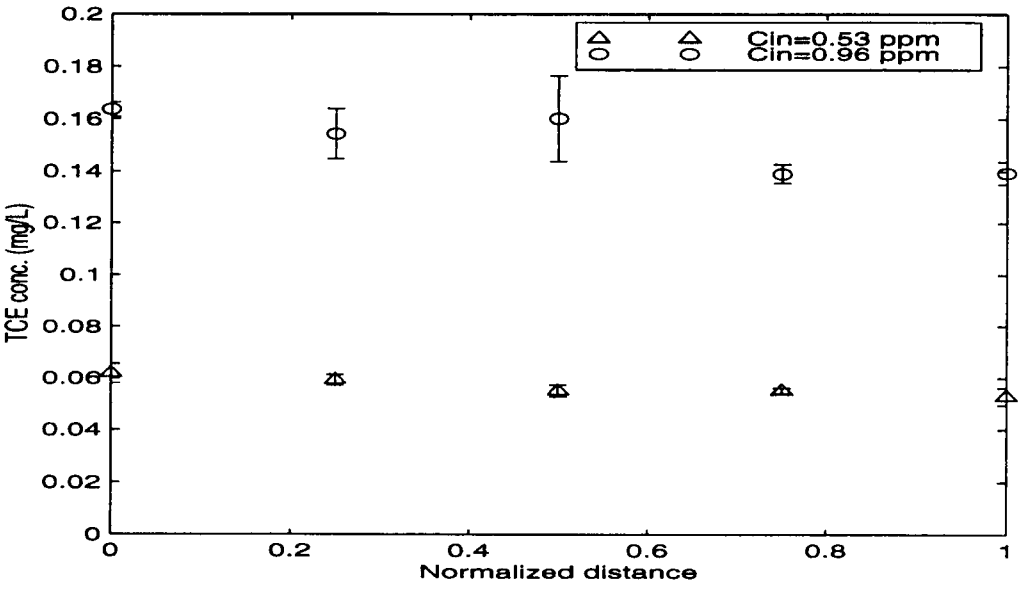



Figure 8.10: Gas Phase TCE Distribution in the Column

and 43%, respectively.

## 8.6 Oxygen Affects TCE and Toluene Degradation

Oxygen as a final electron acceptor takes part in the regeneration of reducing power of NADH, which is necessary in the oxidation reaction. In the beginning of the experiment, no TCE was introduced into the column, and the oxygen supply was cut off. Originally the design of the storage column was to store oxygen. According to a calculation based on the theoretical value of $Y_{o/tol}$ of 2.7 mg $O_2$/mg

toluene (Appendix C), it should last about 10.5 hours for degradation of 0.1483 g/day toluene. Because there was still some oxygen left in the reactor and in the storage column, effluent toluene concentration kept at zero for the first several hours. At about 4 hours, toluene flowed out from the column. This indicates that the oxygen concentration in the column was not 100%. Some $CO_2$ from metabolism existed. Effluent toluene concentration increased continuously until it reached its influent value at about 34.3 ppm. The reaction rate decreased as oxygen getting small. This was the process of oxygen limitation. At about 25 hours, TCE feeding started. Effluent TCE concentration went up very quickly. Four hours later, it equaled to influent concentration. This matches the abiotic TCE experiment. A little more time needed may have been caused by cell adsorption. Oxygen feeding was restarted again. It can be seen from Figure 8.11 that both effluent toluene and TCE concentration decreased immediately.

## 8.7 Summary of the Column Experiments

The entire column experiment with the measurements of TCE influent and effluent liquid phase samples was summarized in Figure 8.12. During the operation, because of the growth of the biomass, the column was clogged several times, so back wash was employed to get rid of some extra cells. New biofilm grew back very quickly by the introducing of toluene. This reactor is effective for aerobic volatile

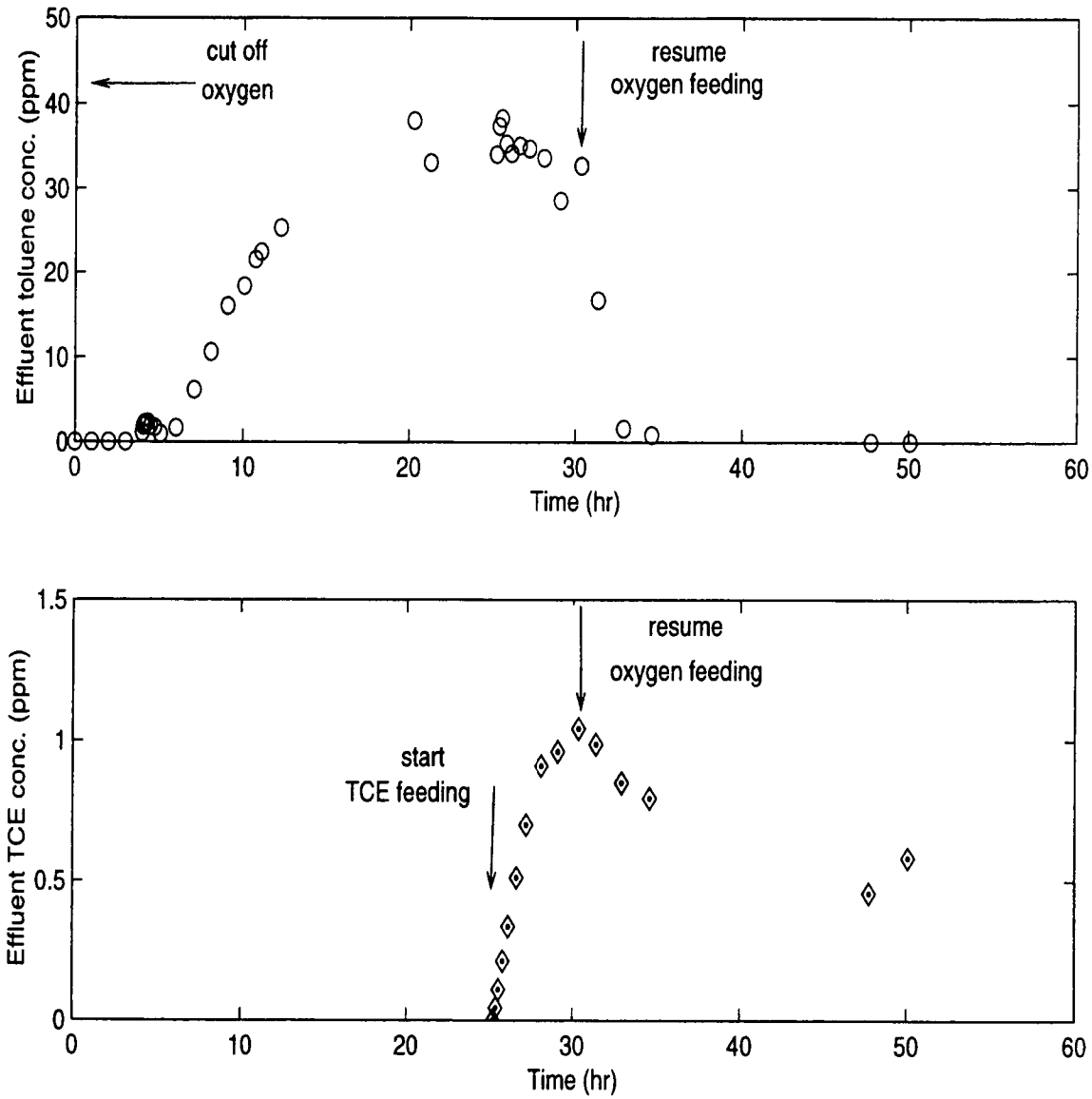



Figure 8.11: Oxygen Affects Toluene and TCE Degradation

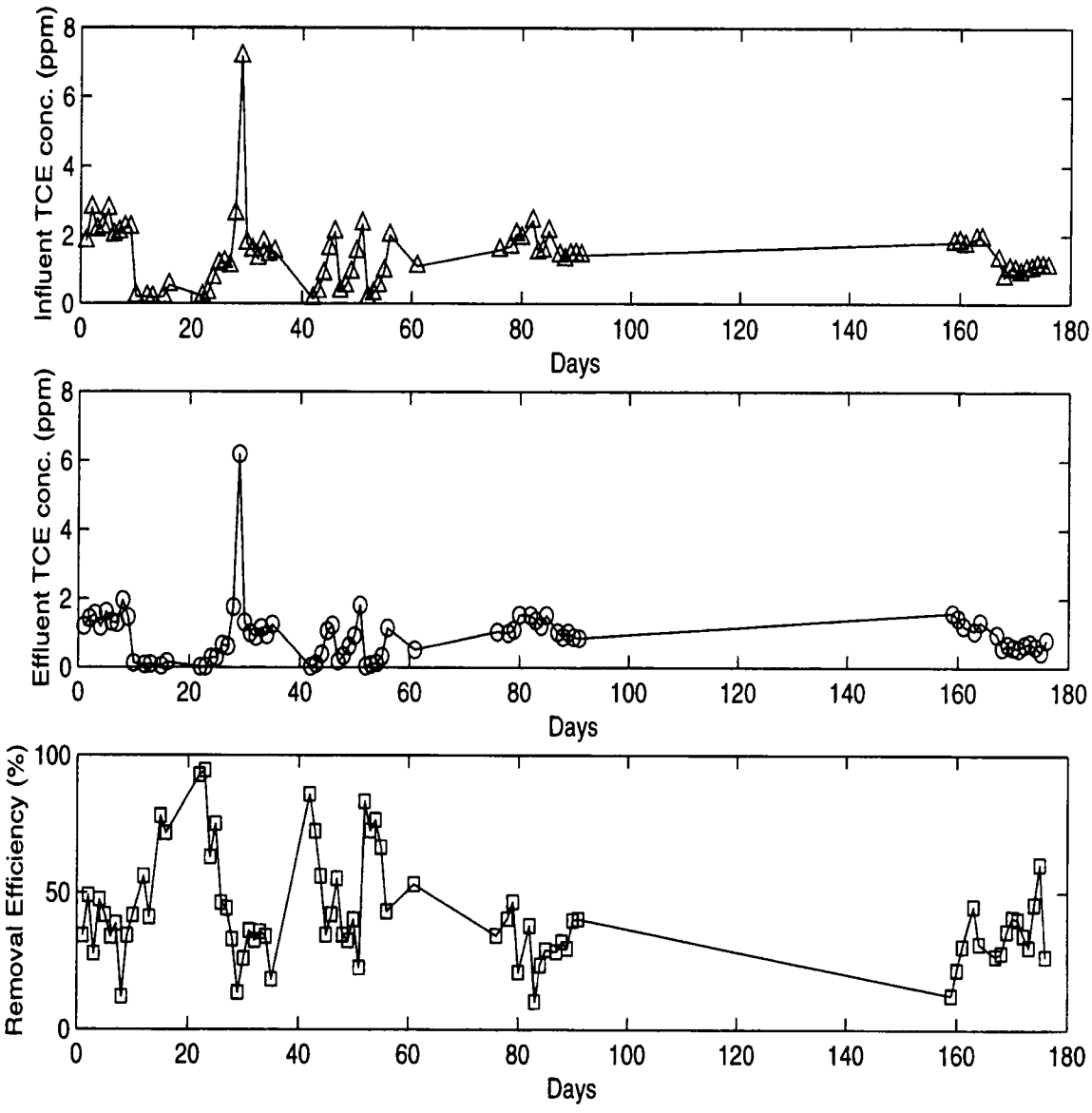



Figure 8.12: Summary of TCE Degradation in the Packed Bed Reactor

compound aqueous phase biological treatment. It can maintain a steady-state operation for TCE degradation. Toluene competitive inhibition was minimized, and oxygen limitation, which is a common problem in the groundwater treatment, was eliminated. TCE degradation is a reaction-controlled process. And product toxicity is the main reason for low removal efficiency at high TCE concentration. What remains to be improved for the reactor is to increase the retention time. Glass beads were used as model supporting material for the experiments. Packing material with larger surface area needs to be used for immobilization of microorganisms. Shortcut happened during the operation, and flowing was not uniformly in the radial direction, thus affecting removal efficiency. A good distributor or redistributor within the column will enhance mass transfer and increase column efficiency greatly.

# Chapter 9

# Biofilm Model

Cells can be immobilized in a bioreactor. They grow in a form of biofilm attached to the surface of a supporting material. Due to high biomass concentrations and immobilization, biofilm reactors are easier to operate than a conventional suspended cell reactor. Usually high efficiency can be achieved in a small volume in a high volumetric flow without worrying about wash out problem. These advantages make biofilm reactors have wide applications in waste water treatment[20][36], especially in the degradation of recalcitrant organic compounds. In order to design a biofilm reactor and optimize the operation process, an understanding of the mechanism of the biological and physical process in the biofilm is very important. Rittmann and McCarty (1980)[55] first proposed a steady-state biofilm model for a single compound biotransformation in the biofilm. They coupled the process

of molecular diffusion and biochemical reaction with the steady-state growth of biofilm. The growth of the biofilm was characterized by the thickness of the biofilm, through utilizing the substrate. Other biofilm models were developed based on their work [57][58][66] for multispecies, dual substrates, and steady-state biofilm with biofilm growth. There are very few reports for biofilm modeling of TCE cometabolism. Anderson and McCarty (1994)[2] studied treatment of TCE by methanotrophic biofilms. In their work, transformation capacity was first introduced in the biofilm modeling, which was used widely in the suspended resting cell system. And biomass was corrected as an active biomass for TCE degradation. However, the model did not predict experimental data very well.

*Pseudomonas putida* F1 uses toluene as a primary substrate for growth. At the time it degrades toluene, TCE can be cometabolically oxidized by dioxygenases, which has a broad substrate inspecificity. Unlike Methanotrophic bacteria[2][63], the expression of enzyme is not limited by the existance of copper in the ground water. Thus, using *Pseudomonas putida* F1 biofilm in the treatment of contaminated ground water is promising.

The object of this study is to develop a biofilm model for TCE cometabolism in the *Pseudomonas* biofilm; quantitatively describe the biological process including competitive inhibition, TCE toxicity effects, and the growth of the biofilm. The model could be used in the engineering design of a biofilm reactor and process

optimization.

## 9.1 Model Development

The biofilm model developed here is based on the steady-state biofilm kinetics. In the system of interest, two compounds are related to the kinetics of biofilm: toluene and TCE. Toluene is the primary substrate which supports the growth of biofilm, while TCE is the secondary substrate. As the enzyme degrades toluene, it cometabolically transforms TCE. Because of the toxicity of the TCE transformation product, its presence in the biofilm will cause the loss of active cells for TCE degradation. This toxic effect is quantified by $Tc$, transformation capacity, defined as the maximum mass of compound that can be degraded per mass of cell (Alvarez-Cohen, 1991)[1]. Principle assumptions made for the model are:

- The biofilm is composed of living cells and dead cells. Toluene determines the growth of the biofilm. So it is characterized by its effective thickness value, which is the point where the gradients of TCE and toluene go to zero. The effective thickness is much smaller than actual thickness.

- Cells that only access to toluene have the activity to degrade TCE. The toxicity of TCE affects these active biomass amounts, which also affects its own degradation, while the inactivated cells are still capable of toluene degra-

dation. Thus biofilm is divided into several sublayers, and each sublayer is treated as a completely mixing unit. Active cell mass balance is then made under the influence of TCE toxicity to correct for TCE degradation in each subunit.

- The overall biofilm density is assumed constant.
- Oxygen is not a limiting factor for biodegradation.
- The thickness of the biofilm is much smaller than the main dimension of supporting material, thus, rectangular geometry is used.

The system is then determined by bulk concentrations of toluene, TCE, and their biological kinetic parameters. The conceptual bases of the biofilm model are mass transfer and bioreaction. The schematic biofilm model is shown in Figure 9.1. First substrates were transferred from bulk fluid to the surface of biofilm. Due to mass transfer resistance of liquid film around the particle, a concentration gradient established in the layer of depth L. The flux across the diffusion layer is calculated by Fick's first law:

$$J_i = -D_i \frac{C_{bi} - C_{si}}{L} \tag{9.1}$$

where $i = 1, 2$ for toluene and TCE. $C_{bi}$ is the bulk concentration, $C_{si}$ is surface concentration. $D_i$ is the diffusion coefficient of substrate in the fluid. The approx-

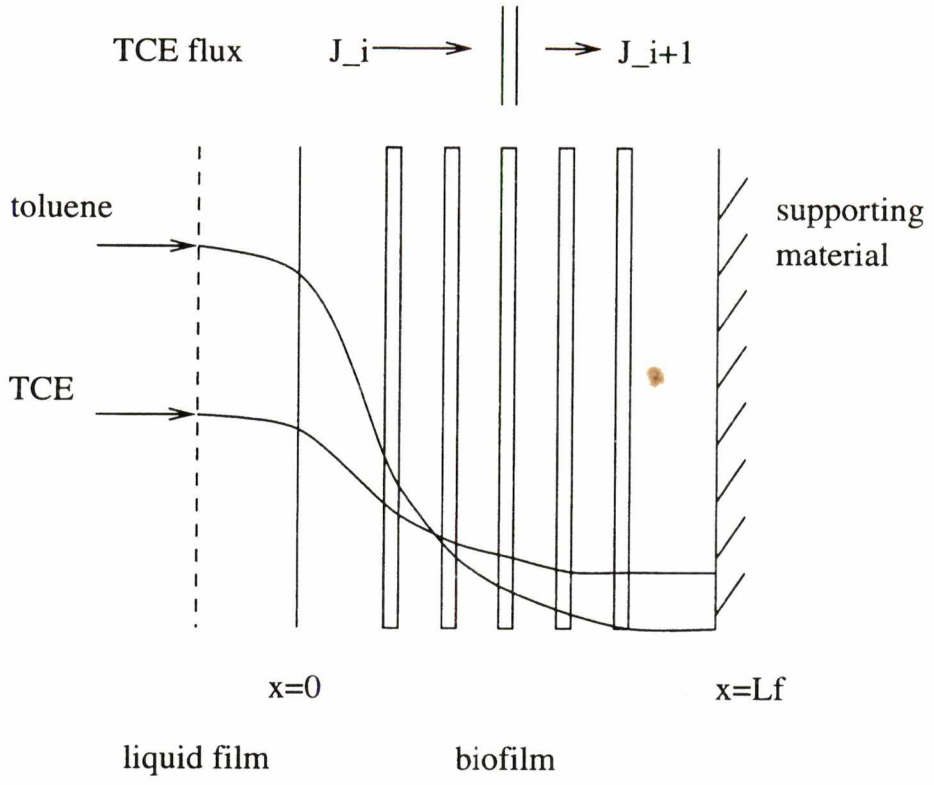



Figure 9.1: Biofilm discretization and toluene TCE concentration profiles

imate relationship of Wilke and Change is used to estimate diffusivities of toluene and TCE in the dilute solution[27]:

$$D = 7.4 \times 10^{-8} \frac{(\psi_b M_b)^{0.5} T}{\mu V_a^{0.6}} \tag{9.2}$$

where $\psi_b$ is the association parameter, it equals to 2.6 for water; $M_b$ is the molecular weight of solvent (18 for water); $T$ is the absolute temperature in K; $\mu$ is the absolute viscosity of solution in cp; $V_a$ is the molar volume of solute as liquid at its boiling point. It can be estimated from the atomic volume of their atoms. The

correlation for fixed bed is employed to calculate the liquid film thickness[59]:

$$L = \frac{D(R_{em})^{0.75} S_c{}^{0.67}}{5.7u} \tag{9.3}$$

in which $u$ is the fluid superficial velocity in the reactor; $S_c$ is Schmit number:

$$S_c = \frac{\mu}{\rho D} \tag{9.4}$$

and $R_{em}$ is Renolds number:

$$R_{em} = \frac{2\epsilon d_p \rho}{(1-\epsilon)\mu} \tag{9.5}$$

where $\mu$ is the absolute viscosity of liquid; $\rho$ is the density of solution; $\epsilon$ is the actual porosity of bed; and $d_p$ is the diameter of spherical particles.

Molecular diffusion is the main mechanism of substrate transport within the biofilm. It follows Fick's second law:

$$\frac{dC_{pi}}{dt} = D_{fi}\frac{d^2 C_{pi}}{dx^2} \tag{9.6}$$

where $C_{pi}$ and $D_{fi}$ are the substrate concentration and diffusion coefficient in the biofilm, respectively. The value of the substrate diffusion coefficient equates to the diffusivity in water corrected by a factor depending on the biofilm density (Fan et al, 1990)[19]:

$$\frac{D_{fi}}{D_i} = 1 - \frac{0.43 X_m{}^{0.92}}{11.19 + 0.27 X_m{}^{0.99}} \tag{9.7}$$

Under the action of microorganisms, substrates are degraded. Toluene and TCE reactions at any point of biofilm are assumed to follow a typical enzyme competitive inhibition model. At a steady state, the concentration profile doesn't change with time. Mass balance for toluene and TCE in the biofilm yields two sets of coupled ordinary differential equations:

$$D_{f1}\frac{d^2C_{p1}}{dx^2} - \frac{k_1 X_f C_{p1}}{C_{p1} + K_1(1 + \frac{C_{p2}}{K_2})} = 0 \tag{9.8}$$

for toluene, and

$$D_{f2}\frac{d^2C_{p2}}{dx^2} - \frac{k_2 X_f C_{p2} f_a}{C_{p2} + K_2(1 + \frac{C_{p1}}{K_1})} = 0 \tag{9.9}$$

for TCE. Where $D_{f1}$ and $D_{f2}$ are toluene and TCE diffusivities in the biofilm; $C_{p1}$ and $C_{p2}$ are toluene and TCE concentrations in the biofilm; $f_a$ is the correction factor of active biomass for TCE degradation. These secondary ordinary differential equations are subjected to the following boundary conditions: at the interface of liquid film and biofilm where $x = 0$,

$$-\frac{dC_{p1}}{dx}|_{x=0} = k_{L1}(C_{b1} - C_{p1}|_{x=0}) \tag{9.10}$$

and

$$-\frac{dC_{p2}}{dx}|_{x=0} = k_{L2}(C_{b2} - C_{p2}|_{x=0}) \tag{9.11}$$

where $k_{L1}$ and $k_{L2}$ are mass transfer coefficients for toluene and TCE. They are determined by the ratio of diffusivity $D$ to the liquid film thickness $L$:

$$k_{Li} = \frac{D_i}{L} \tag{9.12}$$

$C_{b1}$ and $C_{b2}$ are concentrations of toluene and TCE in the bulk fluid phase. At $x = L_f$, the surface of packing material,

$$\frac{dC_{pi}}{dx} = 0 \tag{9.13}$$

where $i = 1, 2$ for toluene and TCE; $L_f$ is the effective thickness of the biofilm, which is a function of toluene concentration only. Its value is determined by total biofilm growth balance:

$$YJ_1 = b^{'} X_f L_f \tag{9.14}$$

where $Y$ is the yield coefficient of toluene, $J_1$ is the total flux of toluene into the biofilm, $b'$ is the overall biofilm decay constant which consists of natural decay ($b_d$) and shear loss ($b_s$):

$$b^{'} = b_s + b_d \tag{9.15}$$

In the computation, $b_d$ is set to 0.12 1/day[14]. Shear loss term is estimated by the following expression (Rittmann, 1982)[56]:

$$b_s = 8.42 \times 10^{-2} \sigma^{0.58} \tag{9.16}$$

where $b_s$ is in the unit of 1/day; $\sigma$ is the shear stress:

$$\sigma = \frac{100 \mu u (1 - \epsilon)^3}{{d_p}^2 \epsilon^3 A_s (7.46 \times 10^9)} \tag{9.17}$$

where $A_s$ is the specific area of particle.

In order to calculate the active biomass distribution within the biofilm, the biofilm was divided into several sublayers (see Figure 9.1). Active biomass for TCE degradation in each subunit is balanced by growth from toluene, toxic effect from TCE, and biofilm decay and shear loss:

$$({J_1}^i - {J_1}^{i+1})Y - ({J_2}^i - {J_2}^{i+1})\frac{1}{T_c} = {f_a}^i \delta l X_f b' \tag{9.18}$$

where $i$ refers to the $i$th node; thickness of the sublayer is $\delta l$; ${f_a}^i$ is the active biomass factor in that sublayer.

## 9.2 Non-Dimensionalization of Model Equations

Model equations were non-dimensionalized. The following dimensionless groups were introduced[46]:

$$\bar{C_{bi}} = \frac{C_{bi}}{K_i},\ \bar{C_{pi}} = \frac{C_{pi}}{K_i}$$

$$\eta = \frac{x}{t_a},\ \bar{L_f} = \frac{L_f}{t_a}$$

$$\bar{L_i} = \frac{L_i}{t_i},\ \bar{D_{fi}} = \frac{D_{fi}}{D_i}$$

$$\bar{J_i} = J_i t_i/(D_i K_i)$$

$i = 1, 2$ for toluene and TCE. $t_i$ is the standard biofilm depth dimension of toluene and TCE:

$$t_i = (\frac{K_i D_{fi}}{k_i X_f})^{1/2} \tag{9.19}$$

and $t_a$ is their geometric average, defined here as:

$$t_a = \sqrt{t_1 t_2} \tag{9.20}$$

The mass balance equations are then transformed into following dimensionless forms:

$$\frac{d^2\bar{C_{p1}}}{d\eta^2} - \frac{t_2}{t_1}\frac{\bar{C_{p1}}}{\bar{C_{p1}} + 1 + \bar{C_{p2}}} = 0 \tag{9.21}$$

for toluene, and

$$\frac{d^2\bar{C_{p2}}}{d\eta^2} - \frac{t_1}{t_2}\frac{f_a\bar{C_{p2}}}{\bar{C_{p1}} + 1 + \bar{C_{p2}}} = 0 \tag{9.22}$$

for TCE. The boundary conditions are: at $\eta = \bar{L_f}$,

$$\frac{\bar{C_{pi}}}{d\eta} = 0 \tag{9.23}$$

at $\eta = 0$,

$$\frac{\bar{C_{pi}}}{d\eta} = -Sh_i(\bar{C_{bi}} - \bar{C_{pi}}|_{\eta=0}) \tag{9.24}$$

where

$$Sh_i = \frac{k_{Li}t_a}{D_{fi}} \tag{9.25}$$

are Sherwood number for toluene and TCE. Total flux of toluene is calculated from:

$$\bar{J_1} = -\bar{D_{f1}}\int_0^{\bar{L_f}} \frac{t_2}{t_a}\frac{\bar{C_{p1}}}{1 + \bar{C_{p1}} + \bar{C_{p2}}}d\eta \tag{9.26}$$

The effective biofilm thickness is found by:

$$\bar{L_f} = \bar{J_1}/(\frac{t_a}{t_1})\bar{D_{f1}}\theta_s \tag{9.27}$$

where $\theta_s$ is the standard biofilm time for toluene:

$$\theta_s = b^{'}/(Yk_1) \tag{9.28}$$

The original form of active cell mass balance for TCE degradation was used during the computation.

## 9.3 Effectiveness Factor

Effectiveness factor $\eta_e$ is defined as the ratio of actual flux in the biofilm to the flux that would occur if the entire biofilm were fully penetrated at surface concentration:

$$\eta_e = \frac{\int_0^{L_f} r_f dx}{L_f r_f|_{x=0}} \tag{9.29}$$

For toluene and TCE, they are expressed as:

$$\eta_{e1} = \frac{\int_0^{\bar{L_f}} \frac{C_{p1}}{1+C_{p1}+C_{p2}} d\eta}{\frac{C_{p1}|_{\eta=0}}{1+C_{p1}|_{\eta=0}+C_{p2}|_{\eta=0}} \bar{L_f}} \tag{9.30}$$

and

$$\eta_{e2} = \frac{\int_0^{\bar{L_f}} \frac{C_{p2} f_a}{1+C_{p1}+C_{p2}} d\eta}{\frac{C_{p2}|_{\eta=0}}{1+C_{p1}|_{\eta=0}+C_{p2}|_{\eta=0}} \bar{L_f}} \tag{9.31}$$

The effectiveness factor tells whether the process is controlled by mass transfer or by biochemical reaction. Concerning TCE, the effectiveness factor also involves TCE toxicity.

## 9.4 Solving Procedure

Because the effective biofilm thickness is unknown, the whole biofilm system is solved by iteration method. A biofilm thickness is guessed first; from the bulk concentrations, the 2nd order nonlinear ODE's are solved. The new biofilm thickness is then calculated out from steady-state biofilm growth mass balance. Active biomass has to be corrected at this time. The new value of biofilm thickness is compared with the old one until their difference is smaller than the tolerance. The flow diagram is shown in Figure 9.2.

## 9.5 Numerical Implementation by Finite Element Method

The finite element method is a procedure for constructing an approximate solution to the initial boundary value partial differential equation (PDE) system in engineering and mathematical physics (Baker, 1996)[5][6][7]. The fundamental axiom of finite element theory is to construct an approximate solution. Any solution is a function of space and time which is distributed smoothly over the problem domain and boundaries. Finite element theory requires selecting a set of functions that exhibits properties which appropriate, and then use it as the "trial space" for supporting the approximation. It formalizes the ingredients of

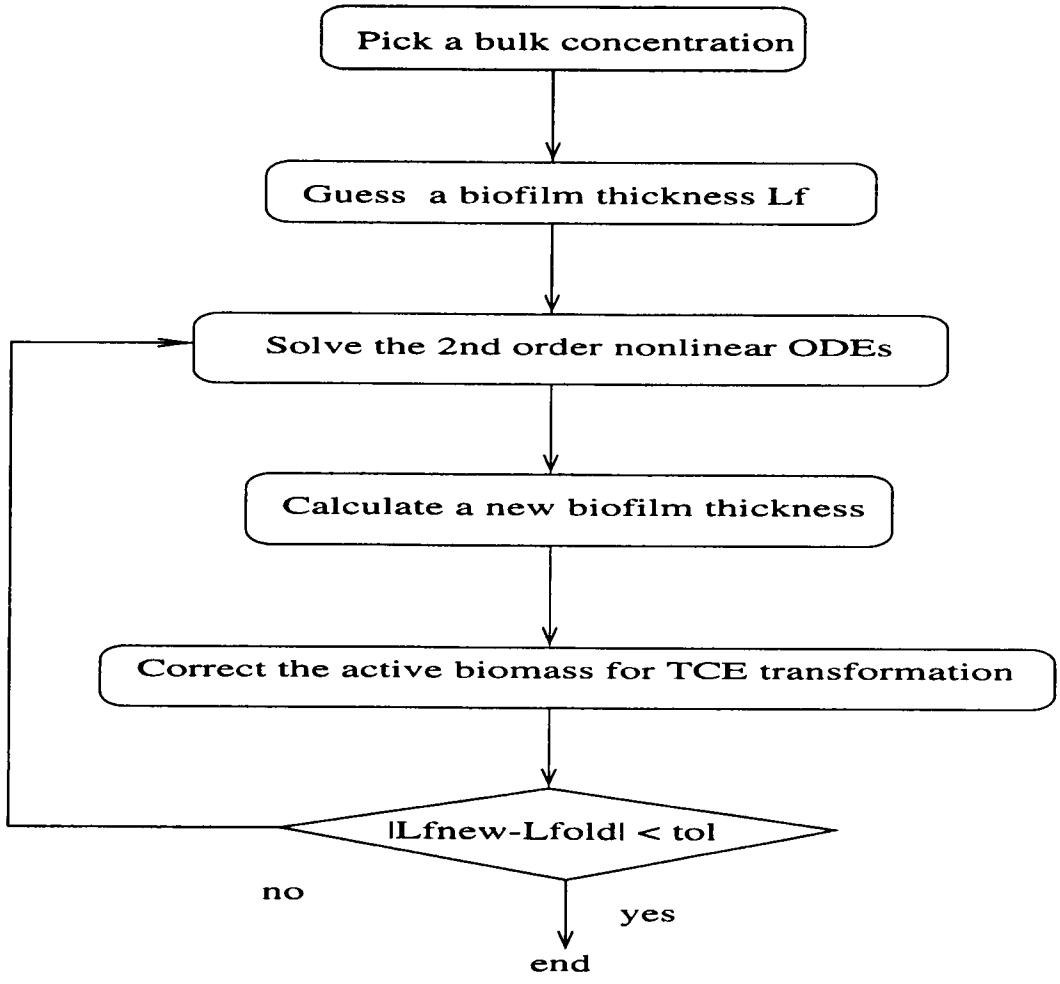



Figure 9.2: Solving Procedure for the Biofilm System

approximate solution construction in terms of trial space, test space, and rending the resultant error minimal in the appropriate measure, called a "norm". Discretization of a weak statement is the operational step that creates an algebraic statement amenable for computing, which combines the calculus and vector field

theory, and concepts of extremization, orthogonality and completeness. Defining $q = f(q_1, q_2)$, where $q_1 = \bar{C_{p1}}$, $q_2 = \bar{C_{p2}}$, and

$$q(\eta) \approx q^N \equiv q^h \equiv U_e q_e(\eta)$$

The Galerkin weak statement for the biofilm phase equation is:

$$GWS^N = \int_\Omega \phi_i L(q^N) d\tau = 0 \tag{9.32}$$

Written for each component:

$$GWSCP1^N = \int_\Omega \phi_i (-\frac{d^2 \bar{C_{p1}}^N}{d\eta^2} + \frac{t_2}{t_1} \frac{\bar{C_{p1}}^N}{\bar{C_{p1}}^N + 1 + \bar{C_{p2}}^N}) d\tau = 0 \tag{9.33}$$

and

$$GWSCP2^N = \int_\Omega \phi_i (-\frac{d^2 \bar{C_{p2}}^N}{d\eta^2} + \frac{t_1}{t_2} \frac{\bar{C_{p2}}^N f_a}{\bar{C_{p1}}^N + 1 + \bar{C_{p2}}^N}) d\tau = 0 \tag{9.34}$$

where $\phi_i$ are set of trial functions that span the physical domain. A function is defined to simplify the operation of reaction term:

$$F = \frac{1}{\bar{C_{p1}}^N + 1 + \bar{C_{p2}}^N} \tag{9.35}$$

$F$ is a function of $\bar{C_{p1}}$ and $\bar{C_{p2}}$, and can be interpolated. With integration by parts and substituting with boundary conditions, Equations 9.33 and 9.34 become:

$$\begin{aligned} GWSCP1^N &= S_e([A211]\{CP1\}_e - Sh1[ONE]\{CB1\} + Sh1[ONE]\{CP1\}|_{\eta=0} \\ &\quad + \frac{t_2}{t_1}\{F\}_e{}^T[A3000]\{CP1\}_e) = \{0\} \end{aligned} \tag{9.36}$$

and

$$GWSCP2^N = S_e([A211]\{CP2\}_e - Sh2[ONE]\{CB2\} + Sh2[ONE]\{CP2\}|_{\eta=0} + \frac{t_1}{t_2}\{f_a * F\}_e{}^T[A3000]\{CP2\}_e) = \{0\} \quad (9.37)$$

Linear bases were used. [A211] and [A3000] are the computational matrices. They are listed in Appendix E.3. The $[ONE]$s are matrices with zero entries except 1 for the corresponding boundary. Due to the nonlinearity, the biofilm equations are solved by Newton algorithm. The corresponding Jacobian form is given by the following expression:

$$\begin{bmatrix} JCP1CP1 & JCP1CP2 \\ JCP2CP1 & JCP2CP2 \end{bmatrix}^p \begin{Bmatrix} \delta CP1 \\ \delta CP2 \end{Bmatrix}^{p+1} = -\begin{Bmatrix} FCP1 \\ FCP2 \end{Bmatrix}^p \quad (9.38)$$

where

$$JCP1CP1 = [A211] + \frac{t_2}{t_1}\{F\}^T[A3000] - \frac{t_2}{t_1}\{CP1\}^T[A3000]\lceil F^2 \rfloor_e + Sh1[ONE] \quad (9.39)$$

$$JCP1CP2 = -\frac{t_2}{t_1}\{CP1\}_e{}^T[A3000]\lceil F^2 \rfloor_e \quad (9.40)$$

and

$$JCP2CP2 = [A211] + \frac{t_1}{t_2}\{f_a * F\}^T[A3000] - \frac{t_1}{t_2}\{CP2\}^T[A3000]\lceil f_a * F^2 \rfloor_e + Sh2[ONE] \quad (9.41)$$

$$JCP2CP1 = -\frac{t_1}{t_2}\{CP2\}_e{}^T[A3000]\lceil f_a * F^2 \rfloor_e \quad (9.42)$$

Sample formations of Jacobians are demonstrated in Appendix E.2. The template is in Appendix F.1. The code is written in Matlab syntax (Appendix F.2 and F.3). The element assembling code was written by Mike Taylor (Appendix F.4). Notations used in the finite element method for the biofilm model are explained in Appendix E.1.1.

## 9.6 Computational Results

Other biological parameters were found from batch experiments in this study. They are listed in Table 9.1. Several different studies showed that biofilm density lies in the range of 20-168 $kgm^{-3}$[3][21][60] for Methanotroph or toluene and phenol oxidizers. A value of 60 $kgm^{-3}$ was assumed for the biofilm density in the calculations. The concept of transformation capacity ($T_c$) was used for TCE degradation by a resting cell system. Batch study gave different values. It is not a fixed number, depending on cell condition. Adding formate to the system results in the enhancement of TCE degradation rate and transformation capacity[43][22]. The maximum value obtained here is 0.02 mg TCE/mg cell. For a fully developed biofilm system with continuous exposure to toluene, TCE associated toxicity might be much less (Woo, 1998)[83]. In this model simulation, $T_c = 0.5, 1, 5, 10$ were tested respectively to see different levels of toxicity. Bulk concentrations of toluene and TCE were set at 4 ppm and 1 ppm.

Table 9.1: Parameters Used in the Biofilm Model Calculation

| Parameters | Value | Unit |
|---|---|---|
| toluene rate constant: $k_1$ | 8.4385 | mg/mg/day |
| TCE rate constant: $k_2$ | 1.5783 | mg/mg/day |
| toluene saturation parameter: $K_1$ | 1.106 | mg/L |
| TCE saturation parameter: $K_2$ | 1.524 | mg/L |
| toluene yield coefficient: $Y$ | 0.4872 | mg cell/mg toluene |
| toluene diffusivity in water: $D_1$ | 0.8899 | $cm^2$/day |
| TCE diffusivity in water: $D_2$ | 0.78 | $cm^2$/day |
| toluene diffusivity in biofilm: $D_{f1}$ | 0.2452 | $cm^2$/day |
| TCE diffusivity in biofilm: $D_{f2}$ | 0.2150 | $cm^2$/day |
| toluene liquid film thickness: $L_1$ | 0.0020 | cm |
| TCE liquid film thickness: $L_2$ | 0.0019 | cm |
| biofilm density: $X_f$ | 60 | mg biomass/$cm^3$ |
| total decay constant: $b'$ | 0.68 | 1/day |

In the numerical simulation, accuracy and convergence of the finite element approximate solution improved as the mesh $\Omega^h$ was refined. 50 nodes with a progressional ratio of 1.05 was determined to produce a smooth solution. Toluene and TCE concentration and active biomass distribution in the biofilm are plotted in Figures 9.3 and 9.4. Under this toluene concentration, the effective biofilm thickness was about 65 $\mu$m. TCE related toxicity didn't affect this value. The same toluene consumptions were achieved in all cases (Figure 9.5). However, TCE degradation in the biofilm was quite different. Small $T_c$ means high toxicity which gives less TCE degradation, and the flux of TCE into the biofilm is small (Figure 9.6). Increasing $T_c$ increases TCE removal capacity of the biofilm. Results with $T_c = 5$ and $T_c = 10$ are almost the same. Under this condition of 1 ppm bulk TCE concentration, $T_c$ =5 mg/mg cell can be viewed as no product toxicity. This conclusion agreed with what Anderson (1994)[2] assumed in their research. The active biomass results are also consistent with the calculation results of TCE concentration profile. Active biomass greater than one near the surface of biofilm could be explained as that the original biomass density was set small. Computer simulation results show that when $T_c$ is small, transformation product toxicity is significant. It can not be neglected in the process of design.

Toluene as a primary growth substrate is very important to maintain the activity of enzymes. Arcangeli and Arvin (1997)[3] developed a biofilm model

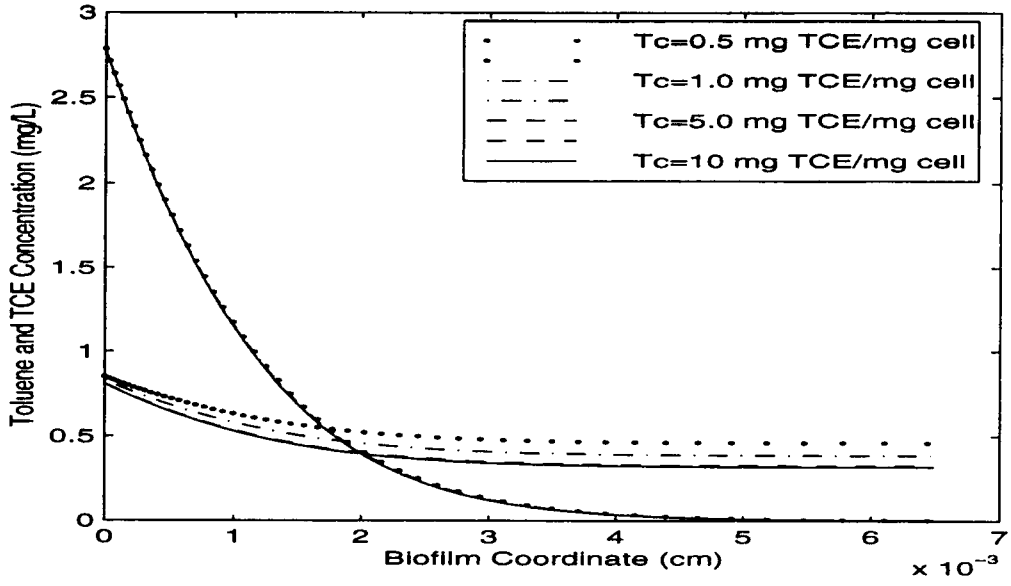



Figure 9.3: Toluene and TCE Concentrations in the Biofilm

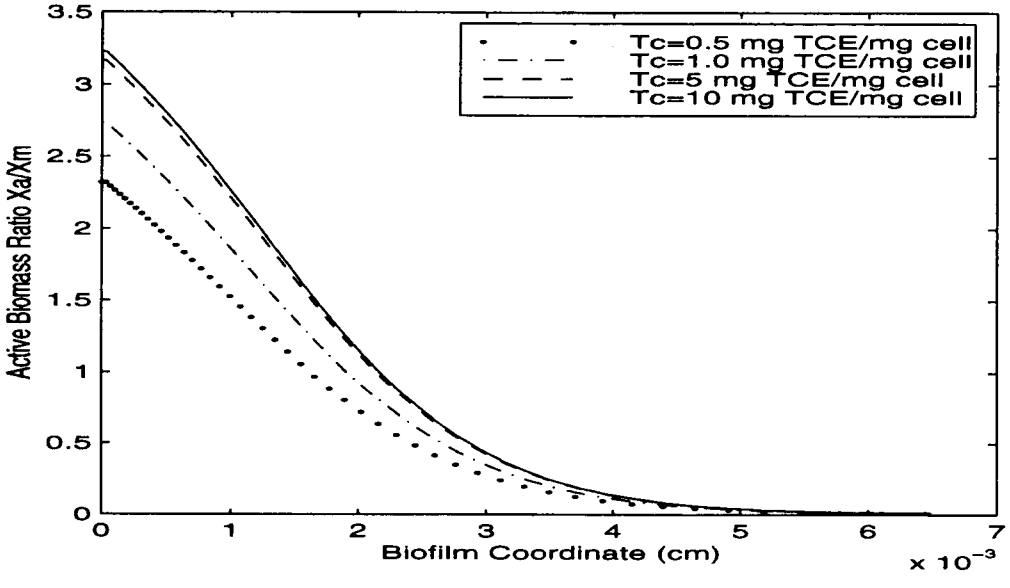



Figure 9.4: Active Biomass Distributions in the Biofilm

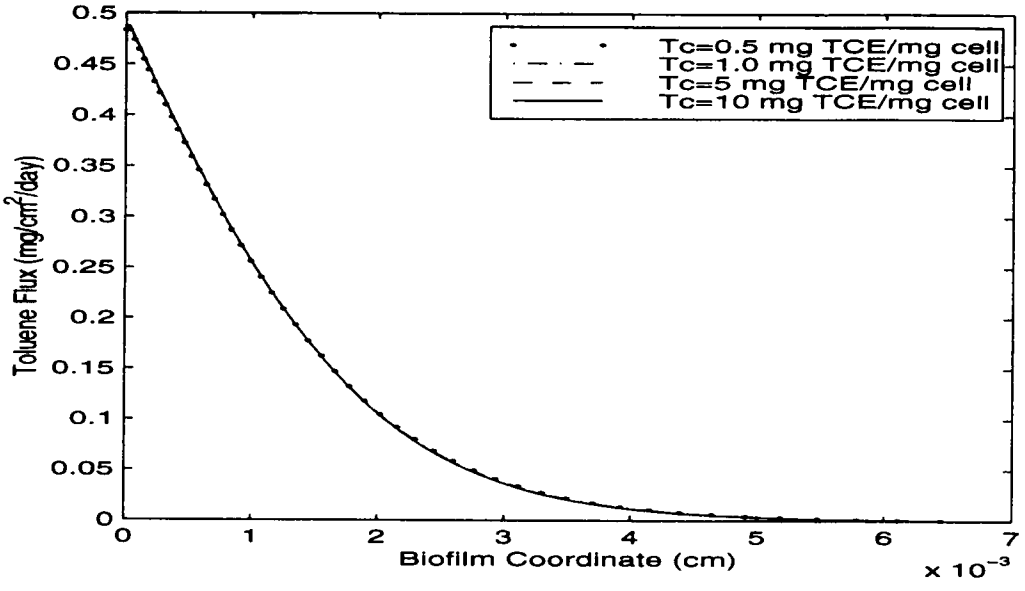



Figure 9.5: Toluene Flux in the Biofilm

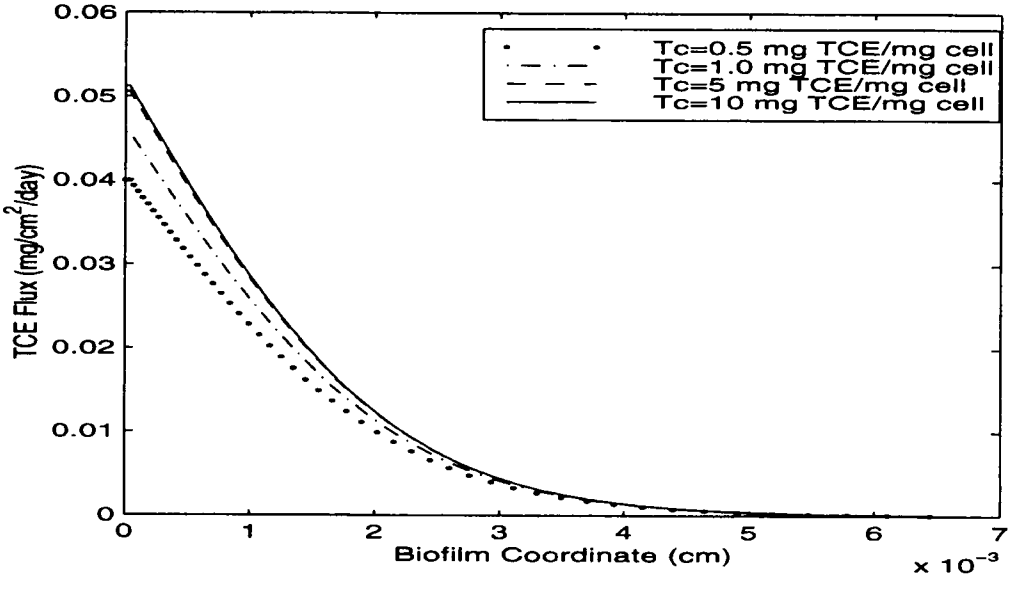



Figure 9.6: TCE Flux in the Biofilm

for TCE degradation by toluene-oxidizing bacteria. Although no information was provided about TCE toxicity, TCE cooxidation activity was corrected by multiplying a toluene concentration related term in the form of $S_{tol}/(S_{tol} + K_s)$ in the TCE reaction equation. In this research, the active TCE degradation cells were not only correlated by the accessment of toluene, but also by the toxicity of TCE transformation products in every discretized biofilm subunit. Computational results with bulk toluene concentrations set at 1 ppm, 3 ppm, and 5 ppm are shown in Figures 9.7, 9.8, 9.9 and 9.10. Increasing toluene concentration increases the depth of effective biofilm thickness, and also increases the amount of active biomass. The increasing of toluene flux to the biofilm was more than the increasing of TCE flux (Figure 9.11). The degradation of TCE in the biofilm was improved. Further increasing of toluene from 5 ppm, to 7 ppm and 10 ppm (Figure 9.12) didn't improve TCE degradation significantly, especially near the surface of the biofilm; TCE degradations were almost the same for these three toluene concentrations. This indicates toluene competitive inhibition to the TCE cometabolism. The calculation was carried out by using $T_c$ = 0.5 mg TCE/mg cell.

TCE concentrations were also investigated in toluene and TCE degradation in the biofilm. In the simulation, bulk toluene concentration was fixed at 5 ppm, and TCE concentrations were set at 0.5 ppm, 1 ppm, and 1.5 ppm, respectively. TCE

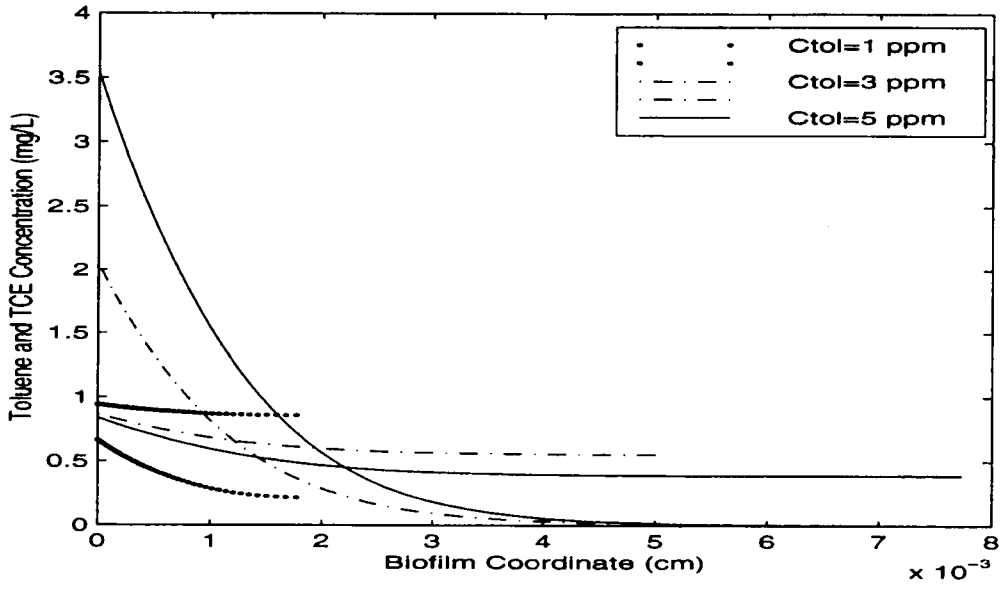



Figure 9.7: Toluene and TCE Concentrations in the Biofilm

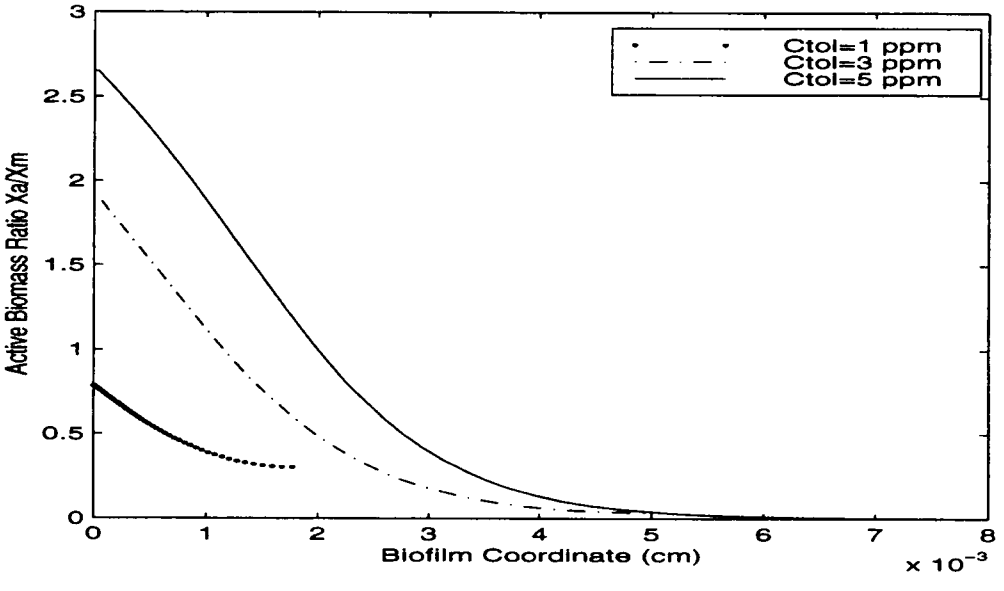



Figure 9.8: Active Biomass in the Biofilm

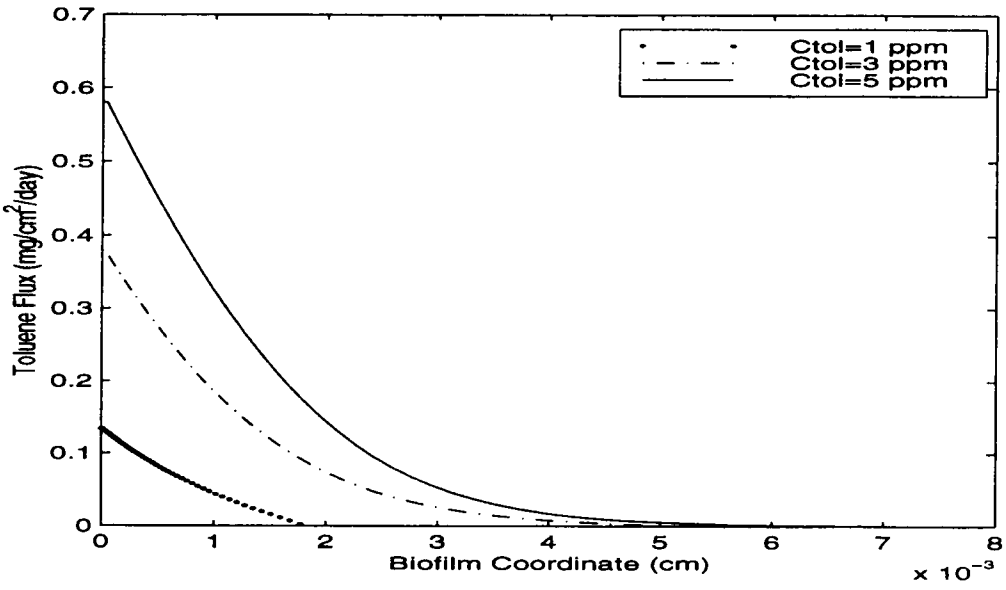



Figure 9.9: Toluene Flux in the Biofilm

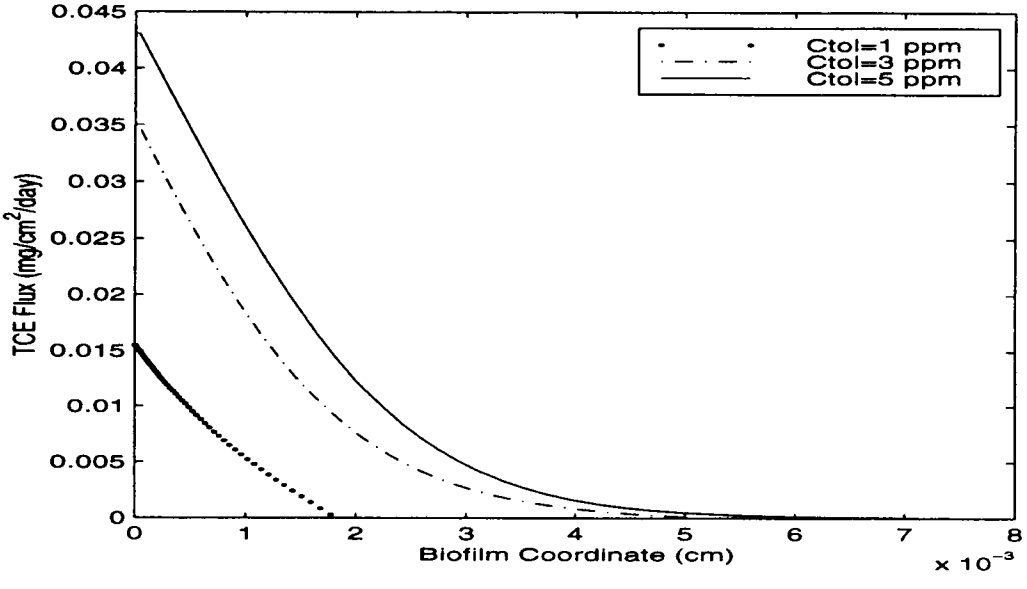



Figure 9.10: TCE Flux in the Biofilm

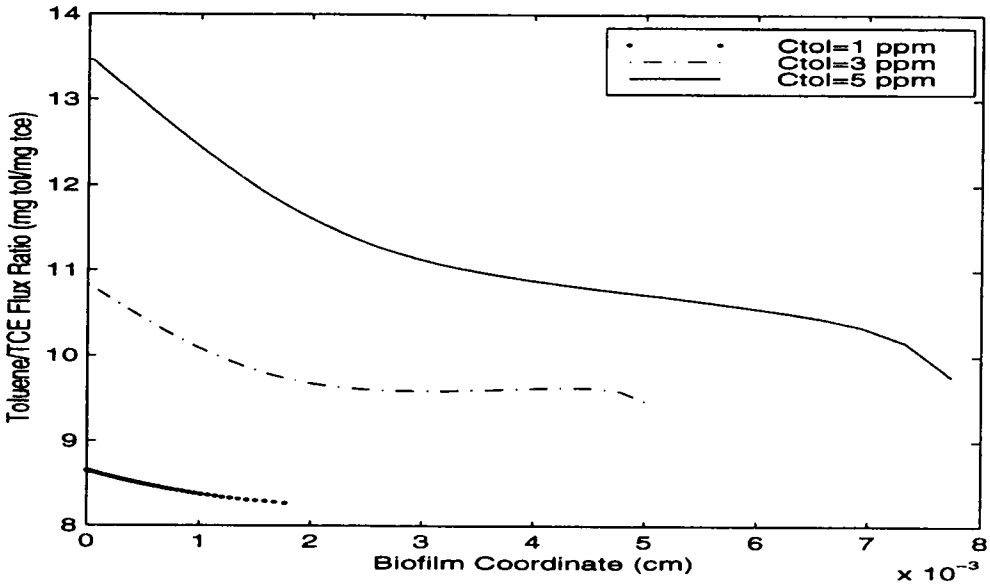



Figure 9.11: Toluene/TCE Flux Ratio in the Biofilm

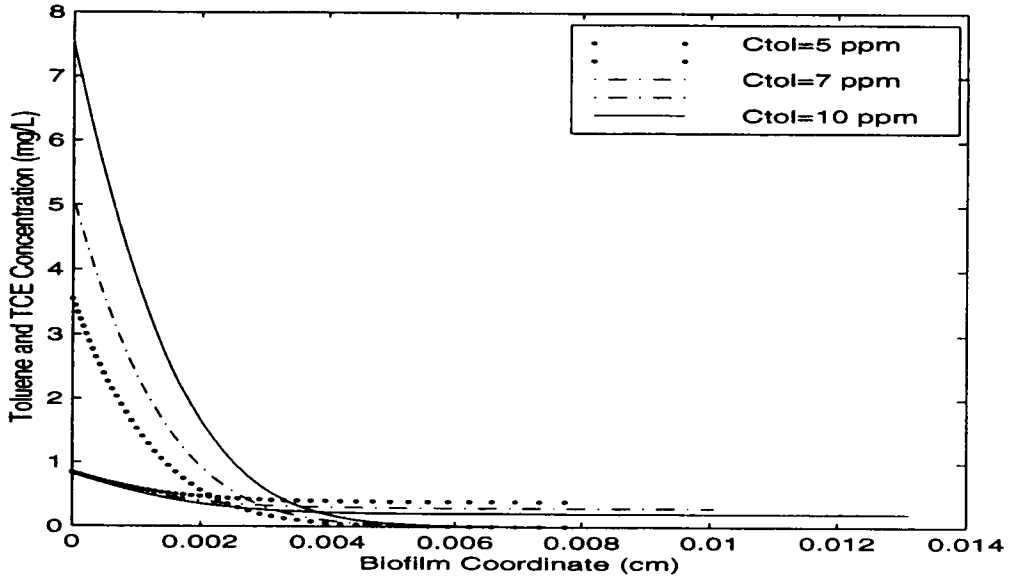



Figure 9.12: Toluene and TCE Concentrations in the Biofilm

concentration has a great effect on active biomass in the biofilm and its degradation (Figures 9.13 and 9.14). TCE removal efficiency dropped from 50% to 40% in the biofilm with bulk TCE concentration raised from 0.5 to 1.5 ppm. Because the tested TCE concentration range is relatively small compared to toluene concentration, toluene degradation rate was not affected significantly (Figure 9.15). It can be predicted that further increasing of the TCE concentration will result in the decreasing of toluene flux. The flux ratio of toluene to TCE was decreased (Figure 9.17) due to the increasing of TCE flux (Figure 9.16). The effective thicknesses of biofilm were: 80 $\mu$m, 77 $\mu$m, and 75 $\mu$m, respectively. It can be seen that the influence of TCE concentration to the effective thickness of biofilm is not as significant as toluene.

Mass transfer also plays an important role in the biodegradation. Since there is always a liquid film around the biofilm, mass transfer resistance causes a concentration gradient across this liquid film. Flow conditions in the bioreactor decides the mass transfer resistance. Three different levels of liquid film were examined: with one calculated from reactor operation condition ($L = [0.0020\ 0.0019]$ cm for toluene and TCE), the others 50% smaller of $L$, and 100% smaller of $L$. Bulk concentrations were set to 5 ppm toluene and 1 ppm TCE. The thinner the liquid film, the higher substrate concentration was achieved at the interface of liquid film and biofilm (Figure 9.18), and more substrates would come into the biofilm

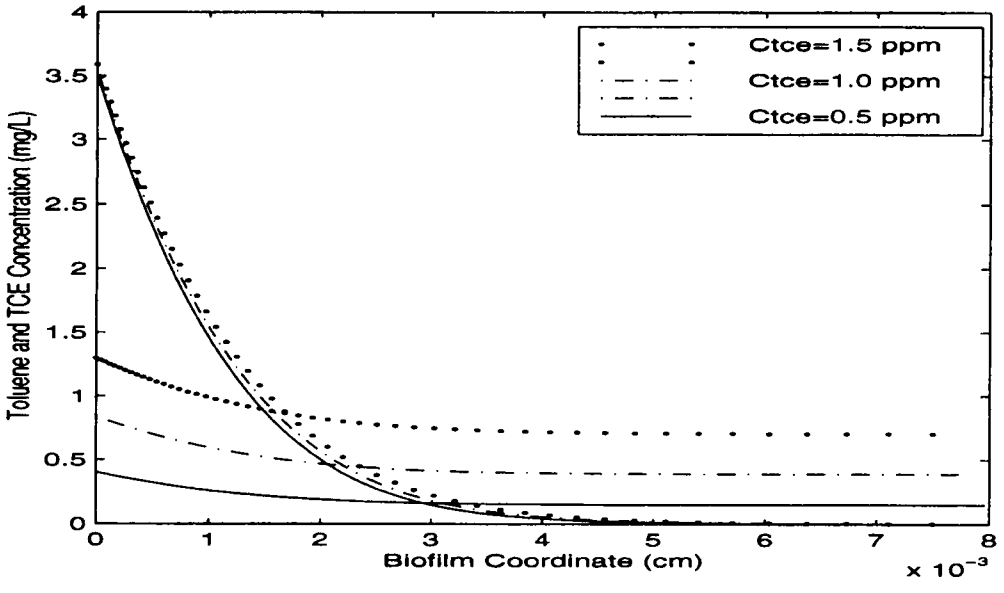



Figure 9.13: Toluene and TCE Concentrations in the Biofilm

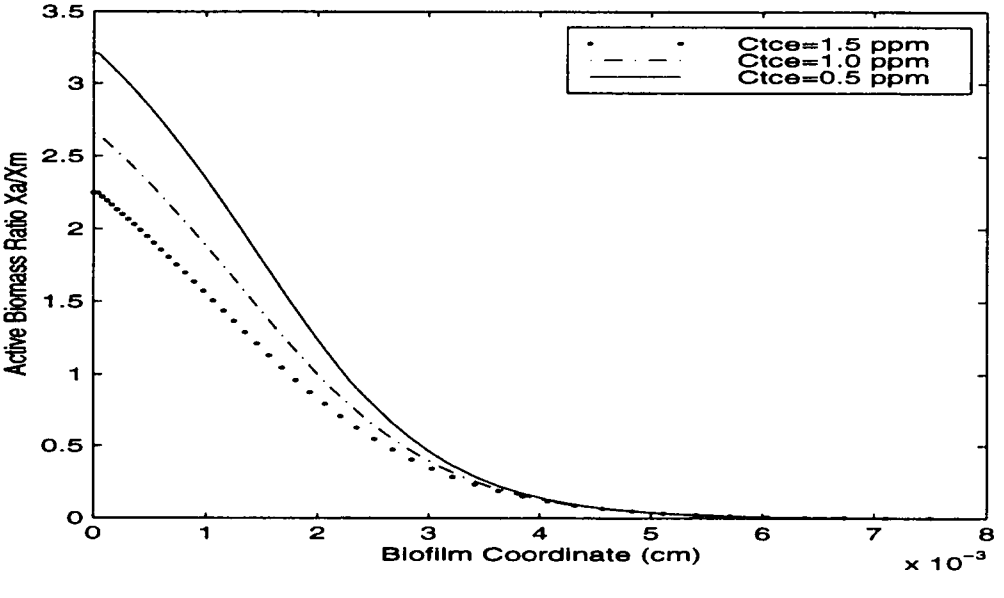



Figure 9.14: Active Biomass in the Biofilm

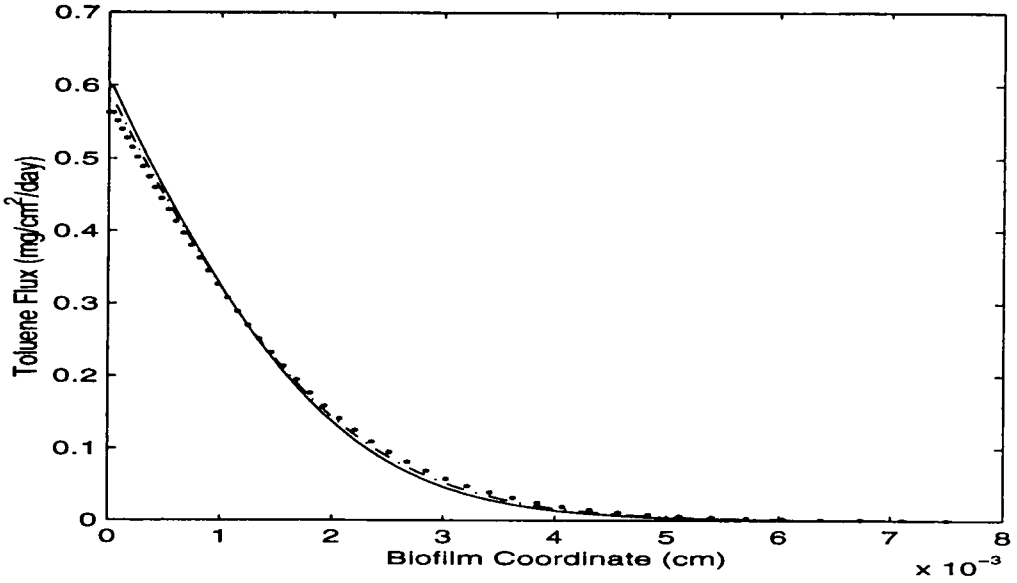



Figure 9.15: Toluene Flux in the Biofilm

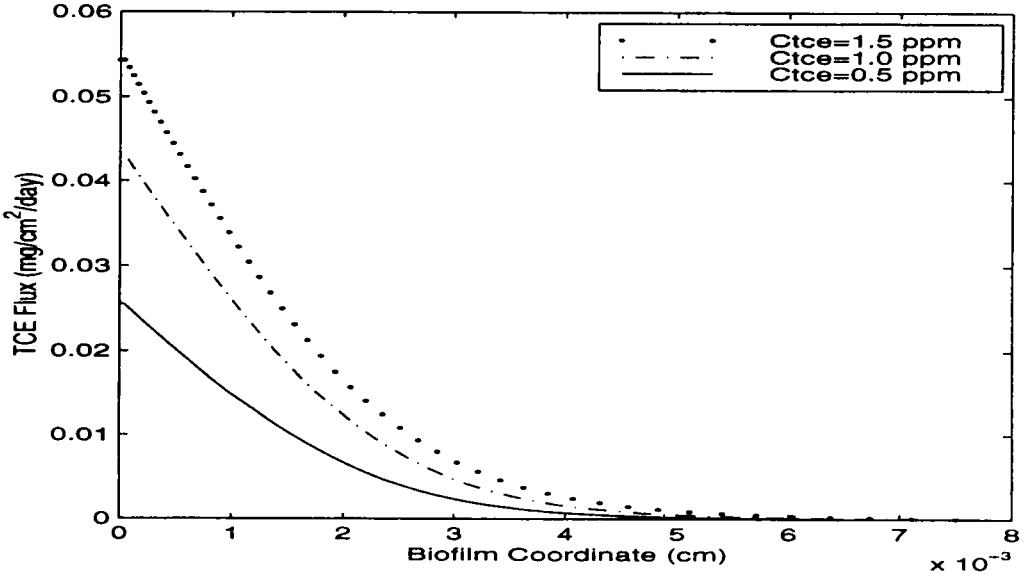



Figure 9.16: TCE Flux in the Biofilm

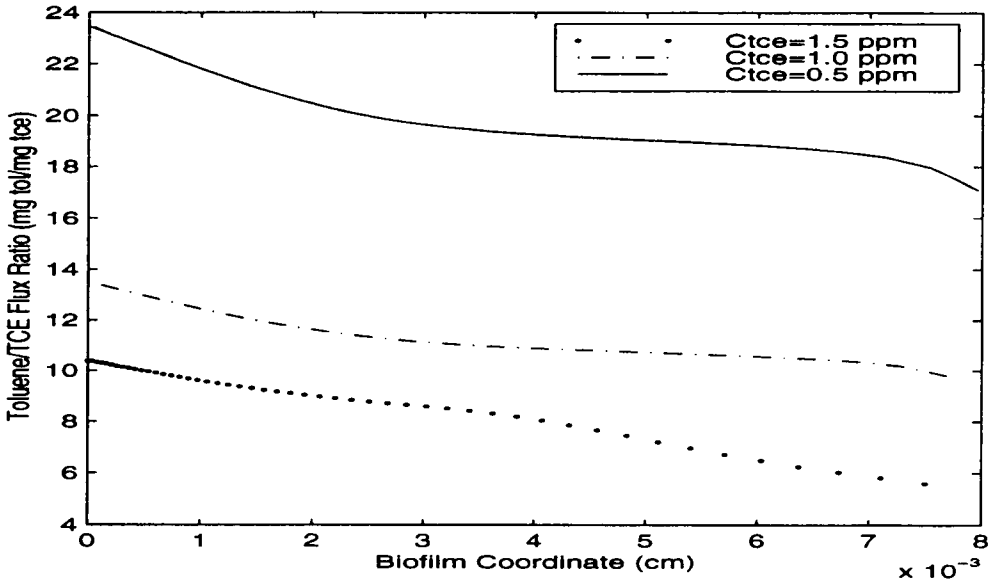



Figure 9.17: Toluene/TCE Flux in the Biofilm

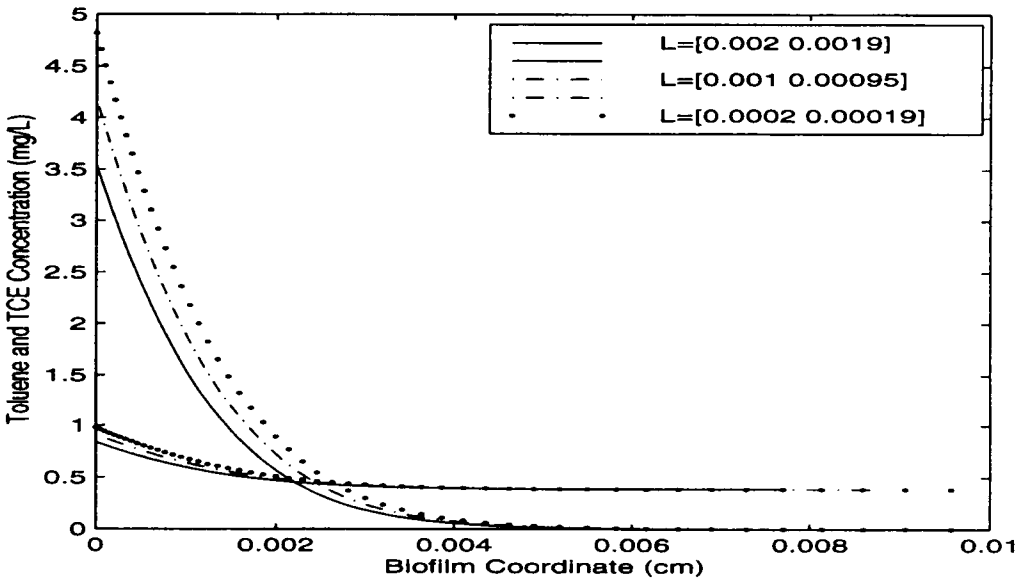



Figure 9.18: Toluene and TCE Concentrations in the Biofilm

(Figures 9.19 and 9.20). The active biomass is a function of both toluene and TCE concentration. As the increasing flux of toluene was bigger than the increasing flux of TCE (Figure 9.21), the active biomass still increased as mass transfer resistance decreased (Figure 9.22). The effective thickness of biofilm increased from 77 $\mu$m, 87 $\mu$m, to 96 $\mu$m.

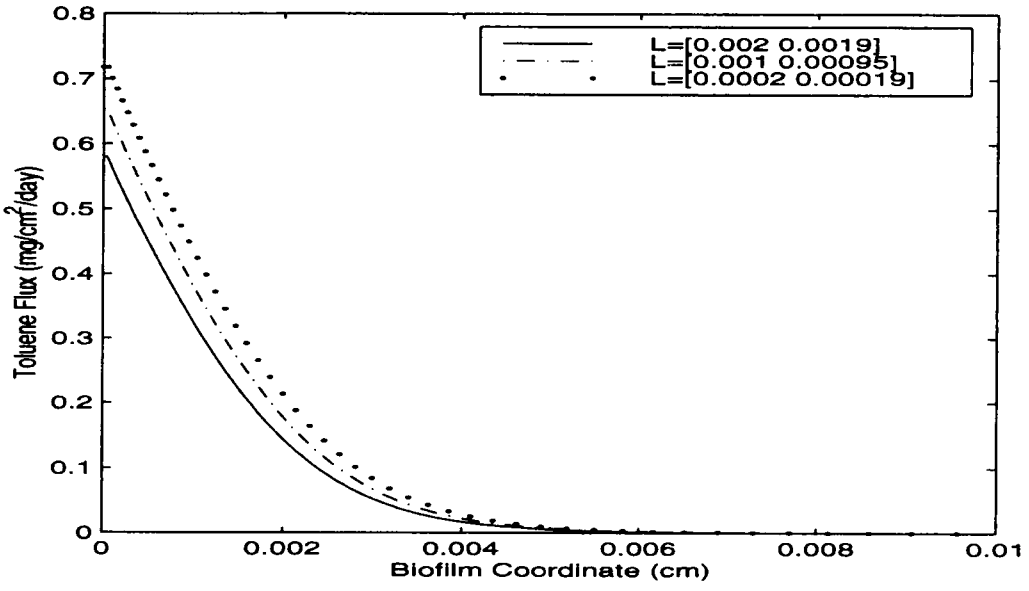



Figure 9.19: Toluene Flux in the Biofilm

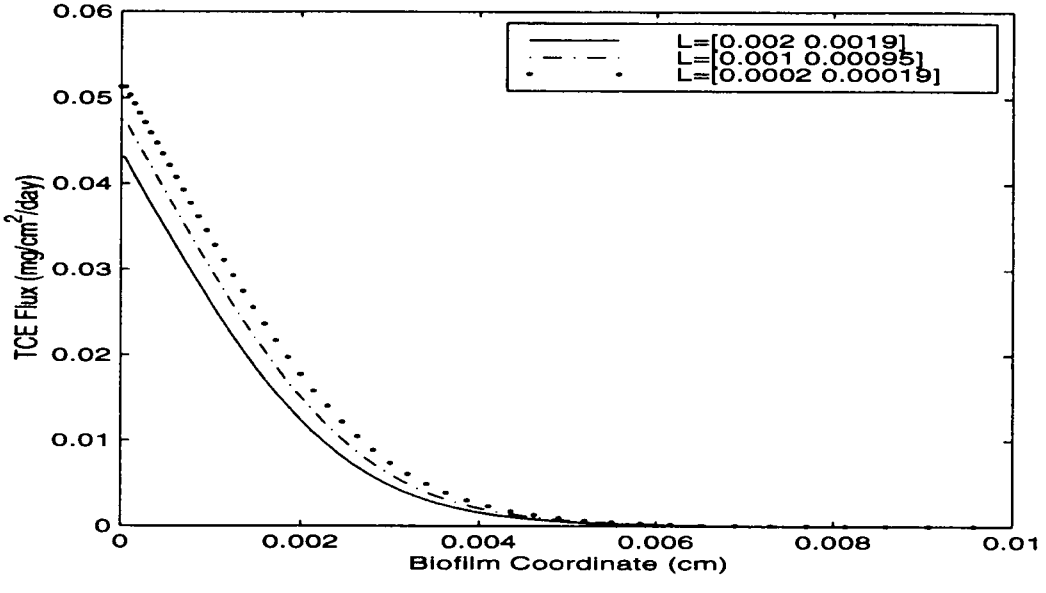



Figure 9.20: TCE Flux in the Biofilm

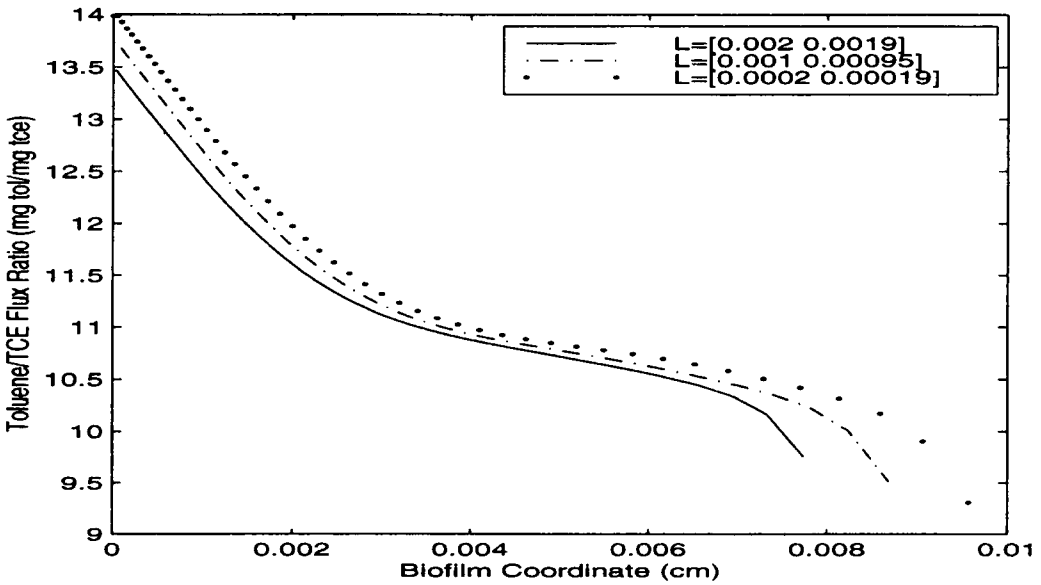



Figure 9.21: Toluene/TCE Flux in the Biofilm

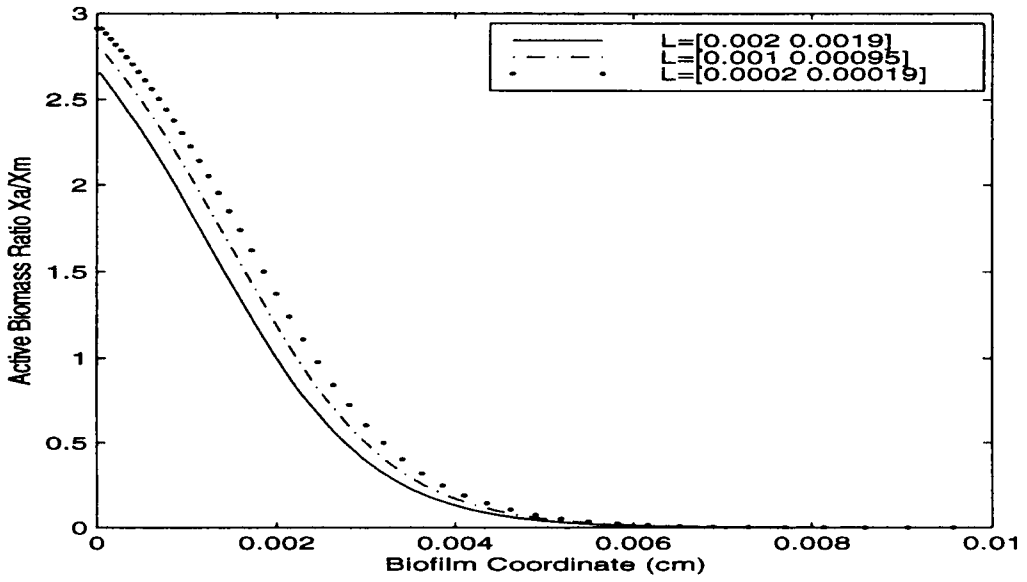



Figure 9.22: Active Biomass in the Biofilm

# Chapter 10

# Bioreactor Model

Mass transfer and biochemical reaction co-existing in the biofilm reactor makes the biotransformation process very complicated. The characteristics of the flow of bulk fluid affects the performance of the bioreactor also. Modeling of the bioreactor is essential for the further understanding of fundamental chemical and microbiological processes of TCE degradation. The entire process for the biodegradation of TCE and toluene is described in Figure 10.1. Microorganisms grow on the surface of packing material in a form of biofilm. As the fluid passes through the column, TCE and toluene are transferred from bulk fluid through a liquid film to the biofilm, where they undergo biodegradation. A bioreactor model was developed based on the steady-state biofilm model with TCE transformation product toxicity discussed in the previous chapter. Combined with dispersion, convection,

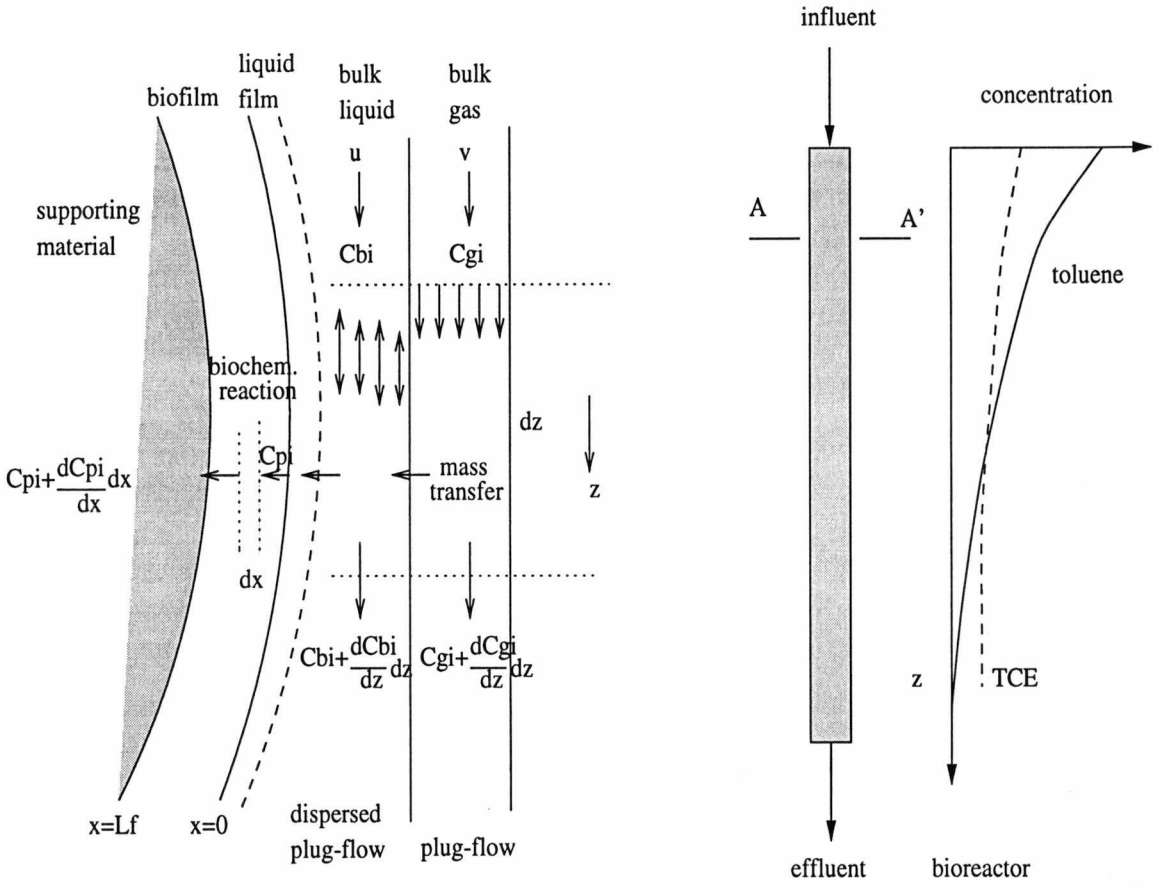



Figure 10.1: Illustrations of Numerical Model for the Biofilm and Bioreactor

mass transfer between biofilm phase and liquid phase, and physical equilibrium between between gas phase and liquid phase, the model could be applied to interpolate experimental data, predict results, optimize the whole process, and reactor design in the future.

## 10.1 Model Development

The principle assumptions made in the biofilm reactor model are as follows:

- Reactor operates under isothermal conditions.
- Substrates are uniformly distributed in the radial cross-section of the reactor in both gas phase and liquid phase.
- Plug flow is assumed in the gas phase.
- Concentration of suspended biomass is neglected compared to the attached biomass.
- Solution is diluted, so Henry's law can be applied.

Besides the equations in the biofilm, mass balances of toluene and TCE in the liquid phase and gas phase should also be made. In liquid phase, the terms needed to be considered include convection, axial dispersion, mass transfer between liquid phase and biofilm phase, and mass transfer between liquid phase and gas phase:

$$\theta_L E_i \frac{d^2 C_{bi}}{dz^2} - u(1+R)\frac{dC_{bi}}{dz} - \theta_L k_{Li} a (C_{bi} - C_{pi}|_{x=0}) - \theta_L k_{Gi} a (C_{bi} - C_i^*) = 0 \quad (10.1)$$

where $i = 1, 2$ refers to toluene and TCE, $\theta_L$ is the liquid holdup, $a$ is the total surface area per unit volume of packed bed, $u$ is the superficial velocity of influent fluid, $R$ is the recycle ratio, $k_{Gi}$ is the mass transfer coefficient of toluene or

TCE between liquid phase and gas phase, $k_{Li}$ is the liquid phase mass transfer coefficient. $C_i^*$ is the gas-liquid interfacial concentration of toluene or TCE, $E_i$ is the dispersion coefficient which can be estimated from Hiby's relation[59]:

$$E = 0.67D + 0.6d_0u[1 + 6.7(\frac{D}{d_0u})^{0.5}] \tag{10.2}$$

where $d_0$ is the Sauter mean diameter and D is the molecular diffusion coefficient. Assuming most mass transfer resistance comes from the liquid film, the gas phase mass transfer coefficient could be considered to be the same as liquid mass transfer coefficient $k_{Li}$; and $k_{Li}$ can be calculated out by:

$$k_{Li} = \frac{D_i}{L} \tag{10.3}$$

where $D_i$ is the diffusion coefficient, and $L$ is the thickness of the liquid film which can be estimated from the method described in the previous chapter. The evaluation of liquid hold-up is from chapter 6.4. The above second order differential equations are subjected to the following boundary conditions: at $z = 0$,

$$\theta_L E_i \frac{dC_{bi}}{dz} = u(1 + R)(C_{bi} - {C_{bi}}^{in}) \tag{10.4}$$

and at $z = L_r$,

$$\frac{dC_{bi}}{dz} = 0 \tag{10.5}$$

where $L_r$ is the length of the reactor, ${C_{bi}}^{in}$ is concentration of toluene or TCE in the inlet of the reactor, which is a function of both influent and effluent concentrations:

$${C_{bi}}^{in} = \frac{{C_{bi}}^{if} + R{C_{bi}}^{ef}}{1 + R} \tag{10.6}$$

in which ${C_{bi}}^{if}$ is the influent toluene or TCE concentration, and ${C_{bi}}^{ef}$ is the effluent toluene or TCE concentration.

At steady-state, gas toluene and TCE concentrations in the storage column don't change. They equal equilibrium concentrations in the effluent. Thus, mass balances of toluene and TCE in the gas phase along the reactor are:

$$-\frac{dC_{gi}}{dz}v + \theta_G k_{Gi} a(C_{bi} - C_i^*) = 0 \tag{10.7}$$

with initial condition at $z = 0$:

$$C_{gi} = {C_{gi}}^{ef} \tag{10.8}$$

where $i = 1, 2$ for toluene and TCE, $v$ is the gas superficial velocity.

## 10.2 Dimensionless Form of Model Equation

In order to facilitate mathematical operations, model equations needed to be non-dimensionalized. Dimensionless variables were introduced:

$$\bar{C_{bi}} = \frac{C_{bi}}{K_i}, \bar{C_{gi}} = \frac{C_{gi}}{K_i}, \zeta = \frac{z}{L_r}$$

Mass balance equations are then transformed into the following expression: in liquid phase,

$$\frac{1}{Pe_i}\frac{d^2\bar{C_{bi}}}{d\zeta^2} - (1+R)\frac{d\bar{C_{bi}}}{d\zeta} - \alpha_i(\bar{C_{bi}} - \bar{C_{pi}}) - \beta_i(\bar{C_{bi}} - \frac{\bar{C_{gi}}}{H_i}) = 0 \tag{10.9}$$

where $H_i$ is the Henry's law constant for toluene or TCE. $Pe_i$, $\alpha_i$, and $\beta_i$ are dimensionless groups. They are defined as:

$$Pe_i = \frac{L_r u}{\theta_L E_i}, \text{ (Peclet number)}$$

$$\alpha_i = \frac{L_r \theta_L}{u} / \frac{1}{k_{Li} a}, \text{ (Liquid-Biofilm mass transfer number)}$$

$$\beta_i = \frac{L_r \theta_L}{u} / \frac{1}{k_{Gi} a}, \text{ (Liquid-Gas mass transfer number)}$$

The boundary conditions are changed to: at $\zeta = 0$,

$$\frac{d\bar{C}_{bi}}{d\zeta} = Pe_i(1+R)(\bar{C}_{bi} - \bar{C}_{bi}^{\,in}) \tag{10.10}$$

and $\zeta = 1$,

$$\frac{d\bar{C}_{bi}}{d\zeta} = 0 \tag{10.11}$$

Dimensionless form in the gas phase will be:

$$-\frac{d\bar{C}_{gi}}{d\zeta} + \gamma_i(\bar{C}_{bi} - \frac{\bar{C}_{gi}}{H_i}) = 0 \tag{10.12}$$

where $\gamma_i$ is the gas phase mass transfer number, defined as

$$\gamma_i = \frac{L_r \theta_G}{v} / \frac{1}{k_{Gi} a}$$

where $\theta_G$ is the gas holdup in the column. The initial condition is:

$$\bar{C}_{gi}^{\,in} = \frac{C_{gi}^{\,in}}{K_i} \tag{10.13}$$

## 10.3 Solving Procedure

After being non-dimensionalized, the convection, dispersion, and mass transfer equations for both toluene and TCE in the liquid phase down the reactor were arranged in such a way (Equation 10.9) that Peclet numbers are not so big to cause numerical oscillation[6]. Finite element method was also used for solving the bulk fluid equations coupled with biofilm equations. Due to the unknown value of concentrations in the interface of liquid phase and biofilm phase, the system was solved by iteration. Figure 10.2 illustrates the solving procedure. Biofilm surface concentrations of TCE and toluene were set as initial guess values to solve bulk concentration profiles in the reactor, then go to the inner loop for computing concentration profiles in the biofilm phase. With those new values of biofilm surface concentrations, the bulk fluid equations were resolved. This process was repeated until new values and old values of bulk concentrations were within the computational tolerance.

## 10.4 Finite Element Method

Assuming $q$ is the state variable, a weak statement for equations in the bulk fluid can be written in following expression:

$$GWSq^N = \int_\Omega \phi_i[-\frac{1}{Pe}\frac{d^2q^N}{d\zeta^2} + \frac{dq^N}{d\zeta} + \alpha(q^N - T|_{\eta=0}) + \beta(q^N - \frac{Q}{H})]d\tau = 0 \quad (10.14)$$

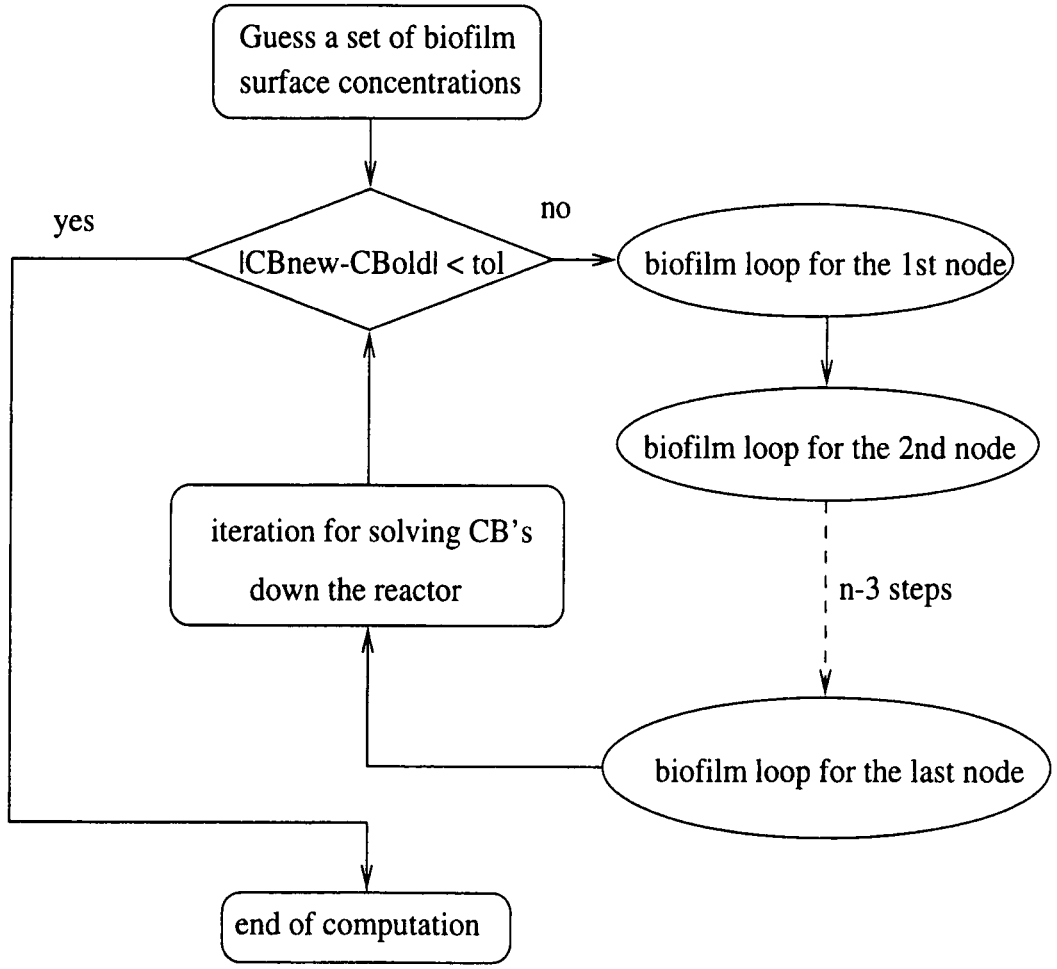



Figure 10.2: Solving Procedure for Concentrations in the Bioreactor

where $Q$ is the state variable for toluene or TCE concentration in the gas phase; $\phi_i$ are sets of trial functions that span the physical domain. Integrating the above equation, a weak statement written in element matrices for each component turns

out to be:

$$
\begin{aligned}
GWSCBi \;=\; & \frac{1}{Pe_i}[A211]\{CBi\}_e + (1+R)[ONE]\{CBi\} - [ONE]\{CBi^{if}\} \\
& -R[ONE]\{CBi^{ef}\} + (1+R)[A201]\{CBi\}_e + \alpha_i[A200]\{CBi\}_e \\
& -\alpha_i[A200]\{CPi\}_e|_{\eta=0} + \beta_i[A200]\{CBi\}_e \\
& -\frac{\beta_i}{H_i}[A200]\{CGi\}_e = \{0\} \qquad (10.15)
\end{aligned}
$$

where $i = 1, 2$, for toluene and TCE; [A201] and [A200] are element library matrices (Appendix E.3). In order to deal with equations in the gas phase, which have no second order term, finite difference was introduced[5][7]. Taking Taylor series for CG and using trapezoidal rule with $\theta = 0.5$ gives the following expression:

$$
(CG)_{j+1} = (CG)_j + \frac{\Delta\zeta}{2}\left(\frac{d(CG)_{j+1}}{d\zeta} + \frac{d(CG)_j}{d\zeta}\right) \qquad (10.16)
$$

where $j$ is the node point. Substituting mass balance equation in the gas phase into equation 10.16 in corresponding node and rearranging it yields:

$$
\begin{pmatrix} 0 & 0 \\ -1 & 1 \end{pmatrix}\{CGi\}_e + \gamma_i\frac{l_e}{2}\begin{pmatrix} 0 & 0 \\ 1 & 1 \end{pmatrix}\{CBi\}_e + \frac{\gamma_i}{H_i}\frac{l_e}{2}\begin{pmatrix} 0 & 0 \\ 1 & 1 \end{pmatrix}\{CGi\}_e = \{0\} \qquad (10.17)
$$

where $l_e$ is the length of the element. Thus a weak statement form for gas phase is:

$$
FCGi = [A201F]\{CGi\}_e - \gamma_i[A200F]\{CBi\}_e + \frac{\gamma_i}{H_i}[A200F]\{CGi\}_e = \{0\} \qquad (10.18)
$$

where $i = 1, 2$ refer to toluene and TCE. Matrices [A201F] and [A200F] are shown in Appendix E.3. Since two components in the liquid and gas phase do not interact with each other, Equations 10.15 and 10.18 can be solved separately by Newton's algorithm:

$$\begin{bmatrix} JCBiCBi & JCBiCGi \\ JCGiCBi & JCGiCGi \end{bmatrix} \begin{Bmatrix} \delta CBi \\ \delta CGi \end{Bmatrix}^{p+1} = -\begin{Bmatrix} FCBi \\ FCGi \end{Bmatrix}^{p} \tag{10.19}$$

where

$$JCBiCBi = \frac{1}{Pe_i}[A211] + (1+R)[A201] + \alpha_i[A200] + \beta_i[A200] + (1+R)[ONE] \tag{10.20}$$

$$JCBiCGi = -\frac{\beta_i}{H_i}[A200] \tag{10.21}$$

$$JCGiCBi = -\gamma_i[A200F] \tag{10.22}$$

$$JCGiCGi = [A201F] + \frac{\gamma_i}{H_i}[A200F] \tag{10.23}$$

The template is in Appendix G.1, and the code for solving the whole system is in Appendix G.2, G.3, and G.4. Detailed explanations of the notations used in the finite element method for this bioreactor model are in Appendix E.1.2.

## 10.5 Sample Model Calculation Results

Conditions set for the sample run were: influent TCE and toluene concentrations at 0.2130 mg/L and 33.66 mg/L, respectively. The influent flow rate was 3.02

ml/min and recycle rate was 27.5 ml/min, which made the recycle ratio equate to 9.1. When examining the solution quality, small mesh size was inadequate to get a smooth solution. Numerical oscillation was observed near the inlet of the reactor where the effluent gas stream met the liquid stream. Asymptotic convergence should be achieved on a sufficiently refined mesh $\Omega^h$[6]. Thus, thirty nodes were selected for the reactor in the z direction with progressional ratio 1.1 to meet the accuracy requirement. Thirty nodes were also chosen in the biofilm with progression 1.2 in the $x$ direction. Numerical oscillation and stability were greatly improved by using non-uniform mesh both in the biofilm and in the reactor. Smooth solutions were obtained. The results are shown in Figures 10.3 - 10.9.

Since influent TCE concentration was very low, no toxicity effect was assumed in the model simulation ($T_c$ = 10 mg TCE/mg cell)[2]. The concentration profiles of toluene and TCE within the reactor are similar; that both are decreasing along the reactor indicates biodegradation (Figures 10.3 and 10.4). Small picks of gas phase concentration near the inlet of the reactor resulted from the gas recirculation and fast equilibrium achieved with the liquid phase stream introduced to the column, which was the influent after dilution by the partially recycled effluent. Model predicted removal efficiency for TCE and toluene are 88.12% and 93.28%. However, the experimental measurement data were 92.86 and 100 percent degradation of toluene. The error may come from some parameters chosen

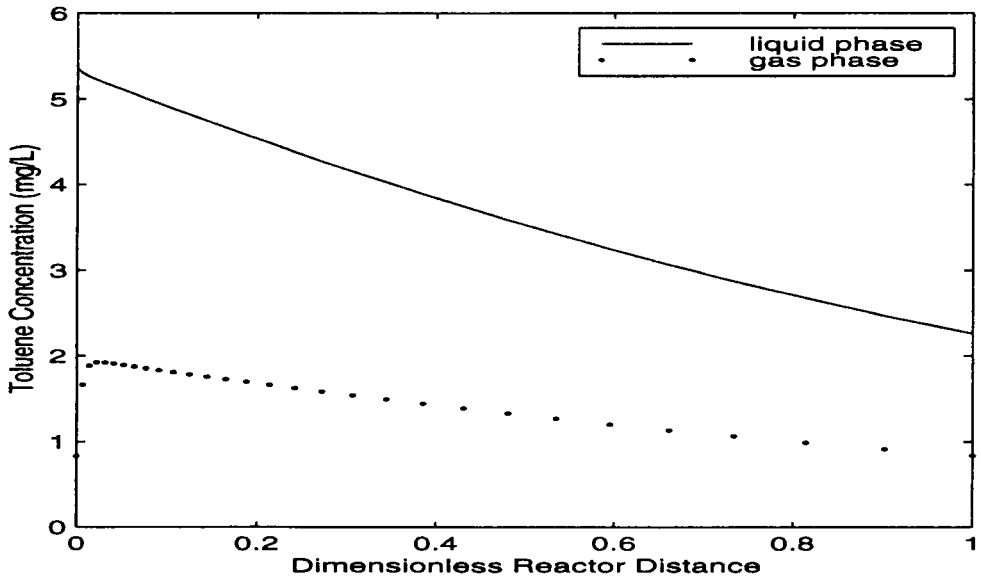



Figure 10.3: Toluene Concentrations in the Bioreactor

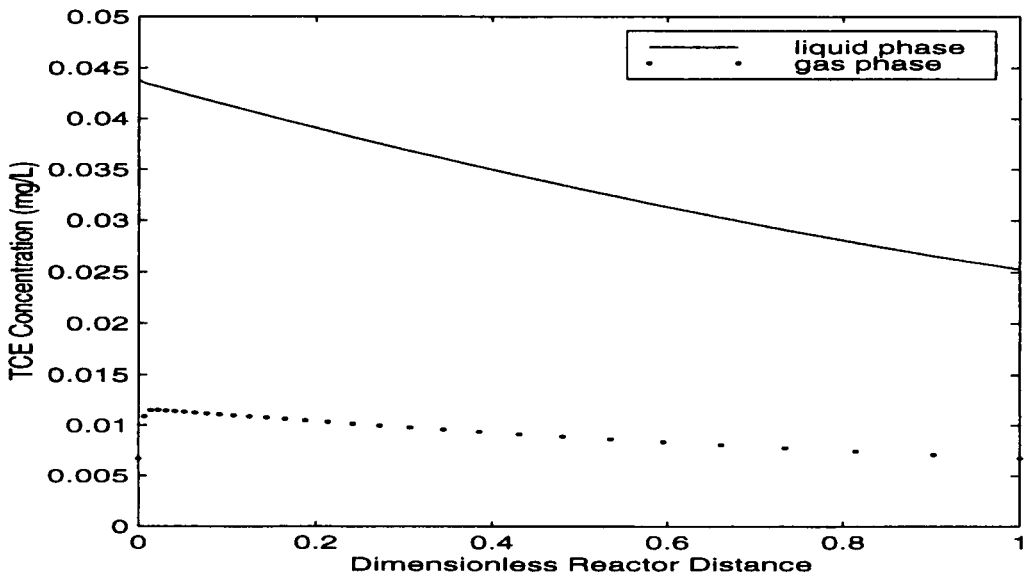



Figure 10.4: TCE Concentrations in the Bioreactor

in the model computation. Toluene concentrations determined the growth of the biofilm. Hence, there was an effective biofilm thickness distribution along the reactor as the model assumed (Figure 10.5). The values are much smaller than could be visualized during the experimental period. The depth of the biofilm and the active biomass within the biofilm determined TCE consumption in the biofilm. As shown by the concentration profiles in the biofilm, the biofilm is deep to toluene (Figure 10.6), where concentration goes to zero, and shallow to TCE (Figure 10.7), in which TCE could only partially penetrated. No TCE degradation existed at the point where no toluene was present. The flux of toluene was much larger than that of TCE (Figure 10.8). They all decreased down to the reactor because of the reduction of concentration gradient. In contrast, the effectiveness factor of TCE is much higher than that of toluene (Figure 10.9). This indicates that in the biodegradation, toluene is diffusion control, while TCE is reaction control. Due to recycling, the entire toluene and TCE concentrations in the reactor were reduced. And the partition of components to the gas phase also lower the concentration levels in the liquid phase. This unique reactor design eliminates the toluene competitive inhibition to the TCE degradation, which is quite common in conventional reactor operations.

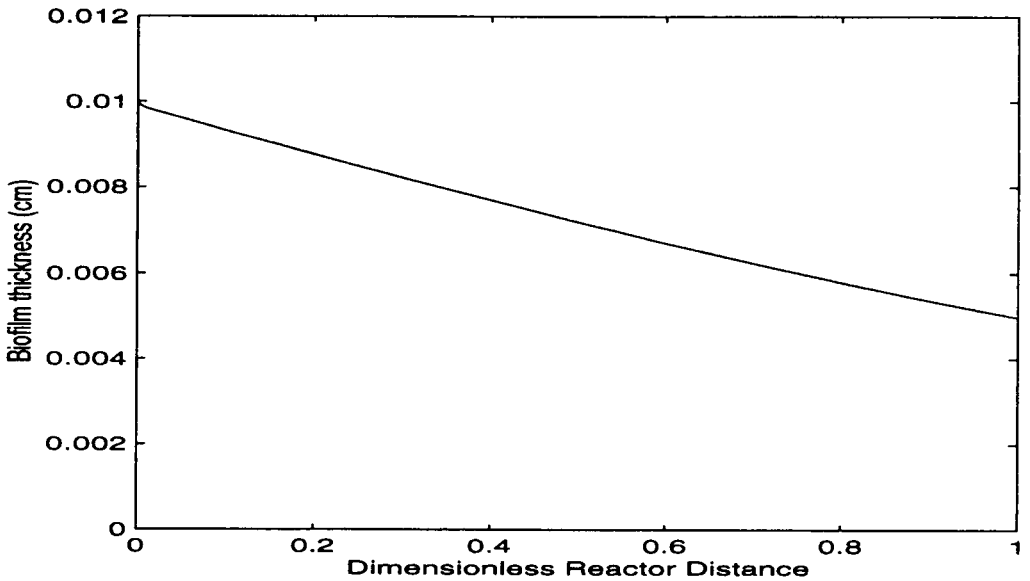



Figure 10.5: Biofilm Thickness Distribution in the Reactor

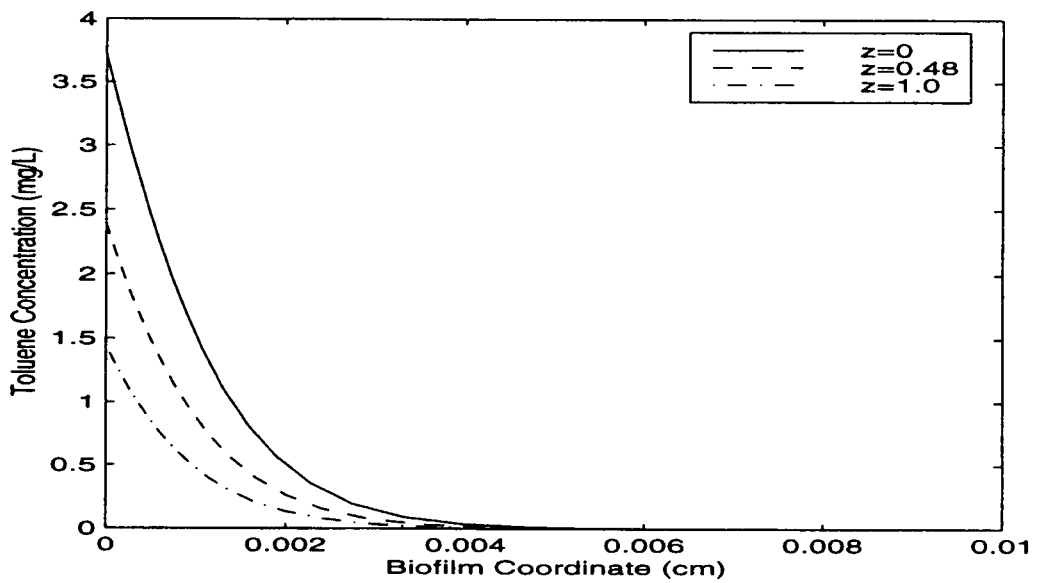



Figure 10.6: Toluene Concentrations in the Biofilm

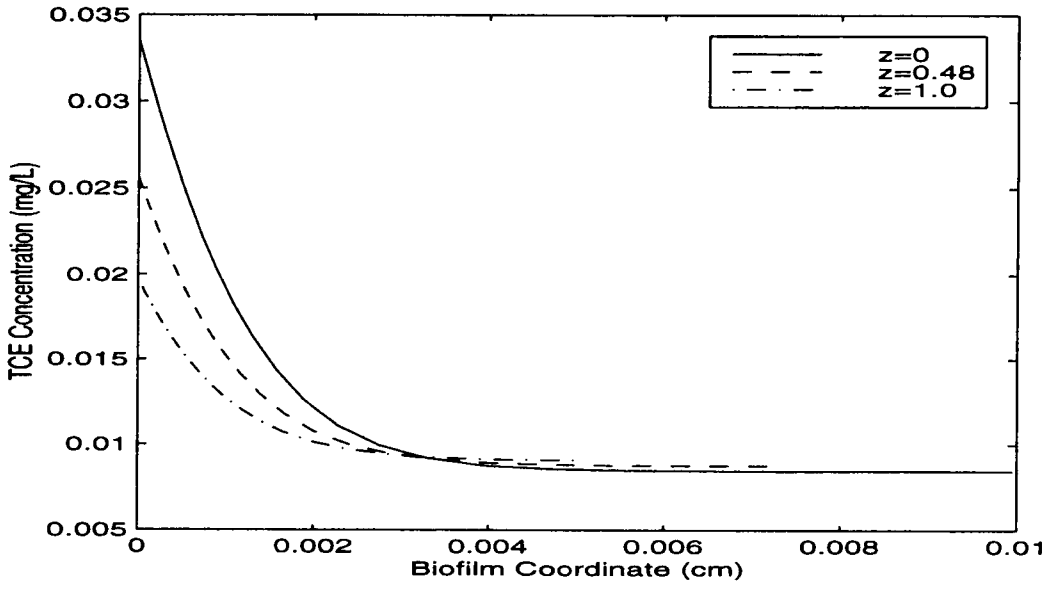



Figure 10.7: TCE Concentrations in the Biofilm

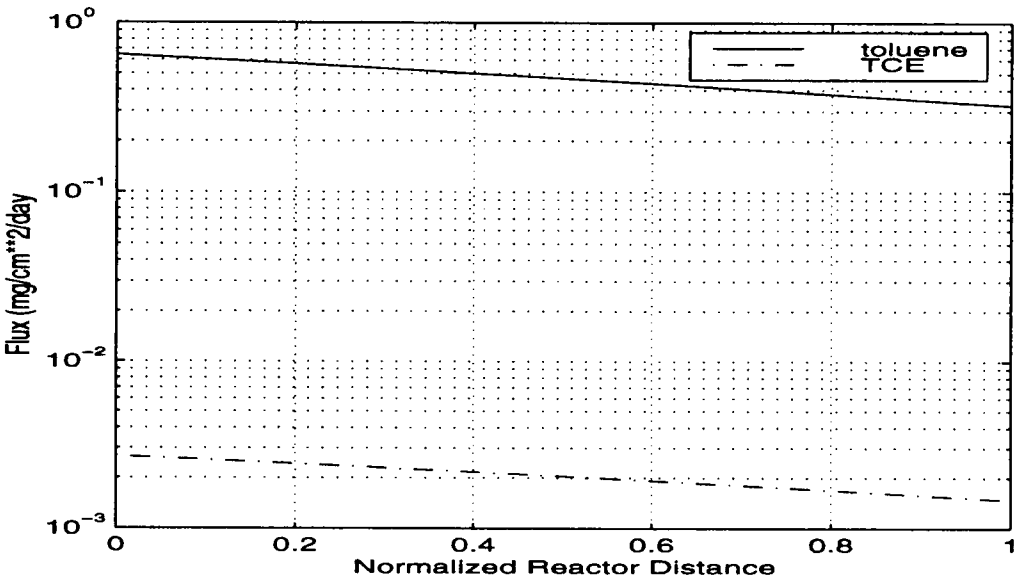



Figure 10.8: Toluene and TCE Flux in the Reactor

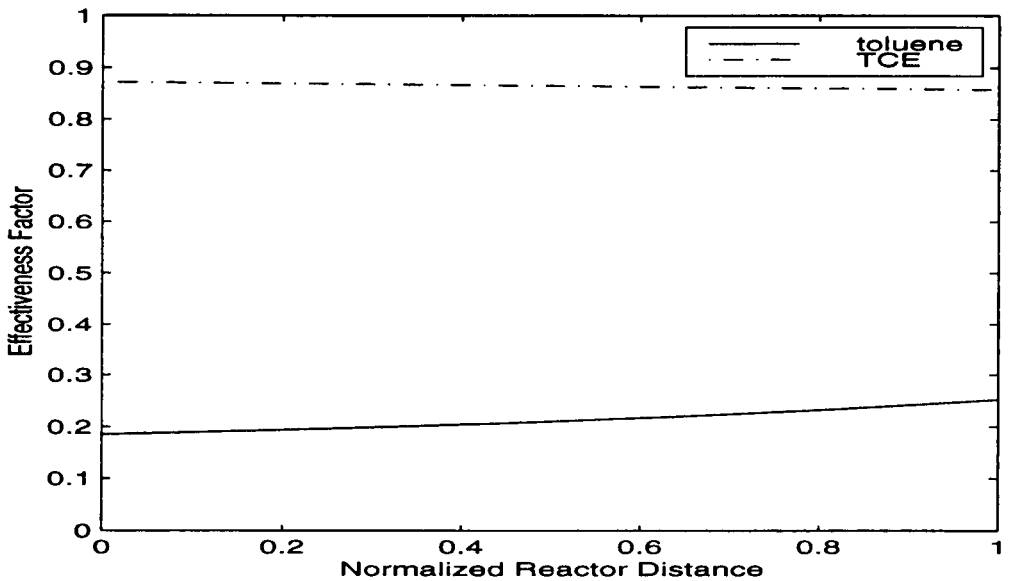



Figure 10.9: Toluene and TCE Effectiveness Factor

## 10.6 Model Sensitivity Analysis

Model sensitivity analysis was carried out by changing different parameters in the model. TCE degradation information can be found when sometimes experiments can hardly reach. Input parameters for the computations are listed in Table 9.1. Other input conditions include: influent flow rate $Q_i$: 3.3 ml/min; influent TCE concentration: 0.75 mg/L; influent toluene concentration: 30.19 mg/L; and recycle rate: 27.5 ml/min. TCE and toluene removal efficiencies were chosen for the final evaluations. The target parameters are: toluene yield coefficient $Y$; TCE transformation capacity $T_c$; specific area for mass transfer; reactor length; TCE

saturation parameter $K_2$; and recycle ratio.

### 10.6.1 Toluene Yield Coefficient

TCE saturation parameter was set to 4 mg/L, and TCE transformation capacity was set to 0.05 mg TCE/mg cell in the following model simulation. Toluene yield coefficient represents growth efficiency by toluene. However, toluene removal was not changed significantly. In the development of the biofilm model, constant biofilm density was assumed. The increasing of cell yield goes to two parts: one to the increasing of active biomass for TCE degradation, the other to the increasing of the depth of the biofilm. The larger the toluene yield coefficient, the more active cells can be obtained, and the more TCE degradation will be gotten. The calculation results verify the point (Figure 10.10). Different from TCE degradation within the biofilm, toluene concentration was always zero at the depth of effective thickness. That's probably the reason why toluene removal efficiency didn't increase much with the changing of its yield coefficient.

### 10.6.2 TCE Transformation Capacity $T_c$

TCE transformation product has been reported to be toxic to the cells and enzymes[26][35][83]. This makes TCE become a recalcitrant compound in the environment. Alvarez-Cohen and McCarty[1] proposed the concept of transfor-

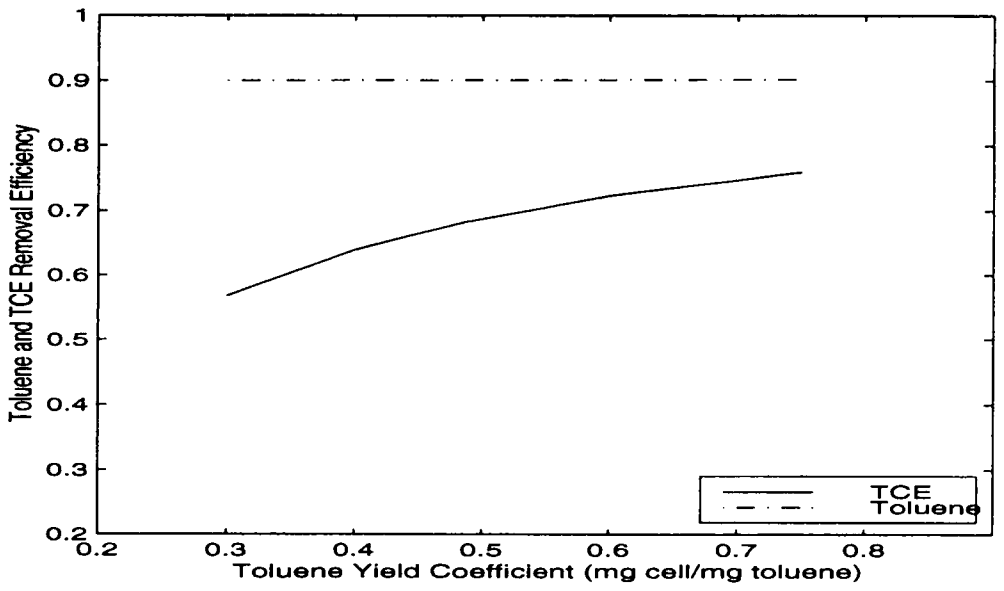



Figure 10.10: Toluene Yield Coefficient Affects TCE Degradation

mation capacity ($T_c$) to quantify the cell inactivation by TCE transformation products for the resting cell. It can be predicted that this effect also exists in the system when toluene and TCE are both present, and can be more serious if TCE concentration is high. Five $T_c$ values were examined: 0.05, 0.1, 1, 5, 10 mg TCE/mg cell. The results are plotted in Figure 10.11. At this toluene and TCE concentration range, toxicity can be ignored if $T_c$ is greater than 0.5: the removal efficiency stays in the maximum amount. TCE removal efficiency will decrease if $T_c$ is below 0.5. The importance of TCE transformation toxicity in the TCE degradation will be discussed in more detail in the next section. Toluene removal was not affected. This matches the experiments. Even cells were inactivated, and

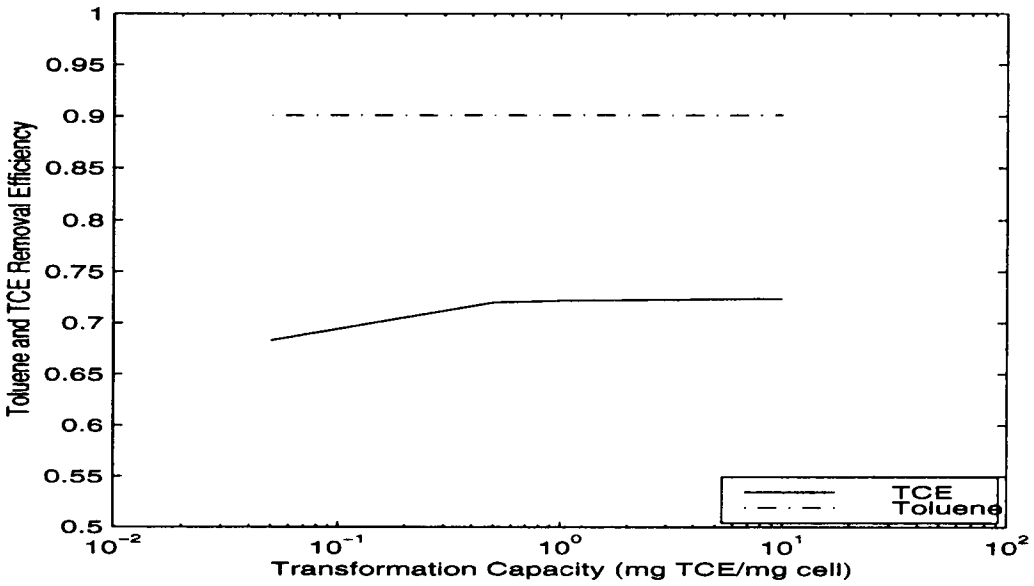



Figure 10.11: TCE Product Toxicity Affects Its Degradation

no TCE could be degraded; they were still alive[84]. Once toluene is present in the environment, reaction take place immediately.

### 10.6.3 Specific Area of Mass Transfer and Reactor Length

Calculations of physical configuration are for the purpose of design. When all biological parameters are fixed, the reactor length and packing material have to be calculated out to achieve certain removal efficiency at a particular contaminated water loading rate. As shown in Figure 10.12, smaller particles have more specific area that provides more space for the growth of biomass and mass transfer, enhancing both TCE and toluene degradation. Hence, packing media with large

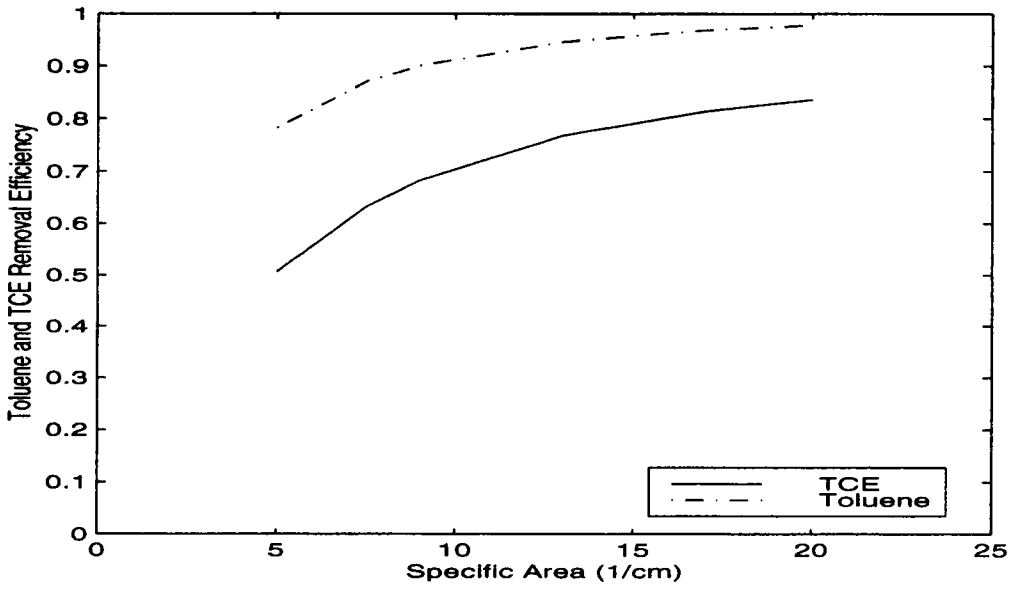



Figure 10.12: Specific Area Affects TCE Degradation

specific area but small resistance for fluid flow should be selected in reality. High removal efficiency can also be reached by increasing the length of the reactor in the event of increasing retention time in the reactor (Figure 10.13). If no toluene can be detected in the effluent, the limiting factors for TCE degradation are not the physical configurations any more.

### 10.6.4 TCE Saturation Parameter $K_2$

Saturation parameter $K_2$ characterizes TCE affinity to the enzyme system which was competitively inhibited by toluene. $K_2$ was found to be 1.524 mg/L in this study. Although physical conditions within biofilm are not the same as suspended

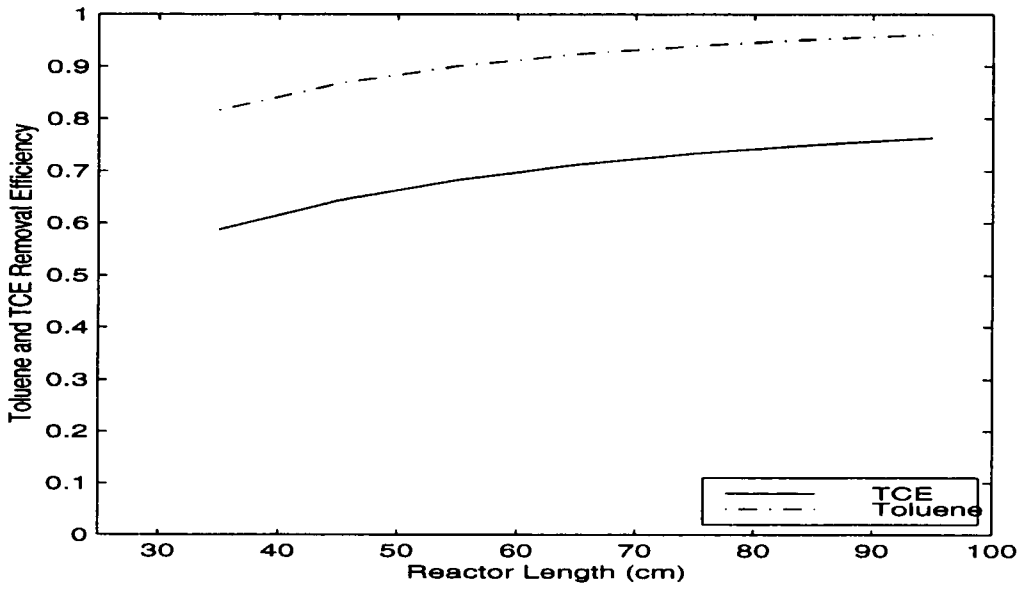



Figure 10.13: Reactor Length Affects TCE Degradation

solution where mass transfer conditions are much better, batch experiments are the best approximation. The values are quite different from all reported, ranging from 0.173 mg/L[3] to 8.64 mg/L[14]. The calculation results are shown in Figure 10.14. There is almost no influence of $K_2$ on toluene degradation, while it is very sensitive to TCE transformation. TCE removal efficiency dropped as $K_2$ value increased. This explains the competitive inhibition during the cometabolism.

### 10.6.5 Recycle Ratio

Recycle ratio is another operational condition that has to be considered. Recycling part of the effluent to the reactor dilutes toluene concentration in the in-

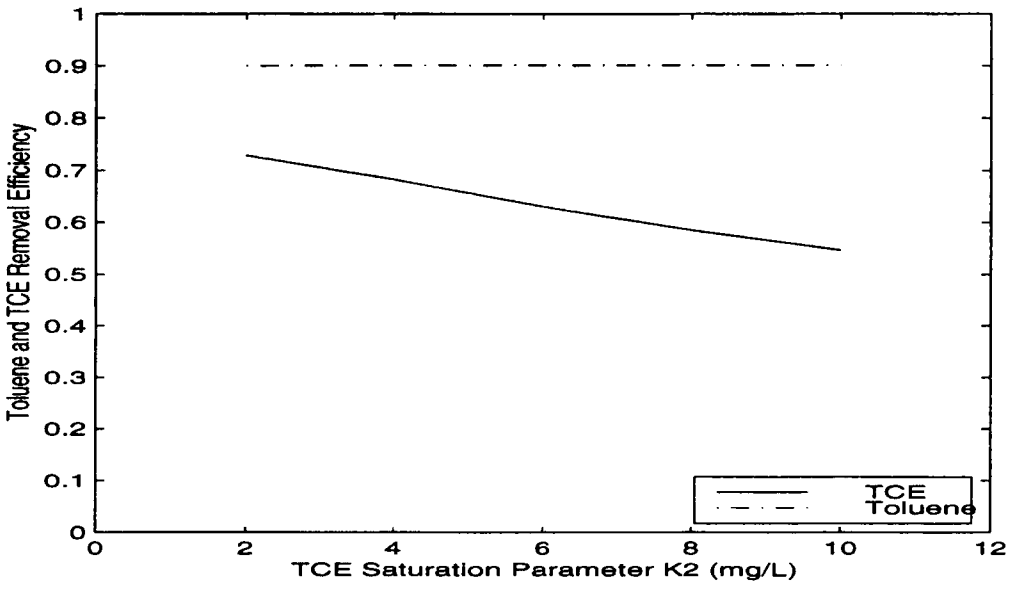



Figure 10.14: TCE Saturation Parameter Affects TCE Degradation

fluent. This is particularly important in the cometabolism system. Thus toluene concentration can be controlled below the competitive inhibition level for TCE degradation. Model computation showed that increasing the recycle ratio will improve the removal efficiency (Figure 10.15). Furthermore, larger recycling results in a high interstitial fluid velocity in the reactor, which enhances mass transfer from the bulk fluid to the biofilm. However, removal efficiency will not increase significantly when the recycle ratio gets to a certain value. In this case, complete mixing may be achieved in the reactor.

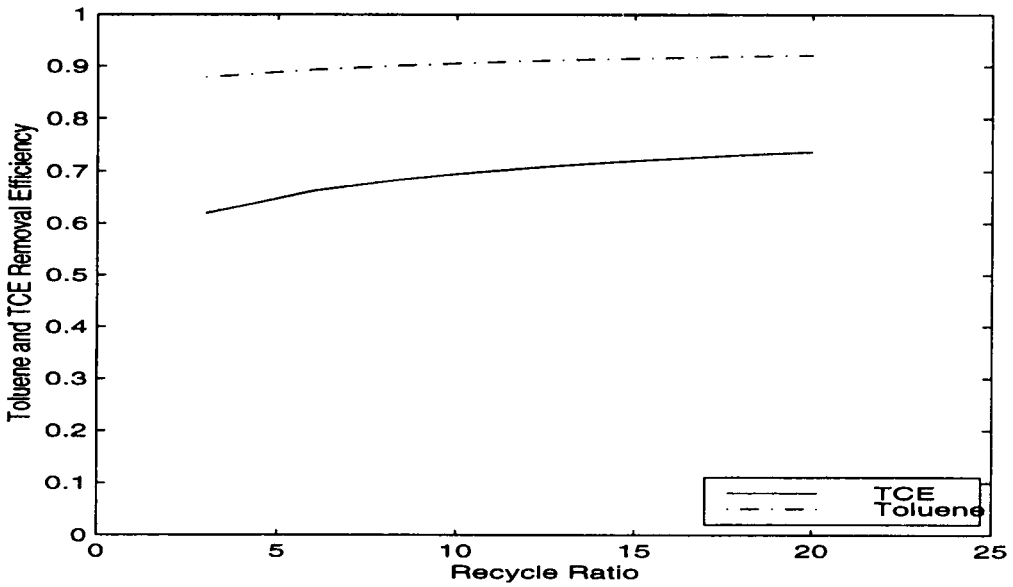



Figure 10.15: Recycle Rate Affects TCE Degradation

## 10.7 Comparison of Model with Experimental Results

Finally, model computation results were compared with the experimental data. Although many studies have been conducted experimentally in the TCE biodegradation either by methanotrophic bacteria, toluene oxidizer, or mixed culture, due to the complexity of the cometabolic and toxic system, no report which quantitatively describes the whole biological process in the aqueous phase biofilm reactor has been found. Parameters used in the model computation were calculated from Appendix G.6.

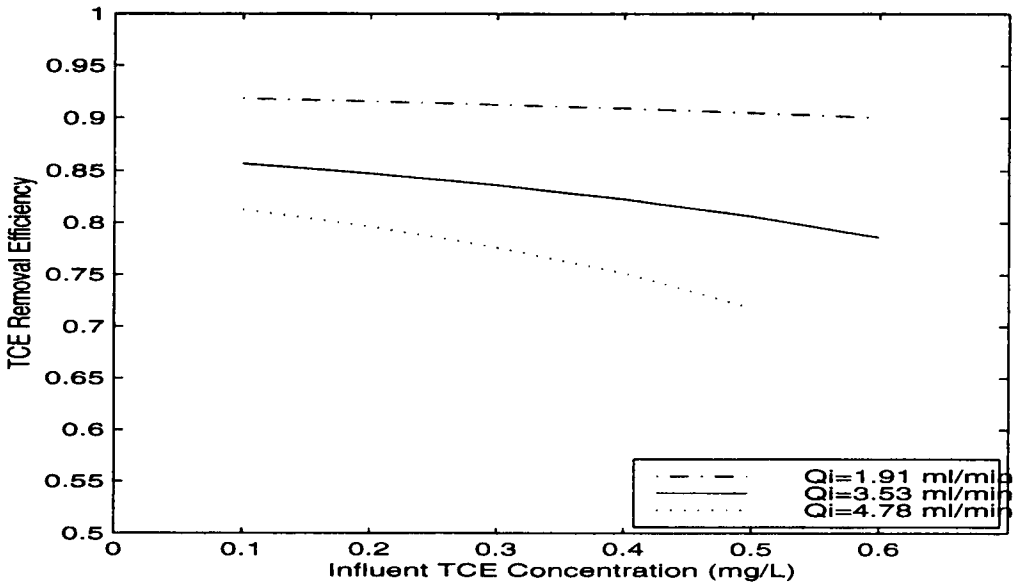



Figure 10.16: Influent Flow Affects TCE Degradation

### 10.7.1 Influent Flow Rate Affects TCE Degradation

Influent flow affects TCE degradation by affecting fluid retention time in the reactor. Since the column was not operated in submerged mode, the liquid hold-up is relatively small. Thus, the retention time is also small compared with conventional packed bed reactors. Three influent flow rates were investigated with the same toluene loading rate at about 0.103 mg/min. Removal efficiencies in the low influent TCE concentration range were plotted in Figure 10.16. As observed in the experiments, increasing the influent flow rate lowered TCE removal efficiency. Since the interested TCE concentration range was small, the toxicity was not that significant. $T_c$=0.05 mg TCE/mg cell was used in the model computation. Using

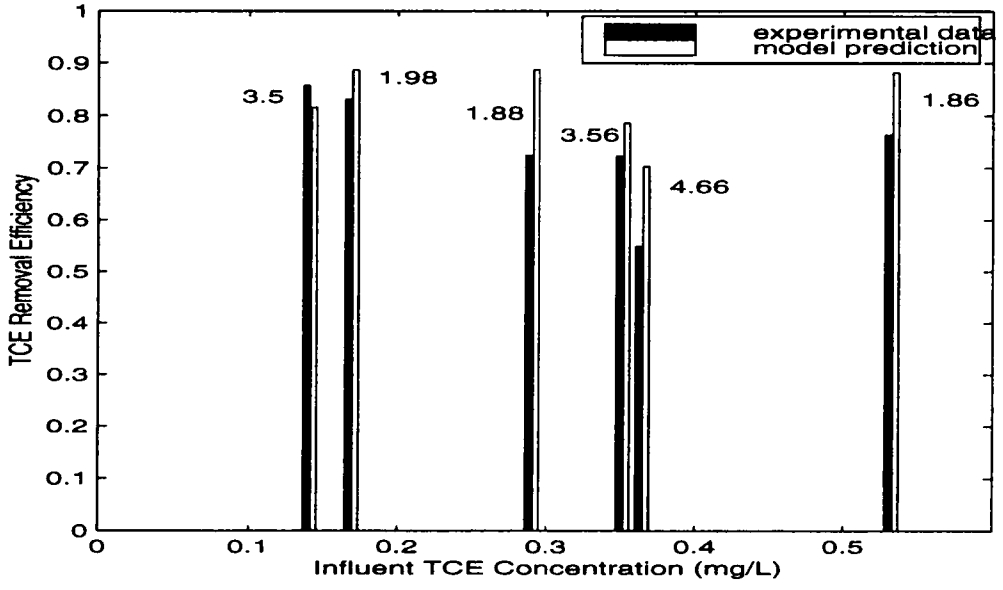



Figure 10.17: Comparison of Model Predictions with Experimental Results at Different Flow Rate. (Numbers refer to influent flow rates in the unit of in ml/min)

actual influent flow rates, influent toluene concentrations, and influent TCE concentrations in the column experiments as model input, TCE removal efficiencies were predicted. Fairly good agreement was achieved between the model predictions and the experimental results (Figure 10.17). Model prediction errors were below 30%.

### 10.7.2 TCE Loading Rate Affects TCE Degradation

Influent TCE concentrations in the range of 0.2 to 3 mg/L were selected. Transformation product toxicity is very important when TCE concentration is high. As

Anderson and McCarty(1994)[2] pointed out, $T_c$=10 mg/L could be considered as no TCE toxic effect on its degradation. Model prediction results didn't match with the experimental data. Low $T_c$ value has to be used. However, it was hard to get the program converged. There are some possible explanations. Due to the physical nature of the biofilm process in the cometabolism of TCE and the effect of its toxicity, the flux of TCE to the biofilm is not continuous if TCE concentration in the bulk fluid is high. Once all the biomass was inactivated by the TCE transformation product, no TCE concentration gradient would exist within the biofilm. Further degradation of toluene induces new enzymes, recovering the degradation of TCE, and TCE is transported to the biofilm again. The process repeats. This also happened in the biofilm model calculation. At high TCE concentration, if the $T_c$ value is small, in the step of correction of active biomass $f_a$'s, they will turn out to be negative values (zero was set in the program in case of this). And in the next iteration, toluene transformation reproduces the active cells. This causes the program to never be converged. The problem was fixed by calculating TCE removal efficiency at different high values of transformation capacity at different influent TCE concentrations under the same other operational conditions. Plotting of the inverse of removal efficiency vs the inverse of $T_c$ results exactly a series of second order polynomials (Figure 10.18). Each set of coefficients corresponds to a certain set of conditions. A simple algebraic relation was obtained between

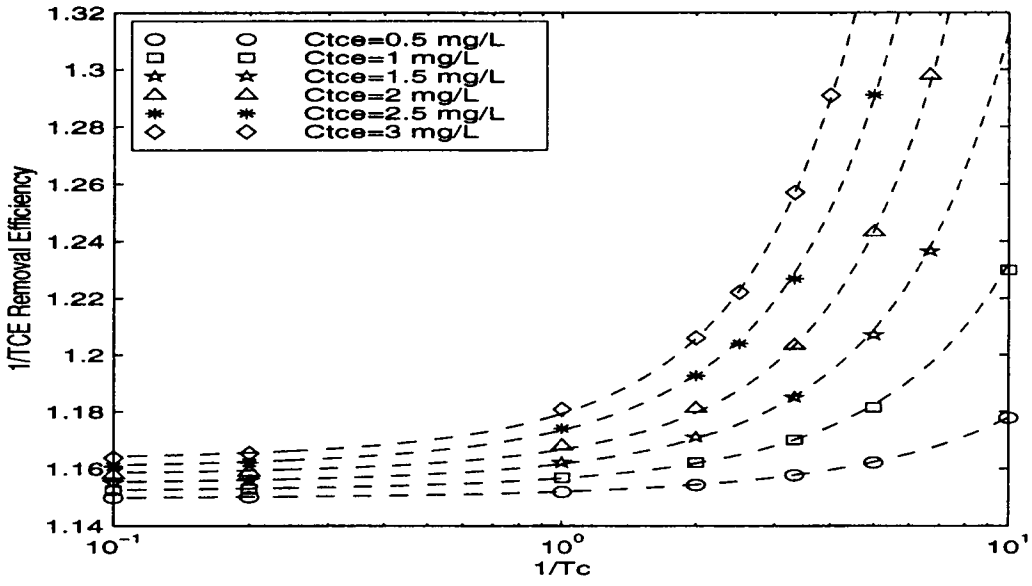



Figure 10.18: Correlation of Removal Efficiency vs $T_c$

TCE removal efficiency and transformation capacity $T_c$:

$$Rm = \frac{T_c^2}{aT_c^2 + bT_c + c} \tag{10.24}$$

where a, b, and c are fitting parameters. By extrapolating data, TCE removal efficiency can be found in the low range of $T_c$ values (Figure 10.19). Removal efficiency vs. influent TCE concentration at different $T_c$ were plotted in Figure 10.20. The shapes of the curves are completely different at low $T_c$ from high $T_c$. In batch studies, the maximum transformation capacity was 0.02 mg TCE/mg cell in the system of the resting cell. This may be underestimated when toluene is present in the environment. Computation results from $T_c$ set to 0.02 (lower limit), 0.035, and 0.05 (upper limit), were compared with the experimental results (Figure 10.21).

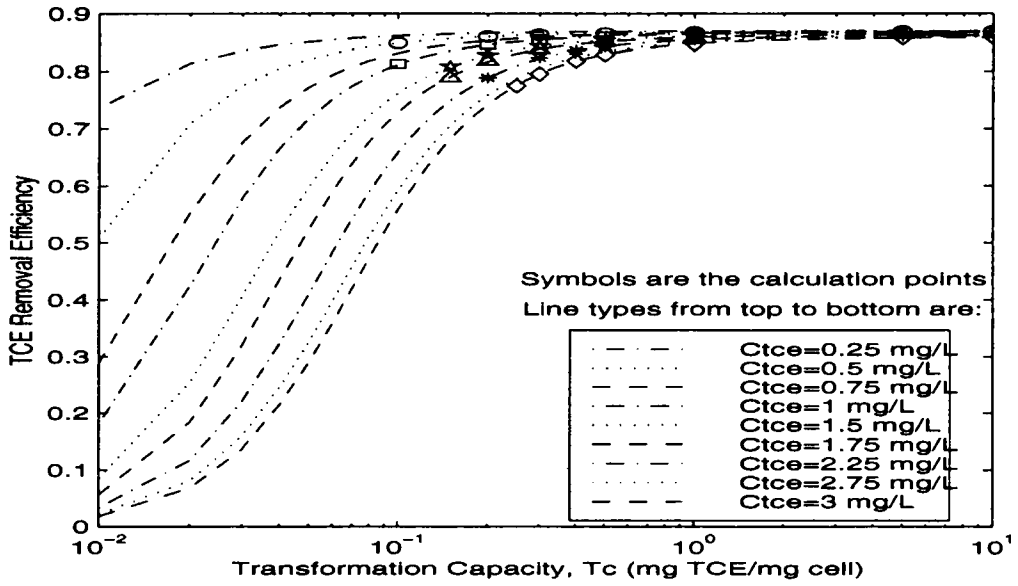



Figure 10.19: Extrapolation of TCE Removal Efficiency at Low $T_c$ Value

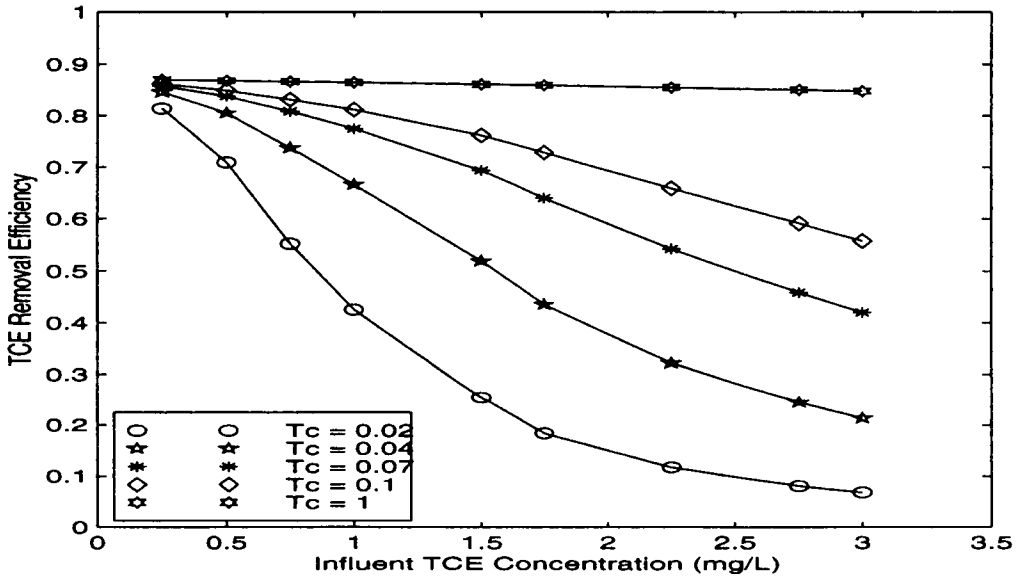



Figure 10.20: TCE Removal Efficiency at Different TCE Concentrations

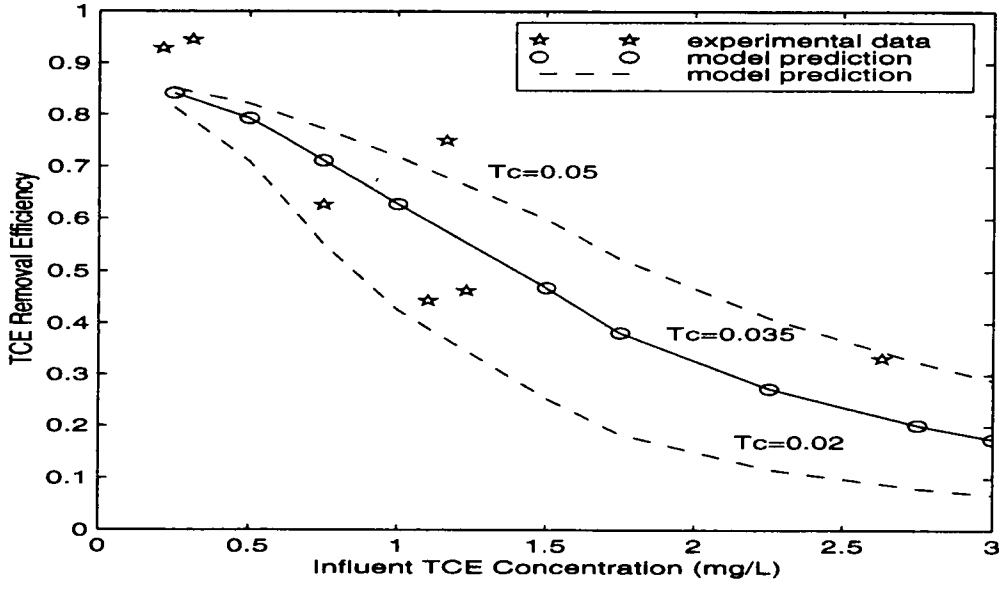



Figure 10.21: Comparison of Model Prediction with Experimental Data

They match fairly well.

### 10.7.3 Toluene Affects TCE Degradation

Toluene as a primary substrate for *Pseudomonas putid* F1 not only provides the carbon source but also acts as an inducer of enzyme for TCE degradation. Because both TCE and toluene share the same enzyme, the competitive inhibition by toluene causes a negative effect on TCE degradation (Section 4.3, Figure 4.3). Toluene loading rate for a fixed TCE loading is very important in order to get a high TCE removal efficiency in a continuous system. The objective is always to achieve better TCE degradation with little or no toluene competition. Influ-

ent toluene concentrations varying from 10 mg/L to 70 mg/L were tested at the same TCE loading rate of 1.0551 mg/L TCE concentration (influent flow rate was fixed at 2.8 ml/min). The same method as in the last section was used. Removal Efficiencies at $T_c$=0.02 mg/L were extrapolated from the correlations in which $T_c$ varies from 0.1 to 1 mg TCE/mg cell at different toluene loading. Results are given in Figure 10.22. Computer generating data shows that the TCE toxic effect was more serious at low toluene loading than at high toluene loading. Plotting of TCE removal efficiency vs. influent toluene concentration (Figure 10.23) illustrates that TCE removal efficiency will not be improved if toluene concentration is higher than 30 mg/L in the influent, and gradually decreases when toluene concentration excess 40 mg/L, if TCE product toxicity is neglected ($T_c$=10). This is the effect of competitive inhibition and can be viewed more clearly in Figure 10.24, which is an enlarged part of Figure 10.22 with influent toluene concentrations at 40, 50, 60, and 70 mg/L. However, unlike the batch reaction, TCE removal efficiency didn't drop tremendously at a high level of toluene in the column reaction. This could be contributed from the recycled stream dilution effect and the partition of volatile compounds to the gas phase that lowered component concentrations in the liquid phase. Actual toluene concentration entering the column was much smaller than toluene concentration in the influent. The relationship between influent toluene concentration and concentration of toluene entering the column

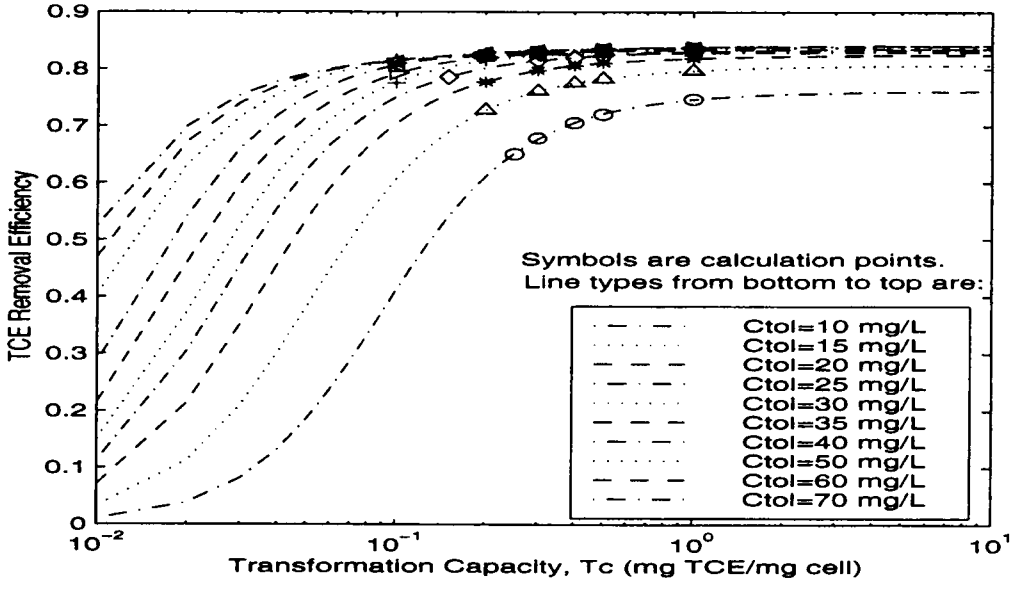



Figure 10.22: Correlation of TCE Removal Efficiency to $T_c$

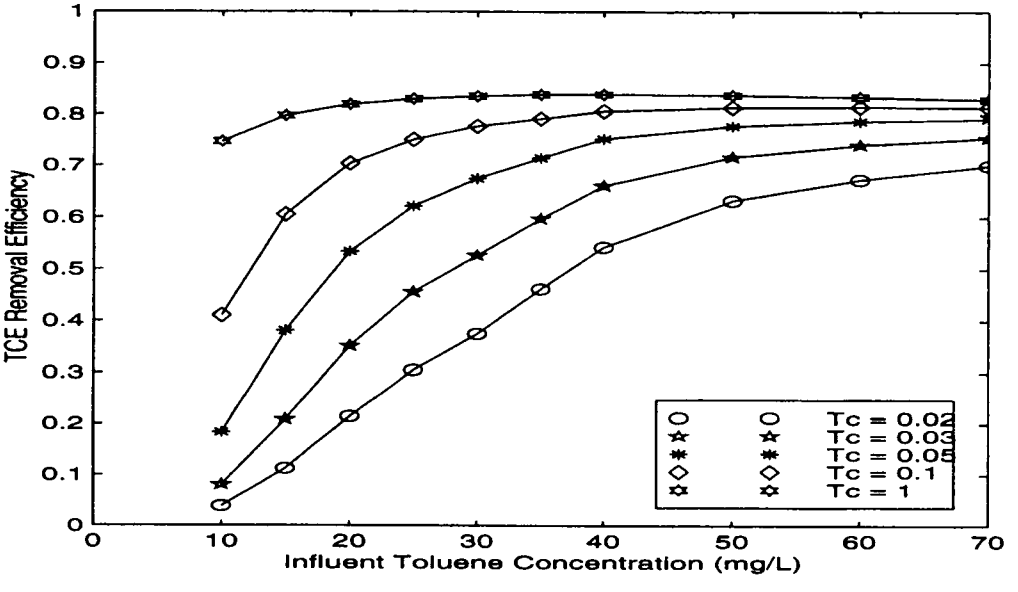



Figure 10.23: TCE Removal Efficiency at Different Influent Toluene Concentration

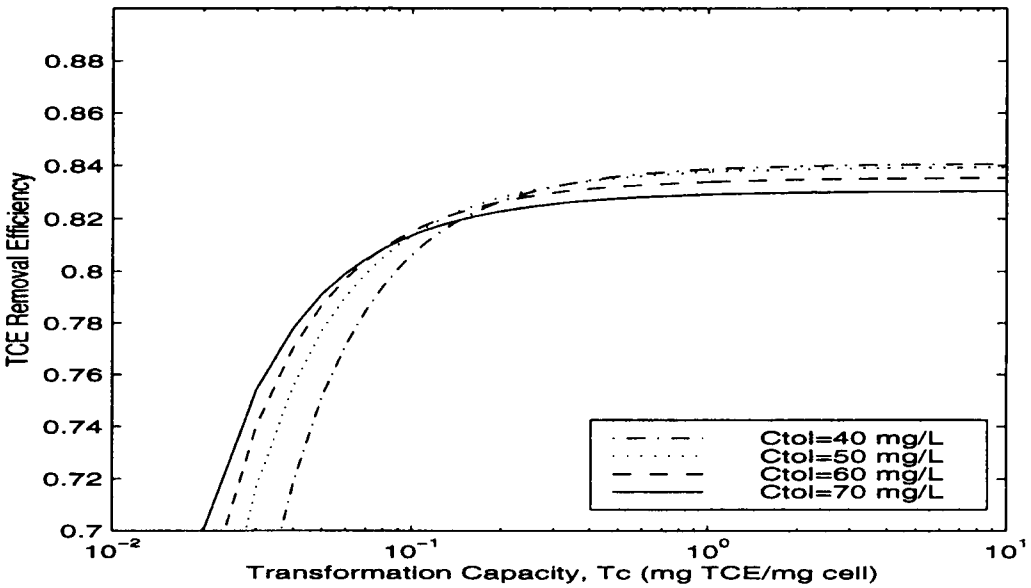



Figure 10.24: Correlation of TCE Removal Efficiency vs $T_c$ at High Toluene Concentrations

under the recycle ratio 9.82 is plotted in Figure 10.25. In the figure, 100% toluene was assumed being degraded as observed in the experiments. In this case, even 70 mg/L toluene in the influent would result in only 6 mg/L toluene transferred into the top of the reactor. In the model calculation, 10% error was obtained in toluene degradation. Only 90% toluene was degraded. Thus, the corresponding concentration of toluene entering the column was higher than that in the experiments. Evidence from batch experiments (Chapter 4, Section 4.3) demonstrated that total toluene concentration below 10 ppm didn't show significant competitive inhibition in the TCE degradation at a volume ratio of headspace to liquid 4:1.

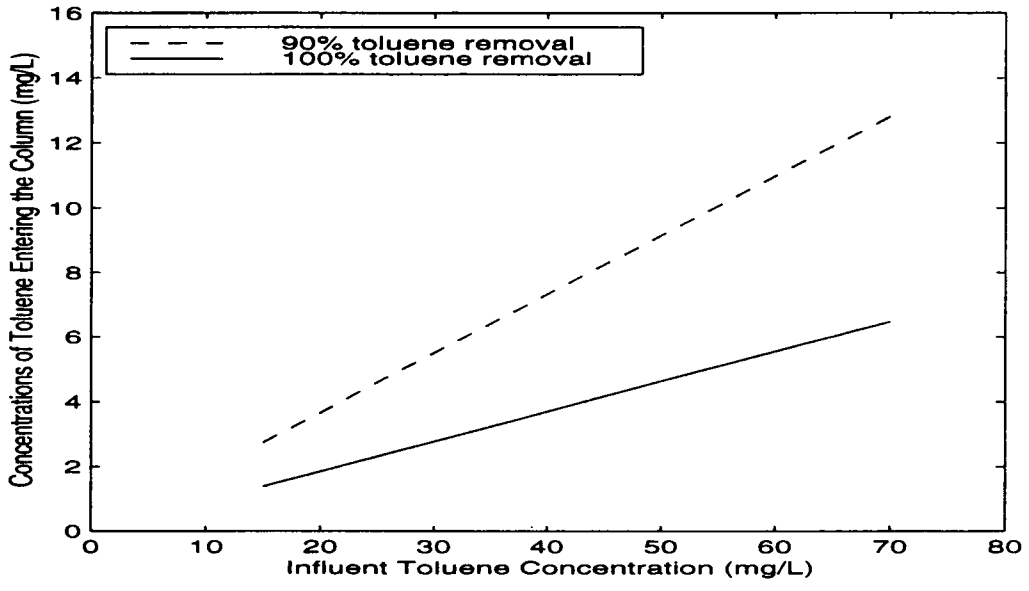



Figure 10.25: Toluene Concentration Entering the Reactor at Its Corresponding Influent Toluene Concentration under Recycle Ratio 9.82

Under reactor experimental flow and packing condition, the ratio of gas hold-up to liquid hold-up in the column was close to 4:1. After partitioning to the gas phase, toluene concentration in the liquid phase would be even smaller than 6 mg/L. Unlike the batch conditions, as the liquid flowed down the reactor, toluene was degraded. Toluene concentration dropped quickly. The effect of competitive inhibition became much less. Therefore, the physical condition at each point along the reactor was different. In addition, due to TCE transformation product toxicity, more toluene is required to maintain cell activity and achieve the same removal efficiency[41]. These all could be used to explain the reason why TCE removal

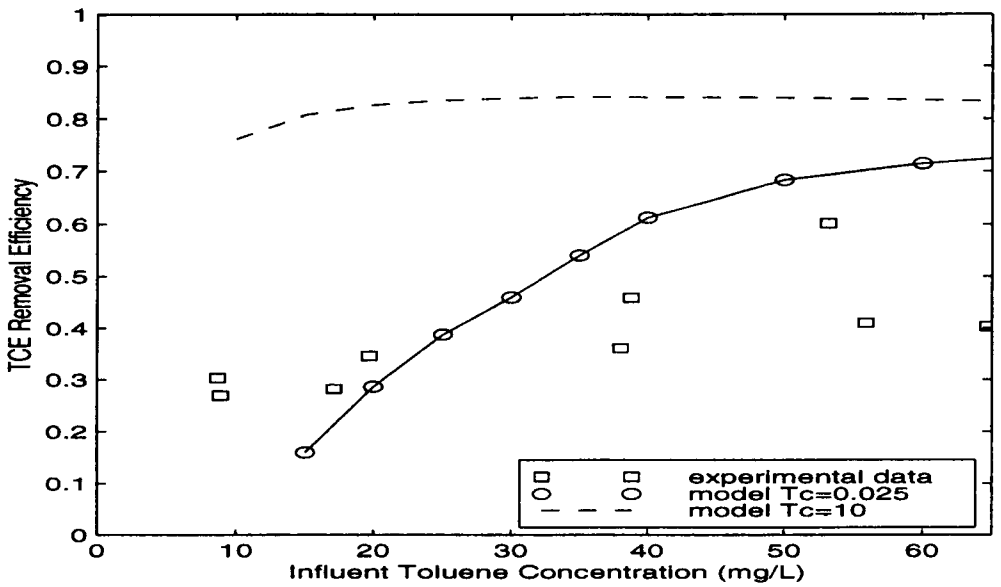



Figure 10.26: Comparison of Model Prediction with Experimental Data

efficiency increases with the increase of toluene concentration in this study. A transition point was observed in Figure 10.23, which separated the curve into two parts for $T_c = 0.02$ mg TCE/mg cell. One is toluene concentration below 40 mg/L in which the slope seems high, and the other is above 40 mg/L with a smaller slope. The first one may be explained as the overcoming of TCE toxicity, which dominated TCE degradation, and in the second one as the increasing of toluene inhibition effect. Model predictions are also compared with the experimental data (Figure 10.26). Removal efficiency at high toluene concentration drops in the experiments might come from non-ideal behavior in the reactor, such as short cut flow, poor gas recirculation in the reactor, instant shortage of oxygen, and so on.

# Chapter 11

# Conclusions

The biodegradation of TCE by toluene dioxygenase system of *Pseudomonas putida* F1 was investigated in this work. Based on the understanding of cometabolism and toxicity from batch experiments, an effective biofilm reactor system was developed for the removal of TCE in aqueous phase. A relatively comprehensive steady-state biofilm model was proposed for TCE cooxidation by *Pseudomonas putida* F1 using toluene as a primary substrate. Combining this biofilm model with dispersion, convection, and mass transfer between different phases, a bioreactor model was established, which can be applied for future design and system optimization.

### Conclusions from the Batch Studies and Kinetic Calculations

1. Toluene as a primary substrate can be degraded very quickly without any resistance by *Pseudomonas putida* F1. The reaction kinetics follows the Monod equation.

2. Three regions can be classified for TCE degradation in the presence of a high initial concentration of toluene: competitive inhibition region, where no TCE is degraded; fast degradation region, in which TCE concentration drops rapidly; and decay region, where toluene is completely consumed and enzyme starts to decay, and the TCE degradation rate decreases with time.

3. At the headspace volume and liquid volume ratio to 4, competitive inhibition of toluene to TCE transformation was not significant if the total toluene concentration below was 10 ppm. A maximum TCE degradation rate can be achieved at the point where total toluene concentration is below 1 ppm.

4. Transformation product toxicity is the limiting factor for TCE removal by resting cells. Computer simulation showed that the active biomass decreased with time.

5. A set of kinetic parameter values were obtained for *Pseudomonas putida* F1.

**Conclusions from Column Experiments**

1. The biofilm reactor system could maintain a stable TCE degradation by

continuous feeding of toluene. Partially recycled effluent diluted the influent toluene. The column was operated without significant toluene competitive inhibition. Oxygen limitation was eliminated by direct contact of gas phase to liquid phase, and the flow of both liquid phase and gas phase enhanced mass transfer.

2. TCE removal efficiency was below 20% if influent toluene concentration was less than 10 mg/L at 1.86 $\sim$ 2.22 mg/L influent TCE concentration. Increasing toluene increased TCE degradation. However, if toluene concentration was over 50 mg/L, the increasing of TCE removal efficiency was not significant in the step increasing of toluene concentration experiment. Steady-state degradation showed that TCE removal efficiency decreased at 68 ppm influent toluene concentration.

3. TCE removal is a function of influent TCE concentration. Low removal efficiency was observed at high TCE loading. The relationship of influent and effluent TCE concentrations were linear.

4. Increasing of recycle rate increased mass transfer and toluene could result in more uniform distribution in the column. However, TCE removal efficiency won't increase at certain levels of recycle rate.

5. The influence of influent flow rate on TCE degradation occurred through

the retention time. Small influent flow gave high removal efficiency.

6. TCE removal efficiencies ranged from 94.5% to 60% with TCE influent concentrations of 0.31 to 1.06 ppm, and influent toluene concentrations of 30 to 53 ppm, respectively. The performance of this bioreactor could be greatly improved if uniform flow, longer retention time, and large specific reaction and mass transfer area could be achieved.

### Conclusions from Biofilm Model

1. TCE associated toxicity affects active biomass in the biofilm. It reduces TCE flux into the biofilm, thus decreasing TCE degradation. Higher TCE concentration results in smaller amounts of active cells.

2. Toluene determines the effective thickness of the biofilm. Increasing bulk toluene concentration increases the flux of TCE into the biofilm. However, further increasing the toluene concentration above 5 ppm doesn't improve TCE degradation much due to competitive inhibition.

3. Mass transfer affects both toluene and TCE degradation in the biofilm. The thinner the liquid film around the biofilm, the more toluene and TCE will be transported into the biofilm for degradation.

4. The biofilm model has a limit when transformation capacity is small. This

may result from the properties of physical process in the enzyme deactivation and regeneration for TCE degradation in the presence of toluene within the biofilm.

### Conclusions from Bioreactor Model

1. The model matches with experimental data fairly well when TCE concentration is low. Compared with the experiments, the model prediction errors were below 30%.

2. The inverse of TCE removal efficiency is predicted as a function of the inverse of TCE transformation capacity in a form of second order polynomial. Thus, TCE degradation can be estimated by extrapolation at high TCE concentration. Close agreement was achieved between the model prediction and experimental data.

3. The competitive inhibition was moderated by TCE product toxicity effect. More toluene will be needed to overcome enzyme inactivation by TCE related toxicity for TCE removal in the system. Model calculation values were higher than experimental data at high influent toluene concentrations, which might be caused by non-ideal behavior of the reactor operations.

4. Model calculation by changing the recycle rate and influent flow rate is consistent with the experimental results.

5. Increasing specific mass transfer-reaction area and reactor length increase the degradation of both toluene and TCE. The model can be used for reactor design to achieve certain removal efficiency.

6. Model sensitivity analysis was conducted. Increasing the toluene yield coefficient increased the removal of TCE. $T_c$ = 10 mg TCE/mg cell, can be viewed as no toxicity. The lower value of $T_c$ gives less TCE degradation. High TCE saturation parameter results in low removal efficiency.

# BIBLIOGRAPHY

# Bibliography

[1] Alvarez-Cohen, L. and P. L. McCarty. 1991. Two-Stage Dispersed-Growth Treatment of Halogenated Aliphatic Compounds by Cometabolism. *Environ. Sci. Technol.* **25**: 1387-1393.

[2] Anderson, J. E., and P. L. McCarty. 1994. Model for Treatment of Trichloroethylene by Methanotrophic Biofilms. *J. Envir. Engrg.* **120**: 379-400.

[3] Arcangeli, Jean-Pierre and E. Arvin. 1997. Modeling of the Cometabolic Biodegradation of Trichloroethylene by Toluene-Oxidizing Bacteria in a Biofilm System. *Environ. Sci. Technol.* **31**: 3044-3052.

[4] Bailey, J. E., and D. F. Ollis. 1986. Biochemical Engineering Fundamentals. Second Edition, McGraw-Hill, New York.

[5] Baker, A. J. 1996. Finite Element Computational Fluid Mechanics. University of Tennessee, Knoxville.

[6] Baker, A. J., and D. W. Pepper. 1991. Finite Elements 1-2-3. McGraw-Hill, Inc.

[7] Baker, A. J. 1983. Finite Element Computational Fluid Mechanics. Hemisphere Publishing Corporation, New York.

[8] Barrio, G. et al. 1986. Sequential Dehalogenation of Chlorinated Ethenes. *Environ. Sci. Technol.* **20**: 96-99.

[9] Bouwer, E. J., and P. L. McCarty. 1983. Transformation of 1- and 2-Carbon Halogenated Aliphatic Organic Compounds Under Methanogenic Conditions. *Appl. Environ. Microbiol.* **45**: 1260-1294.

[10] Bouwer, E. J., and P. L. McCarty. 1985. Utilization Rates of Trace Halogenated Organic Compounds in Acetate-Grown Biofilm. *Biotech. Bioeng.* **27**: 1564-1571.

[11] Bouwer, E. J. 1985. Secondary Utilization of Trace Halogenated Organic Compounds in Biofilms. *Environ. Prog.* **4**: 43-45.

[12] Carranza, F. E. 1990. Biodegradation of Trichloroethylene by Unsaturated Aerobic Fixed-Film Bioreactor Using Methane as the Primary Substrate. *Ph.D Dissertation.* The University of Oklahoma.

[13] Chang, Hsiao-Lung and L. Alvarez-Cohen. 1997. Two-Stage Methanotrophic Bioreactor for the Treatment of Chlorinated Organic Wastewater. *Wat. Res.* **31**: 2026-2036.

[14] Chang, Hsiao-Lung and L. Alvarez-Cohen. 1995. Model for the Cometabolic Biodegradation of Chlorinated Organics. *Environ. Sci. Technol.* **29**: 2357-2367.

[15] Criddle, C. S. 1993. The Kinetics of Cometabolism. *Biotechnol. Bioeng.* **41**: 1048-1056.

[16] Dalton, H., D. I. Stirling. 1982. Co-metabolism. *Phil. Trans. R. Soc. Lond. Ser.* **B297**: 481-496.

[17] Ensley, B. D. 1991. Biochemical Diversity of Trichloroethylene Metabolism. *Annu. Rev. Microbiol.* **45**:283-99.

[18] Fan, A. M. 1988. Trichloroethylene: Water Contamination and Health Risk Assessment. *Reviews of Environmental Contamination and Toxicology.* Vol. 101, G. W. Ware, ed., Springer-Verlag, New York, N. Y., 55-92.

[19] Fan, L. S., R. Leyva-Ramos, K. D. Wisecarver, and B. J. Zehner. 1990. Diffusion of Phenol through a Biofilm Grown on Activated Carbon Particles in a Draft-Tube Three-Phase Fluidized-Bed. *Biotech. Bioeng.* **35**: 279-286.

[20] Fennel, D. E., Y. M. Nelson, S. E. Underhill, T. E. white, and W. J. Jewell. 1993. TCE Degradation in a Methanotrophic Attached-Film Bioreactor. *Biotechnol. Bioeng.* **42**: 859-872.

[21] Fitch, M. W., D. Weissman, P. Phelps, G. Georgiou, and G. E. Speitel Jr. 1996. Trichloroethylene Degradation by *Methylosinus Trichosporium* OB3B Mutants in a Sequencing Biofilm Reactor. *Wat. Res.* **30**: 2655-2664.

[22] Fitch, M. W., G. E. Speitel, Jr., and G. Georgiou. 1996. Degradation of Trichloroethylene by Methanol-Grown Cultures of *Methylosinus trichosporium* OB3b PP358. *Appl. Environ. Microbiol* **62**: 1124-1128.

[23] Folkard, G. K. 1986. The Significance, Occurrence and Removal of Volatile Chlorinated Hydrocarbon Solvents in Ground Water. *Water Pollution Control.* 63-69.

[24] Folsom, B. R, and P. J. Chapman. 1991. Performance Characterization of a Model Bioreactor for the Biodegradation of Trichloroethylene by *Pseudomonas cepacia* G4. *Appl. Environ. Microbiol.* **57**: 1602-1608.

[25] Greenberg, A. E., J. J. Connors, and D. Jenkins. 1981. Standard Methods, For the Examination of Water and Wastewater. Fifteenth Edition. APHA-AWWA-WPCE.

[26] Heald, S., and R. O. Jenkins. 1994. Trichloroethylene Removal and Oxidation Toxicity is Mediated by Toluene Dioxygenase of *Pseudomonas putida*. *Appl. Environ. Microbiol.* **60**: 4634-4637.

[27] Hines, A. L., and R. N. Maddox. 1985. Mass Transfer: Fundamentals and Applications. P T R Prentice-hall Inc.

[28] Hopkins, G. D., J. Munakata, L. Semprini, and P.L. McCarty. 1993. Trichloroethylene Concentration Effects on Pilot Field-Scale in-Situ Groundwater Bioremediation by Phenol-Oxidizing Microorganisms. *Environ. Sci. Technol.* **27**: 2542-2547

[29] Hopkins, G. D., L. Semprini, and P. L. McCarty. 1993. Microcosm and in Situ Field Studies of Enhanced Biotransformation of Trichloroethylene by Phenol-Utilizing Microorganisms. *Appl. Environ. Microbiol.* **59**: 2277-2285.

[30] Hopkins, G. D, and P. L. McCarty. 1995. Field Evaluation of in-Situ Aerobic Cometabolism of Trichloroethylene and Three Dichloroethylene Isomers Using Phenol and Toluene as Primary Substrates. *Environ. Sci. Technol.* **29**: 1628-1637.

[31] Krans, D. L., and A. L. Dunn. 1983. Trichloroethylene Occurrence and Ground Water Restoration in Highly Anisotropic Bedrock: A Case Study. Proceedings of the Third National Symposium and Exposition on Aquifer

Restoration and Ground Water Monitoring. National Water Well Association, Worthington, Ohio. 76-81.

[32] Landa, A. S., E. M. Sipkema, J. Weijma, A. A. C. M. Beenackers, J. Dolfing, D. B. Janssen. 1994. Cometabolic Degradation of Trichloroethylene by *Pseudomonas cepacia* G4 in a Chemostat with Toluene as the Primary Substrate. *Appl. Environ. Microbiol.* **60**: 3368-3374.

[33] Leahy, J. G., A. M. Byrne, and R. H. Olsen. 1996. Comparison of Factors Influencing Trichloroethylene Degradation by Toluene-Oxidizing Bacteria. *Appl. Environ. Microbiol.* **62**: 825-833.

[34] Lee, M. D., et al. 1988. Biorestoration of Aquifers Contaminated with Organic Compounds. *CRC Critical Reviews in Environmental Control.* **18**: 29-89.

[35] Li, S., and L. P. Wackett. 1992. Trichloroethylene Oxidation by Toluene Dioxygenase. *Biochem. Biophys. Res. Commun.* **185**: 443-451.

[36] Livingston, A. G. 1991. Biodegradation of 3,4-Dichloroaniline in a Fluidized Bed Bioreactor and a Steady-State Biofilm Kinetic Model. *Biotechnol. Bioeng.* **38**: 260-272.

[37] Love, Jr., O. T., and R. G. Eilers. 1982. Treatment of Drinking Water Containing Trichloroethylene and Related Industrial Solvents. *J. Am. Water Works Assoc.* **74**: 413-425.

[38] Mackay, D. M., and J. A. Cherry. 1989. Groundwater Contamination: Pump-and-Treat Remediation. *Environ. Sci. Technol.* **23**: 630-636.

[39] Maltoni, C., and G. Lafemine. 1974. Carcinogenicity Bioassays of Vinylchloride. I. Research Plan and Early Results. *Environ. Res.* **7**: 387-396.

[40] Mars, A. E, J. Houwing, J. Dolfing, and D. B. Janssen. 1996. Degradation of Toluene and Trichloroethylene by *Burkholderia cepacia* G4 in Growth-Limited Fed-Batch Culture. *Appl. Environ. Microbiol.* **62**: 886-891.

[41] Mars, A. E, G. T. Prins, P. Wietzes, W. de Koning, and D. B. Janssen. 1998. Effect of Trichloroethylene on the Competitive Behavior of Toluene-Degrading Bacteria. *Appl. Environ. Microbiol.* **64**: 208-215.

[42] McCarty, P. L., L. Semprini, M. E. Dolan, T. C. Harmon, C. Tiedeman, S. M. Gorelick. 1992. *In Situ* Methanotrophic Bioremediation for Contaminated Groundwater at St. Joseph, Michigan. In On-Site Bioreclamation: Processes for Xenobiotic and Hydrocarbon Treatment. Butterworth-Heineman, Boston, Mass., 16.

[43] McFarland, M. J., C. M. Vogel, and J. C. Spain. 1992. Methanotrophic Cometabolism of Trichloroethylene (TCE) in a Two Stage Bioreactor System. *Wat. Res.* **26**: 259-265.

[44] Mercer, J. W, D. C. Skipp, and D. Griffin. 1990. Basics of Pump-and-Treat Groundwater Remediation Technology. *Robert S. Kerr Environmental Research Laboratory*, Office of Research and Development U. S. EPA. Ada. OK. EPA-600/8-90/003.

[45] Miller, R. E., and F. P. Quengerich. 1982. Oxidation of Trichloroethylene by Liver Microsomal Cytochrome P-450: Evidence for Chlorine Migration in a Transition State not Involving Trichloroethylene Oxide. *Biochemistry.* **21**: 1090-1097.

[46] Namkung, E. 1985. Kinetics and Mechanisms of Low-Concentration Multisubstrate Utilization by Biofilms. Ph.D Dissertation, University of Illinois at Urbaba-Champaign.

[47] Nelson, M. J, S. O. Montgomery, and P. H. Pritchard. 1988. Trichloroethylene Metabolism by Microorganisms That Degrade Aromatic Compounds. *Appl. Environ. Microbiol.* **54**: 604-606.

[48] Neufeld, R. D., S. Niaki, C. Badali, P. K. T. Liu, and D. Powers. 1994. Activated Biofilm Removal of Low Concentrations of Toluene. *Wat. Environ. Res.* **66**: 899-904.

[49] Oldenhuis, R., R. L. J. M. Vink, D. D. Janssen, B. Witholt. 1989. Degradation of Chlorinated Aliphatic Hydrocarbons by *Methylosinus trichosporium* OB3b Expressing Soluble Methane Monooxygenase. *Appl. Environ. Microbiol.* **55**: 2819-2826.

[50] Parvatiyar, M. G., R. Govind, and D. F. Bishop. 1996. Treatment of Trichloroethylene (TCE) in a Membrane Biofilter. *Biotechnol. Bioeng.* **50**: 57-64.

[51] Phelps, T., J. J. Niedzielski, K. J. Malachowsky, R. M. Schram, S. E. Herbes, and D. C. White. 1991. Biodegradation of Mixed-Organic Wastes by Microbial Consortia in Continuous-Recycle Expanded-Bed Bioreactors. *Environ. Sci. Technol.* **25**: 1461-1465.

[52] Pieters, J. G., J. Sanseverino, C. L. Wright, C. L. Cheng, K. Liu, K. G. Robinson, C. D. Cox, S. R. Kehrmeyer, B. M. Applegate, and G. S. Sayler. May 5-7, 1997. Bioluminescence and Cometabolic Degradation of Toluene and Trichloroethylene by *Pseudomonas putida* TVA8. *Proceedings of 52nd Purdue Waste Industrial Conference*, West Lafayette, IN.

[53] Quail, B. E. and G. A. Hill. 1991. A Packed-Column Bioreactor for Phenol Degradation: Model and Experimental Verification. *J. Chem. Tech.Biotechnol.* **52**: 545-557.

[54] Reardon, K. F., J. R. Conuel, D. C. Mosteller. 1992. In *Proceedings of the 9th Conference on Hazardous Waste Remediation*; Erickson, L. E., Ed.; EPA.

[55] Rittmann, B. E. and P. L. McCarty. 1980. Model of Steady-State Biofilm Kinetics. *Biotechnol. Bioeng.* **17**: 2343-2357.

[56] Rittmann, B. E. 1982. The Effect of Stress on Biofilm Loss Rate. *Biotechnol. Bioeng.* **114**: 501-506.

[57] Rittmann, B. E., J. A. Manem. 1992. Development and Experimental Evaluation of Steady-State Multispecies Biofilm Model. *Biotechnol. Bioeng.* **39**:914-922.

[58] Rittmann, B. E., and K. Dovantzis. 1983. Dual Limitation of Biofilm Kinetics. *Water Res.* **17**: 1727-1734.

[59] Rittmann, B. E. 1982. Comparative Performance of Biofilm Reactor Types. *Biotech. Bioeng.* **24**: 1341-1370.

[60] Segar Jr., R. L, S. L. De Wys, G. E. Speitel Jr. 1995. Sustained Trichloroethylene Cometabolism by Phenol-Degrading Bacteria in Sequencing Biofilm Reactors. *Water Environ. Res.* **65**: 764-774.

[61] Shahalam, A. B., R. El-Samra, G. M. Ayoub, and A. Acra. 1996. Parametric Sensitivity of Comprehensive Model of Aerobic Fluidized-Bed Biofilm Process. *J. Envir. Engrg.* **122**: 1085-1093.

[62] Shields, M. S., S. O. Montgomery, P. J. Chapman, S. M. Cuskej, and P. H. Pritchard. 1989. Novel Pathway of Toluene Catabolism in the Trichloroethylene-Degrading Bacterium G4. *Appl. Environ. Microbiol.* **55**: 1624-1629.

[63] Shimomura T., F. Suda, H. Uchiyama and O. Yagi. 1997. Biodegradation of Trichloroethylene by *Methylocystis* SP. Strain M Immobilized in Gel Beads in a Fluidized-Bed Bioreactor. *Eat. Res.* **31**: 2383-2386.

[64] Shin, H. S., and J. L. Lim. 1996. Performance of a Packed-Bed Bioreactors for the Cometabolic Degradation of Trichloroethylene by Penol-Oxidizing Microorganisms. *Environ. Technol.* **17**: 1351-1359.

[65] Shurtliff, M. M, G. F. Parkin, L. J. Weathers, and D. T. Gibson. 1996. Biotransformation of Trichloroethylene by a Phenol-Induced Mixed Culture. *J. Envir. Engrg.* **122**: 581-589.

[66] Skowlund, C. T. 1990. Effect of Biofilm Growth on Steady-State Biofilm Models. *Biotech. Bioeng.* **35**: 502-510.

[67] Stanier, R. Y., N. J. Palleroni, and M. Doudoroff. 1966. The aerobic Pseudomonads: a taxonomic study. *J. General Microbiol.* **41**: 159-127.

[68] Strand, S. E., M. D. Bjelland and H. D. Stensel. 1990. Kinetics of Chlorinated Hydrocarbon Degradation by Suspended Cultures of Methane-Oxidizing Bacteria. *Res. J. WPCF* **62**: 124-129.

[69] Strand, S. E., J. V. Wodrich, and H. D. Stensel. 1991. Biodegradation of Chlorinated Solvents in a Sparged Methanotrophic Biofilm Reactor. *Research Journal WPCF* **63**: 859-867.

[70] Strandberg, G. W., T. L. Donaldson, and L. L. Farr. 1989. Degradation of Trichloroethylene and trans-1,2 Dichloroethylene by a Methanotrophic Consortium in a Fixed-Film Packed-Bed Bioreactor. *Environ. Sci. Technol.* **23**: 1422-1425.

[71] Stratton, R. G., E. Namkung, B. E. Rittmann. 1983. Secondary Utilization of Trace Organics by Biofilms on Porous Media. *American Water Works Association Journal* **75**: 463-469.

[72] Sun, A. K., and T. K. Wood. 1996. Trichloroethylene Degradation and Mineralization by Pseudomonads and *Methylosinus trichosporium* OB3b. *Appl. Microbiol. Biotechnol.* **45**: 248-256.

[73] Tschantz, M. F., J. P. Bowman, T. L. Donaldson, P. R. Bienkowski, J. M. Strong-Gunderson, A. V. Palumbo, S. E. Herbes, and G. S. Sayler. 1995. Methanotrophic TCE Biodegradation in a Multi-Stage Bioreactor. *Environ. Sci. Technol.* **29**: 2073-2082.

[74] Tsien, H. C., G. A. Brusseau, R. S. Hanson, and L. P. Wackett. 1989. Biodegradation of Trichloroethylene by *Methylosinus trichosporium* OB 3b. *Appl. Environ. Microbiol.* **55**: 3155-3161.

[75] U.S. EPA. 1984. National Primary Drinking Water Standard. *Proposed. Fed. Regist.* **49**: 24329.

[76] Van Duren, B. L., and S. Banerjee. 1978. Covalent Binding of the Carcinogen Trichloroethylene to Hepatic Microsomal Proteins and to Exogenous DNA in vitro. *Cancer Res.* **38**: 776-780.

[77] Vannelli, T., M. Logan, D. M. Arciero, A. B. Hooper. 1990. Degradation of Halogenated Aliphatic Compounds by the Ammonia-Oxidizing Bacterium *Nitrosomonas europea*. *Appl. Environ. Microbiol.* **56**: 1169-1171.

[78] Vogel, T. et al. 1987. Transformation of Halogenated Aliphatic Compounds. *Environ. Sci. Technol.* **21**

[79] Wackett, L. P, G. A. Brusseau, S. R. Householder, and R. S. Hanson. 1989. Survey of Microbial Oxygenases: Trichloroethylene Degradation by Propane-Oxidizing Bacteria. *Appl. Environ. Microbiol.* **55**: 2960-2964.

[80] Wackett, L. P., and D. T. Gibson. 1988. Degradation of Trichloroethylene by Toluene Dioxygenase in Whole-Cell Studies with *Pseudomonas putida* F1. *Appl. Environ. Microbiol.* **54**: 1703-1708.

[81] Westrick, J. J., J. W. Mello, and R. I. Thomas. 1984. The Groundwater Supply Survey. *J. Am. Water Works Assoc.* **76**: 52-59.

[82] Wilson, J. T., and B. H. Wilson. 1985. Biotransformation of Trichloroethylene in Soil. *Appl. Environ. Microbiol.* **29**: 242-243.

[83] Woo, H. J. 1998. Cometabolic Oxidation of TCE (Trichloroethylene) by *Pseudomonas putida* F1 in Biofiltration. Ph. D Dissertation. The University of Tennessee, Knoxville.

[84] Wright, C. L. 1998. Engineering a Packed Bed Biofilter for the Cometabolic Biodegradation of Trichloroethylene by the Bioluminescent Strain *Pseu-*

*domonas putida* TVA8. Master Thesis, The University of Tennessee, Knoxville.

[85] Zylstra, G. J., L. P. Wackett, and D. T. Gibson. 1989. Trichloroethylene Degradation by *Escherichia coli* Containing the Cloned *Pseudomonas putida* F1 Toluene Dioxygenase genes. *Appl. Environ. Microbiol.* **55**: 3162-3166.

# APPENDICES

# Appendix A

# Calibration Curve of O.D vs Biomass

Cells grown at exponential phase were centrifuged and washed by phosphate buffer. The settled down biomass was resuspended in MSB media and diluted in series at different O.D with final volume of 20 ml in glass tubes. Samples were prepared duplicately. 0.1 $\mu$l pore size cellulose nitrate filter in 47 mm diameter(Micro Filtration System) was used for filtration. Before the experiment, pretreatment of filter was needed. The filters were placed on a membrane filter apparatus and vacuum was applied. The filters were then washed several times with about 20 ml deionized water, dried in oven at 103°C $\sim$ 105°C for an hour, placed in the desiccator to cool down, and weighted. This procedure was repeated for the measurement of cell mass in the samples. The cell mass concentration was calculated by the following expression:

$$W = \frac{(A - B) * 1,000}{V_{sample}, ml} \tag{A.1}$$

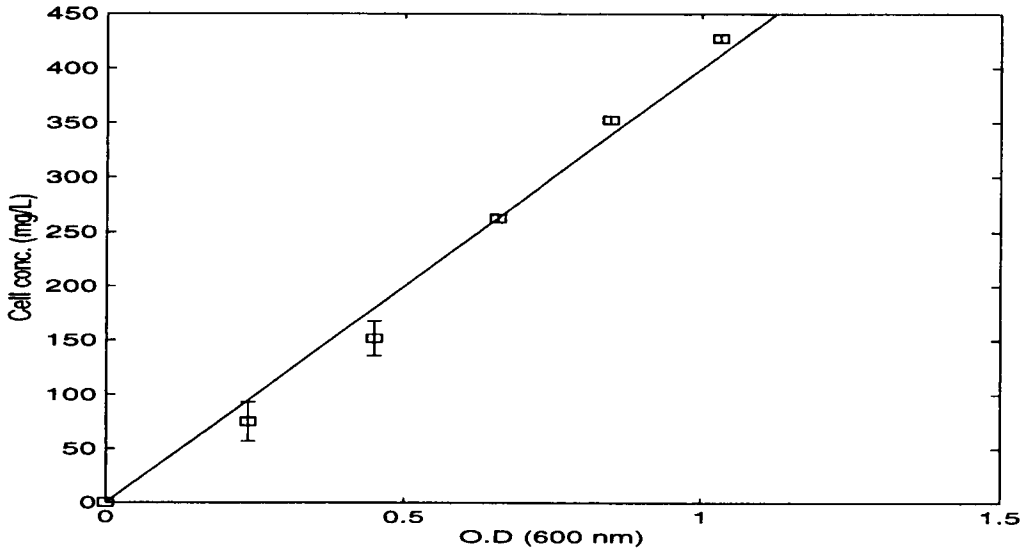



Figure A.1: Calibration Curve of O.D vs Dried Mass

Where A is the total weight of filter plus cell mass (mg), B is the weight of filter (mg), W is mg total dried cell mass. The calibration curve is plotted in Figure A.1. The slope is 399.68. This procedure is from the Standard Methods[25].

# Appendix B

# Procedure for Making Solution B

1. Nitrilo triacetic acid (NTA) is dissolved in 1500 ml of $H_2O$ with the addition of 75 g KOH per 100 g of NTA.

2. $MgSO_4$ is dissolved in a separate volume (1500 ml) of $dH_2O$; CaCl is dissolved in a separate volume (1500 ml) of $dH_2O$. The $MgSO_4$ solution is then added to the NTA solution (No.1 above)slowly to avoid any clouding of the mixture. Once these solutions are mixed, begin the gradual addition of the CaCl solution. Again do not allow the mixture to become cloudy as this result in an insoluble precipitate. Prepare a 1500 ml solution of $(NH_4)_6Mo_7O_{24}$ and $FeSO_4$. Add this solution to the mixture already prepared. At this stage of mixing, precipitate is not to be worried about. The mixture turns a pale yellow color.

3. Now add 500 ml of Metals 44 (this solution should be a very distinctive aquamarine blue). This addition will result a deeper yellow color development of

the bulk mixture.

4. Bring the total volume to 10 liters with $d\mathrm{H_2O}$. Now titrate the bulk solution to pH 6.8 using 10 N NaOH solution. This must be done very slowly and do not exceed pH 7.0, as this will result in an insoluble precipitate. As NaOH is added, precipitate will be seen. Stir the solution continuously until the precipitate is gone, then continue with the NaOH additions.

# Appendix C

# Calculation of Oxygen Demanding in the Column

Theoretical value of oxygen conversion coefficient is: $Y_{O/tol} = 2.7$ mg $O_2$/mg toluene[83]. If the flow rate of toluene saturated water is 0.2 ml/min, the mass flow rate will be:

$$F_{tol} = 0.2 \text{ ml/min} \times 515 \text{ mg/L} = 0.103 \text{ mg/min}$$

where 515 mg/L is the solubility of toluene in water at room temperature. Oxygen required for complete toluene oxidation is:

$$F_{O_21} = 0.103 \text{ mg/L} \times 2.7 \text{ mg/mg} = 0.2781 \text{ mg/min}$$

Under 1 atmosphere, gas behavior follows ideal gas law ($PV = nRT$), then the volumetric flow rate of oxygen can be found by:

$$V_{O_21} = 0.278/16 \times 0.082 \times 298/1 = 0.425 \text{ ml/min}$$

For oxygen dissolved in media, assuming that the total feed flow rate is 3.5 ml/min, and the saturated dissolved oxygen under room temperature is 7 mg/L, then oxygen needed for saturation will be:

$$F_{O_22} = 3.5 \times 7 \times 10^{-3} = 0.0245 \text{ mg/min}$$

Converted to volumetric flow rate by using ideal gas law again, $V_{O_22} = 0.0374$ ml/min. Thus total oxygen input needs to be:

$$V_{O_2} = 0.425 + 0.0374 = 0.462 \text{ ml/min}$$

The volume of oxygen storage column is 290 ml. Time lasted for toluene biodegradation under this condition is:

$$T = 290/0.462 = 10.46 \text{ hr}$$

# Appendix D

# Code for Kinetic Calculation

```
%****** Kinetics of TCE and Toluene Cometabolism ******
clear all

% parameter input

Htol=0.27; %Henry's Law constant for toluene
Htce=0.36; %Henry's Law constant for TCE
Vl=5; %liquid phase volume (ml)
Vg=20; %gas phase volume (ml)
A=1/(1+Htol*Vg/Vl);
B=1/(1+Htce*Vg/Vl);

Ks=1.106; %toluene half-saturated constant (mg/L)
Kc=1.524; %TCE half-saturated constant (mg/L)
ks=8.439/(24*60); %toluene rate constant (mg tol/mg cell/day)
kc=1.578/(24*60); %TCE rate constant (mg TCE/mg cell/day)
Y=0.4872; %toluene yield coefficient (mg cell/mg toluene)
Tc=0.0047; %TCE transformation capacity (mg TCE/mg cell)

% initial conditions

s0=[0*A 4.7*B]; %initial liquid phase concentration (mg/L)
x0=400; %cell concentration (mg/L)

% time discretization
```

```
n=1471;
delt = 0.04;
x=zeros(n,4);
r=zeros(n,2);
rn=zeros(n,2);

% initial conditions

x(1,1) = s0(1);x(1,2)=s0(2);x(1,3)=x0;x(1,4)=x0;
r(1,1) = A*ks*x(1,1)*x(1,3)/(Ks*(1+x(1,2)/Kc)+x(1,1));
r(1,2) = B*kc*x(1,2)*x(1,3)/(Kc*(1+x(1,1)/Ks)+x(1,2));
rn(1,1) = r(1,1)/x(1,3);
rn(1,2) = r(1,2)/x(1,4);
t=zeros(n,1);
t(1)=0;

% finite difference method to solve the ode system


for i = 2:n

t(i) = t(i-1) + delt;
r(i,1)=A*ks*x(i-1,1)*x(i-1,3)/(Ks*(1+x(i-1,2)/Kc)+x(i-1,1));
r(i,2)=B*kc*x(i-1,2)*x(i-1,4)/(Kc*(1+x(i-1,1)/Ks)+x(i-1,2));
x(i,1) = x(i-1,1) - r(i,1) * delt;
x(i,2) = x(i-1,2) - r(i,2) * delt;
x(i,3) = x0 + Y * (s0(1) - x(i,1));
x(i,4) = x0 + Y * (s0(1) - x(i,1)) - (s0(2) - x(i,2))/Tc;
rn(i,1) = r(i,1)/x(i,3);
rn(i,2) = r(i,2)/x(i,4);

end

r = r/x(1,3);
r(:,1) = r(:,1)/A; r(:,2) = r(:,2)/B;
rn(:,1) = rn(:,1)/A; rn(:,2) = rn(:,2)/B;
x(:,1)=x(:,1)/A; %transfer back to total concentration
x(:,2)=x(:,2)/B;

[t x];
```

```
figure(1)
subplot(2,1,1)
plot(t,x(:,1))
xlabel('time (min)')
ylabel('Toluene conc. (mg/L)')
title ('Toluene Concentration Changes with Time ')
axis([0 max(t) 0 10]);
hold on

subplot(2,1,2)
plot(t,x(:,2))
xlabel('time (min)')
ylabel('TCE conc. (mg/L)')
title ('TCE Concentration Changes with Time')
axis([0 max(t) 0 10]);
hold on

figure(3)
subplot(2,1,2)
plot(t,x(:,4))
xlabel('time (min)')
ylabel('Biomass conc. (mg/L)')
title ('Biomass Concentration Changes with Time')
axis([0 max(t) 0 420]);
hold on

figure(3)
subplot(2,1,1)
plot(t,r(:,2))
xlabel('time (min)')
ylabel('TCE rx (mg tol/mg initial cell/min)')
title ('Toluene and TCE Reaction Rate Changes with Time')
hold on

figure(4)
plot(x(:,2),rn(:,2))
xlabel('TCE conc. (mg/L)')
ylabel('-1/x*dC/dt, (mg tol/mg cell/min)')
```

```
title('Specific TCE Reaction Rate Changes with ...
TCE Concentration')

figure(5)
plot(x(:,1),rn(:,1))
xlabel('toluene conc. (mg/L)')
ylabel('-1/x*dS/dt, (mg tol/mg cell/min)')
title('Specific Toluene Reaction Rate Changes with ...
Toluene Concentration')
hold on
```

# Appendix E

# Finite Element Method Related Issues

## E.1 Notations Used in the Finite Element Methods

### E.1.1 Notations in the Biofilm Model

CPi: Dimensionless node concentration of toluene or TCE in the biofilm

F: A defined function of toluene and TCE concentrations in the biofilm

FCPi: Function form of weak statement of CPi

$GWS^N$: Galerkin weak statement

$GWSCPi^N$: Galerkin weak statement for toluene or TCE equation in the biofilm

JCPiCPi: The first derivative of GWSCPi with respect to CPi

JCP1CP2: The first derivative of GWSCP1 with respect to CP2

JCP2CP1: The first derivative of GWSCP2 with respect to CP1

$\eta$: Dimensionless biofilm distance

$\delta$CPi: The difference between present iteration and previous iteration by Newton method

$\phi_i$: Set of trial functions

i=1: for toluene, and i=2: for TCE

### E.1.2 Notations in the Bioreactor Model

CBi: Dimensionless concentration of toluene or TCE in the bulk liquid phase

CGi: Dimensionless concentration of toluene or TCE in the gas phase

FCBi: Function form of weak statement in liquid phase for toluene or TCE

FCGi: Function form of weak statement in gas phase for toluene or TCE

GWSCBi: Galerkin weak statement for toluene or TCE equation in the bulk liquid phase

JCBiCBi: The first derivative of GWSCBi with respect to CBi

JCBiCGi: The first derivative of GWSCBi with respect to CGi

JCGiCBi: The first derivative of GWSCGi with respect to CBi

JCGiCGi: The first derivative of GWSCGi with respect to CGi

$l_e$: Element length in the z direction

$q$: State variable for liquid phase equations

$Q$: State variable for gas phase equations

$\delta$CBi,$\delta$CGi: The difference between present iteration and previous iteration by Newton method

$\phi_i$: Set of trial functions

$\zeta$: Dimensionless bioreactor distance

i=1: for toluene, and i=2: for TCE

## E.2 Sample Operation of Jacobian Form in the Biofilm Model

In forming jacobian form of Equations 9.36 and 9.37 in the biofilm, first derivatives should be taken with respect to each component. The following examples are illustrations in the formation of JCP1CP1 and JCP1CP2 in Equation 9.38:

$$\begin{aligned} JCP1CP1 &= \frac{\partial GWSCP1}{\partial\{CP1\}} \\ &= [A211] + Sh1[ONE] + \frac{\partial((\frac{t_2}{t_1})\{F\}_e{}^T[A3000]\{CP1\})}{\partial\{CP1\}} \end{aligned} \quad \text{(E.1)}$$

Since F is a function of CP1, last term in Equation E.1 turns out to be:

$$(\frac{t_2}{t_1})\{F\}_e{}^T[A3000] + (\frac{t_2}{t_1})\{CP1\}^T[A3000]\frac{\partial\{F\}}{\partial\{CP1\}} \quad \text{(E.2)}$$

According to the definition of F in Equation 9.35, the derivative of F with respect to CP1 will be:

$$\frac{\partial\{F\}}{\partial\{CP1\}} = -\frac{1}{(CP1+1+CP2)^2} \quad \text{(E.3)}$$

which equates to the negative of F square. Substituting Equation E.3 into E.2, and then to Equation E.1 gives the following form of JCP1CP1:

$$JCP1CP1 = [A211] + \frac{t_2}{t_1}\{F\}^T[A3000] - \frac{t_2}{t_1}\{CP1\}^T[A3000]\lceil F^2\rfloor_e + Sh1[ONE] \tag{E.4}$$

where $\lceil F\rfloor$ is a diagonal matrix. F is also a function of CP2. Thus, the first derivative of GWSCP1 with respect to CP2 will be:

$$\begin{aligned} JCP1CP2 &= \frac{\partial((\frac{t_2}{t_1})\{F\}_e{}^T[A3000]\{CP1\})}{\partial\{CP2\}} \\ &= (\frac{t_2}{t_1})\{CP1\}^T[A3000]\frac{\partial\{F\}}{\partial\{CP2\}} \\ &= -(\frac{t_2}{t_1})\{CP1\}^T[A3000]\lceil F^2\rfloor \end{aligned} \tag{E.5}$$

## E.3 Finite Element Library Matrices

```
[A3000L] =

    0.2500    0.0833
    0.0833    0.0833
    0.0833    0.0833
    0.0833    0.2500

[A3001L] =

   -0.3333    0.3333
   -0.1667    0.1667
   -0.1667    0.1667
   -0.3333    0.3333

[A3011L] =

    0.5000   -0.5000
```

```
    0.5000   -0.5000
   -0.5000    0.5000
   -0.5000    0.5000

[A3000F] =

         0         0
         0         0
    0.2500    0.2500
    0.2500    0.2500

[A3001F] =

         0         0
         0         0
   -0.5000    0.5000
   -0.5000    0.5000
```

NOTE: Matrices [A211], [A201], [A200], [A201F], [A200F] in the text correspond to matrices [A3011L], [A3001L], [A3000L], [A3001F], [A3000F], respectively, in the computation.

# Appendix F

# Code for Solving Biofilm Model

## F.1 Template for Solving Biofilm Concentrations

```
% Template for Solving Biofilm Equations

RESIDUALS

CP1   2#

   (     )(   )(   )(0;-1)(A211)(CP1)
+  (tc/ts)(   )( F )(0; 1)(A3000)(CP1)

CP1   3#

   ( -SH1)(   )(   )(0; 0)(ONE)(CB1)
+  (  SH1)(   )(   )(0; 0)(ONE)(CP1)

CP2   2#

   (     )(   )(   )(0;-1)(A211)(CP2)
+  (ts/tc)(   )(F*fa)(0;1)(A3000)(CP2)

CP2   3#

   ( -SH2)(   )(   )(0; 0)(ONE)(CB2)
+  (  SH2)(   )(   )(0; 0)(ONE)(CP2)
```

```
JACOBIANS

CP1   CP1   2#

   (     )(   )(   )(0;-1)(A211)(   )
+  (tc/ts)(   )( F )(0; 1)(A3000)(   )
+ (-tc/ts)(   )(CP1)(0; 1)(A3000)(F^2)

CP1   CP1   3#

   ( SH1 )(   )(   )(0; 0)(ONE)(   )

CP1   CP2   2#

  (-tc/ts)(   )(CP1)(0; 1)(A3000)(F^2)

CP1   CB1   3#

   ( -SH1)(   )(   )(0; 0)(ONE)(   )

CP2   CP2   2#

   (     )(   )(   )(0;-1)(A211)(   )
+  (ts/tc)(   )(F*fa)(0;1)(A3000)(  )
+ (-ts/tc)(   )(CP2)(0; 1)(A3000)(F^2*fa)

CP2   CP2   3#

   ( SH2 )(   )(   )(0; 0)(ONE)(   )

CP2   CP1   2#

  (-ts/tc)(   )(CP2)(0; 1)(A3000)(F^2*fa)

CP2   CB2   3#

   ( -SH2)(   )(   )(0; 0)(ONE)(   )
```

## F.2 Main Program for Biofilm Equations

```
%#################################################################%
%                                                                 %
% Code written for calculating the thickness of biofilm and       %
% flux for toluene and TCE degradation ** non-uniform mesh **     %
%                                                                 %
%#################################################################%

clear all

% biofilm kinetic parameters for substrate

k = [8.4385 1.5783]; % reaction constant, mg/mg/day
Ks = [1.106 1.524]; % saturation parameter, mg/L
D = [0.8899 0.78]; % diffusivity in aqueous phase cm^2/day
Df = [0.2452 0.2150]; % Df in the biofilm cm^2/day
L = [0.0020 0.0019]; % liquid film thickness cm
kL = D./L; % mass transfer coefficient cm/day
Y = 0.4872; % yield coefficientY = 0.771;
Tc = 0.5; % TCE transformation capacity
bm = 0.68; % cell decay constant 1/day
Xf = 60; % biofilm density mg biomass/cm^3

% Dimensionless parameters

theta = [bm/(Y*k(1)) Tc*bm/k(2)]; % standard biofilm time
tau = (Ks.*Df./(k.*Xf)/1000).^0.5;
                        % standard biofilm depth dimension
taubar = (tau(1)*tau(2))^0.5; % geometric average
DDf = Df./D;
sh = kL.*taubar./Df; % Sherwood number
a = tau(2)/tau(1);
b = 1/a;

% Bulk concentration for substrates

Cb = [5 1]; % toluene, TCE conc. mg/L
CB = Cb./Ks; % converted to dimensionless form
CB1bar = CB(1);
```

```
CB2bar = CB(2);

%Initial guess for biofilm thickness and effective biomass

tlf = 0.0085; % unit in cm
TLF = tlf/taubar; % dimensionless form

% discretization in space

nnodesx = 50;

% setup the initial conditions

CP1 = zeros(nnodesx,1);
CP2 = zeros(nnodesx,1);
QP = [CP1;CP2];
sum = zeros(2,1);
y1 = zeros(nnodesx,1); % for integration
y2 = zeros(nnodesx,1);
DJ = zeros(2,1);
J = zeros(nnodesx,2);
fa = ones(nnodesx,1);

% set max iteration count for Newton algorithm

maxits = 50; % max iterations
eps = 1E-4; % convergence criteria for Newton algorithm

% load the matrix library
load femlib

% begin iteration

TLFnew = TLF;
TLFold = 0;
ki = 0;
while abs(TLFnew - TLFold) > eps

ki = ki +1
alphaa = 0.6;
```

```
TLFnext = alphaa * TLFnew + (1 - alphaa) * TLFold;
TLFold = TLFnext;
x = ratlist(0,TLFold,nnodesx-1,1.05);

for m = 1:maxits
% [resCP,jacCP] = resjacCP(QP,x)
resjacCPtest4
dQP = jacCP\(-1*(resCP)); % Newton algorithm
QP = QP + dQP;
jiteration = m %display iteration count
dQmax = max(abs(dQP)); % convergence criteria
if dQmax < eps % test convergence against tolerance
break
end
end
CP1 = QP(1:nnodesx,1);
CP2 = QP((nnodesx+1):2*nnodesx,1);
CP0 =[CP1(1) CP2(1)];
CPP = [CP1 CP2];

% integration by using trapezoidal rule

y1 = tau(2)/taubar*CP1./(1+CP1+CP2);
y2 = fa .* tau(1)/taubar.*CP2./(1+CP2+CP1);
sum(1) = trapz(x,y1);
sum(2) = trapz(x,y2);

% calculate the substrates flux

DJ = sum.*DDf';
% J = kL .* (CB - CP0).*Ks/1000 ;
% DJ = J.*tau./(D.*Ks);

% calculate the new biofilm thickness

TLFnew = DJ(1)/(taubar/tau(1)*DDf(1)*theta(1));
TLFnew;
TLF = TLFnew * taubar;
xx = ratlist(0,TLF,nnodesx-1,1.05);
```

```
% correct for the active biomass for TCE degradation

JJ = DJ'.*D.*Ks./tau/1000;
J(1,:) = kL .* (CB - CPO).*Ks/1000;
for i=2:nnodesx
deltah = xx(i) - xx(i-1);
J(i,:) = Df.*(CPP(i-1,:) - CPP(i,:))/deltah/1000;
fa(i-1) = ((J(i-1,1)-J(i,1))*Y-1/Tc*(J(i-1,2)-J(i,2))) ...
/(bm*Xf*deltah);
if fa(i-1) <= 0
fa(i-1) = 0.0005;
else
end
end
fa(nnodesx)=fa(nnodesx-1);
fa(1) = fa(2);
fa
J
J(1,:) = J(2,:);
end

% calculate the effectiveness factor

eta1 = sum(1) * taubar/tau(2)/(TLFnew*CP1(1)/(1+CP2(1)+CP1(1)))
eta2 = sum(2) * taubar/tau(1)/(TLFnew*CP2(1)/(1+CP2(1)+CP1(1)))

% convert dimensionless terms to physical domain

CP1 = CP1 * Ks(1)
CP2 = CP2 * Ks(2)
TLF
fa
x = ratlist(0,TLF,nnodesx-1,1.05);

figure(1)
%plot(x,CP1,'ro')
%hold on
%plot(x,CP2,'r*')
plot(x,CP1,'.')
hold on
```

```
plot(x,CP2,'.')
xlabel('Biofilm Coordinate (cm)')
ylabel('Toluene and TCE Concentration (mg/L)')
%title('Influene of Mass Transfer on Toluene and ...
 TCE Concentrations in the Biofilm')
%legend(r,toluene concentration,g,TCE concentration)
hold on
axis square

figure(2)
plot(x, fa,'.')
hold on
%plot(x, fa)
xlabel('Biofilm Coordinate (cm)')
ylabel('Active Biomass Ratio Xa/Xm')
%title('Influence of Mass Transfer on Active Biomass ...
 Distribution in the Biofilm')
axis square


figure(3)
plot(x,J(:,1),'.')
%plot(x,J(:,1))
xlabel('Biofilm Coordinate (cm)')
ylabel('Toluene Flux (mg/cm^2/day)')
%title('Influene of Mass Transfer on Toluene ...
 Flux in the Biofilm')
%legend(r,toluene concentration,g,TCE concentration)
hold on
axis square

figure(4)
plot(x,J(:,2),'.')
%plot(x,J(:,2))
xlabel('Biofilm Coordinate (cm)')
ylabel('TCE Flux (mg/cm^2/day)')
%title('Influene of Mass Transfer on TCE Flux ...
 in the Biofilm')
%legend(r,toluene concentration,g,TCE concentration)
hold on
```

```
axis square

figure(5)
plot(x,J(:,1)./J(:,2),'.')
xlabel('Biofilm Coordinate (cm)')
ylabel('Toluene/TCE Flux Ratio (mg tol/mg tce)')
%title('Influene of Mass Transfer on Toluene and ...
 TCE Flux in the Biofilm')
%legend(r,toluene concentration,g,TCE concentration)
hold on
axis square
```

## F.3 Residuals and Jacbians for Concentrations in the Biofilm

```
%%%%%%%%%%%%%%%%%%%%%%%%%%%%%%%%%%%%%%%%%%%%%%%%%%%%%%%%%%%%%%%%%%
%Calculation of residuals of state variable CPs for TCE  %
%and toluene biodegradation in a packed bed reactor      %
%%%%%%%%%%%%%%%%%%%%%%%%%%%%%%%%%%%%%%%%%%%%%%%%%%%%%%%%%%%%%%%%%%


%function [resCP,jacCP] = resjacCPnew(QP,x);

global nnodex

% res -                 residuals
% QP -                  state variables[CP1 CP2]
% x -                   grid data in biofilm
% j -                   index in the z direction
% i -                   index in the x direction
% CP1, CP2 -            conc. in the x direction at any z position
%                       are 1 x i vector

% divide QP into CP1 and CP2

CP1 = QP(1:nnodesx,1);
CP2 = QP(nnodesx+1:2*nnodesx,1);
```

```
% interpolate the reaction terms

F = 1./(CP1 + 1 + CP2);

% calculate the residuals

CP1_sp = ass1d ([],[],[],-1,A3011L,x);
CP1_sp = CP1_sp + ass1d (a,[],F',1,A3000L,x);
CP1_sp = CP1_sp*CP1;              % domain terms

CP1_sp(1,1) = CP1_sp(1,1) + sh(1)*CP1(1) - sh(1)*CB1bar;
                                  % add boundary terms
                                  % CB1bar = CB1(k,j) in main algorithm

CP2_sp = ass1d ([],[],[],-1,A3011L,x);
CP2_sp = CP2_sp + ass1d (b,[],(F.*fa)',1,A3000L,x);
CP2_sp = CP2_sp*CP2;              % domain terms

CP2_sp(1,1) = CP2_sp(1,1) + sh(2)*CP2(1) - sh(2)*CB2bar;
                                  % add boundary terms
                                  % CB2bar = CB2(k,j) in main algorithm

resCP = [CP1_sp;CP2_sp];


% calculate the jacobians

JCP1CP1 = ass1d ([],[],[],-1,A3011L,x);
JCP1CP1 = JCP1CP1 + ass1d (a,[],F',1,A3000L,x);
JCP1CP1 = JCP1CP1 + ass1d (-a,[],CP1',1,A3000L,x) * diag(F.^2);
                                  % domain terms

JCP1CP1(1,1) = JCP1CP1(1,1) +sh(1);
                                  % add boundary terms

JCP1CP2 = ass1d (-a,[],CP1',1,A3000L,x) * diag(F.^2);


JCP2CP2 = ass1d ([],[],[],-1,A3011L,x);
```

```
JCP2CP2 = JCP2CP2 + ass1d (b,[],(F.*fa)',1,A3000L,x);
JCP2CP2 = JCP2CP2 + ass1d (-b,[],CP2',1,A3000L,x) * diag(F.^2.*fa);
                                % domain terms

JCP2CP2(1,1) = JCP2CP2(1,1) +sh(2);
                                % add boundary terms

JCP2CP1 = ass1d (-b,[],CP2',1,A3000L,x) * diag(F.^2.*fa);

% assembling of the jacobians

jacCP = [JCP1CP1 JCP1CP2;JCP2CP1 JCP2CP2];
```

## F.4 Code for Element Assembling

```
function gmat=ass1d(gscalar,escalar,hyp,mexp,lmat,mesh);
%  usage:  ass1d(gscalar,escalar,hyp,mexp,lmat,mesh)
%
%  Assembles 1d finite element matrices.  Assumes that each basis that went
%  into the element library matrix is of the same degree.  Returns the
%  assembled  global matirx.
%
%  gscalar - global scalar data (default unity)
%  escalar - element data (row matrix, default unity)
%  hyp     - hypermatrix contraction data  (row matrix, default unity)
%  mexp    - mesh measure exponent
%  lmat    - element library matrix
%  mesh    - nodal values of the mesh  (row matrix)
%
%  Any of the first three arguments may be omitted by supplying an
%  empty matrix ([]) in their place.    Ones will be inserted for any
%  legally omitted arguments.

nnodes = size(mesh,2);   %  number of nodes in the mesh
enodes = size(lmat,2);  % num of columns in lmat is num of nodes per element
emat = zeros(enodes);   % allocate space for element matrix
nelements = (nnodes-1)/(enodes-1); % number of elements
```

```
% Allocate memory for global matrix (full matirx is stored)
gmat = zeros(nnodes,nnodes); % creates nnodes by nnodes matirx of zeros

%  provide for empty arguments
if length(gscalar)==0;
  gscalar = 1;
end;
if length(escalar)==0;
  escalar = ones(1,nelements); % row of ones
end;
if length(hyp)==0
  hyp = ones(1,nnodes);  % row of ones
end;


%  initialize left and right node addresses for current element
mleft = 1;
mright = enodes;

% Main loop
for i=1:nelements;
  ehyp = hyp(mleft:mright);   %  get part of hyp for current element
  le = mesh(mright) - mesh(mleft);  % length of the element

% contract library hypermatrix; use mesh measure, element scalar and
%    global scalar to form element matrix
  emat = hmult(ehyp,lmat) * le^mexp * escalar(i) * gscalar;

% assemble element matrix into global matrix
  gmat(mleft:mright,mleft:mright) = gmat(mleft:mright,mleft:mright) + emat;

% update left and right node addresses for the next element
  mleft = mleft + enodes - 1;
  mright = mright + enodes -1;

end;
```

# Appendix G

# Code for Solving Bioreactor Model

## G.1 Template for Bulk Fluid Equations

```
RESIDUALS

CB1 2#

     (1/Pe1)( )( )(0;-1)(A211)(CB1)
+     (1+R) ( )( )(0; 0)(A201)(CB1)
+    (alph1)( )( )(0; 1)(A200)(CB1)
+   (-alph1)( )( )(0; 1)(A200)(CP1)|x=0
+    (beta1)( )( )(0; 1)(A200)(CB1)
+(-beta1/H1)( )( )(0; 1)(A200)(CG1)


CB1 3#

      (1+R)( )( )(0; 0)(ONE)(CB1)
+       (-)( )( )(0; 0)(ONE)(CB1in)
+      (-R)( )( )(0; 0)(ONE)(CB1out)


CB2 2#

     (1/Pe2)( )( )(0;-1)(A211)(CB2)
```

```
+      (1+R) ( )( )(0; 0)(A201)(CB2)
+     (alph2)( )( )(0; 1)(A200)(CB2)
+    (-alph2)( )( )(0; 1)(A200)(CP2)|x=0
+     (beta2)( )( )(0; 1)(A200)(CB2)
+(-beta2/H2)( )( )(0; 1)(A200)(CG2)


CB2 3#

       (1+R)( )( )(0; 0)(ONE)(CB2)
+        (-)( )( )(0; 0)(ONE)(CB2in)
+       (-R)( )( )(0; 0)(ONE)(CB2out)


CG1 2#

        ( )( )( )(0; 0)(A201F)(CG1)
+  (-gam1)( )( )(0; 1)(A200F)(CB1)
+(gam1/H1)( )( )(0; 1)(A200F)(CG1)


CG1 2#

        ( )( )( )(0; 0)(A201F)(CG2)
+  (-gam2)( )( )(0; 1)(A200F)(CB2)
+(gam2/H2)( )( )(0; 1)(A200F)(CG2)


JACOBIANS


CB1 CB1 2#

     (1/Pe1)( )( )(0;-1)(A211)
+      (1+R)( )( )(0; 0)(A201)
+    (alph1)( )( )(0; 1)(A200)
+    (beta1)( )( )(0; 1)(A200)

CB1 CB1 3#
```

```
   (1+R)( )( )(0; 0)(ONE)( )


CB1 CP1 2#


   (-alph1)( )( )(0; 1)(A200)( )

CB1 CG1 2#

 (-beta1/H1)( )( )(0; 1)(A200)( )


 CB2 CB2 2#

    (1/Pe2)( )( )(0;-1)(A211)
+     (1+R)( )( )(0; 0)(A201)
+   (alph2)( )( )(0; 1)(A200)
+   (beta2)( )( )(0; 1)(A200)

CB2 CB2 3#

   (1+R)( )( )(0; 0)(ONE)( )


CB2 CP2 2#


   (-alph2)( )( )(0; 1)(A200)( )

CB2 CG2 2#

 (-beta2/H2)( )( )(0; 1)(A200)( )


 CG1 CG1 2#

       ( )( )( )(0; 0)(A201F)( )
+(gam1/H1)( )( )(0; 1)(A200F)( )
```

```
CG1 CB1 2#

 (-gam1)( )( )(0; 1)(A200F)( )


  CG2 CG2 2#

       ( )( )( )(0; 0)(A201F)( )
+(gam2/H2)( )( )(0; 1)(A200F)( )


CG2 CB2 2#

 (-gam2)( )( )(0; 1)(A200F)( )
```

## G.2 Main Program for Bioreactor Model

```
%%%%%%%%%%%%%%%%%%%%%%%%%%%%%%%%%%%%%%%%%%%%%%%%%%%%%%%%%%%%%%%%%%%%%%%%
%This code is written for solving a set of differential %
%equations in biofilm phase, liquid phase and gas phase %
%for biodegradation of TCE and toluene in a fixed film  %
%packed bed reactor.                                    %
%%%%%%%%%%%%%%%%%%%%%%%%%%%%%%%%%%%%%%%%%%%%%%%%%%%%%%%%%%%%%%%%%%%%%%%%

clear all

% Condition input

Qr = 27.5; % recycle rate; ml/min
Qi = 3.02; % total flow rate; ml/min

Cbin = [33.66 0.2130]; % influent toluene and TCE conc. mg/L
Tc = 10;

tin = 0.0065; % initial guess of biofilm cm

nnodesx = 30;
```

```
nnodesz = 30;

%%%%%%%%%
parameters % parameters estimation
%%%%%%%%%
alpha = alpha * thetaL;
beta = alpha;
gamma = gamma * thetaG;


CBin = Cbin./Ks; % dimensinless influent concentration

%discretization in space

z = ratlist(0,1,nnodesz-1,1.1); % grid in bulk fluid

% load the matrix library
load femlib

% load the matrix library for finite difference method
load mylib

% set max iteration count for Newton algorithm

maxits = 50; % max iterations
eps = 1E-4; % convergence criteria for Newton algorithm
eps1 = 1E-3;

%%%%
dim % matrix dimension set-up
%%%%

% begin iterations

dQ1max = max(abs(Qnew(:,1) - Qold(:,1)));
dQ2max = max(abs(Qnew(:,2) - Qold(:,2)));

l = 0;
while max([dQ1max dQ2max]) > eps
```

```
l = l + 1

Qold = Qnew;
QCPold = QCPnew;

for i = 1:2
CBIN = CBin(i); % solve in liquid & air phase
pe1 = pe(i);
alpha1 = alpha(i);
H1 = H(i);
beta1 = beta(i);
gamma1 = gamma(i);
CPbar = QCPold((i-1)*nnodesz+1:i*nnodesz,:);
Q = Qold(:,i);

for m = 1:maxits
% [res,jac] = resjacCBCG(Q,z)
resjacCBCG218
dQ = jac\(-1*(res)); % Newton algorithm
Q = Q + dQ;
Q(nnodesz+1) = Q(nnodesz)*H1;% undo dQ for Dirichlet node
iteration = m % display iteration count
dQmax = max(abs(dQ)); % convergence criteria
if dQmax < eps % test convergence against tolerance
break
end
end
Qnew(:,i) = Q; % store new value for Q
end

        Qnew1 = Qnew(1:nnodesz,1);
Qnew2 = Qnew(1:nnodesz,2);
QCPold1 = QCPold(1:nnodesz,:);
QCPold2 = QCPold((nnodesz+1):2*nnodesz,:);

for j = 1:nnodesz % solve in biofilm

QP = [QCPold1(j,:)';QCPold2(j,:)'];
CB1bar = Qnew1(j);
CB2bar = Qnew2(j);
```

```
%%%%%%%%
biofilmcp2 % call for biofilm calculation
%%%%%%%%

QCPnew1(j,:) = QP(1:nnodesx,1)';
QCPnew2(j,:) = QP((nnodesx+1):2*nnodesx,1)';

faf(j,:) = fa';
Jf (j,:) = J(:,1)';
Jf(nnodesz+j,:) = J(:,2)';
xr(j,:) = xx;

end

QCPnew(1:nnodesz,1:nnodesx) = QCPnew1;
QCPnew((nnodesz+1):2*nnodesz,1:nnodesx) = QCPnew2;

dQ1max = max(abs(Qnew(:,1) - Qold(:,1)));
dQ2max = max(abs(Qnew(:,2) - Qold(:,2)));

end

% Convert dimensionless term to physical domain

Qnew1 = Qnew(1:nnodesz,1) * Ks(1);
Qnew2 = Qnew(1:nnodesz,2) * Ks(2);
QCPnew1 = QCPnew1 * Ks(1);
QCPnew2 = QCPnew2 * Ks(2);
CG1 = Qnew(nnodesz+1:2*nnodesz,1);
CG2 = Qnew(nnodesz+1:2*nnodesz,2);
CG1 = CG1 * Ks(1);
CG2 = CG2 * Ks(2);
TLFF = TLFF * taubar;

QCPnew1
QCPnew2
CB = [Qnew1 Qnew2]
CG =[CG1 CG2]
TLFF
```

```
eta

% Remove efficiency

eff1 = (Cbin(1) - Qnew1(nnodesz))/Cbin(1)
eff2 = (Cbin(2) - Qnew2(nnodesz))/Cbin(2)


save out2 TLFF CB CG QCPnew1 QCPnew2 JJ eta faf Jf xr z eff1 ...
 eff2 Qi Qr Cbin Tc Ks Y As
```

## G.3 Residuals and Jacobians for Bulk Fluid Equations

```
%%%%%%%%%%%%%%%%%%%%%%%%%%%%%%%%%%%%%%%%%%%%%%%%%%%%%%%%%%%%%%%%%%%%%%%%%%%%
%   Calculation of residuals and jacobians of state variable    %
%   CBs and CGs in the bulk liquid phase and air phase for      %
%   toluene, TCE and oxygen.                                    %
%                           October 7, 1997                     %
%%%%%%%%%%%%%%%%%%%%%%%%%%%%%%%%%%%%%%%%%%%%%%%%%%%%%%%%%%%%%%%%%%%%%%%%%%%%

%function [res, jac] = resjacCBCG(Q,z)

global nnodesz

% res -residuals
% Q -state variables [CB CG]
% z -grid data in axial direction

% divide Q into CB and CG

CB = Q(1:nnodesz,1);
CG = Q(nnodesz+1:2*nnodesz,1);

% calculation of residuals

CB_res = ass1d (1/pe1,[],[],-1,A3011L,z);
CB_res = CB_res + ass1d (1+R,[],[],0,A3001L,z);
```

```
CB_res = CB_res + ass1d (alpha1,[],[],1,A3000L,z);
CB_res = CB_res + ass1d (beta1,[],[],1,A3000L,z);
CB_res = CB_res * CB + ass1d (-alpha1,[],[],1,A3000L,z) * CPbar(:,1);
CB_res = CB_res + ass1d (-beta1/H1,[],[],1,A3000L,z) * CG;
                                        % domain terms

CB_res(1,1) = CB_res(1,1) + (1+R)*CB(1) - CBIN;
                                        % add boundary terms
CB_res(1,1) = CB_res(1,1) - R * CB(nnodesz);

CG_res = ass1d ([],[],[],0,A3001F,z);
CG_res = CG_res + ass1d (gamma1/H1,[],[],1,A3000F,z);
CG_res =CG_res * CG + ass1d(-gamma1,[],[],1,A3000F,z) * CB;
% finite difference

res = [CB_res;CG_res];


% calculation of jacobians

JCBCB = ass1d (1/pe1,[],[],-1,A3011L,z);
JCBCB = JCBCB + ass1d (1+R,[],[],0,A3001L,z);
JCBCB = JCBCB + ass1d (alpha1,[],[],1,A3000L,z);
JCBCB = JCBCB + ass1d (beta1,[],[],1,A3000L,z);

%JCBCB(1,1) = JCBCB(1,1) + 1;
JCBCB(1,1) = JCBCB(1,1) + 1 + R;
%JCBCB(nnodesz,nnodesz) = JCBCB(nnodesz,nnodesz) - R;

JCBCG = ass1d (-beta1/H1,[],[],1,A3000L,z);

JCGCG = ass1d ([],[],[],0,A3001F,z);
JCGCG = JCGCG + ass1d (gamma1/H1,[],[],1,A3000F,z);

JCGCG(1,1) = 1E10;

JCGCB = ass1d(-gamma1,[],[],1,A3000F,z);

jac = [JCBCB JCBCG;JCGCB JCGCG];
```

## G.4 Subroutine for Solving the Biofilm Equations

```
%#################################################################
%                                                                 %
% Code written for calculating the thickness of biofilm and      %
% flux for toluene and TCE degradation                           %
%                                                                 %
%#################################################################


% setup the initial conditions

%CP1 = zeros(nnodesx,1);
%CP2 = zeros(nnodesx,1);
%QP = [CP1;CP2];

if j == 1 & l == 1
TLF = tin/taubar; % initial guess of the biofilm thickness
elseif j == 1
TLF = TLFF(1);
else
TLF = TLFF(j-1);
end

J = zeros(nnodesx,2);
fa = ones(nnodesx,1);

% begin iteration

TLFnew = TLF;
TLFold = 0;
ki = 0;
while abs(TLFnew - TLFold) > eps1

ki = ki +1
alphaa = 0.6;
TLFnext = alphaa * TLFnew + (1 - alphaa) * TLFold;
```

```
TLFold = TLFnext;
x = ratlist(0,TLFold,nnodesx-1,1.2);

for m = 1:maxits
% [resCP,jacCP] = resjacCP(QP,x)
resjacCPtest4
dQP = jacCP\(-1*(resCP)); % Newton algorithm
QP = QP + dQP;
jiteration = m; %display iteration count
dQmax = max(abs(dQP)); % convergence criteria
if dQmax < eps % test convergence against tolerance
break
end
end
CP1 = QP(1:nnodesx,1);
CP2 = QP((nnodesx+1):2*nnodesx,1);
CPO =[CP1(1) CP2(1)];
CPP = [CP1 CP2];



% integration by using trapezoidal rule

y1 = tau(2)/taubar*CP1./(1+CP1+CP2);
y2 = fa.*tau(1)/taubar.*CP2./(1+CP2+CP1);
sum(1) = trapz(x,y1);
sum(2) = trapz(x,y2);

% calculate the substrates flux

DJ = sum.*DDf';

% update the bs
% tlf = TLFold * taubar; % cm
% if tlf > 0.003
% bs = 0.0842 * (sigmma/(1+443.2*(tlf-0.003)))^0.58;
% else
bs = 0.0842 * sigmma^0.58;
% end
% bprime= bm + bs;
```

```
% theta = [bprime/(Y*k(1)) Tc*bprime/k(2)]; % standard biofilm time

% calculate the new biofilm thickness

TLFnew = DJ(1)/(taubar/tau(1)*DDf(1)*theta(1));
TLFnew
TLFnon = TLFnew * taubar;
xx = ratlist(0,TLFnon,nnodesx-1,1.2);

% correct for the active biomass for TCE degradation

JJ(j,:) = DJ'.*D.*Ks./tau/1000;
J(1,:) = JJ(j,:);
for i=2:nnodesx
deltah = xx(i) - xx(i-1);
J(i,:) = Df.*(CPP(i-1,:) - CPP(i,:))/deltah/1000;
fa(i-1) = ((J(i-1,1)-J(i,1))*Y-1/Tc*(J(i-1,2)-J(i,2)))/(bprime*Xf*deltah);
if fa(i-1) < 0
fa(i-1) = 0;
else
end
end
fa(nnodesx)=fa(nnodesx-1);
fa(1) = fa(2);
J(1,:) = J(2,:);
fa;

end

% calculate the effectiveness factor

eta(j,1) = sum(1) * taubar/tau(2)/(TLFnew*CP1(1)/(1+CP2(1)+CP1(1)));
eta(j,2) = sum(2) * taubar/tau(1)/(TLFnew*CP2(1)/(1+CP2(1)+CP1(1)));
%JJ(j,:) = DJ'.*D.*Ks./tau/1000;
JJ(j,:) = J(1,:);

TLFF(j)=TLFnew

xx = ratlist(0,TLFnew*taubar,nnodesx-1,1.2);
```

## G.5 Matrices Dimension Set-up

```
% setup the initial conditions

Qold = ones(2*nnodesz,2); % initial guess value
QCPold = ones(2*nnodesz,nnodesx);

Qnew = 1E-2 * Qold;
QCPnew = 0 * QCPold;

QCPnew1 = zeros(nnodesz,nnodesx);
QCPnew2 = zeros(nnodesz,nnodesx);

TLFF = zeros(nnodesz,1);
sum = zeros( 2,1);
DJ = zeros(2,1);

eta = zeros(nnodesz,2);
JJ = zeros(nnodesz,2);
Jf = zeros(2*nnodesz,nnodesx); % flux in the biofilm
faf= zeros(nnodesz,nnodesx); % active biomass ratio
xr = zeros(nnodesz,nnodesx);
```

## G.6 Parameter Evaluation

```
%%%%%%%%%%%%%%%%%%%%%%%%%%%%%%%%%%%%%%%%%%%%%%%%%%%%
%                                                  %
%          PARAMETER FILE       Oct. 18, 1997      %
%                                                  %
%%%%%%%%%%%%%%%%%%%%%%%%%%%%%%%%%%%%%%%%%%%%%%%%%%%%

% biofilm kinetic parameters for substrate
```

```
k = [8.4385 1.5783]; % reaction constant, mg/mg/day
Ks = [1.106 1.524]; % saturation parameter, mg/L
Y = 0.4872; % yield coefficient
Tc = 0.05; % TCE transformation capacity
bm = 0.12; % cell decay constant 1/day
Xf = 60; % biofilm density mg biomass/cm^3

% Physical parameters of toluene and TCE

D = [0.8899 0.78]; % diffusivitiesin aqueous phase cm^2/day
H = [0.3687 0.2656]; % Henry's law constant
vis = 864; % viscosity of water g/cm/day
ro = 1; % density of water g/cm***3

Df = (1-0.43*Xf^0.93/(11.19+0.27*Xf^0.99))*D;
% diffusivity in biofilm cm**2/day

% Reactor parameters

Vr = 270; % total reactor volumn ml
Lr = 55; % reactor length cm
Dr = 2.5; % reactor diameter cm
d = 0.4; % beads diameter cm

% Estimation parameters

A = pi/4*Dr^2; % reactor cross section area cm**2
As = 11; % spesific mass transfer area /cm
R = Qr/Qi; % recycle ratio
u = Qi/A*60*24; % superficial velocity cm/day
DE = 0.67*D+0.65*d*(1+R)*u*(1+6.7*(D/(d*(1+R)*u)).^0.5);
                          % dispersion coefficient cm**2/day

% Parameters and gas flow, liquid hold-up estimation

c1 = 1.4287; % fitting parameters from experiments
c2 = 0.4065;
thetaL = c1 * (Qi*(1+R)/A*0.01/60)^c2; % liquid hold-up
a1 = 2.9879;
a2 = 0.3674;
```

```
Qg = a1 * Qi^a2 * 60 *24; % Gas recycle rate ml/day
thetaP = 0.6; % beads holp-up
thetaG = 1 - thetaL - thetaP; % Gas hold-up
v = Qg/A; % gas superficial velocity cm/day

Sc = vis./(ro*D);                % Schmit number
Re = 2*thetaL*d*u*(1+R)*ro/((1-thetaL-thetaG)*vis);
                                 % Renolds number
L = D*Re^0.75.*Sc.^0.67/(5.7*u*(1+R));
                                 % Liquid film thickness cm
kL = D./L;

% Dimensionless parameters

%theta = [bm/(Y*k(1)) Tc*bm/k(2)]; % standard biofilm time
tau = (Ks.*Df./(k.*Xf)/1000).^0.5;
                          % standard biofilm depth dimension
taubar = (tau(1)*tau(2))^0.5; % geometric average
DDf = Df./D;
sh = kL.*taubar./Df; % Sherwood number
a = tau(2)/tau(1);
b = 1/a;

% Reactor dimensionless group

pe = Lr*u./(thetaL*DE); % Peclet number
alpha = Lr*kL*As/u; % mass transfer number for L-B
beta = alpha; % for L-G; ~ area is the same
gamma = Lr*kL*As/v; % gas phase mass transfer number

% Shear stress  Re < = 10 (yes)

sigmma = 100*vis*u*(1+R)*(1-thetaL-thetaG)^3...
/(d^2*thetaL^3*As*7.46*10^9);
bs = 0.0842 * sigmma^0.58;
bprime = bm + bs;
theta = [bprime/(Y*k(1)) Tc*bprime/k(2)];

prmout
```

## Vita

Feng Yu was born in Hangzhou, China. She graduated from Hangzhou No. 4th Middle School in 1982. After a highly competitive entrance examination, she was admitted to Zhejiang Institute of Technology where she received her B. S. in Microbial Engineering four years later. She continued her graduate study in Wuxi Institute of Light Industry and got M. S. degree in the same area in December 1988. She worked as a research assistant later as a lecturer in the Department of Chemical Engineering, Zhejiang University from January 1990 to June 1993. She went to The University of Tennessee, Knoxville in Fall 1993 and received her Ph. D degree in Chemical Engineering in August 1998.